

Preparación, Caracterización y Aplicaciones de Carbones Activados preparados a partir de Lignina Kraft




WOOD BIOPOLYMERS GROUP
Department of Chemical Engineering - CTM-Q - Rovira i Virgili University

Vanessa Torné Fernández

Tesis dirigida pels

Dr. Vanessa Fierro y Dr. Daniel Montané

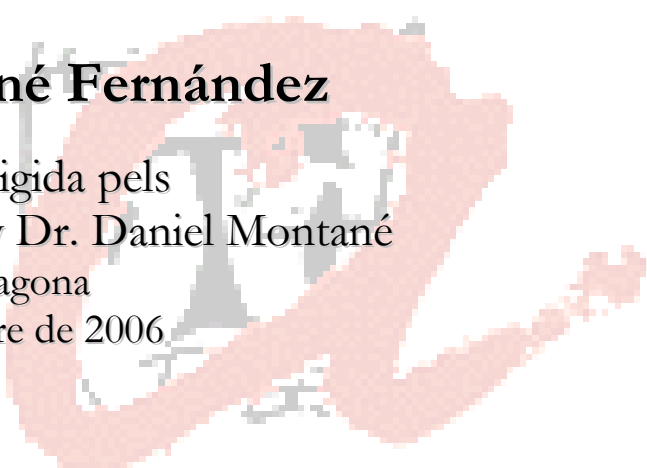
PREPARACIÓN, CARACTERIZACIÓN Y APLICACIONES DE CARBONES ACTIVADOS PREPARADOS A PARTIR DE LIGNINA KRAFT

Memòria de la tesis presentada al
Departament d'Enginyeria Química de la
Universitat Rovira i Virgili

per a optar al títol de
Doctor per la Universitat Rovira i Virgili

Vanessa Torné Fernández

Tesis dirigida pels
Dr. Vanessa Fierro y Dr. Daniel Montané
Tarragona
Septembre de 2006



Preparación, caracterización y aplicaciones de carbones activados preparados a partir de lignina Kraft.

Tesis doctoral

Autora : Vanessa Torné Fernández

Fotografies i il·lustracions: Vanessa Torné Fernández

Disseny i maquetació : Vanessa Torné Fernández

© del text, 2006, Vanessa Torné Fernández

© de les imatges i il·lustracions, 2006, Vanessa Torné Fernández

Primera edició: setembre 2006-09-02

Reservats tots els drets

No està permesa la reproducció total o parcial d'aquest llibre, ni el seu tractament informàtic, ni la transmissió de cap manera o per qualsevol mitjà, ja sigui electrònica, mecànica, per fotocòpies, per registre o altres mètodes, sense el permís previ i per escrit dels titulars del Copyright.

Tirada: 20 exemplars

ISBN: 84-690-0707-6

Nº Registre: 06/66749

A la meva gent.

Al meu passat,
i al meu present.

El tiempo es al amor
lo que la vela al viento.
Si sopla con suavidad lo hará llegar muy lejos.
Si sopla con brusquedad lo acabará rompiendo.

“León Bocanegra”.
Alberto Vázquez-Figueroa

UNIVERSITAT ROVIRA I VIRGILI
PREPARACION, CARACTERIZACIÓN Y APLICACIONES DE CARBONES ACTIVADOS
PREPARADOS A PARTIR DE LIGNINA KRAFT
VANESSA TORNÉ FERNÁNDEZ
ISBN: 978-84-690-7600-2
DL.T.1387-2007

UNIVERSITAT ROVIRA I VIRGILI
PREPARACION, CARACTERIZACIÓN Y APLICACIONES DE CARBONES ACTIVADOS
PREPARADOS A PARTIR DE LIGNINA KRAFT
VANESSA TORNÉ FERNÁNDEZ
ISBN: 978-84-690-7600-2
DL.T.1387-2007

UNIVERSITAT ROVIRA I VIRGILI
PREPARACION, CARACTERIZACIÓN Y APLICACIONES DE CARBONES ACTIVADOS
PREPARADOS A PARTIR DE LIGNINA KRAFT
VANESSA TORNÉ FERNÁNDEZ
ISBN: 978-84-690-7600-2
DL.T.1387-2007

PREPARACIÓN, CARACTERIZACIÓN Y APLICACIONES DE CARBONES ACTIVADOS PREPARADOS A PARTIR DE LIGNINA KRAFT

Tribunal de tesis:

Dr. Peter Carrott (Vocal)
Universidad de Evora (Portugal)

Dr. Ana Lea Cukierman (Vocal)
Universidad de Buenos Aires (Argentina)

Dr. Xavier Farriol (President)
Universitat Rovira i Virgili de Tarragona (Catalunya)

Dr. María Martín (Vocal)
Universitat de Girona (Catalunya)

Dr. Flor Siperstein (Secretaria)
Universitat Rovira i Virgili de Tarragona (Catalunya)

Dr. Sergi Díez (Suplent)
CSIC (Catalunya)

Dr. Francesc Ferrando (Suplent)
Universitat Rovira i Virgili de Tarragona (Catalunya)

Avaluadors externs:

Dr. Lourdes Ballinas Casarrubias
Universidad Autónoma de Chihuahua (México)

Dr. Guy Furdin
Université Henri Poincaré (Francia)

UNIVERSITAT ROVIRA I VIRGILI
PREPARACION, CARACTERIZACIÓN Y APLICACIONES DE CARBONES ACTIVADOS
PREPARADOS A PARTIR DE LIGNINA KRAFT
VANESSA TORNÉ FERNÁNDEZ
ISBN: 978-84-690-7600-2
DL.T.1387-2007

Els sotasignants

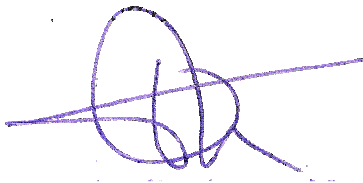
FAN CONSTAR

que el present treball, que porta per títol

**PREPARACIÓN, CARACTERIZACIÓN Y APLICACIONES DE CARBONES
ACTIVADOS PREPARADOS A PARTIR DE LIGNINA KRAFT**

i que presenta na Vanessa Torné Fernández per a optar al grau de Doctor per la Universitat Rovira i Virgili, ha estat realitzat en aquesta universitat sota les seves direccions, i que tots els resultats presentats i l'anàlisi corresponent són fruit de la investigació realitzada per l'esmentat candidat.

I per a que se'n prengui coneixement i als efectes que correspongui, signa aquest certificat,



Dr. Vanessa Fierro Pastor
Groupe Matériaux Carbonés
Université Henri Poincaré
Faculté des Sciences et Techniques
Nancy (França)



Dr. Daniel Montané i Calaf
Grupo de Biopolimeros Vegetales
Departament d'Enginyeria
Química
Universidad Rovira i Virgili
Tarragona (Catalunya)

Tarragona, 05 de juliol de 2006.

UNIVERSITAT ROVIRA I VIRGILI
PREPARACION, CARACTERIZACIÓN Y APLICACIONES DE CARBONES ACTIVADOS
PREPARADOS A PARTIR DE LIGNINA KRAFT
VANESSA TORNÉ FERNÁNDEZ
ISBN: 978-84-690-7600-2
DL.T.1387-2007

ÍNDICE GENERAL

ÍNDICE GENERAL	i
Índice de figuras y tablas	vii
<u>AGRAÏMENTS</u>	xiii
<u>1. RESUMEN GENERAL</u>	1
<u>2. INTRODUCCIÓN</u>	5
<u>2.1. El carbón activado</u>	5
<u>2.1.1. Aplicaciones del carbón activo</u>	6
<u>2.1.2. Obtención de materiales carbonosos</u>	8
<u>2.1.2.1. Activación Física</u>	11
<u>2.1.2.2. Activación Química</u>	13
<u>2.1.3. Química de la activación</u>	17
<u>2.1.3.1. Activación con ácido fosfórico</u>	17
<u>2.1.3.2. Activación con hidróxidos</u>	19
<u>2.1.4. Caracterización de carbones activados</u>	20
<u>2.2. La lignina</u>	24
<u>2.2.1. Estructura química</u>	25
<u>2.2.2. Ligninas técnicas y comerciales</u>	27
<u>2.2.3. Aplicaciones de la lignina</u>	29
<u>2.2.4. Lignina, precursor para carbones activados</u>	31
<u>3. OBJETIVOS</u>	33
<u>4. MATERIALES Y MÉTODOS</u>	35
<u>4.1. Materias primas</u>	35
<u>4.2. Preparación de carbones activados</u>	37

4.3. Caracterización de carbones activados	41
4.3.1. Composición química y caracterización estructural	41
4.3.1.1. Análisis Elemental	42
4.3.1.2. Análisis Inmediato	43
4.3.1.3. Espectroscopía de infrarrojo	44
4.3.2. Morfología y caracterización textural	46
4.3.2.1. Adsorción de nitrógeno	46
4.3.2.2. Análisis óptico: SEM	51
4.3.3. Química de superficie	52
4.3.4. Análisis de adsorción	58
4.3.4.1. Adsorción de azul de metileno	58
4.3.4.2. Adsorción de yodina	59
4.3.4.3. Determinación de metales	61
4.3.4.4. Determinación de componentes orgánicos	62
4.4. Aplicaciones de carbones activados	65
5. DISCUSIÓN DE RESULTADOS	67
5.1. Preparación y caracterización de carbones activados	72
5.1.1. Activated carbons from lignin: kinetic modeling of the pyrolysis of Kraft lignin activated with phosphoric acid	72
5.1.2. Study of the decomposition of Kraft lignin impregnated with orthophosphoric acid	85
5.1.3. Kraft lignin as a precursor for microporous activated carbons prepared by impregnation with orthophosphoric acid: synthesis and textural characterisation	93
5.1.4. Influence of the demineralisation on the chemical activation of Kraft lignin with orthophosphoric acid	102
5.1.5. Highly microporous carbons prepared by activation of Kraft lignin with KOH	130
5.1.6. Methodical study of the chemical activation of Kraft lignin with KOH and NaOH	147
	181

<u>5.2. Aplicaciones de carbones activados</u>	
<u>5.2.1. Removal of Cu (II) from aqueous solutions by adsorption on activated carbons prepared from Kraft lignin</u>	181
<u>5.2.2. Optimization of the synthesis of highly microporous carbons by chemical activation of Kraft lignin with NaOH</u>	194
<u>5.2.3. Sorption study of organic compounds on highly microporous carbons prepared from Kraft lignin</u>	236
<u>5.2.4. Polymeric composite membranes based on carbon/PSf</u>	278
<u>5.2.5. Removal of lignin and associated impurities from xylo-oligosaccharides by activated carbon adsorption</u>	288
<u>6. CONCLUSIONES GENERALES</u>	299
<u>7. BIBLIOGRAFÍA</u>	305
<u>8. NOMENCLATURA</u>	317
<u>ANEXOS</u>	327
<u>Anexo A.</u>	329
Use of Kraft lignin for Cu(II) removal in industrial water. 9th Mediterranean Congress (Póster). Barcelona - Catalunya (2002).	
<u>Anexo B.</u>	333
Activated carbons prepared from Kraft lignin by phosphoric acid impregnation. Carbon (Póster). Oviedo – España (2003).	
<u>Anexo C.</u>	337
Removal of Cu (II) from aqueous solutions by adsorption on activated carbons prepared from Kraft lignin. Carbon (Póster). Oviedo - España (2003).	

<u>Anexo D.</u>	341
Uptake of Cu(II) and Zn from aqueous solution by Kraft lignin. 4th European Congress in Chemical Engineering (Póster). Granada - España (2003).	
<u>Anexo E.</u>	345
Highly microporous carbons prepared by activation of Kraft lignin with KOH. 7th International Symposium on the characterization of porous Solids (Póster). Aix-en-Provence - Francia (2005).	
<u>Anexo F.</u>	349
Enzymatic composite membranes based on carbon/polysulfone. Engineering with membranes: medical and biological applications (Póster). Camogli - Italia (2005).	
<u>Anexo G.</u>	353
Influence of the ash content on the microporosity of activated carbons derived from Kraft lignin. Carbon (Póster). Corea (2005).	
<u>NOTAS PARTICULARES</u>	357

ÍNDICE DE FIGURAS Y TABLAS

<u>Figura 1.1.</u>	Ejemplos de estructuras de: zeolitas (derecha) y materiales carbonosos (derecha) con estructura porosa desarrollada.	2
<u>Figura 2.1.</u>	Distribución de la capacidad de producción mundial de carbón activado.	6
<u>Figura 2.2.</u>	Estructuras tridimensionales para (a) el ordenamiento cristalográfico del carbón negro con capas hexagonales paralelas pero desordenadas, (b) cristal hexagonal de grafito y (c) estructura microcristalina del carbón activado.	9
<u>Figura 2.3.</u>	Representación esquemática típica de la microestructura del AC.	10
<u>Figura 2.4.</u>	Monómeros propios de la lignina con sus posibles puntos de enlace entre unidades (\rightarrow). Unidad guayacilo abundante en coníferas (izquierda) y unidad siringilo típica en frondosas (derecha).	26
<u>Figura 2.5.</u>	Estructura aleatoria de la lignina procedente de madera blanda (“hardwood lignin”) propuesta por W. G. Glasser en 1981.	27
<u>Figura 4.1.</u>	Esquema de la etapa de preparación de CA (etapa 1).	36
<u>Figura 4.2.</u>	Materias primas utilizadas en la preparación de CA: a) NaOH, b) KOH, c) ácido fosfórico y d) LK, e) LK _d y f) CA obtenido.	36
<u>Figura 4.3.</u>	Detalle del horno empleado en la activación con ácido fosfórico.	37
<u>Figura 4.4.</u>	Detalle del reactor horizontal empleado, horno eléctrico y panel de control de las condiciones de operación.	38
<u>Figura 4.5.</u>	Tratamiento realizado al CA obtenido: oxidación, lavado y secado.	39
<u>Figura 4.6.</u>	Resumen de las condiciones de operación para la producción de CA.	40
<u>Figura 4.7.</u>	Esquema de la etapa de caracterización de CA (etapa 2).	41
<u>Figura 4.8.</u>	Analizador elemental Carlo Erba modelo CHNS-O EA1108, provisto de automuestreador.	42
<u>Figura 4.9.</u>	Proceso térmico para el análisis inmediato (\diamond) y termograma ejemplo (Δ).	43
<u>Figura 4.10.</u>	Termobalanza Perkin Elmer TGA-7.	44

<u>Figura 4.11.</u>	Equipo de infrarrojo Jasco FT/IR-680 Plus y detalle del accesorio ATR.	45
<u>Figura 4.12.</u>	Ejemplo de espectro obtenido por IR para CA-Na preparados a temperaturas entre 400°C y 800°C.	46
<u>Figura 4.13.</u>	Diferentes tipos de porosidad presente en el carbón activado.	47
<u>Figura 4.14.</u>	Isotermas de adsorción de nitrógeno a 77 K según la clasificación BDDT.	48
<u>Figura 4.15.</u>	Llenado de poros de moléculas de adsorbato en función de la presión parcial.	49
<u>Figura 4.16.</u>	Ejemplo de isoterma experimental de adsorción (●) y desorción (○) para muestras microporosas obtenidas a partir de un carbón activado con hidróxido de sodio a 750°C.	50
<u>Figura 4.17.</u>	Equipo de medida de superficie ASAP 2020.	51
<u>Figura 4.18.</u>	Equipo de microscopía electrónica de barrido.	52
<u>Figura 4.19.</u>	Curva obtenida en la valoración de: a) carbonatos, b) bicarbonatos, c) hidróxido de sodio y d) etóxido sódico.	54
<u>Figura 4.20.</u>	Estructuras propuestas para los grupos oxigenados ácidos más representativas de la superficie del CA.	55
<u>Figura 4.21.</u>	Posibles estructuras de los grupos oxigenados básicos más representativas de la superficie del CA.	56
<u>Figura 4.22.</u>	Valorador automático CRISON Compact Titrator Versión D.	57
<u>Figura 4.23.</u>	Equipo para análisis de TPD Termo Finnigan modelo TPDR 1100 (izquierda) conectado a un analizador de masas Pfeiffer Vacuum Omnistar GSD 301 O (derecha).	57
<u>Figura 4.24.</u>	Espectrofotómetro Dinko Instruments UV-VIS 8500 y detalle de su interior.	59
<u>Figura 4.25.</u>	Ejemplo de isoterma de adsorción de yodo en CA.	60
<u>Figura 4.26.</u>	Equipo de Absorción Atómica para la determinación de cobre (II) y lámpara específica.	61
<u>Figura 4.27.</u>	Sistema de análisis empleado para la adsorción de metales.	62
<u>Figura 4.28.</u>	HPLC: Cromatógrafo de líquidos Agilent 1100 Series.	63
<u>Figura 5.1.</u>	Resumen de los reports realizados a partir de la obtención de datos en las etapas 1, 2 y 3.	68

<u>Tabla 2.1.</u>	Condiciones de operación del proceso de activación química para la obtención de AC.	15
<u>Tabla 2.2.</u>	Condiciones de operación del proceso de activación física para la obtención de AC.	16
<u>Tabla 2.3.</u>	Relación de técnicas empleadas en la caracterización estructural.	21
<u>Tabla 2.4.</u>	Relación de técnicas empleadas en la caracterización textural.	22
<u>Tabla 2.5.</u>	Relación de técnicas empleadas en el estudio de la química de superficie.	22
<u>Tabla 2.6.</u>	Contenido de la pared celular de diversas materias vegetales (expresado como materia seca).	24
<u>Tabla 4.1.</u>	Condiciones de operación para el AC-K, AC-Na y AC-P base.	39

AGRAÏMENTS

Els agraïments són una de les parts més complicades d'escriure però, sense cap dubte, també és una de les parts més boniques.

En primer lloc vull donar les gràcies als meus dos tutors de tesi. A la Dr. Fierro, pel temps dedicat en aquesta tesi. Al Dr. Montané, per fer l'esforç en pujar-se a un tren que ja estava en marxa i quasi arribant a la fi del trajecte. Això sí, segurament, l'estació d'arribada hagués estat una altra de no ser per vostè. Gràcies per animar-me quan em van entrar els nervis finals.

També vull donar les gràcies a la Universitat Rovira i Virgili per la beca concedida per a la realització d'aquesta tesis i gràcies a tots els projectes involucrats d'on han sortit equips vitals per finalitzar-la.

Als membres del grup de Biopolímers Vegetals, que tots han col·laborat, directa o indirectament, en acabar aquests quatre anys, en especial al Dr. García. Ricard, tu vas ser el que em vas convèncer a començar aquest període

de la meua vida i tot i que han hagut moments per a tot, mai m'he penedit d'haver començat. He après a saber com és la gent i a estar al meu lloc, tenint en compte les circumstàncies, i segurament mai ho hagués après d'una altra manera.

També vull fer menció al Dr. Bonet, al Dr. Medina i a la Dr. Vega amb els qui he pogut parlar sempre que ho he necessitat des d'un punt de vista forà. Gràcies per preguntar sense que ho hagués demanat. Gràcies Dr. Castells i Dr. Mateo per sempre anar amb un somriure a la cara i fer el dia a dia més feliç.

No pot faltar la gent amb qui he investigat. Des del començament fins ara, ha passat molta gent per la meua vida. La Cati Casals, el Guillermo, la Lulu amb qui vaig mantenir llargues converses sense que perdés el somriure, la Xiao, el Dayong amb qui encara no estic gaire segura de que entengués bé de què parlàvem, el Carles que sempre ha estat amb la mà estesa i desinteressada quan ho he necessitat, a tots els que han aguantat els meus maldecaps en els pitjors moments, el meu gran amic i conversador İu..., la Jorgelina, el Luizildo, Camilo, la Debora, la Pepa, el Jose Antonio i el Nour-Eddine. I als grans profes que tenim: Ricard, Joan, Farriol, Dani, Francesc, i Marta, que primer de tot són persones.

Però també a altra gent del programa de doctorat que m'ha ajudat tant als moments menys fàcils: la Maria Eugenia, la Alicia, la Maretva i l'Esther que han estat sempre per recolzar-me i preguntar-me com anaven les coses. I al Xavi per les estones de riure per la ramoni.

La Clara, la Sònia i la Ilham de qui he après moltes coses, de les que s'ensenyen als llibres i de les que no. I com no, a tots els estudiants que han passat durant aquest temps pel laboratori fent-me preguntes de tot tipus i descobrint-me nous perquè del que feiem: el Jordi (de las Heras), l'Eva (Baba), la Gemma i la Mireia, el Rubén, la Juvanteny, el JoanJo, la Montse i l'Ana i per una altra banda, el Sergi B., l'altre Sergi Q., la Ivanka, la Gemma i la Maite. I les meves darreres companyes d'experiments: la Vero i la Pili.

I també companys i excompanys de despatx i de docència: Isabela, Haydée, Paula, Gaval, Teresa, Restrepo, Ricardo Chimentao, Roni, Noe, Eva, Isabel, Iouliana, Henry, Antonio... i segur que em deixo a més d'un... gràcies pel dia a dia.

Gràcies també al Servei de Recursos Científics i Tecnològics per ensenyar-me els "intrínquils" de les màquines que he pogut utilitzar. Especialment a Francesc Guirado que m'ha ajudat durant tant de temps.

Fora d'aquest ambient, també voldria agrair els constants intents d'entendre el que feia per part de la gent que m'envolta.

Als de la penya: la Horten i el Raul, el Dani, Sue i Ivan, Susi, Fernando i companyia, la Viki i Roberto, la Mari i l'Esteban, l'Esther i Ana.

A la meva "família postissa", els meus sogres, Josefa i Julian, i cunyants (la Rosi i el Joan, l'Olga i Delfín, Belinda i Diego, Alberto i Rosa, Yuli, Armando i Eva) i nebots (Aleix i Laia, Arnau i Sara, Martina i el nou vingut Albert) que encara ara em pregunteu com van els polímers...

I també a la gent del basquet: els del C.B. Valls i els del C.B.T. Al Manolo, al Lluís, a la Isa, la Nuria, les meves Moni i Miriam, la Devi, la Lu, a l'Aleix i l'Esther, a Claudia, a Rosalia, a la Borrell, a Vicky i a Eva. Aquests anys hi han hagut ascensos a lliga femenina 2 i un manteniment in extremis. Emocions que ensenyen i motiven i que sobretot, et formen com a persona i aprens qui realment mereix la pena en aquesta vida. Us estimo a tots i a totes.

Finalment, i com a part molt important, a la meva família. Als meus pares, el Josep i la Nandi, als meus germans, Yoli i Txema, als meus abuelos, Manolo (†) i Fina (†), i avis, el Sr. Joan i la Sra. Antònia i als oncles i cosins. Al Rintin (†)... Aquests darrers anys han estat molt difícils per a tots. Hi han hagut moltes pujades i baixades i sembla que no hi ha una bona sense una dolenta... M'agradaria dedicar especialment aquesta tesi a tots vosaltres que sempre heu estat al meu costat i als que ja no estan físicament però que sempre estaran als nostres cors. Tots heu marcat la meva vida. Sóc com sóc gracies a vosaltres i a algunes petites aportacions personals i en cada bateg del meu cor us sento dins meu i us estimo com si fos el darrer dia tot i que no us ho sàpiga demostrar.

Per acabar, aquesta tesi també està dedicada a en Jesús. El meu dia a dia. No és fàcil ser-hi en els mals moments i tu has aguantat estoïcament. Espero saber fer el mateix per tú si cap dia ho necessites. TQM. Sempre busco les millors paraules per dedicar-te i potser mai se trobar la més adient per a tu. Potser no et puc donar cap que estigu a l'alçada del que et mereixes però crec que són millor els fets. Fets que espero i desitjo poder-te donar tota la vida. Ets el meu company, el meu amic i el meu somni.

Segurament, estic oblidant a molta gent. Gent que ha esta al meu costat no només aquests darrers quatre anys, sino mes temps inclús o potser menys. Ja saveu com sóc d'oblidadissa i tot i que no m'en recordi de les dades senyalades o de les petites coses, sempre us porto al pensament. Gràcies per fer-me viure la vida que tinc...

UNIVERSITAT ROVIRA I VIRGILI
PREPARACION, CARACTERIZACIÓN Y APLICACIONES DE CARBONES ACTIVADOS
PREPARADOS A PARTIR DE LIGNINA KRAFT
VANESSA TORNÉ FERNÁNDEZ
ISBN: 978-84-690-7600-2
DL.T.1387-2007

1. RESUMEN GENERAL

La creciente demanda de productos altamente purificados requiere el desarrollo tecnológico de métodos de separación cada vez más selectivos y el entendimiento de los procesos físicos y químicos que tienen lugar. Actualmente, los materiales que se usan principalmente en los métodos de separación y purificación son los adsorbentes porosos basados en zeolitas y los de naturaleza carbonosa.

En ambos casos, su estructura microporosa permite la separación basada en el tamaño y/o forma de las moléculas de los componentes que se pretenden separar. A pesar de ello, los materiales carbonosos tienen algunas ventajas respecto a los tamices moleculares desarrollados a partir de zeolitas: selectividad por la forma (moléculas planas), alta hidrofobicidad, alta resistencia en medios alcalinos y ácidos y estabilidad térmica a temperaturas más altas en atmósferas inertes.



Figura 1.1. Ejemplos de estructuras de zeolitas (derecha) y materiales carbonosos (derecha) con estructura porosa desarrollada.

Los materiales carbonosos se pueden obtener a partir de carbones minerales, materiales biomásicos y sintéticos. El uso de productos secundarios en diferentes procesos industriales es una opción recomendada, no únicamente desde el punto de vista medioambiental, sino también en el económico. La lignina Kraft es un subproducto muy abundante en la industria de fabricación de papel que puede ser utilizado como precursor en la producción de carbones activos.

De esta manera, el uso de lignina Kraft como precursor de carbón activado preparado por activación física con dióxido de carbono (CO_2) y por activación química con cloruro de zinc (ZnCl_2) y ácido fosfórico (H_3PO_4), ha sido objeto de estudio en diversos trabajos anteriores^[1-7]. Estos carbones aunque tienen una alta microporosidad pueden presentar también una mesoporosidad muy desarrollada a condiciones de operación determinadas.

El objetivo de este estudio es la obtención de carbones esencialmente microporosos por activación química con H_3PO_4 e hidróxidos (NaOH y KOH). Las variables de operación que se han estudiado son la relación agente activante / lignina Kraft, la temperatura de carbonización, el tiempo de activación, el caudal de la atmósfera durante el proceso de pirólisis y la velocidad de calentamiento. Estas condiciones de trabajo afectan a las propiedades físicas y químicas del carbón obtenido. Los parámetros que se han tenido en cuenta en este estudio para caracterizar los carbones activados preparados han sido diversos. Entre ellos están el rendimiento a carbón, análisis de superficie (área superficial y tamaño y distribución de poros), los grupos funcionales de superficie, análisis ópticos (microscopía electrónica de barrido (SEM)), análisis termogravimétricos, el análisis elemental e inmediato y adsorción de azul de metileno. Estos análisis se han realizado mediante

diferentes técnicas como valoración modificada de Boehm, análisis de área superficial por adsorción de gas, espectroscopía por infrarrojo, etc.

Como consecuencia de este estudio, se han elaborado conclusiones relacionadas con las reacciones que tienen lugar debido a la presencia de diferentes tipos de agentes activantes, los productos de las reacciones producidas y las condiciones de operación del proceso. Esto ha permitido entender la razón por la cual algunas variables tienen un efecto más importante en las características finales del carbón, con el fin de poder controlar el desarrollo de estas propiedades y, por tanto, la aplicación final del producto.

Los resultados obtenidos muestran la complementación de los métodos de análisis en la explicación de las hipótesis que se presentan, que han permitido explicar la relación entre las condiciones de operación y el desarrollo de las propiedades físico-químicas del carbón activo.

En el caso de la activación con ácido fosfórico, el aumento de la relación entre la cantidad de ácido añadido y la de lignina Kraft favorece el desarrollo de la estructura interna del CA hasta valores de relación másica de 1.0, a partir del cual no se producen cambios en el proceso de pirólisis que afecten a sus propiedades más importantes. A relaciones mayores de 1.4 comienza a disminuir el área superficial BET y el volumen total de poros promovido por el agresivo ataque del ácido fosfórico. El uso de ácido fosfórico en exceso produce óxidos de fósforo que protegen la estructura del carbón de la oxidación externa y cuando esta especie se evapora a temperaturas mayores de 580°C, el carbón se oxida totalmente en aire mientras que en presencia de nitrógeno, la producción de carbón se mantiene constante. Por otro lado, el aumento de la temperatura de activación produce un decremento en el volumen de ultramicroporos pero un aumento en la microporosidad total. Sin embargo, a partir de 600°C, seguir aumentando la temperatura conlleva la reducción del volumen total de poros y de área superficial BET debido al colapso y al exceso de oxidación del material.

En el caso de la activación con hidróxidos, tanto la relación agente activante – lignina Kraft como la temperatura de carbonización producen un descenso en el rendimiento a carbón, debido principalmente a que se favorece la reacción de activación, obteniendo productos de reacción volátiles. El incremento de caudal de nitrógeno produce un aumento del rendimiento debido a la eliminación de reactivo mientras que el tiempo de activación y la velocidad de calentamiento no afectan de forma significativa a este parámetro. La mayor influencia sobre el rendimiento se encuentra cuando el carbón se activa con

grandes proporciones de agente activante, propiciando el colapso de la estructura y con variaciones en el caudal de nitrógeno, que afectan de manera diferente a las muestras activadas con diferentes hidróxidos. Los grupos ácidos y básicos de superficie experimentan un mayor desarrollo al aumentar la relación agente activante / lignina y temperatura de carbonización. Los análisis de adsorción de nitrógeno (N_2) han confirmado la obtención de carbones esencialmente microporosos con superficies específicas de hasta $3000 \text{ m}^2/\text{g}$ que unidos a la fuerte acidez de la superficie los convierten en materiales adsorbentes muy atractivos.

2. INTRODUCCIÓN

2.1. El carbón activado

Los materiales de origen vegetal forman carbones al ser calentados en una atmósfera inerte. Éstos pueden activarse para producir carbón activo (CA). Las materias primas que se utilizan principalmente para producir CA son carbones naturales, materiales sintéticos y diferentes tipos de biomasa como turba, y cáscaras de diferentes tipos de materiales biomásicos (coco, maíz, arroz, corcho y huesos de fruta).

En la actualidad, se preparan de manera global cada año, alrededor de 40000 toneladas de carbón activo que se producen principalmente en E.E.U.U. (ver *Figura 2.1*), los cuales requieren aproximadamente un millón de toneladas de materia prima^[8].

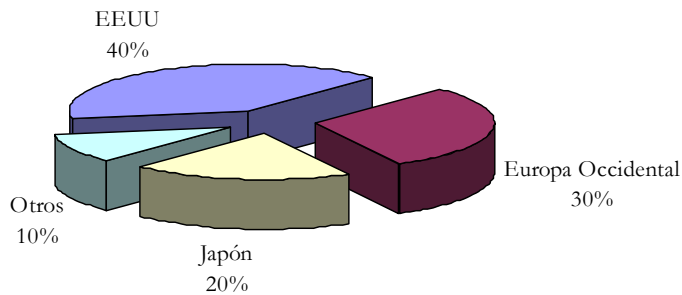


Figura 2.1. Distribución de la capacidad de producción mundial de carbón activado^[9].

En el mundo, existen unas 150 compañías que fabrican carbones activos y entre las que producen mayor cantidad están Calgon Carbon Corporation (19%), American Noria (12%), MeadWestvaco (7%), Pica S.A. (7%) y Ceca S.A. (6%).

2.1.1. Aplicaciones del carbón activado

La importancia del CA estriba en sus numerosas aplicaciones^[8, 10, 11] en campos tan diversos como en la industria alimenticia, farmacéutica, química, nuclear, petrolífera, tratamiento de aguas de consumo y depuración de efluentes industriales tanto líquidos como gaseosos, tratamiento de aire y otros gases, entre otros.

El carbón activo tiene una gran capacidad de adsorción y se utilizan en la purificación y separación de líquidos y gases. Existe una flexibilidad considerable en el proceso de preparación de carbones activos, favoreciendo la variación de sus propiedades y su capacidad de adsorción, utilizándose generalmente en forma granular o en polvo, aunque también se puede preparar en forma de fibras de carbón activo (ACF).

Los casos más generales de aplicación de CA se encuentran en sistemas de fluidos, por ejemplo, el tratamiento de aguas potables y de uso doméstico, la purificación de antibióticos, vitaminas y otros productos farmacéuticos, en la industria alimenticia en la decoloración de azúcares y la mejora de las propiedades de color, olor y sabor de bebidas y aceites comestibles. También en la purificación del aire en museos para evitar el dióxido sulfúrico perjudicial para las pinturas, en la recirculación de aire desde el exterior en aeropuertos y en hospitales y en diversos filtros que se utilizan para los

vapores de fundición, en campanas extractoras, respiradores industriales y militares, etc. Comúnmente, también se puede encontrar CA para desodorizar neveras, paquetes que contengan productos farmacéuticos con fuerte olor, en áreas relacionadas con la higiene en artículos deportivos y en los filtros de los cigarrillos de tabaco y pipas de fumar con el objetivo de reducir el contenido de alquitrán y nicotina en el humo.

A nivel industrial, el CA puede ser utilizado de manera muy eficiente para la eliminación de vapores orgánicos de gases incluso a presiones relativas bajas, siendo muy útil para la producción de gases muy puros y en la protección del medio ambiente. Por ejemplo, pequeñas cantidades de sulfuro de hidrógeno se pueden convertir en sulfuro elemental en presencia de oxígeno mediante un CA activado químicamente con yoduro de potasio en un proceso conocido como proceso Sulfosorbon^[11]. Al igual que éste, hay diferentes procesos comerciales que se utilizan a nivel industrial con el propósito expuesto, como es el caso del proceso Sulfren o el proceso Desorex^[11].

Otra aplicación industrial muy extendida es el uso de CA como catalizador, por ejemplo, en la síntesis de fosgeno a partir de monóxido de carbono y clorina y en la producción de cloruro de surfurilo a partir de dióxido de sulfuro y clorina, entre muchos procesos conocidos.

Además el CA también se utiliza en plantas nucleares en la separación de xenón y criptón, en la producción de baterías de mercurio e incluso en la protección de componentes electrónicos.

Particularmente, el CA se utiliza en algunos países para evitar la contaminación atmosférica de vapores de gasolina en los vehículos a motor, donde se utilizan filtros de CA que adsorbe este vapor en el puerto de ventilación de los tanques de gasolina cuando el automóvil se deja al sol y provoca la evaporación del combustible.

Son varias las tecnologías^[12] que se están desarrollando para sustituir la gasolina en motores de combustión interna debido a la disminución de las reservas de combustibles fósiles y la tendencia a utilizar combustibles cada vez más limpios y menos costosos.

En este campo, una aplicación interesante de los CA es el desarrollo de una tecnología y un proceso para almacenar metano en carbón activado con gran capacidad de adsorción. El metano es un combustible mucho más limpio que el carbón o los derivados del petróleo, sin embargo, su transporte es problemático ya que es muy difícil de licuar. El gas natural adsorbido en los carbones microporosos a 4 MPa y 298 K es una alternativa prometedora al gas natural comprimido (20 MPa y 298 K) como combustible limpio para

vehículos para transporte de mercancías a granel. Entre los adsorbentes disponibles, los carbones activados tienen la mayor capacidad adsorptiva.

Además del almacenamiento de metano, el CA puede ser utilizado para almacenar hidrógeno. La problemática es fruto de la dificultad de almacenarlo en el menor volumen posible: en estado líquido a bajas temperaturas (21 K)^[13], como gas comprimido, como hidruros metálicos^[13-16] o como gas adsorbido en sólidos porosos en sistemas criogénicos^[17] o adecuando las propiedades del adsorbente^[12, 18-20]. Este último caso es factible a temperatura ambiente y permite almacenar cantidades de hidrógeno mayores que como gas comprimido.

En la industria alimentaria, química y farmacéutica se consume aproximadamente el 40%^[21] de la producción mundial de carbono activo en forma granular, de regeneración fácil, y en polvo, generalmente desechable, ya que la adsorción/desorción principalmente suele ser en fase líquida. En las aplicaciones en fase gas se emplea principalmente carbón granular aunque su uso en polvo está aumentando debido al mejor contacto gas/sólido que se produce. En la catálisis se produce un consumo inferior al 5%^[21] en procesos muy específicos, como soporte para catalizadores. Otro 40%^[21] de la producción de carbón activo, se consume en el tratamiento de aguas, tanto en su potabilización como en el tratamiento de aguas residuales, en combinación con otros procesos físico-químicos o biológicos, en polvo o granular dependiendo de la reactivación, el tipo de compuesto a adsorber, el estado de la tecnología disponible o la necesidad de mayor o menor área de contacto.

2.1.2. Obtención de materiales carbonosos

Los carbones activos se obtienen después de extraer los componentes volátiles de los materiales carbonosos, mediante un calentamiento en atmósfera inerte. Posteriormente se puede activar con diferentes gases (dióxido de carbono o vapor) y a veces por la adición de agentes químicos (cloruro de zinc, ácido fosfórico, hidróxidos, etc.) antes, durante o después del proceso de carbonización con el fin de incrementar sus propiedades adsorbentes. Los CA se pueden preparar a partir de cualquier precursor orgánico de origen natural o sintético. El parámetro que rige de manera más severa la elección de la materia prima es el económico que se basa tanto en la disposición del material como en el bajo coste de suministro. Ejemplos de suministros de estas materias primas son los materiales de origen botánico (madera, cáscara de coco y huesos de frutas) y material biomásico degradado o carbonizado (turba, lignitos y todo tipo de carbones). En porcentajes, la

distribución de precursores^[18] se estima en el 35% para madera, 28% de carbón, 14% de lignitos, 10% de cáscara de coco, 10% de turba y 3% de otros. Los precursores obtenidos a partir de biomasa no degradada son la fuente más económica ya que son fuentes renovables, abundantes y de bajo coste donde los residuos obtenidos de la agricultura se utilizan extensamente. Cabe reseñar que el uso de cáscara de coco está retomando importancia, por delante de las cáscaras de almendra y los huesos de melocotón, albaricoque, ciruela, cereza y nuez^[22].

En la carbonización de cualquier precursor orgánico se genera una determinada distribución de tamaño de poro (PSD) debido principalmente a que gran parte de los elementos unidos al carbono se gasifican por la descomposición pirolítica. Simultáneamente, el carbón se agrupa en formaciones microcristalinas que se organizan entre sí de manera irregular creando huecos intersticiales libres que se bloquean como consecuencia de la descomposición y deposición de alquitranes^[23], tal y como se puede observar en la *Figura 2.1-c*.

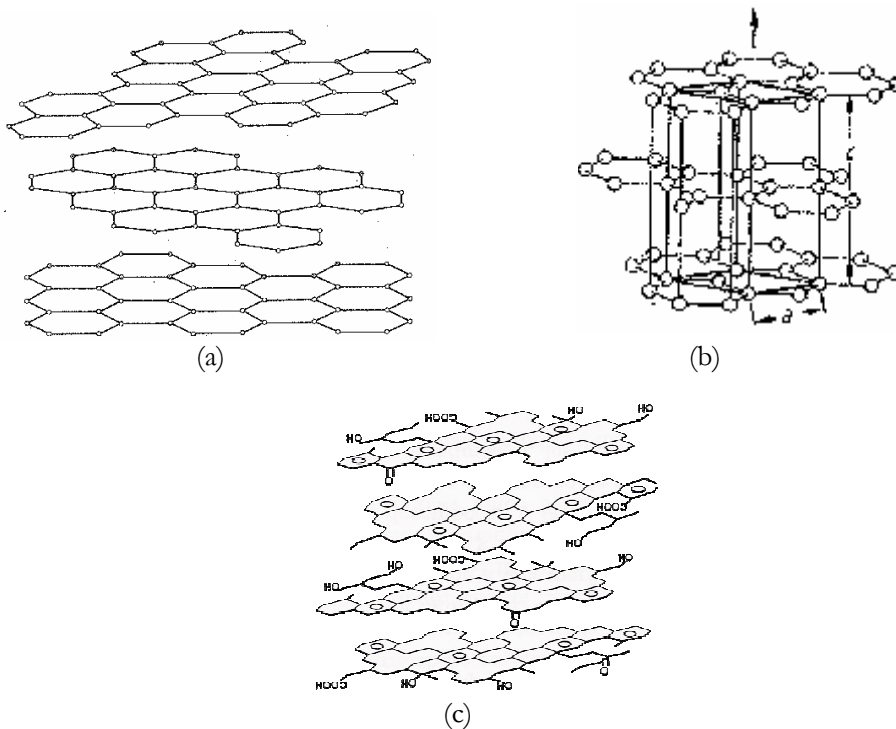


Figura 2.2. Estructuras tridimensionales para (a) el ordenamiento cristalográfico del carbón negro con capas hexagonales paralelas pero desordenadas^[10], (b) cristal hexagonal de grafito^[11] y (c) estructura microcristalina del carbón activado.

La estructura química del carbón activado suele ser estudiada por comparación de la estructura microcristalina del grafito (ver *Figura 2.2-b*) que es una forma alotrópica del carbono que presenta un apilamiento de láminas planas de átomos de carbono en sistemas de anillos hexagonales condensados. Los enlaces químicos que existen entre los átomos de cada lámina son covalentes, mientras que los enlaces entre láminas son por fuerzas débiles de van der Waals. Ello determina que la distancia entre átomos contiguos de una misma lámina (0.14 nm) sea menor que la correspondiente entre los átomos más próximos de las láminas adyacentes (0.34 nm). En realidad existen dos modificaciones del grafito que difieren en la ordenación de las capas: en la forma hexagonal la secuencia de apilamiento es del tipo ABAB (*Figura 2.1-a*) mientras que en la forma rombohédrica el orden de apilado es ABCABC.

El carbón activado también presenta una estructura tridimensional de átomos de carbonos en láminas planas de anillos hexagonales pero, a diferencia del grafito, no existe ningún orden cristalográfico en la tercera dimensión, pudiendo darse el entrecruzamiento de las láminas. Por otro lado, las imperfecciones estructurales en las capas bidimensionales son mucho más frecuentes en los carbones activados que en el grafito, existiendo incluso ciclos de cinco y siete átomos de carbono, así como numerosos anillos aromáticos (ver *Figura 2.1-c*). Ésto da lugar a una estructura microcristalina muy desordenada denominada estructura turboestática que es la que confiere a los carbones activados una mayor superficie accesible a las fases gaseosa y líquida que el propio grafito. Además, las imperfecciones del carbón activado favorecen la reactividad de los átomos de carbono situados en las partes periféricas de los cristales.

También es usual encontrar el modelo de estructura presentado para carbones activados típicos en la *Figura 2.3* desarrollada de acuerdo con las observaciones realizadas mediante microscopía electrónica de transmisión (TEM) [18].



Figura 2.3. Representación esquemática típica de la microestructura del AC.

Aunque este carbón puede utilizarse en determinadas aplicaciones, sus propiedades físicas pueden ser mejoradas mediante el uso de un agente activante. El uso de determinados agentes químicos sobre el precursor utilizado en el proceso de carbonización, actúa como agente deshidratante y restringe la formación de alquitranes modificando la química de pirólisis en una sola etapa. Como resultado, se pierde menos carbón con los volátiles y se obtiene una PSD diferente dependiendo del activador utilizado.

Otras modificaciones de la PSD se pueden producir por la gasificación del material con vapor o dióxido de carbono eliminando selectivamente átomos de carbono de las paredes de los poros originales. El oxígeno no es un agente físico activante adecuado ya que es una molécula muy reactiva que actúa principalmente en la superficie del carbón sin incrementar por tanto su PSD y únicamente se utiliza en casos particulares. Por otro lado, se pueden utilizar otras especies químicas fuertemente oxidantes para variar la PSD, que se depositan en la entrada de los poros y, al ser grupos de gran tamaño, reducen las dimensiones de éstos.

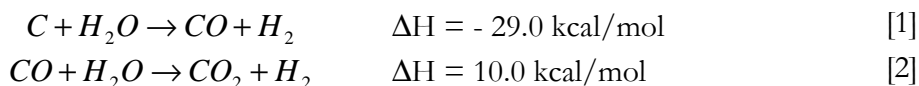
En resumen, el carbón natural, la biomasa o los materiales sintéticos proveen la materia prima para la preparación de carbón activo el cual se trata para desarrollar la estructura porosa interna, tanto para aumentar su volumen como para incrementar el diámetro de los poros creados, durante el proceso de carbonización y crear nuevos^[18] mediante procesos de activación tales como los presentados a continuación.

2.1.2.1. Activación Física

La activación física tiene lugar en dos etapas. En primer lugar el material se carboniza en un producto intermedio, cuyos poros son demasiado pequeños como para que sea un absorbente útil. El desarrollo de la estructura porosa para producir un área de superficie interna accesible, se logra favoreciendo la reacción del producto carbonizado con una atmósfera de vapor, CO₂, aire o una mezcla de estos gases (gasificación parcial) a temperaturas entre los 800°C y los 1100°C. Dicha temperatura se consiguen mediante la combustión de gas natural, cuando es posible, ya que es el más económico pues el calor requerido y el agente de la activación se proveen simultáneamente. La reacción ocurre en toda la estructura del carbón aumentando el tamaño del poro. El control de la temperatura es crítico ya que si está fuera del rango mencionado, la velocidad de la reacción es demasiado lenta, produciendo la reducción del tamaño de partícula y dejando el interior inactivo. Lo que se consigue en este tipo de activación es que se desprendan las partes más reactivas de la matriz del carbón como óxido y

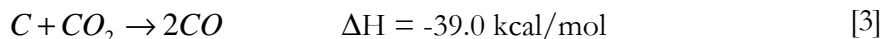
dióxido de carbono dependiendo de la naturaleza del gas empleado y de la temperatura de activación (reacción [1] para la activación con vapor de agua y reacción [3] en la activación por CO₂) mientras que paralelamente pueden tener lugar reacciones de formación de dióxido de carbono e hidrógeno (reacción [4]).

La activación con vapor^[18] se lleva a cabo a temperaturas entre 850-950°C en ausencia de oxígeno ya que su presencia provoca una disminución en el rendimiento a carbón y en la porosidad. La reacción de vapor con el carbón es catalizada por óxidos y carbonatos de metales alcalinos, hierro, cobre y otros metales. La gasificación del material carbonizado con vapor tiene lugar mediante la reacción endotérmica [1] y paralelamente, el vapor se cataliza exotérmicamente por la superficie del carbón mediante la reacción [2].



El hidrógeno formado se adsorbe en los centros activos de la superficie del carbón reduciendo la activación del material producida, a la vez que disminuye la velocidad de reacción

La activación con CO₂^[18] (reacción [3]) implica una reacción menos energética en comparación con la del vapor (reacción [1]) y requiere temperaturas mayores (850-1100°C). Al ser el CO₂ una molécula de mayor tamaño que la del agua, se produce una difusión más lenta a través de la estructura porosa del carbón, disminuyendo así la cantidad de microporos. En este caso, la reacción de activación es:

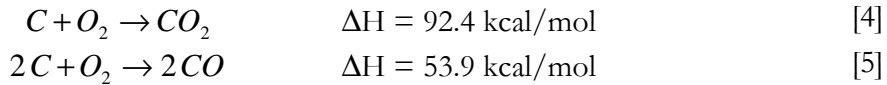


La formación de CO puede aumentar la velocidad de su quimisorción en los centros activos, tal y como sucede con el hidrógeno en la activación física por vapor, aunque está documentado que la presencia de CO favorece una activación más uniforme^[24] proporcionando más homogeneidad al CA final.

Debido a que las reacciones entre el carbón y el vapor o el dióxido de carbono son endotérmicas, el proceso de activación necesita un control adecuado de la temperatura, donde un aporte externo es necesario en el horno en el que se lleva a cabo la activación. En los procesos industriales utilizados en la actualidad, el agente activante usado es generalmente un gas al

que se le añade una cierta cantidad de vapor obteniendo una activación combinada entre vapor y CO₂.

El uso de oxígeno^[18] como agente de activación es menor que en los casos anteriores debido a la dificultad de mantener unas condiciones de operación estacionarias en el horno ya que la reacción es extremadamente exotérmica (reacción [4]) y produce sobrecalentamientos locales que disminuyen la homogeneidad del carbón activo final.



Por otro lado, la acción del oxígeno no se limita a la oxidación de los poros sino que también produce una gran cantidad de óxidos sobre la superficie y una disminución en el rendimiento a carbón. Por estas razones, este tipo de activación raramente es utilizada.

2.1.2.2. Activación Química

La activación química se realiza normalmente con precursores de base orgánica, aunque tal y como se ha visto anteriormente, también se utiliza carbón, coque, y derivados del petróleo, de los que se produce CA con altas áreas superficiales. El material precursor se somete a una impregnación con un agente químico activante que degrada el material orgánico. En la impregnación, generalmente se utiliza una solución concentrada que se mezcla con el material inicial y se deja actuar durante un tiempo determinado a una temperatura inferior a 100°C. En algunos casos, la mezcla se realiza cuando el agente activante está en estado sólido, y por tanto, no es necesaria la impregnación. Transcurrido este período, se aplica un proceso pirolítico donde la carbonización y la activación se dan a la vez en ausencia de aire en un rango de temperaturas entre 400°C y 900°C. En esta etapa, la impregnación química deshidrata la materia prima y aromatiza el carbón creando una estructura porosa tridimensional rígida favorecida por el entrecruzamiento de la matriz del AC. Posteriormente, el producto pirolizado se enfría y se lava para eliminar el exceso de agente activante.

Los agentes químicos activantes más utilizados son el hidróxido de sodio y potasio, ácido fosfórico, cloruro de zinc y ácido sulfúrico, aunque también se utiliza el sulfuro de potasio, hidróxido de tiocianato de potasio, carbonatos metálicos y cloruros de calcio, magnesio y hierro. Estos activantes tienen en

común que son agentes deshidratantes que influyen en la descomposición que tiene lugar durante el proceso de pirólisis a la vez que inhiben la formación de alquitranes, ácido acético y metanol, entre otras especies, y aumentan la producción de carbón.

De esta manera, se ha observado que la forma de los poros de los carbones activados químicamente es diferente a los obtenidos mediante activación física. En el primer caso, los poros tienen forma de cuello de botella mientras que con la activación física, los poros son cónicos^[18]. Los poros de cuello de botella se forman durante la activación química a temperaturas alrededor de 500°C y se asocia a que el material carbonoso pirolizado está en un estado plástico. Así pues, cuando los gases que se forman durante la descomposición térmica escapan de la estructura crean unos agujeros en el material plástico por donde escapan a través de pequeños pasillos.

Por otro lado, durante la activación física con vapor de agua a temperaturas entre 850-950°C, se produce un gradiente de concentración entre la entrada y el centro de los poros. Por tanto, el proceso de oxidación que tiene lugar, que es la causa de la activación, ocurre de manera más importante alrededor de la entrada del poro, donde se concentra la mayor cantidad de agente activante, en comparación con el centro de éste y por tanto, es más usual obtener poros cónicos con amplias entradas.

En la activación química llevada a cabo con cloruro de zinc ($ZnCl_2$)^[18], la temperatura óptima está en 600-700°C, por debajo de las temperaturas utilizadas en la activación física, favoreciendo el desarrollo de la estructura porosa. La distribución de tamaño de poros en el CA final está fuertemente influenciada por el grado de impregnación. Generalmente, al aumentar el grado de impregnación aumenta el diámetro de poro del carbón. Sin embargo, debido a los problemas medioambientales que genera el uso de cloruro de zinc, este agente activante cada vez se utiliza menos, en pro de otros como los ácidos y los hidróxidos.

En el caso de la activación con ácido fosfórico (H_3PO_4)^[18], la temperatura de activación desciende a 350-500°C produciendo carbones de características similares a los anteriores. Por ejemplo, este agente activante es el más utilizado cuando el precursor es serrín. En este caso, el serrín se seca y se mezcla con una solución concentrada de ácido fosfórico formando una pasta que se piroliza dentro del rango de temperaturas mencionado produciendo un carbón de granulometría muy pequeña. Este tipo de CA que tienen aspecto de polvo, tienen una alta capacidad de adsorción y se utilizan para capturar grandes moléculas en procesos de decolorización.

Cuando se utilizan hidróxido de potasio hidratado (KOH)^[18] como agente activante, la preparación del CA es similar a los anteriores. Una de las formas de preparar este tipo de CA es mediante la impregnación del material previamente calcinado en un rango de temperaturas entre 300°C y 450°C durante más de 4 horas aunque la forma más común de prepara este tipo de CA es mediante un proceso de activación y pirólisis simultánea. La temperatura de proceso en este caso aumenta hasta 700-750°C y posteriormente el CA obtenido se enfría en una atmósfera inerte y se lava con agua destilada para eliminar el agente activante presente en exceso. De esta manera, se obtienen carbones altamente microporosos de área superficial del orden de 1800-4000 m²/g.

Son autores diversos los que han estudiado desde hace tiempo la activación de diferentes tipos de precursores con diferentes sales de potasio como hidróxido de potasio, o sulfatos, cloruros, carbonatos o bicarbonatos de potasio. En estos casos, se obtienen de igual manera CA de áreas superficiales altas. Por ejemplo, la activación de carbón con cloruro de potasio^[25] a 900°C en presencia de nitrógeno da como resultado CA de 1100-1500 m²/g y cuando el precursor es carbón y se activa con compuestos alcalinos como hidróxidos de sodio o potasio^[26] se alcanzan áreas de 1600 m²/g y volúmenes de microporo de 0.63 cm³/g.

En las siguientes tablas, se puede ver una comparativa de estos datos para CA preparados a partir de diferentes materias primas y agentes activantes en activación física (*Tabla 2.1*) y activación química (*Tabla 2.2*)

Tabla 2.1. Condiciones de operación del proceso de activación física para la obtención de AC^[18].

Material	R (Agente Activante/MP) ⁴	Ta (°C) ⁵	tp (h) ⁶	Atm ⁷	S _{BET} (m ² /g) ⁸	V _{microporo} (cm ³ /g) ⁹
Lignito	1.4/1	900	-	Vapor	920	0.83
	1.4/1	900	-	CO ₂	900	0.36
	2/1	900	-	O ₂	750	0.27

⁴ R: relación entre agente activante y materia prima en peso.

⁵ Ta: temperatura de activación.

⁶ tp: tiempo de activación.

⁷ Atm: atmósfera durante la pirólisis.

⁸ S_{BET}: área superficial efectiva.

⁹ V_{microporo}: volumen de microporos.

Tabla 2.2. Condiciones de operación del proceso de activación química para la obtención de AC.

Material	R (Agente Activante/MP) ¹⁰	Ta (°C) ¹¹	tp (h) ¹²	Atm ¹³	S _{BET} (m ² /g) ¹⁴	V _{microporo} (cm ³ /g) ¹⁵
H₃PO₄ ^[1, 3, 22, 27]						
Carbón Comercial	1.87/1	700	-	Argón	1688	0.70
Carbón Natural	2/3	500	3	Nitrógeno	850	0.40
Biomasa	1/1	700	2	-	945	0.35
Lignina	1/1	600	-	Nitrógeno	1000	0.40
KOH ^[2, 28-33]						
Carbón Comercial	3/1	700	2	Nitrógeno	3646	1.35
Carbón Natural	3/1	800	1	Nitrógeno	3900	1.17
Biomasa	4/1	750	2	Nitrógeno	3302	1.73
Lignina	0.25/1	700	1	Nitrógeno	514	0.21
NaOH ^[1, 28, 34-37]						
Carbón Comercial	8/1	750	1	Nitrógeno	3033	1.02
Carbón Natural	3/1	750	1	Nitrógeno	2193	0.60
Biomasa	3/1	750	1.5	Nitrógeno	2952	>1.60
Lignina	1	800	-	Nitrógeno	1400	0.55

Como se puede observar en las tablas anteriores, las condiciones de activación más severas se utilizan en las activaciones físicas en cuanto a temperatura de carbonización. El uso de diferentes tipos de activación favorece ciertas propiedades del producto final adecuándolo a una determinada aplicación. La activación que más favorece el desarrollo del área superficial es la activación con hidróxidos, debido en parte, al desarrollo más acentuado de la microporosidad. La activación física en un determinado rango de temperaturas, favorece el desarrollo de la mesoporosidad y por

¹⁰ R: relación entre agente activante y materia prima en peso.

¹¹ Ta: temperatura de activación.

¹² tp: tiempo de activación.

¹³ Atm: atmósfera durante la pirólisis.

¹⁴ S_{BET}: área superficial efectiva.

¹⁵ V_{microporo}: volumen de microporos.

tanto, la utilización de este tipo de carbones será diferente a los obtenidos por activación química.

Dependiendo del agente activante utilizado y de las condiciones de pirólisis aplicadas, se obtendrán diferentes tipos de carbones con propiedades físicas y químicas diferentes. Así, por ejemplo, los carbones más mesoporosos se utilizarán en tratamientos de efluentes líquidos contaminados con metales pesados, colorantes, componentes orgánicos no iónicos (NOC), etc. y los carbones más microporosos, en efluentes tanto líquidos como gaseosos, en la eliminación de contaminantes, almacenamiento de gases, etc. De igual manera, la química de superficie del carbón es importante determinando su campo de aplicación final.

2.1.3. Química de la activación

A continuación, se presentan en detalle los procesos de activación química de los CA que se han preparado para la realización de esta memoria y que corresponden a la preparación de CA procedentes de lignina Kraft activados por un lado con ácido fosfórico y por el otro con hidróxidos de sodio y de potasio.

2.1.3.1. Activación con ácido fosfórico

En la bibliografía se encuentran algunos modelos^[38-42] que intentan explicar la cinética de la descomposición térmica de la biomasa y sus fracciones cuando se activan químicamente con ácido fosfórico. La aproximación más común es en la que asume que los componentes que forman parte de la biomasa, tales como celulosa, hemicelulosa y lignina, reaccionan simultánea e independientemente de los otros componentes presentes mediante una serie de reacciones paralelas.

El proceso de activación de maderas “hardwood”^[42] puede ayudar a entender la activación de la lignina. Este proceso se puede dividir en dos etapas.

La primera se desarrolla a temperaturas inferiores a 150°C y en ella se observa, según diferentes técnicas de análisis, los diferentes fenómenos relacionados con la reacción entre la materia prima con el ácido fosfórico. El análisis elemental muestra una disminución del contenido en hidrógeno y oxígeno que continua hasta los 500°C que corresponde a la deshidratación de la muestra y conlleva una disminución de la producción de carbón. En los estudios en esta etapa con resonancia magnética nuclear y espectroscopía por infrarrojo, se observa la pérdida de carboxilos y grupos metilo de la

hemicelulosa y cambios en la composición de la lignina. A partir de 100°C la celulosa reacciona para formar cetonas, aumenta la aromaticidad y disminuyen los grupos alifáticos, carbonilos y carboxilos comenzando así el entrecruzamiento de la materia.

La segunda etapa de la activación se da a temperaturas por encima de los 150°C. Principalmente, de los análisis microscópicos se desprende que se produce una depolimerización parcial de los biopolímeros y se redistribuye el material, especialmente en el caso de la lignina. En las pruebas de adsorción de gases se observa un aumento de la microporosidad a partir de 150°C y de la mesoporosidad a partir de 250°C. A temperaturas elevadas, se produce una disminución de la porosidad provocada por una contracción estructural. A partir de 300°C incrementa la producción de carbón debido al entrecruzamiento de la estructura que se produce y la retención de ciertos volátiles. A partir de 450°C y mediante resonancia magnética nuclear y espectroscopía de infrarrojo, se comprueba una disminución acusada de la aromaticidad de la muestra, cetonas y ésteres debido a la disminución del reordenamiento estructural.

Estas etapas se corresponden al modelo presentado a continuación, aplicado a la activación de lignina, aunque tal y como se ha comentado con anterioridad, es complicada la predicción exacta de un modelo para la activación de una macromolécula tan compleja.

Si se aplican estos modelos a la activación de lignina con ácido fosfórico, éste se reduce básicamente a dos reacciones paralelas e independientes. Mientras que en la primera se produce la volatilización del agua presente en la muestra y en la solución de activante utilizada, en la segunda se carboniza la mezcla entre el ácido fosfórico y la lignina para dar el CA y volátiles.

Debido a la complejidad de la molécula de lignina es muy difícil detallar todas las reacciones que tienen lugar, pero se puede presentar un modelo^[43] de la activación química usando ácido fosfórico como agente activante y describir los pasos que tienen lugar como una serie de pasos simplificados que describen los múltiples procesos reactivos involucrados. Este modelo se presenta en detalle en el apartado 5.1.

En primer lugar, la mezcla entre la lignina y el ácido fosfórico dan lugar a un complejo generado por la reacción entre el ácido y los sitios reactivos de la lignina, que puede durar aproximadamente una hora a temperatura ambiente, y que se finaliza antes de comenzar el proceso térmico.

Posteriormente y una vez se comienza con la pirólisis de la muestra, se produce la conversión del exceso de ácido en P₂O₅ mediante la progresiva pérdida de las moléculas de agua. Este proceso se lleva a cabo mediante

diferentes transformaciones de los derivados de ácido fosfórico. Por una parte, cuando el ácido fosfórico se calienta se deshidrata y forma ácido pirofosfórico ($H_4P_2O_7$) como resultado de la condensación de dos moléculas de ácido fosfórico. El calentamiento sucesivo conlleva la generación de una mezcla formada por ácidos ortofosfórico y polifosfórico llamada ácido superfosfórico. A altas temperaturas se forma ácido metafosfórico (HPO_3) que posteriormente se descompone para formar el P_2O_5 . Este proceso comporta que se produzca una pérdida de peso a $170^\circ C$ hasta $580^\circ C$ que se puede atribuir a las reacciones sucesivas de la deshidratación del P_2O_5 . A temperaturas mayores de $580^\circ C$, el óxido de fósforo se sublima, lo que conlleva que se produzcan pérdidas de peso menores. La formación de este compuesto ayuda al desarrollo de la estructura interna de la muestra actuando como un protector y cuando seguidamente se evapora, constituye el primer paso del desarrollo de su porosidad. Finalmente, la pirólisis completa del complejo generado en el primer paso, da lugar al CA definitivo y volátiles, con lo que se acaba de desarrollar la estructura interna del producto final.

2.1.3.2. Activación con hidróxidos

El efecto de los hidróxidos en la activación de materiales carbonosos se rige principalmente por la formación de sodio o potasio metálico, dependiendo del proceso, hidrógeno y carbonatos. Los mecanismos descritos en la literatura en los que especifica la activación química mediante hidróxidos son equivalentes tanto para hidróxido de sodio (NaOH) como para hidróxido potásico (KOH).

Por tanto, a continuación se detalla el mecanismo para un tipo de hidróxido, el de sodio, extendiendo esta cinética al uso de los dos activantes estudiados.

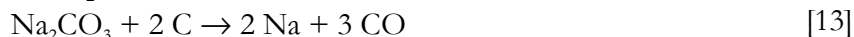
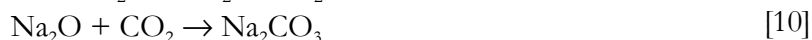
La reacción principal de obtención de los productos mencionados se da entre el hidróxido sódico y el material carbonoso estudiado (reacción [6]), teniendo lugar a partir de $730^\circ C^{[37]}$ para las reacciones con NaOH y a partir de $630^\circ C^{[37]}$ para la activación con KOH a presiones atmosféricas de nitrógeno.



En casos determinados, en la activación con NaOH, la reacción [6] puede darse a temperaturas alrededor de $570^\circ C^{[37]}$ debido a que el uso de la corriente de nitrógeno produce que la presión de los volátiles que se gasifican sea inferior a 1 bar.

Aunque hay autores que presentan otras reacciones como principales^[28, 37, 44, 45] en las que el hidróxido de sodio reacciona con dióxido de carbono para dar carbonato de sodio y agua y, por otro lado, reacciona con el carbono de la estructura para dar sodio metálico, dióxido de carbono y agua, desde el punto de vista termodinámico^[37] es más factible que se de la reacción [6].

Por otro lado, se consideran las reacciones secundarias^[28, 44, 46, 47] de la descomposición del hidróxido de sodio y la reducción del carbón, simultáneamente (reacciones [7] a [13]).



La formación de carbonatos (reacción [10]) es una reacción competitiva con la activación por NaOH o KOH (reacción [6]), y no sólo se forman por el proceso de activación, sino también por la pirólisis previa del material. Cuando la temperatura supera los 750°C, se da la descomposición del Na₂CO₃ formando óxidos de carbono (CO y CO₂) que son también activantes y restos de sodio metálico que, junto a las reacciones [11], [12] y [13], explicaría la presencia de esta sustancia en la muestra carbonizada.

De esta manera, y operando con un calentamiento continuado hasta 750°C, manteniendo una isoterma de 1 hora en atmósfera de nitrógeno y trabajando con una relación de agente activante / materia prima de 3 se pueden conseguir valores de 3000 m²/g de área superficial y volúmenes de microporos mayores de 1.6 cm³/g, cuando se trabaja con cáscara y paja de arroz y carbones sintéticos y naturales^[28, 34, 36, 37, 48-51].

2.1.4. Caracterización de carbones activados

La caracterización de sólidos que se conoce actualmente comprende tres bloques de técnicas bien definidas con las que se puede estudiar la estructura, la textura y la superficie de sólidos.

Por un lado, se haya el grupo de técnicas para el estudio de la composición química y la caracterización estructural, que son aquellas que determinan la distribución en el espacio de los átomos o iones de la parte material del sólido, según la IUPAC. En particular, aplicado a un sólido poroso, la distribución en/o próxima a la superficie.

Tabla 2.3. Relación de técnicas empleadas en la caracterización estructural.

Tipo de análisis	Técnicas
Químicos	<ul style="list-style-type: none">○ Absorción atómica (AA)○ Fluorescencia de rayos X (XRF)
Contenido en agua y volátiles	<ul style="list-style-type: none">○ Termogravimetría (TG y ATD)
Estudio de la estructura química	<ul style="list-style-type: none">○ Difracción de rayos X (DRX)○ Espectroscopía de infrarrojos (IR)
Perfiles de materiales no homogéneos, monocapas y superficies	<ul style="list-style-type: none">○ Raman○ Espectroscopía XPS
Coordinación de cationes	<ul style="list-style-type: none">○ Resonancia magnética nuclear (RMN)

El segundo bloque de técnicas es el que estudia la morfología y la caracterización textural de sólidos, es decir, la geometría detallada del espacio de huecos y poros, según la IUPAC.

La textura es una propiedad de las sustancias que poseen una matriz de material sólido que rodea a un sistema de poros que tienen dimensiones coloidales (de unos amstrongs a un micrómetro). La textura se caracteriza por una gran superficie interna, y en la mayoría de los casos, por una irregularidad marcada del sistema de poros, de tal modo que muchas partes de la red de poros pueden alcanzarse solamente a través de constricciones estrechas. Las técnicas incluidas en este segundo bloque realizan:

Tabla 2.4. Relación de técnicas empleadas en la caracterización textural.

Tipo de análisis	Técnicas
Ópticos	<ul style="list-style-type: none"> ○ Microscopía electrónica (SEM y TEM)
Estudio de la distribución de tamaños	<ul style="list-style-type: none"> ○ Sedimentación ○ Scattering ○ Coulter
Área superficial	<ul style="list-style-type: none"> ○ Diferentes métodos, el más conocido el de la teoría de Brunauer-Emmett-Teller (BET)
Determinación de volumen y distribución de tamaños de poros	<ul style="list-style-type: none"> ○ Densidad real y aparente (volumen total) ○ Intrusión de mercurio (macroporosidad) ○ Adsorción física de nitrógeno, dióxido de carbono y/o argón (meso y microporosidad) ○ Calorimetría de inmersión (meso y microporosidad)

Por último, el tercer bloque de técnicas estudia la química de superficie, tal y como se observa en la siguiente tabla.

Tabla 2.5. Relación de técnicas empleadas en el estudio de la química de superficie.

Tipo de análisis	Técnicas
Hidroxilos	<ul style="list-style-type: none"> ○ TG ○ IR ○ RMN ○ Raman
Centros ácidos	<ul style="list-style-type: none"> ○ adición de aminas ○ IR ○ desorción de amoniaco ○ técnicas de desorción a temperatura controlada (TPD)
Dispersión metálica y no metálica	<ul style="list-style-type: none"> ○ TEM ○ quimisorción selectiva
Cationes de cambio y centros redox	<ul style="list-style-type: none"> ○ Valoración
Valencias superficiales	<ul style="list-style-type: none"> ○ XPS
Especies adsorbidas	<ul style="list-style-type: none"> ○ TPD

Por lo general, la caracterización de un sólido conlleva la medida de varios parámetros o magnitudes fisicoquímicas, recogiendo información a través de varias técnicas experimentales por lo que hay que diagnosticar qué es lo que se busca para decidir qué técnicas y en qué orden se van a aplicar.

En el caso de la caracterización de los CA preparados para la realización de esta memoria, se han utilizado diversas técnicas de las mencionadas anteriormente y que se detallan en el apartado de “Materiales y Métodos”.

2.2. La lignina

En esta memoria se realizan CA a partir de lignina Kraft, por eso es importante conocer las características de esta materia prima con el fin de poder entender mejor las modificaciones que se producen debidas a su activación química y las propiedades finales del carbón obtenido.

La lignina es el segundo componente mayoritario en la madera, en una proporción que oscila entre el 7.2%, en el caso de la alfalfa, y el 24.1%, en madera de abeto, presente en la pared celular de diversas materias primas (*Tabla 2.6*)^[52]. La lignina está localizada en las paredes celulares y en los espacios intracelulares, donde funciona como un agente adhesivo que entrelaza las matrices de las fibras de celulosa formando una estructura rígida.

La lignina realiza múltiples funciones que son esenciales para la vida de las plantas, como en el transporte interno de agua, nutrientes y metabolitos, proporciona rigidez a la pared celular actuando como puente de unión entre las células de la madera, creando un material que es notablemente resistente a los impactos, compresiones y flexiones y proporciona resistencia al ataque de los microorganismos, impidiendo la penetración de las enzimas destructivas en la pared celular^[53].

Tabla 2.6. Contenido de la pared celular de diversas materias vegetales (expresado como materia seca).

Tipo de biomasa vegetal	Contenido (%)			
	Hemicelulosa	Celulosa	Lignina	Otros
Alfalfa (maduración media)	6.0	25.0	7.2	61.8
Dáctilo apelonado ¹⁶	40.0	32.0	4.7	23.3
Paja de centeno	27.2	34.0	14.2	24.6
Madera de abedul	25.7	40.0	15.7	18.6
Madera de abeto	20.9	46.0	24.1	9.0

La fuente más importante de obtención de materias lignicas está en la fabricación de pastas químicas de celulosa^[10, 11] donde se generan como producto secundario en los procesos hidrolíticos que se llevan a cabo en la separación de la fibra celulósica del resto de constituyentes de la madera. El tratamiento de la madera en diferentes etapas de cocción o lejiado dan como resultado una pasta de celulosa y una disolución residual llamada licor negro que contiene una elevada concentración de solutos entre los que predominan

¹⁶ Dáctilo apelonado: *Dactylis glomerata*, de la familia de las gramíneas.

los de naturaleza lignica en una proporción entre 38-45%^[11]. Dependiendo del tratamiento que se realiza al licor negro se obtienen diferentes tipos de lignina entre los que destacan el proceso al bisulfito y el proceso al sulfato, este último, el más utilizado ya que se obtiene la llamada pasta kraft, que es la más importante a nivel comercial.

Por otro lado, la obtención de lignina también está presente en los procesos de conversión de madera en hidrocarburos^[10, 54]. Estos procesos se están desarrollando debido a que hoy en día se dependen en gran medida de productos petroquímicos derivados de hidrocarburos fósiles, líquidos y gaseosos como materias primas para la producción de fibras, plásticos, cauchos, adhesivos, etc. Tanto el petróleo como el gas natural son fuentes no renovables que aumentan su precio a medida que van escaseando y por tanto el uso de otras fuentes de carbono, tales como el carbón de leña o la madera, pueden utilizarse como materias primas alternativas, tal y como se lleva a cabo en una planta piloto de estas características en Oregón desde 1978.

2.2.1. Estructura química

En su forma natural, la lignina es un polímero tridimensional constituido principalmente por unidades fenilpropano polimerizadas al azar (C₉). Ésta naturaleza polimérica ha favorecido el desarrollo de aplicaciones en las cuales se ha explotado sus características estructurales, como por ejemplo, su uso como materia prima en la obtención de carbones activos, en resinas, etc.

La molécula de lignina es una macromolécula, con un elevado peso molecular (840-880 g/mol)^[55], que resulta de la unión de varios ácidos y alcoholes fenilpropílicos (cumarílico, coniferílico y sinapílico). La lignina puede estar unida física y/o químicamente a las hemicelulosas y a la propia α -celulosa conociéndose, en este caso, como protoligninas.

El acoplamiento aleatorio de los radicales^[11, 56, 57] presentados en la *Figura 2.4* da origen a una estructura tridimensional, un polímero amorfo característico de la lignina. La lignina es el polímero natural más complejo con relación a su estructura y heterogeneidad. Por esta razón no es posible describir una estructura definida de la lignina como una combinación simple de uno o más unidades monoméricas o unos pocos tipos de enlaces, como en el caso de la celulosa o las hemicelulosas (poliosas), sino como una serie de modelos que la “aproximan”. La dificultad de determinar una única estructura de la lignina reside en el proceso de extracción de la madera ya que, aún empleando el mismo procedimiento de síntesis, se producen variaciones en la molécula, incluso llegando a afectar el tratamiento inicial que se le da a la madera.

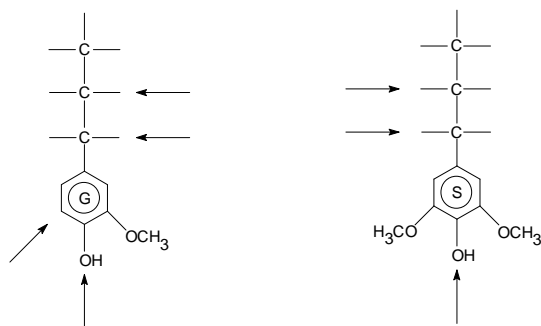


Figura 2.4. Monómeros propios de la lignina con sus posibles puntos de enlace entre unidades (→). Unidad guayacilo abundante en coníferas (izquierda) y unidad siringilo típica en frondosas (derecha).

El primer modelo de la lignina fue descrito por Freudenberg en el año 1964 y se basó en el concepto de polimerización deshidrogenativa. Este modelo representa 18 unidades fenilpropano como una sección de toda la molécula que se asumía mayor de 100 unidades. En 1977, Adler propuso un modelo diferente basado en la presencia de 16 unidades formadas por cadenas de C₉, principalmente derivadas de los experimentos de degradación oxidativa. Posteriormente, en 1980, Sakakibara describió un modelo para las ligninas “softwood” basada en la evaluación de la degradación de productos derivados de hidrólisis poco agresivas y de hidrogenólisis. De esta manera, presentaba una estructura de 28 unidades C₉ con diversos elementos estructurales alternativos que coincidía con los datos analíticos existentes. Finalmente, la mayor estructura modelada para una lignina “softwood” obtenida por ordenador a partir de la combinación aleatoria de varias subestructuras, grupos funcionales y de enlaces conocidos y presentada por primera vez por Glasser y Glasser en 1974 (ver *Figura 2.5*).

Esta estructura se obtuvo al modelizar las reacciones radicalarias del alcohol p-hidroxicinámico y estaba compuesta por 80 unidades fenilpropano. Posteriormente, este modelo fue optimizado a partir de numerosos datos experimentales obtenidos serrín de *Pinus Taeda*, en el que 94 unidades formaban la estructura proporcionando un peso molecular mayor a 170.000.

La estructura de la lignina también varía entre las maderas duras (“hardwoods” o “grass”) y las maderas blandas (“softwoods”). En general, los grupos fenilo en las ligninas procedentes de “hardwoods”, están más substituidos por grupos metoxilos que los de procedencia “softwood”. La consecuencia principal de esta característica es que las ligninas de origen

“hardwood” están menos entrelazadas y por tanto se disuelven mejor en el proceso de pulpación.

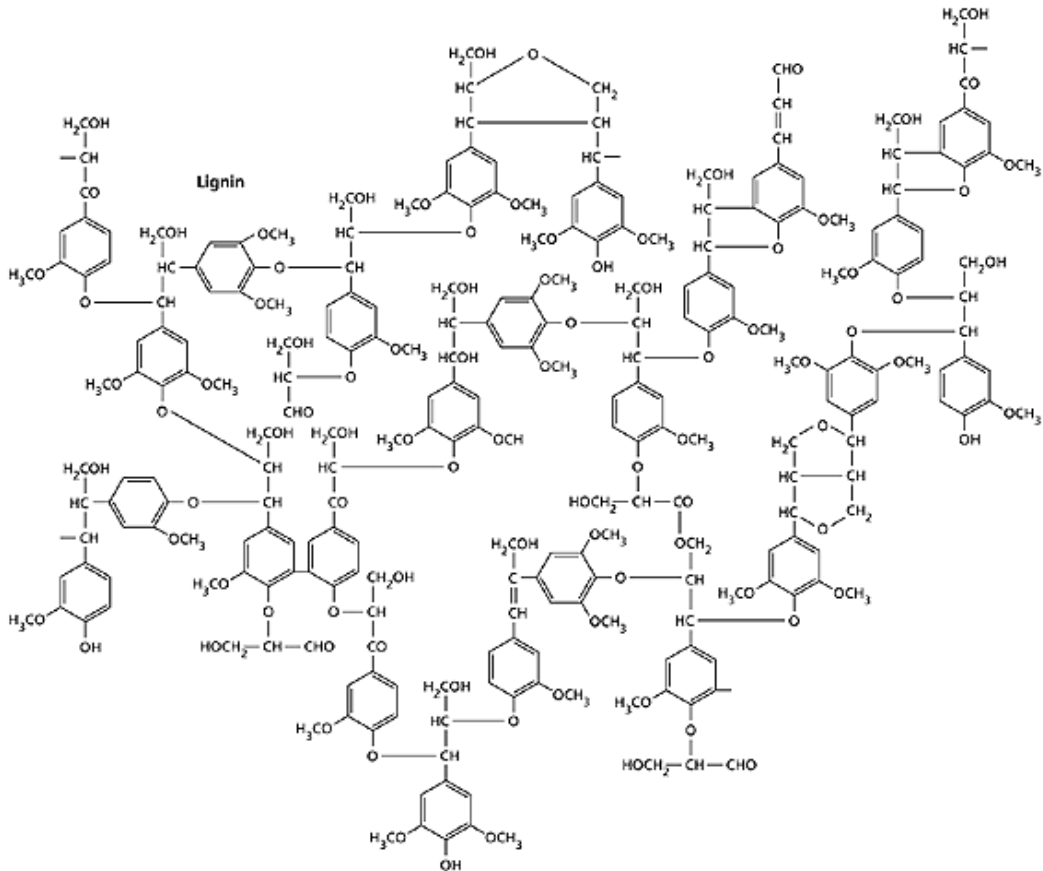


Figura 2.5. Estructura aleatoria de la lignina procedente de madera blanda (“hardwood lignin”) propuesta por W. G. Glasser^[58] en 1981.

2.2.2. Ligninas técnicas y comerciales

Las ligninas industriales son subproductos generados en la industria de la madera y la celulosa. Los lignosulfonatos y la lignina Kraft son los principales tipos de ligninas comerciales disponibles en grandes cantidades. En el caso de los primeros, la producción anual en el mundo occidental se sitúa en $500 \cdot 10^9$ Tm, de las cuales, el 46.3% se produce en Europa y el 25.1% en Estados Unidos. En el caso de la lignina Kraft, la capacidad anual es menor que para los lignosulfonatos, siendo de $100 \cdot 10^3$ Tm repartidas entre Europa (52.6%) y

Estados Unidos (47.4%) principalmente^[10, 59, 60]. Las ligninas Organosolv son disponibles en cantidades limitadas.

- Ligninas Kraft (ligninas al sulfato o alcalinas): obtenidas de la precipitación del licor negro generado durante el proceso de pulpación con hidróxido de sodio y sulfuro de sodio en digestores batch aunque éstos están siendo reemplazados por digestores continuos. Las condiciones de temperatura, agitación y acidez del medio influyen significativamente en las propiedades finales de la lignina. Este proceso se aplica en una gran variedad de tipos de maderas ya que se obtiene una pulpa más blanca en comparación a la resultante en el proceso del sulfito. En contraposición, presenta como desventajas el olor que se genera debido a tioles y sulfuros y el contenido de óxidos de azufre en las aguas del proceso con un pH que oscila entre 8 y 9. éste polímero tiene un peso molecular de 1100 g/mol^[61] aproximadamente.
- Lignosulfonatos (ligninas sulfonadas o ligninas al sulfito): se generan durante el proceso Howard al añadir hidróxido de calcio al licor negro en tres etapas batch en las que se generan y se recirculan en cada una: sulfito de calcio, lignosulfonato cálcico y lignosulfonato con exceso de cal. Posteriormente, los lignosulfonatos se someten a un proceso de calentamiento en presencia de calcio o hidróxido de sodio mediante el cual se produce la desulfonación. Principalmente, la lignina se recupera mediante la hidrólisis y la oxidación del precipitado obtenido debido al medio básico, aunque otro tipo de separaciones se basan en la ultrafiltración y la osmosis inversa. Éste proceso es menos contaminante que el anterior ya que no se producen ni tioles ni sulfuro y admite más variaciones en las condiciones de operación. Sin embargo, el proceso es sensible al estado de la materia prima (ramas, cortezas y resina) que no se disuelve de igual manera que la madera. El polímero de lignosulfonato tiene un peso molecular de 1300 g/mol^[61].
- Lignina Organosolv: procede de tratamientos con solventes orgánicos en el proceso de deslignificación como el metanol, etanol, ácido acético, y ácido fórmico. Las ligninas derivadas de pulpación con alcoholes son comercialmente disponibles en cantidades limitadas. Éste polímero puede alcanzar pesos moleculares de 2800 g/mol^[61] aproximadamente.

- **“Furafil”**: Los restos de cereales son ricos en pentosanos y son fuentes comerciales de furfurales. Los pentosanos son hidrolizados con catalizadores ácidos a pentosas de la cual se obtiene el furfural¹⁷ que se separa por destilación. El residuo de la hidrólisis de la cáscara de mazorca de maíz, arroz y avena contiene entre el 30-40% de lignina y se comercializa bajo el nombre de “furafil”. Se han desarrollado varios usos del “furafil” tales como abonos y fertilizantes, adsorbentes, ingredientes en las arenas para moldear en las fundiciones y como suplementos para varias resinas.
- **Productos de la corteza**: La corteza de los árboles contienen además de fibras de celulosa y otros componentes propios, una cantidad considerable de materiales lignicos que se denominan ácidos fenólicos de corteza. Durante muchos años, se producían preparados que contenían este material y se vendían como aditivos en las perforaciones petrolíferas, pegamento, aditivos de las resinas, dispersantes, etc. La tecnología de manufactura de estos productos es escasa y cara y se basa en la producción de derivados del petróleo para resinas y adhesivos aunque actualmente están siendo más utilizados en la agricultura o como agente energético para ser quemado.
- **Lignina hidrolizada**: La hidrólisis de la madera para producir glucosa ha sido estudiada durante muchos años y se han desarrollado varios procesos, en especial para la producción de azúcares y sus productos de fermentación. Estas ligninas son conocidas como ligninas Scholler y pueden ser modificadas por cloración, nitración, etc., de forma similar a las ligninas alcalinas, formando nitroligninas y cloroligninas que se utilizan en la fabricación y tratamiento de componentes para mantener su resistencia. Este tipo de ligninas se utiliza como abono para el suelo, como aditivo en resinas y gomas y como agente adhesivo en paneles de conglomerado.

2.2.3. Aplicaciones de la lignina

Los productos derivados de la lignina son utilizados principalmente como combustible interno para la recuperación de la energía y reactivos inorgánicos restantes en la producción de papel. La problemática viene dada por la creciente producción de papel que aumenta la producción de lignina que a su

¹⁷ Furfural: compuesto utilizado en la producción de pesticidas, en resinas fenolfurfural y en la producción de tetrahidrofurano, el cual se utiliza como un disolvente comercial y como materia prima en la producción de nylon.

vez incrementa los costes de los hornos de recuperación, lo cual no es una inversión rentable en el caso de la pequeña y mediana empresa papelera. La separación de la lignina y su uso en diferentes campos podrían ser una alternativa a la incineración. Algunas de éstas aplicaciones alternativas^[11, 56, 57, 60, 62-65] a la valorización energética de la lignina son:

- estabilizante en emulsiones de líquidos inmiscibles
- secuestrante de iones metálicos para evitar que reaccionen con otros compuestos y permanezcan disueltos en la solución, manteniéndolos disponibles en plantas de tratamiento de agua y previniendo depósitos en sistemas acuosos
- dispersante, ya que el lignosulfonato es útil en mezclas de cemento, arcilla y cerámica, tintes y pigmentos, tableros de yeso, fangos de perforación petrolífera, pesticidas e insecticidas, etc.
- adhesivo. Muy eficaz y económico (resinas fenólicas), actúa como agente astringente en pellets, lo que es útil en briquetas del carbón, tableros de chapado y de partícula, cerámicas, granos de pienso, aislamiento de fibra de vidrio, fertilizantes y herbicidas, goma del linóleo, estabilizadores del suelo, etc.
- producción de tableros de aglomerado llamados presdwood^[11] a partir de la alteración con vapor a altas temperaturas de la lignina de la madera
- materia prima para la producción de carbón activo^[5-7] como adsorbente en el campo de la electrónica, la catálisis, el almacenamiento de gases^[28, 34, 48, 49, 66] y principalmente en procesos de separación, purificación de afluentes líquidos y gaseosos y en procesos de recuperación debido a la textura porosa y gran capacidad de adsorción del carbón activo.

El uso de materiales de bajo coste y de base carbonosa o lignocelulósica para su utilización como precursores en la producción de carbones activos es la tendencia actual en el campo de investigación de materiales carbonosos. La utilización de la lignina como precursor para la producción de carbón activo ha sido estudiado anteriormente mediante la activación física por gasificación parcial de CO_2 ^[6, 7] en lignina Kraft procedente de eucalipto y en activaciones químicas mediante el uso de ZnCl_2 ^[5], H_3PO_4 ^[1, 3, 4] e hidróxidos como el KOH o el NaOH^[1, 2].

2.2.4. Lignina, precursor para carbones activados

Tal y como se ha mencionado, los subproductos lignocelulósicos obtenidos de la agricultura y de otras fuentes, son de gran interés para la producción de carbones activos. De hecho, la madera es un material ampliamente utilizado como materia prima y entre sus componentes básicos está la celulosa, hemicelulosa y lignina, así que el uso de cualquiera de estos componentes como precursor para CA es más interesante que su utilización como combustible.

Los agentes activantes más utilizados en los procesos de activación de la lignina son principalmente el ácido fosfórico y, en menor escala, el cloruro de zinc.

Desde la perspectiva económica y medioambiental y comparando los procesos de activación química y física, el ácido fosfórico es mejor método de activación ya que la temperatura de proceso es ligeramente menor, del orden de 400-500°C, comparado con la temperatura mínima de 850°C que se necesita en los procesos físicos, con la ventaja añadida que el ácido fosfórico es recuperable.

La activación física de la lignina con dióxido de carbono^[6] permite obtener CA con una microporosidad bien desarrollada y una alta mesoporosidad a temperaturas moderadas (a 550°C el área superficial es de 496 m²/g con una microporosidad de 0.224 cm³/g). A medida que aumenta la temperatura de carbonización, se crean macroporos que permite obtener CA aplicables en diferentes usos dependiendo de las condiciones de preparación (a 800°C se obtiene un área superficial de 1360 m²/g con una microporosidad de 0.528 cm³/g, una mesoporosidad de 0.992 cm³/g y una macroporosidad de 0.510 cm³/g). En este caso, la influencia del contenido en ceniza de la materia prima es importante ya que evita la aparición de la fase plástica en la lignina y por tanto, aumenta la activación física.

Desde el punto de vista de la aplicación, el uso de ácido fosfórico^[67] aumenta el rendimiento a carbón y favorece el desarrollo de la acidez superficial lo cual es de gran utilidad en usos como la adsorción de metales pesados que se encuentran en bajas concentraciones en efluentes líquidos además de ser carbones muy estables química y térmicamente.

En los carbones desarrollados a partir de la lignina y activada con ácido fosfórico, las condiciones de preparación, especialmente la relación de impregnación y la temperatura de activación tienen gran incidencia en el desarrollo de la porosidad, principalmente, de la mesoporosidad (volumen de

microporos de $0.20 \text{ cm}^3/\text{g}$ y de mesoporos de $0.59 \text{ cm}^3/\text{g}$) pudiendo obtener CA de $1459 \text{ m}^2/\text{g}$ a 500°C ^[4, 67].

El desarrollo de la acidez superficial se rige por la presencia de grupos sensibles y los insensibles a la temperatura. El primer grupo consiste en grupos carbonilos de acidez variable mientras que el segundo grupo está compuesto principalmente por grupos fosforosos y en mucho menor grado, otro tipo de grupos carbonilo de menor acidez^[67].

Relaciones de impregnación bajas favorecen la formación de los grupos superficiales ácidos, especialmente carbonilos y el aumento de la relación agente activante – lignina^[67] los grupos fosforosos.

La activación con cloruro de zinc^[5] permite alcanzar CA de áreas superficiales de hasta $1800 \text{ m}^2/\text{g}$, a 500°C y una relación cloruro de zinc – lignina de 2.3, esencialmente microporosos (volumen de microporos de $1.039 \text{ cm}^3/\text{g}$, mesoporos de $0.586 \text{ cm}^3/\text{g}$ y macroporos de $0.143 \text{ cm}^3/\text{g}$). La estructura porosa se desarrolla incluso con relaciones altas entre el cloruro de zinc y la lignina, lo que indica que la distribución del agente activante sobre la lignina es muy homogénea. Incluso cuando la lignina entra en la fase plástica debido al incremento de temperatura, la activación del cloruro de zinc ayuda al desarrollo de la porosidad. Esta etapa plástica puede ser omitida cuando se utiliza lignina con alto contenido en cenizas, de tal manera que el desarrollo de la porosidad que se produzca será diferente aunque sin generar grandes cambios. Los CA obtenidos de esta manera tienen buenas propiedades mecánicas aún cuando la microporosidad es elevada y por tanto se esperase lo contrario.

La activación de lignina con hidróxidos de potasio o de sodio ha sido desarrollada recientemente y con ella se consiguen materiales con áreas superficiales más altas y de mayor microporosidad, comparado con las logradas mediante activación con ácidos. En la activación con KOH se alcanzan áreas superficiales de $2930 \text{ m}^2/\text{g}$ con volúmenes total de poros de $1.656 \text{ cm}^3/\text{g}$ y de microporos de $1.197 \text{ cm}^3/\text{g}$, a 750°C temperatura de carbonización. Si el agente activante es NaOH, los valores son ligeramente inferiores a las mismas condiciones de carbonización: áreas superficiales de $2340 \text{ m}^2/\text{g}$ con volúmenes total de poros de $1.338 \text{ cm}^3/\text{g}$ y de microporos de $0.954 \text{ cm}^3/\text{g}$ ^[68]. De igual manera, el desarrollo de la acidez y la basicidad superficial se lleva a cabo de manera más marcada que en los casos anteriores debido a las condiciones de operación utilizadas donde generalmente se usa una atmósfera de nitrógeno en lugar de una atmósfera oxidante.

3. OBJETIVOS

El estudio presentado en esta memoria pretende conducir a conclusiones relacionadas con las reacciones que tienen lugar debido a la presencia de diferentes tipos de agentes activantes, los productos de las reacciones producidas y las condiciones de operación de los diferentes procesos de activación química investigados. Esto, a la vez, permitirá determinar las variables que tienen un efecto más importante en las características finales del CA obtenido con el fin de poder controlar el desarrollo de estas propiedades y, por tanto, la aplicación final del producto.

Por tanto, el objetivo principal de este trabajo es controlar perfectamente el desarrollo de la estructura porosa de los carbones preparados a partir de lignina Kraft. Para llevar a cabo este objetivo general, se deben tener en cuenta una serie de objetivos secundarios tales como:

- En primer lugar, desarrollar CA microporosos, a partir de un subproducto de la producción de papel, la lignina Kraft, por activación química con ácidos e hidróxidos. Para ello, se realizarán una serie de CA partiendo de unas condiciones de carbonización determinadas y realizando variaciones de una sola de ellas.
- Posteriormente, entender los procesos reactivos que tienen lugar durante la activación química de la lignina Kraft con tres agentes activantes diferentes (ácido fosfórico, hidróxido de sodio e hidróxido de potasio), para poder controlar el proceso de carbonización que tiene lugar y así, entender el desarrollo de las propiedades finales del producto.
- También se realizará la caracterización estructural, textural y de superficie de la materia prima y de los CA y se establecerá una relación entre las propiedades finales de los carbones activos con las diferentes condiciones de operación, con el fin de adecuarlas para desarrollar un producto final que se ajuste a las necesidades de su uso en efluentes líquidos.
- Finalmente, se emplearán los mejores CA obtenidos en los tres tipos de activación química estudiada, en la adsorción de diferentes tipos de contaminantes.

Por un lado, se estudiará la eliminación de cobre (II) en sistemas líquidos por parte de los CA obtenidos por activación con ácido fosfórico.

Por el otro lado, se probarán los tres tipos de CA obtenidos en la adsorción de fenol y benceno, contaminantes típicos en aguas procedentes de industrias.

Por último, como aplicación específica, se participará en el estudio de la incorporación de los CA obtenidos a partir de ácido fosfórico como aditivo en membranas para la obtención de reactores enzimáticos de membrana (EMR), a partir de una matriz polimérica (polisulfona), el cual se usa para adsorber una enzima específica directamente o a partir de un metal con el propósito de purificar oligómeros.

Paralelamente a estos estudios, también se participará en estudios que estriban en los pasos previos a aplicaciones de los carbones producidos para esta tesis. En este caso, se utilizarán carbones comerciales para la purificación de xilo-oligosacáridos que contienen como impurezas principales productos derivados de la lignina.

4. MATERIALES Y MÉTODOS

Para la consecución de los objetivos de este trabajo, se han seguido tres etapas bien definidas basadas en:

- 1) Preparación de CA a partir de la lignina Kraft como materia prima y su activación con diferentes agentes químicos (apartado 4.2).
- 2) Caracterización de los CA preparados en 1) (apartado 4.3).
- 3) Aplicaciones previas de los CA a partir de los datos obtenidos en su caracterización (apartado 4.4).

4.1. Materia primas

La materia prima de la que se parte en la primera etapa, la lignina Kraft, ha sido utilizada de dos formas diferentes: tal y como llegó del proveedor Lignotech Ibérica S.A. (LK) y después de someterla a un tratamiento ácido para la reducción de cenizas (LK_d).

A partir de estas dos materias primas, se ha realizado su activación química a partir de diferentes tipos de agentes activantes (AgA).

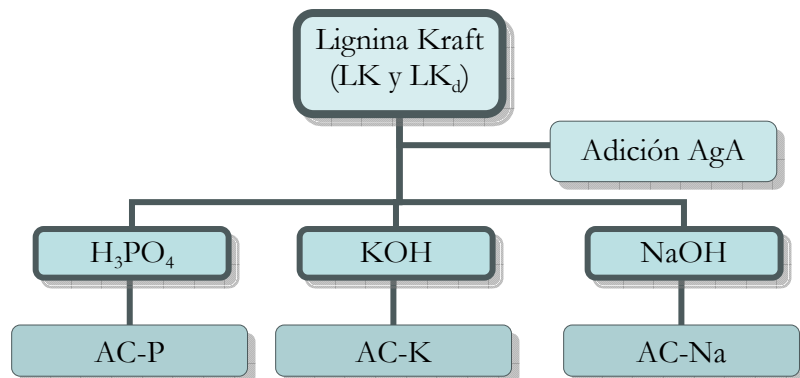


Figura 4.1. Esquema de la etapa de preparación de CA (etapa 1).

Para el caso de la LK, se ha procedido a la activación química con ácido fosfórico e hidróxido de potasio. En el caso de la LK_d, se ha utilizado como agentes activantes ácido fosfórico, hidróxido de potasio e hidróxido de sodio. El usar las dos materias primas con el mismo agente activante tiene como objetivo el estudio del contenido en cenizas de la materia prima en los CA obtenidos. En principio, para los carbones obtenidos con ácido fosfórico (AC-P) se ha utilizado LK y tan solo algún CA se ha preparado a partir de LK_d. En el caso de la activación con hidróxidos (AC-K y AC-Na), la materia prima era fundamentalmente LK_d y tan solo algún experimento comparativo se ha realizado a partir de LK.

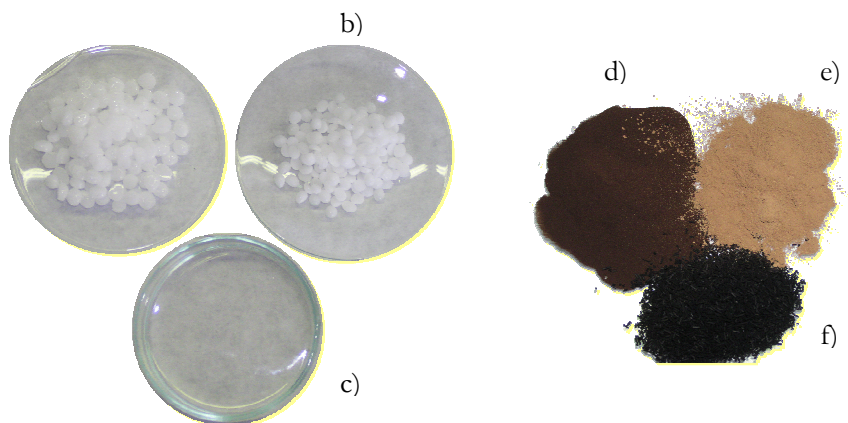


Figura 4.2. Materias primas utilizadas en la preparación de CA: a) NaOH, b) KOH, c) ácido fosfórico, d) LK, e) LK_d y f) CA obtenido.

4.2. Preparación de carbones activados

La preparación de los CA se ha realizado de la siguiente manera. En los carbones activados con ácido fosfórico, en primer lugar se realiza una etapa de impregnación donde se mezcla una cantidad determinada de lignina con una solución de ácido fosfórico al 85% acorde con la relación P/L que se desea obtener. Esta mezcla se deja a temperatura ambiente en atmósfera de aire durante un tiempo determinado, llamado tiempo de activación, antes de pasar a la segunda etapa. Transcurrido este período, se procede a iniciar la etapa de pirólisis, bajo atmósfera de aire, en la cual se introduce la muestra en un horno DUM modelo 10CAF (ver *Figura 4.3*). El horno se calienta a 10°C/min hasta 150°C, temperatura a la que se mantiene constante durante una hora permitiendo así una evolución libre del agua. Posteriormente, el horno se calienta de nuevo a la misma velocidad de calentamiento hasta una temperatura de carbonización entre 400°C y 650°C manteniéndola durante dos horas.

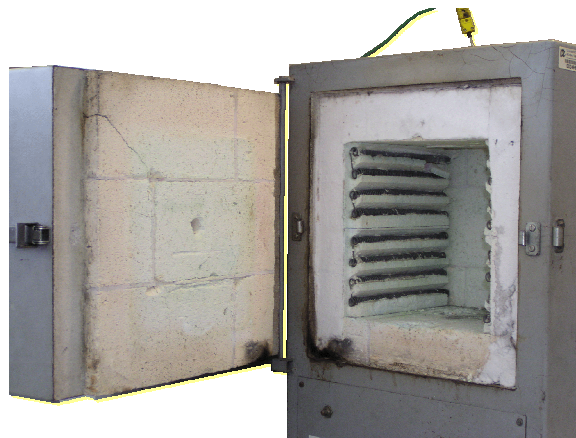


Figura 4.3. Detalle del horno empleado en la activación con ácido fosfórico.

Para eliminar el exceso de ácido fosfórico después de la carbonización, el AC-P se lava repetidamente con agua destilada hasta pH neutro, medido con un pH-ímetro CyberScan PC 510 con un electrodo Hamilton “Flushtrode”. Finalmente, las muestras se dejan secar durante 12 horas en una estufa a 110°C.

Para la preparación de AC-K o AC-Na se dispone de hidróxido de potasio o hidróxido de sodio en lentejas suministradas por Scharlau. Estas lentejas se muelen y se mezclan con la LK_d de acuerdo con la relación R que se desee.

En este caso, no existe una etapa de impregnación y la mezcla se introduce directamente en un reactor horizontal de acero inoxidable y de diámetro interno de 5 cm situado en un horno eléctrico que posee tres zonas de calentamiento independientes controladas por termopares (ver *Figura 4.4*). También se dispone de un termopar situado en el interior del reactor en la zona de reacción, que controla el calentamiento del horno. Mediante un programador automático, se introducen los valores de temperatura de carbonización, tiempo de activación y velocidad de calentamiento. El caudal de nitrógeno en el interior del reactor se controla con un rotámetro. Una vez alcanzada la temperatura de carbonización, esta se mantiene constante durante un tiempo de activación determinado.

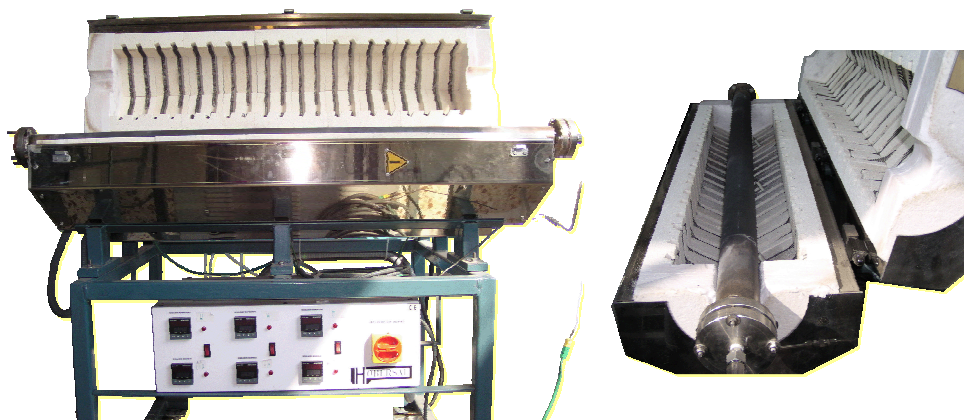


Figura 4.4. Detalle del reactor horizontal empleado, horno eléctrico y panel de control de las condiciones de operación.

Pasado el proceso de carbonización, el CA se expone durante 24 horas a una atmósfera de aire para que se lleve a cabo la oxidación de los restos de sodio o potasio metálico que permanecen en la muestra. Pasado este tiempo, el carbón activo obtenido se lava con 150 ml de HCl 1N para eliminar el exceso de agente activante que pueda quedar y posteriormente se realizan lavados con agua MilliQ hasta neutralizar el pH, medido con un pH-ímetro CyberScan PC 510 con un electrodo Hamilton “Flushtrode”. Finalmente, se seca la muestra durante 12 horas en una estufa a 110°C y se almacena en un bote de tapa roscada de cristal. Estas etapas se detallan básicamente en la *Figura 4.5*.

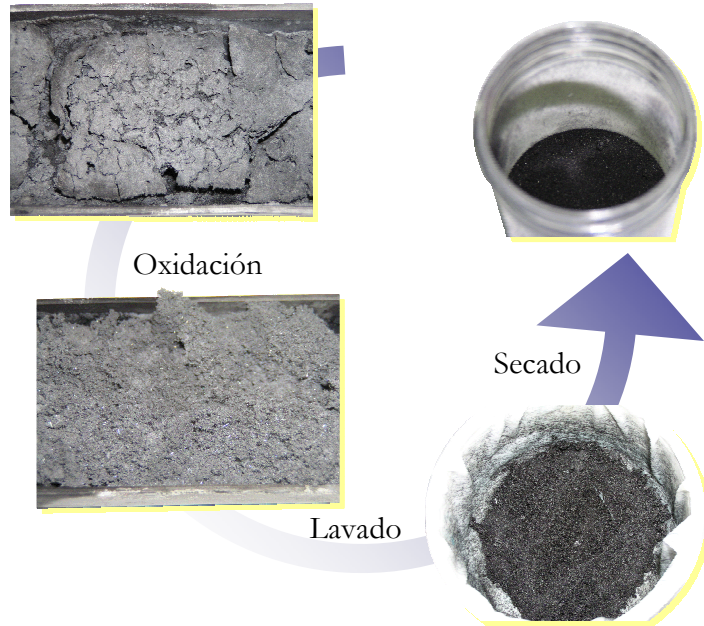


Figura 4.5. Tratamiento realizado al CA obtenido: oxidación, lavado y secado.

La preparación de los carbones se ha realizado a partir de un carbón base que se ha establecido según datos bibliográficos con la premisa de maximizar el área superficial. Estas condiciones de operación se han determinado en base a cinco parámetros centrales de estudio para el caso de la activación con hidróxidos, tal y como se muestra en la siguiente tabla.

Tabla 4.1. Condiciones de operación para el AC-K, AC-Na y AC-P base.

CA	T_a^{18} (°C)	t_p^{19} (h)	R^{20} (%/w)	P/L^{21} (%/w)	$Q_{N_2}^{22}$ (ml N ₂ /min)	r^{23} (°C/min)
AC-Na y AC-K	700	1	3/1	-	200	5
AC-P	450	1	-	1.4/1	-	-

¹⁸ T_a : temperatura de pirólisis

¹⁹ t_p : tiempo de activación

²⁰ R: relación agente activante – LK_d

²¹ P/L: relación agente activante – LK

²² Q_{N_2} : caudal de la atmósfera de nitrógeno durante los experimentos

²³ r: velocidad de calentamiento

En el caso de la activación con ácido fosfórico (AC-P), los parámetros a estudiar han sido tres ya que los experimentos se han realizado en atmósfera estática de aire.

A partir de este carbón base, se han realizado variaciones de un parámetro manteniendo el resto de variables constantes. Los rangos estudiados en los AC-P y AC-K y AC-Na han sido:

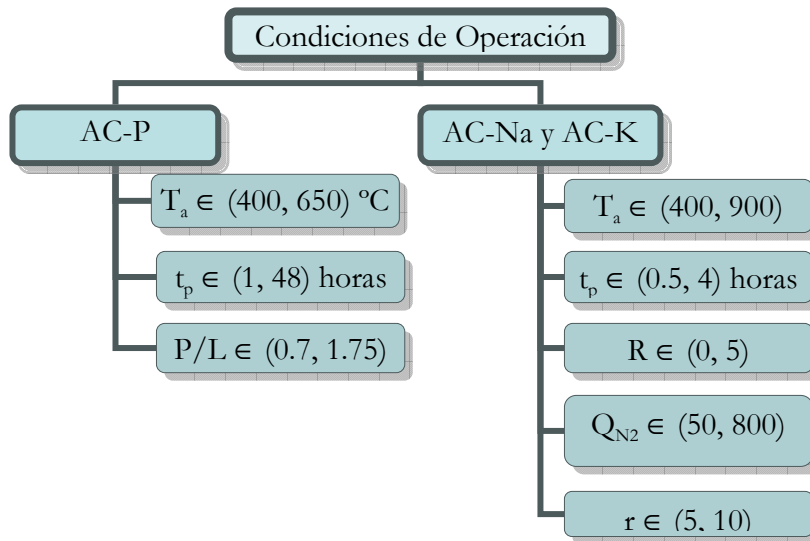


Figura 4.6. Resumen de las condiciones de operación para la producción de CA.

4.3. Caracterización de carbones activados

Una vez obtenido el carbón, se realiza la caracterización del material al objeto de conocer la mayor cantidad de sus propiedades fisicoquímicas.

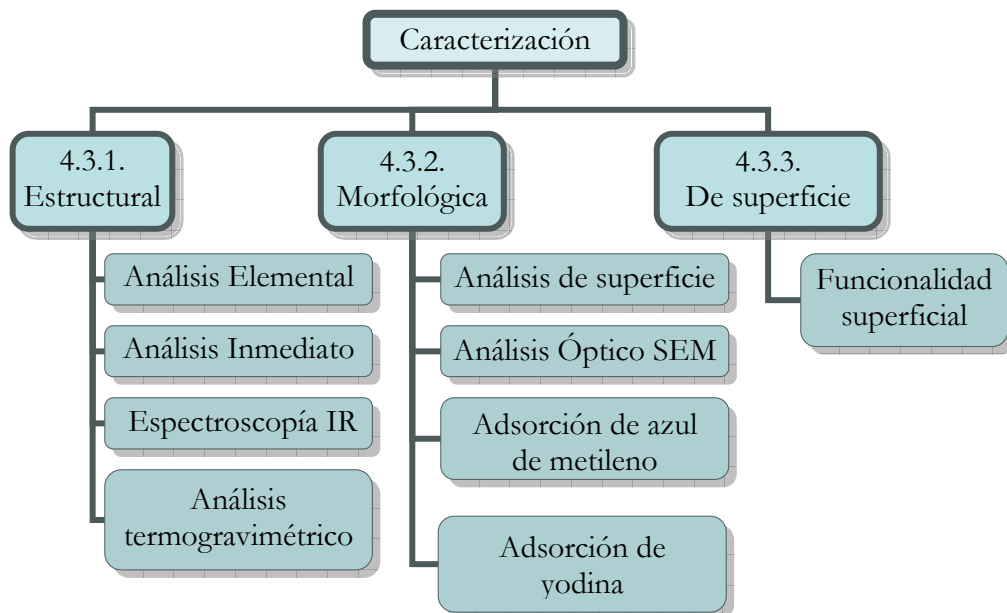


Figura 4.7. Esquema de la etapa de caracterización de CA (etapa 2).

A parte de los análisis que se detallan en la figura anterior, se han realizado estudios termogravimétricos en los AC-P con el objetivo de determinar los mecanismos de activación que tienen lugar y de esta manera adquirir una mayor comprensión sobre la transformación del material y el desarrollo de su porosidad, así como la influencia de ciertas condiciones de operación en el CA final.

4.3.1. Composición química y caracterización estructural

Estos tipos de análisis son complementarios a los resultados de los análisis de los otros dos bloques explicados anteriormente.

4.3.1.1. Análisis Elemental

Fundamento

El análisis elemental es una técnica que proporciona el contenido total de carbono, hidrógeno, nitrógeno y azufre presente en un amplio rango de muestras de naturaleza orgánica e inorgánica tanto sólidas como líquidas, con cantidades relativamente pequeñas de muestra (2-3 mg). La técnica está basada en la completa e instantánea oxidación de la muestra mediante una combustión con oxígeno puro a una temperatura aproximada de 1000°C. Los diferentes productos de combustión CO_2 , H_2O y N_2 , son transportados mediante el gas portador (He) a través de un tubo de reducción para una posterior separación selectiva en columnas específicas y luego desorbidos térmicamente. Finalmente, los gases pasan de forma separada por un detector de conductividad térmica que proporciona una señal proporcional a la concentración de cada uno de los componentes individuales de la mezcla.

Los campos de aplicación de esta técnica son diversos, desde el análisis de combustibles fósiles (carbón, coque, gasolina, aceite minerales, gasoil, etc.) hasta la industria farmacéutica y la química fina, pasando por el análisis de suelos, industrial alimenticia, cerámicas, etc.

Equipamiento

El equipo empleado en este tipo de análisis es un analizador Carlo Erba Elemental Analyser modelo CHNS-O EA1108.



Figura 4.8. Analizador elemental Carlo Erba modelo CHNS-O EA1108, provisto de automuestrador.

El análisis elemental de los CA preparados ha sido útil para poder identificar qué compuestos se forman en las condiciones de operación establecidas. De esta manera, se puede observar el desarrollo de propiedades como por ejemplo, la aromaticidad de los AC.

4.3.1.2. Análisis Inmediato

Fundamento

El análisis inmediato es una técnica desarrollada de acuerdo con los estándares ISO^[69] para la determinación de la humedad (110°C en nitrógeno), el contenido en volátiles (900°C en nitrógeno) y carbón fijo y cenizas (incineración a 900°C en aire) en termobalanza. Esta técnica se basa en la medida de la variación de la masa de una muestra cuando es sometida a un programa de temperatura en una atmósfera controlada.

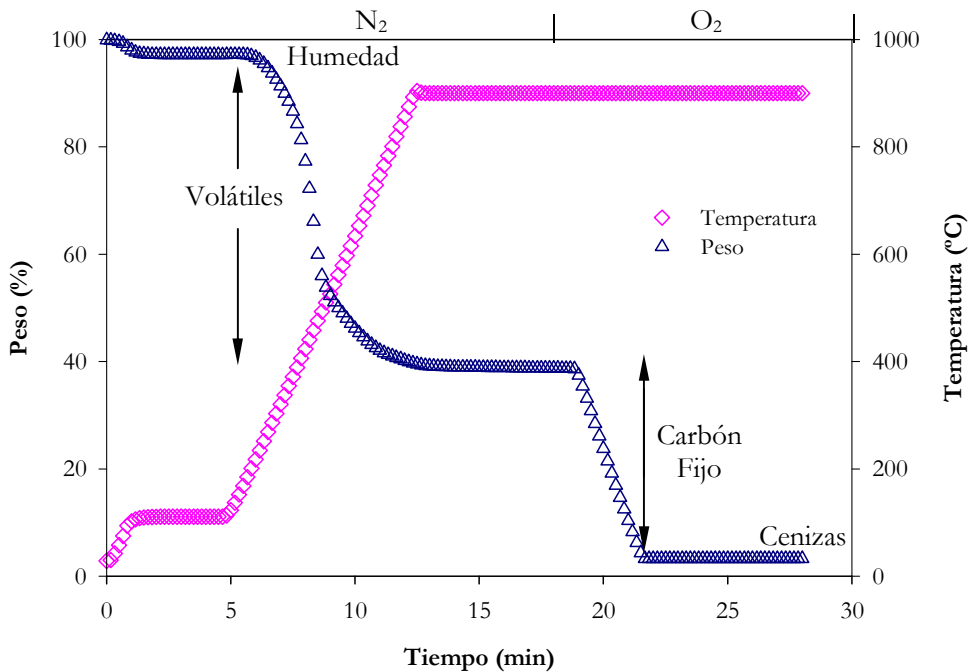


Figura 4.9. Proceso térmico para análisis inmediato (◇) y termograma ejemplo (△).

Todos estos parámetros son importantes para caracterizar el CA obtenido. El contenido en carbón fijo influye en la clasificación de los diferentes tipos de carbón. La turba, la primera etapa en la formación de carbón, tiene un bajo

contenido de carbono fijo y un alto índice de humedad. El lignito, el carbón de peor calidad, tiene un contenido de carbono mayor. El carbón bituminoso tiene un contenido aún mayor, por lo que su poder calorífico también es superior. La antracita o hulla seca, es el carbón con el mayor contenido en carbono y el máximo poder calorífico. La presión y el calor adicionales pueden transformar el carbón en grafito, que es prácticamente carbono puro.

Equipamiento

Este análisis termogravimétrico se ha realizado en una termobalanza Perkin Elmer TGA – 7 con un tiempo de duración aproximado de 30 minutos.



Figura 4.10. Termobalanza Perkin Elmer TGA – 7.

Los análisis inmediatos de las materias primas y los CA preparados han sido útiles para poder determinar las propiedades mencionadas anteriormente ya que es importante para poder explicar datos obtenidos con el uso de otras técnicas de caracterización de los AC.

4.3.1.3. Espectroscopía IR

Fundamento^[70-77]

La espectroscopía infrarroja es una de las técnicas más versátiles para la caracterización cualitativa de materiales sólidos. Sin embargo, la información que aporta en materiales heterogéneos y de naturaleza polimérica es limitada ya que las bandas que aparecen en sus espectros son resultantes de la contribución de diversas especies moleculares con diferentes grupos funcionales y enlaces químicos.

El campo de aplicación de esta técnica es muy amplio ya que se pueden analizar todo tipo de sólidos y líquidos. El estudio de muestras sólidas que presentan dificultades para la preparación de soluciones o pulverización, y sólidos opacos en general se puede realizar utilizando una serie de accesorios comerciales e intercambiables como la reflexión total atenuada (ATR), reflectancia difusa (RRIFT) y detector fotoacústico (PAS). Los espectros de absorción obtenidos son similares y proporcionan la misma información que cuando se trabaja en transmisión. La utilización de este tipo de accesorios comerciales es muy ventajosa ya que permite que la técnica no sea destructiva, acepta formas irregulares de los sólidos, no altera la muestra y no requiere preparación de la muestra o bien ésta es mínima.

Equipamiento

Este análisis se ha llevado a cabo en un JASCO FT/IR-680 Plus que dispone de un ATR de diamante. Para ello, no ha sido preciso ningún tipo de pretratamiento de la muestra. El análisis se ha realizado en un rango de longitudes de onda comprendido entre 600 y 3700 cm^{-1} , con una resolución de 4 cm^{-1} realizando 400 escaneos por análisis y con una velocidad del espejo de 2 mm/s .

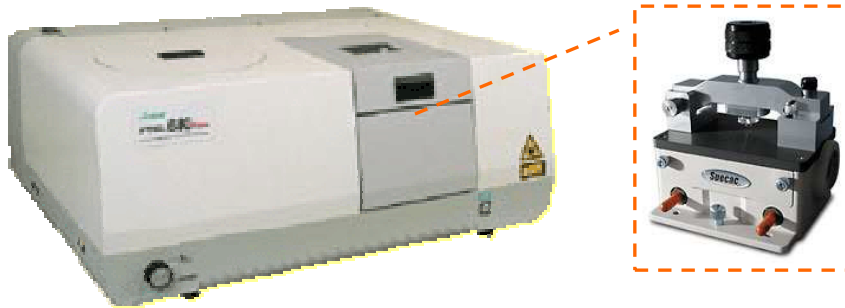


Figura 4.11. Equipo de infrarrojo Jasco FT/IR-680 Plus y detalle del accesorio ATR.

El análisis IR realizado a la materia prima y a los CA preparados, es un análisis complementario a las valoraciones de Boehm para la determinación de grupos superficiales. La realización de estos análisis a la materia prima proporciona espectros con gran cantidad de información debido a la complejidad de la estructura de la lignina^[58]. Sin embargo, el uso de esta técnica en CA^[37, 47, 78-81] tiene complicada interpretación debido al severo tratamiento térmico realizado a las muestras aunque la información obtenida complementa a los datos obtenidos por otras técnicas.

En el caso de los espectros presentados en la siguiente figura, se observa como evolucionan los grupos superficiales del AC-Na a medida que varía la temperatura del proceso de pirólisis, mediante las bandas o picos presentes entre 2000 y 1000 cm^{-1} . La ventaja de este análisis radica en la sencilla apreciación de este tipo de efectos y su rápida obtención ya que la adquisición del espectro no es mayor a 15 minutos.

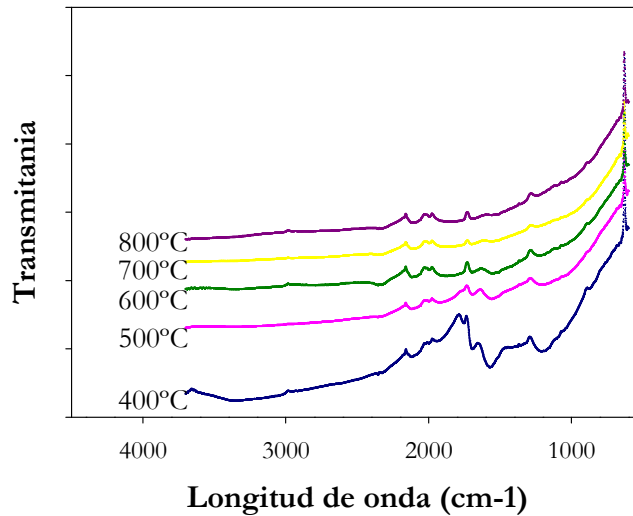


Figura 4.12. Ejemplo de espectro obtenido por IR para AC-Na preparados a temperaturas entre 400°C y 800°C.

4.3.2. Morfología y caracterización textural

4.3.2.1. Adsorción de nitrógeno

Fundamentos^[82-87]

El método de análisis de superficie BET es una técnica que permite evaluar la porosidad total de la muestra y la distribución del tamaño de poro (ver *Figura 4.13*), basándose en la adsorción de un gas inerte a baja temperatura sobre una superficie sólida. En el caso de muestras con una superficie específica expuesta igual o superior a 1.0 m^2/g , el gas analítico utilizado es nitrógeno o dióxido de carbono, en cambio, para materiales con superficies específicas inferiores, el gas utilizado es criptón.

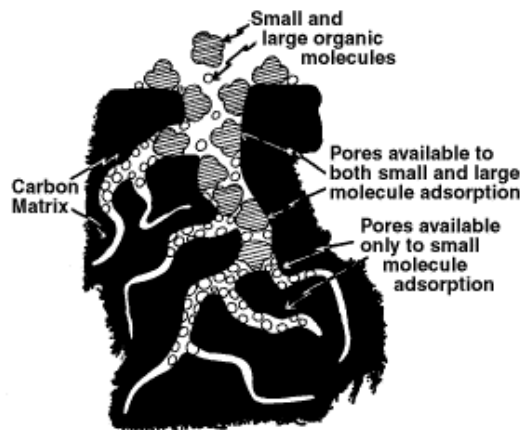


Figura 4.13. Diferentes tipos de porosidad presente en el carbón activado.

Esta técnica es de aplicación importante en productos desarrollados para la industria farmacéutica, cerámicas, materiales catalizadores, refractarios, porosos o microporosos y carbones activos dado que gran parte de la aplicación final dependerá de esta propiedad.

Equipamiento

El equipo empleado es un Micromeritics ASAP 2020 con el que se obtiene la isoterma de adsorción y desorción de nitrógeno a 77K. En una primera etapa, las muestras se desgasifican a 523K durante varias horas para posteriormente estudiar la adsorción de nitrógeno en dos rangos de presiones. En el primer rango, P/P_0 es inferior a 10^{-3} y se aplica el modelo de Horvath-Kawazoe para obtener la distribución de tamaño de microporo. Posteriormente, el rango de presiones estudiado está entre 10^{-5} y 0.99, donde los datos obtenidos se analizan por

- el método BET^[84] para calcular el área superficial específica,
- la ecuación de Dubinin- Radushkevich^[84] para calcular el volumen de microporo, la energía característica del nitrógeno respecto al carbón, y el tamaño promedio de los microporos,
- el método alfa-s^[84, 88] para calcular el volumen de ultramicroporo y el de microporo,
- el volumen total de poro calculado a una presión relativa de 0.99,
- el volumen de mesoporo calculado a partir de las diferencias entre el volumen total de poros y el volumen de microporo calculado por Dubinin- Radushkevich

En 1940, Brunauer, Deming, Deming y Teller, realizaron una sistematización de las isothermas de adsorción de gases basada en datos empíricos obtenidos con diferentes tipos de sólidos porosos y no porosos. La clasificación propuesta por estos autores se conoce como la clasificación BDDT y consta inicialmente de cinco tipos de isothermas aunque posteriormente se añadió una sexta, tal y como se muestran en la *Figura 4.14*.

Bajo estos seis tipos de isothermas es posible clasificar la mayoría de los sólidos de acuerdo con sus propiedades de adsorción. Los CA se ajustan mayoritariamente a la isoterma de tipo I^[84] por se representativas de sólidos microporosos. Este tipo de isoterma se llama también de Langmuir y es característica de sólidos microporosos donde se observa que el proceso de adsorción tiene lugar fundamentalmente a bajas presiones relativas, cuando se produce el llenado de los microporos con el adsorbato. A presiones relativas más altas, la cantidad adsorbida se mantiene constante o aumenta ligeramente si existen suficientes mesoporos. Este tipo de isoterma puede ser debida a la existencia de quimisorción, adsorción en microporos, adsorción en disolución o adsorción física en superficies muy homogéneas. En este último caso se obtiene la isoterma de tipo IV al aumentar la presión. En estos casos, la capacidad de la monocapa puede obtenerse directamente de los datos experimentales o aplicando el modelo de Langmuir.

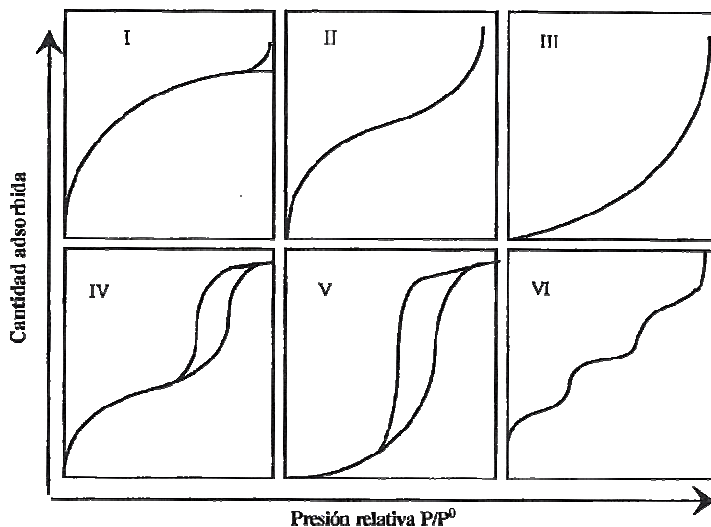


Figura 4.14. Isothermas de adsorción de nitrógeno a 77K según la clasificación BDDT^[84].

La isoterma de tipo II corresponde a adsorción en mono-multicapas, en sólidos no porosos o macroporos, que presentan heterogeneidad superficial. A este tipo de datos experimentales se aplica la teoría de BET.

La isoterma de tipo III aparece cuando la interacción adsorbato/adsorbente es débil, menor que la existente entre las moléculas de adsorbato. En este caso, es preferible cambiar de adsorbato.

La isoterma de tipo IV es similar a la de tipo II en la zona de presiones bajas e intermedias, por lo que también se le aplica el modelo BET. La diferencia entre ambas está en que la presencia de mesoporosidad no aparece hasta presiones relativas superiores a 0.4. En este tipo de isotermas existe un ciclo de histéresis debido a que los procesos de condensación y evaporación capilar transcurren por caminos diferentes.

Las isotermas de tipo V indican una adsorción débil al principio seguida de condensación capilar y lo indicado, al igual que en las isotermas de tipo III, es cambiar el adsorbato.

La isoterma de tipo VI aparece cuando se trata de adsorción en superficies muy homogéneas donde cada capa empieza a formarse cuando la anterior está ya prácticamente completa. En este caso, se puede obtener de manera directa el valor de la monocapa aunque no es un ejemplo habitual en la naturaleza.

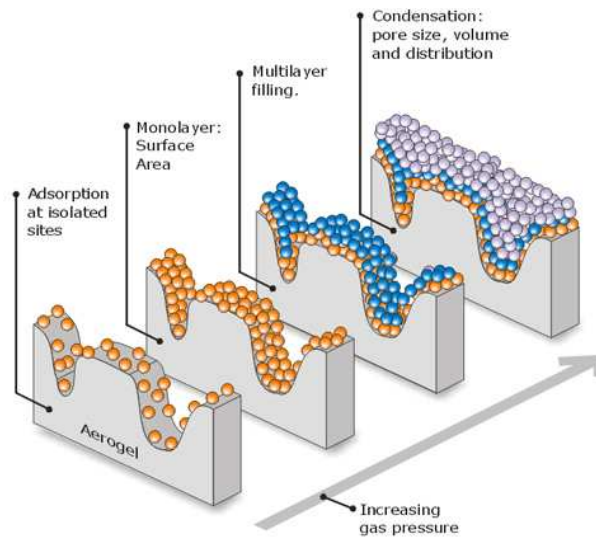


Figura 4.15. Llenado de poros de moléculas de adsorbato en función de la presión parcial^[89].

De estas isotermas puede obtenerse de manera directa o indirecta el valor de monocapa (ver *Figura 4.15*) que es útil para determinar el número de especies adsorbidas que la completan sobre la superficie pudiéndose ser relacionado con el área superficial del sólido mediante el área que ocupa la molécula. Lo más sencillo es determinar la monocapa de moléculas directamente pero debido a que la adsorción en la segunda capa se da sin haberse completado la primera, es necesario el empleo de modelos, siendo el más utilizado el de BET.

La diferencia entre el diámetro de los mesoporos²⁴ y el tamaño de las moléculas de adsorbato asegura un cubrimiento completo de la superficie. Este comportamiento no se corresponde en el caso de los microporos²⁵ debido a la existencia de impedimentos estéricos para cubrir la pared de poros de tamaño entre 0.6 y 1 nm. A partir de 1 nm si se recubre los poros pero el mecanismo que sigue la adsorción es el de llenado de microporos debido al aumento del potencial de adsorción lo cual no permite la formación de la monocapa.

A continuación, en la *Figura 4.16* se muestra una isoterma experimental de adsorción y desorción que se corresponde al tipo I, la cual se ajusta de manera bastante precisa al modelo, presentando escasa histéresis en la etapa de desorción.

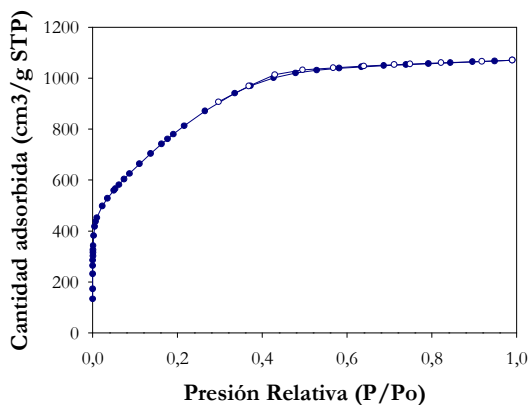


Figura 4.16. Ejemplo de isoterma experimental de adsorción (●) y desorción (○) para muestras microporosas obtenidas a partir de un carbón de lignina Kraft activado con hidróxido de potasio a 750°C.

²⁴ Poros de diámetro entre 2 y 50 nm.

²⁵ Poros de diámetro inferior a 2 nm.

Este tipo de análisis es una parte muy importante de la caracterización de CA ya que se puede deducir diversas propiedades texturales. El equipo empleado para la realización de este estudio es un Micromeritics ASAP 2020 (ver *Figura 4.17*).



Figura 4.17. Equipo de medida de superficie ASAP 2020.

4.3.2.2. Análisis Óptico: SEM

Fundamentos

Cuando un haz de electrones incide sobre la superficie de un sólido, tienen lugar varios fenómenos: reemisión de una parte de la radiación incidente, emisión de luz, electrones secundarios y Auger, rayos X, etc. Todas estas señales se pueden emplear para obtener información sobre la naturaleza de la muestra (morfología, composición, estructura cristalina, estructura electrónica, etc.). Las imágenes que se obtienen en el microscopio electrónico de barrido corresponden a electrones secundarios o electrones retrodispersados emitidos tras la interacción con la muestra de un haz incidente de entre 5 y 30 KeV.

Las aplicaciones de la técnica son muy numerosas tanto en Ciencia de Materiales, como en Ciencia Biomédica. Dentro de la Ciencia de Materiales destacan las aplicaciones en metalurgia, petrología y mineralogía, materiales de construcción, materiales cerámicos tradicionales y avanzados, electrónica, fractografía y estudio de superficies y composición elemental de sólidos en general. La microscopía electrónica de barrido también se aplica en botánica, en el estudio de cultivos celulares, en dermatología, en odontología y biomateriales, en hematología, inmunología y en el estudio de la morfología de preparaciones biomédicas en general y de sólidos porosos.

Equipamiento

El microscopio utilizado es un JEOL JSM-6400 (ver *Figura 4.18*), el cual consta de un detector de electrones retrodispersados con resolución de 3.5, donde la fotografía puede tomarse con 360° de rotación e inclinando la muestra hasta 90° y de un microanalizador de energía dispersiva de rayos X.

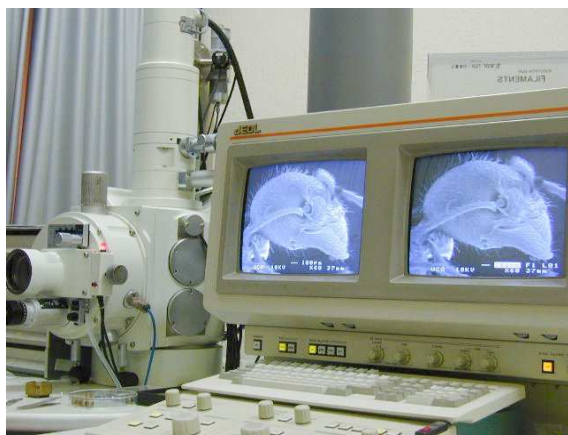


Figura 4.18. Equipo de microscopía electrónica de barrido (SEM).

4.3.3. Química de superficie

Fundamentos^[90-95]

Casi todos los grupos funcionales orgánicos están presentes en la superficie del carbón activo. Los más frecuentes son los carboxílicos, hidroxifenólicos y carbonilos tipo quinona. Los presentes de menor medida son los éter, peróxido, éster en forma de lactonas normales o tipo cíclicos, anhídridos de ácidos carboxílicos, peróxidos cíclicos, entre otros.

Los grupos funcionales presentes en la superficie de carbones están sujetos a una gran variedad de interacciones inter e intramoleculares incluyendo efectos inductivos, mesoméricos, tautoméricos, estéricos y de puentes de hidrógeno. Estas interacciones pueden alterar severamente las características de un ácido/base de Brönsted de tal manera que puede no parecerse a compuestos químicos semejantes. La heterogeneidad en la superficie química hace difícil especificar la relación entre las funcionalidades superficiales del carbón con sus propiedades ácido-base ya que una distribución continua de las propiedades químicas superficiales (acidez, basicidad) se espera para cada tipo de grupo superficial (ácidos carboxílicos, fenoles, etc.) y en muchos

casos el pK dominante se puede solapar con varios grupos químicos diferentes.

Otro factor que afecta a la química de superficie de carbones es que sus propiedades son sensibles al oxígeno, la humedad y la luz y por tanto, pueden variar durante su almacenamiento.

De todas maneras, las propiedades ácidas o básicas de los carbones se puede modificar aplicando tratamientos superficiales apropiados que son la base de muchas aplicaciones industriales. Por tanto, conocer la química de superficie es importante para gran cantidad de procesos tecnológicos, no sólo para la catálisis heterogénea sino también en lubricantes, en la aplicación de gomas y elastómeros, en flotación, en tintas para imprimir, en aditivos textiles, etc.

Existen dos tipos de carbones clasificados según su comportamiento ácido-base, H y L, que se diferencian principalmente en que el pH del carbón H es de naturaleza más básica y los del tipo L más ácida.

En los carbones de tipo H no suele examinarse sus propiedades ácidas, fundamentalmente debido a la dificultad de mantener la superficie limpia una vez se expone al aire. En principio, su superficie está cargada positivamente y la adsorción de ácido que presenta en solución es el resultado de la adsorción específica de aniones en la superficie y subsiguiente adsorción secundaria de protones y cationes en la porción difusa de la doble capa eléctrica una vez en suspensión. Consecuentemente es muy difícil estudiar los grupos funcionales superficiales mediante interacciones ácido-base.

Por otro lado, los carbones de tipo L muestran un amplio rango de interacciones ácido-base que aparentemente proceden de fuerzas relativamente ácidas de los óxidos superficiales. H. P. Boehm empleó un número de bases de amplia gama de fuerzas para medir cuantitativamente e identificar cualitativamente los tipos de óxidos ácidos que están presentes en la superficie de los carbones L. Como bases tituladoras empleó bicarbonato de sodio (NaHCO_3), carbonato de sodio (Na_2CO_3), hidróxido de sodio (NaOH) y etóxido de sodio etanólico (NaOC_2H_5) de concentración 0.1N. Los pKa de los ácidos conjugados de estas bases son 6.37, 10.25, 15.74 y 20.58 respectivamente (ver *Figura 4.19*).

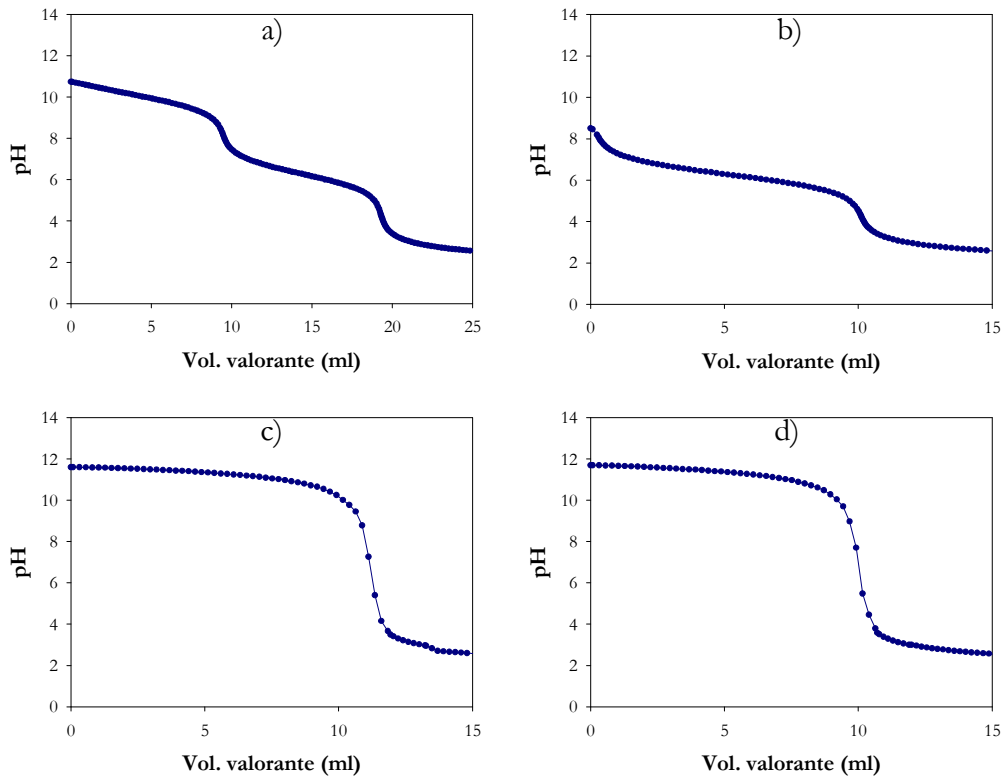


Figura 4.19. Curva obtenida en la valoración de: a) carbonatos, b) bicarbonatos, c) hidróxido de sodio y d) etóxido sódico.

En teoría, debería ser posible titular grupos ácidos con cada una de estas bases con valores de pK_a al menos 2-3 unidades menores que el ácido conjugado de la correspondiente base. Sin embargo, la presencia de un solvente necesario para la titulación puede afectar a la determinación de la acidez. En consecuencia debería ser posible titular óxidos superficiales ácidos de pK_a menores de 4.4, 8.2 y 10 en solución acuosa usando bicarbonato, carbonatos e hidróxido de sodio respectivamente, mientras que con etóxido etanólico será posible valorar estequiométricamente grupos ácidos superficiales con pK_a de 19.

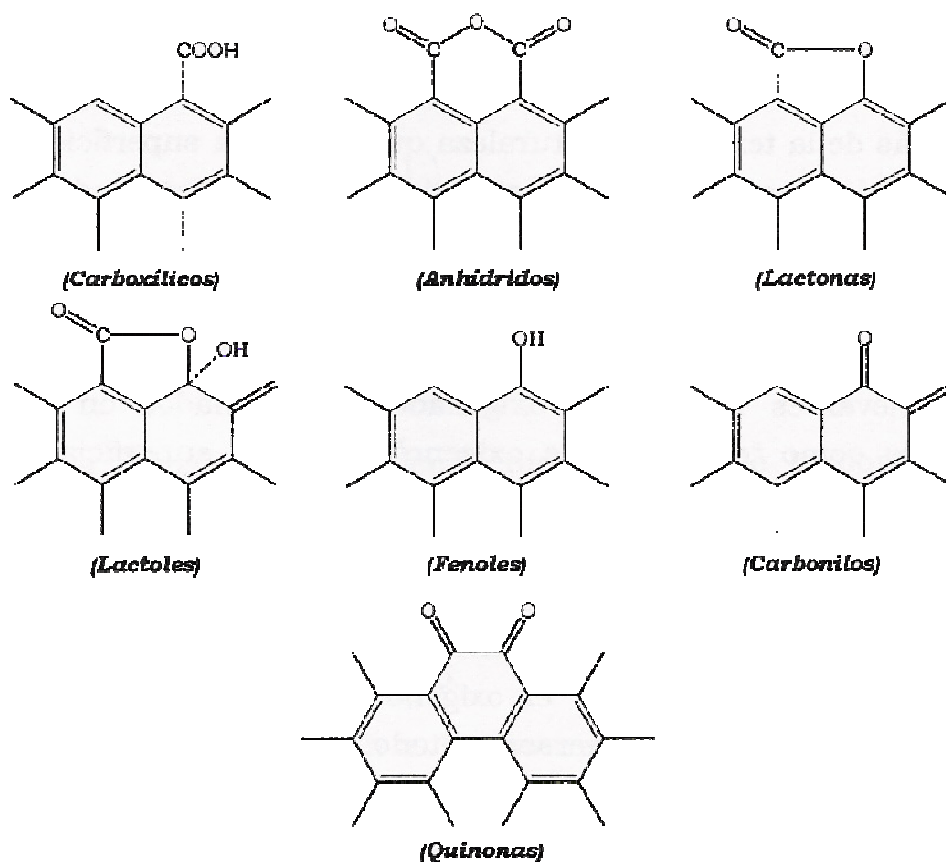


Figura 4.20. Estructuras propuestas para los grupos oxigenados ácidos más representativas de la superficie del CA^[90].

Está generalmente aceptado que NaHCO_3 neutraliza sólo grupos carboxilos, Na_2CO_3 valora grupos carboxilos y lactonas y NaOH neutraliza carboxilos, lactonas y grupos fenólicos (ver *Figura 4.20*). Para la determinación de la basicidad superficial dada por los grupos funcionales presentados en la *Figura 4.21* se utilizará HCl 0.05 N.

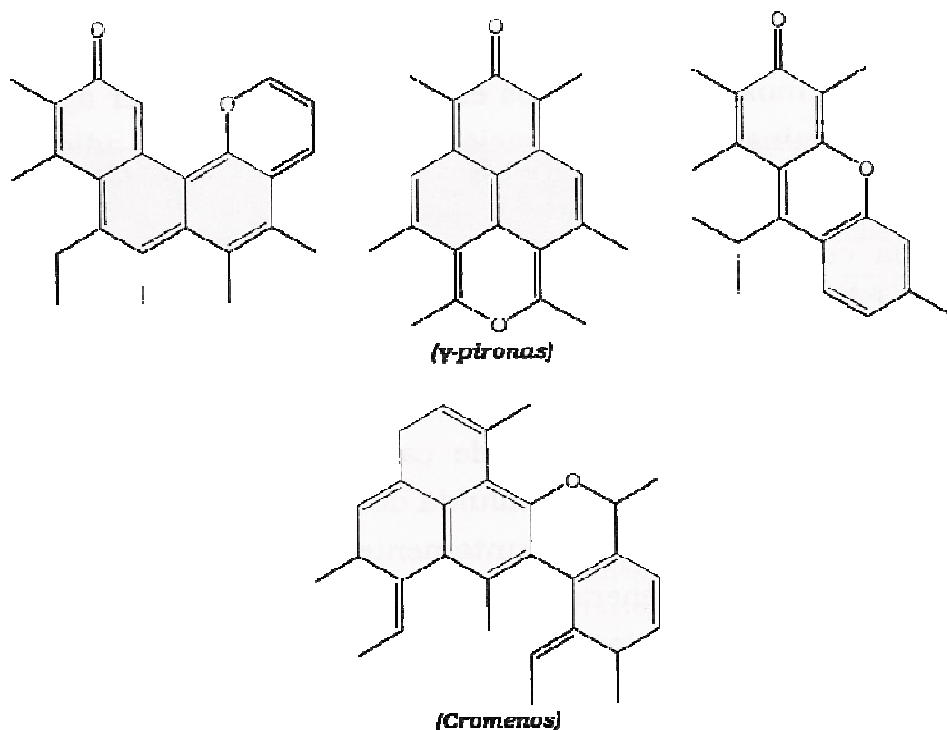


Figura 4.21. Posibles estructuras de los grupos oxigenados básicos más representativas de la superficie del CA^[95].

Equipamiento

El equipo utilizado para llevar a cabo esta serie de valoraciones ha sido un valorador automático CRISON Compact Titrator Versión D con electrodo para soluciones acuosas CRISON (ver *Figura 4.22*).

La solución valorante empleada para determinar la cantidad de grupos ácidos superficiales (ver *Figura 4.20*) fue HCl 0.05 N mientras que la cuantificación de la basicidad total superficial (ver *Figura 4.21*) se realizó con NaOH 0.1 N.

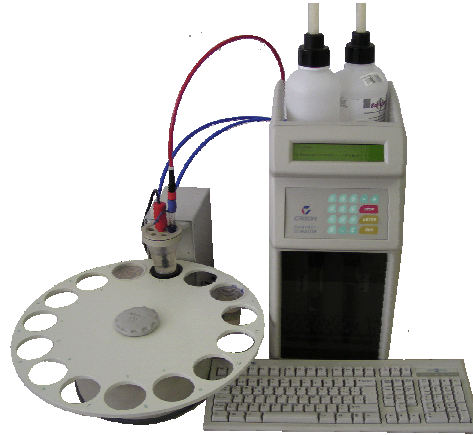


Figura 4.22. Valorador automático CRISON Compact Titrator Versión D.

Por otro lado, diferentes autores recomiendan el uso de técnicas complementarias a la valoración química de Boehm ya que establecen la dificultad de usarla cuando la granulometría de la muestras es muy pequeña y proponen el uso complementario de diferentes técnicas. Por ejemplo, XPS daría un valor aproximado de la composición química de las capas más superficiales del material. Otra técnica adicional sería la espectroscopía IR aunque solo puede ser aplicada a carbones altamente oxidados, es decir, de gran funcionalidad dado que las bandas de absorción no serían de suficiente intensidad.



Figura 4.23. Equipo para análisis de TPD Termo Finnigan modelo TPDR 1100 (izquierda) conectado a un analizador de masas Pfeiffer Vacuum Omnistar modelo GSD 301 O (derecha).

Aunque de todas las técnicas propuestas, Figueiredo^[96, 97] recomienda el uso de métodos de temperatura programada con la que los grupos oxigenados que se encuentran en la superficie se descomponen al calentar en forma de CO y CO₂. Así que se puede relacionar los picos obtenidos por TPD con los grupos superficiales específicos, si bien éstos pueden verse afectados por la textura del material, la velocidad de calentamiento establecida en el experimento y la geometría del sistema experimental utilizado, mediante un TPD conectado en serie con un analizador de masas (ver *Figura 4.23*).

4.3.4. Análisis de adsorción

A la hora de comprobar el comportamiento de los CA preparados, las pruebas realizadas se han basado en la adsorción de contaminantes en efluentes líquidos.

4.3.4.1. Adsorción de azul de metileno

Fundamentos

El método de adsorción de azul de metileno se basa en la isoterma de adsorción de un solo punto para azul de metileno en un medio de ácido acético diluido^[98]. El resultado se expresa en gramos de azul de metileno adsorbidos por 100 gramos de carbón.

El azul de metileno es el compuesto de mayor uso en la evaluación del poder decolorante del carbón activado y su adsorción es indicia de la presencia de macro y mesoporos debido al gran tamaño de esta molécula, la cual es aproximadamente 1.5 nm.

Equipamiento

El equipo utilizado para el análisis de muestras por colorimetría es un espectrofotómetro UV-VIS 8500 de Dinko Instruments que dispone de una lámpara de tungsteno que se utiliza para el análisis de muestras a una longitud de onda de 664.8 nm (ver *Figura 4.24*).

El análisis se ha realizado introduciendo 33.7 mg de CA en base seca con una precisión de 0.1 mg en un bote de plástico con tapa roscada de 50 ml. Posteriormente se ha añadido 50 ml de solución de azul de metileno 3.2 mM, se tapa el bote y se deja agitando la suspensión durante al menos 24 horas. Pasado este tiempo, se filtra la mezcla por gravedad con un papel de poro

medio en un vaso de precipitado limpio y seco, descartando los primeros 5 ml, y del filtrado posterior obtenido, se realizan las diluciones necesarias para que la concentración esté en el rango de medida del aparato utilizado.

La medida de la concentración de orgánico se realiza mediante el espectrofotómetro de la figura anterior, donde también se miden los blancos y los patrones. La cantidad adsorbida se calcula por diferencia entre el valor inicial y el final.

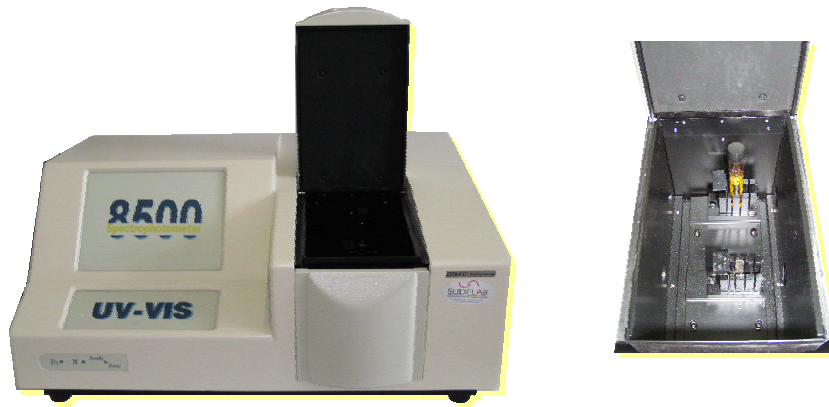


Figura 4.24. Espectrofotómetro Dinko Instruments UV-VIS 8500 y detalle de su interior.

4.3.4.2. Adsorción de yodina

Fundamentos

El número de yodo $\left(\frac{X}{M}\right)$ es un indicador relativo de la porosidad en el carbón activo aunque no da necesariamente una medida de la habilidad del carbón para absorber otras especies, como en el caso de la adsorción de azul de metileno. La adsorción de yodo se realiza con el propósito de establecer la capacidad de los carbones activados preparados por activación química, de adsorber moléculas no polares de diámetro pequeño. El número de yodo se puede utilizar como una aproximación del área superficial, en especial con el volumen de microporos^[99], para algunos tipos de carbones activados aunque su relación no puede generalizarse. Ésta varía con el cambio de materia prima del CA, las condiciones de trabajo y la distribución de volumen de poro.

Éste método se basa en la obtención de una isoterma de adsorción de tres puntos^[100, 101] que se obtiene a partir de la utilización de una solución de yodo

de concentración conocida que se pone en contacto con tres cantidades de CA bajo condiciones de trabajo específicas. Esta suspensión se filtra y se mide la concentración de yodina en la solución restante mediante espectrofotometría.

Equipamiento

El equipo utilizado para el análisis de muestras por colorimetría es un espectrofotómetro UV-VIS 8500 de Dinko Instruments (ver *Figura 4.24*) que dispone de una lámpara de tungsteno que se utiliza para el análisis de muestras a una longitud de onda de 458.4 nm.

El análisis se ha realizado pesando diferentes cantidades de CA (por ejemplo, 0.1, 0.2, 0.3, 0.4 y 0.5 g) en base seca con una precisión de 0.1 mg en un erlenmeyer de cristal limpio y seco. Posteriormente se ha añadido 50 ml de solución de yodina 0.1 N (0.05 M), se tapa el erlenmeyer con parafilm y se deja agitando la suspensión durante al menos 24 horas a oscuras. Pasado este tiempo, se filtra la mezcla por gravedad con un papel de poro medio en un vaso de precipitado limpio y seco y del filtrado obtenido, se realizan las diluciones necesarias para que la concentración esté en el rango de medida del aparato utilizado.

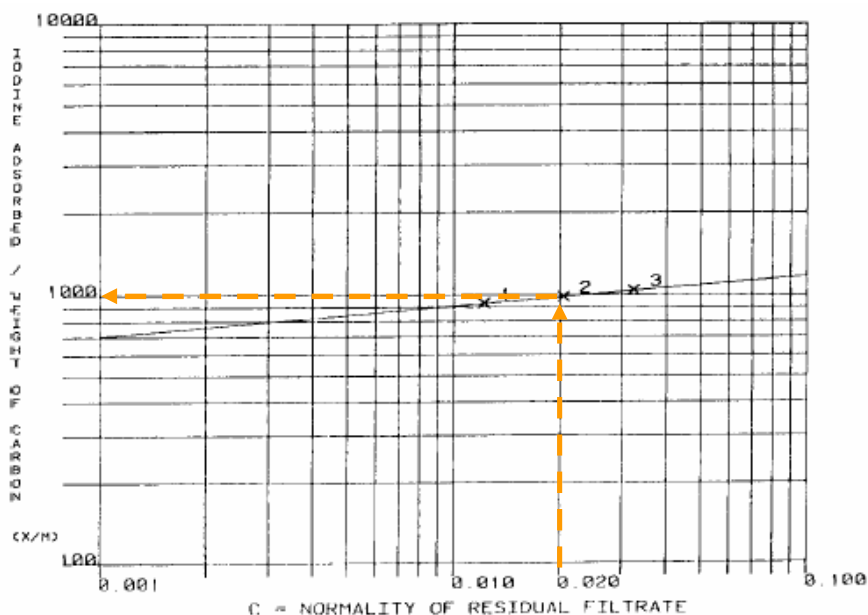


Figura 4.25. Ejemplo de isoterma de adsorción de yodo en CA^[102].

La medida de la cantidad de orgánico por gramo de CA se realiza mediante el espectrofotómetro de la *Figura 4.24*, utilizando como blanco agua MilliQ y donde también se miden los patrones de diferentes concentraciones dentro del rango de linealidad. De las muestras preparadas no solo se mide el número de yodo, sino también un parámetro llamado normalidad del filtrado residual (C). A partir de los datos de X/M y C se realiza una regresión lineal y el valor final para el número de yodo se obtiene cuando C es de $0.02N^{[102]}$, tal y como se muestra en la *Figura 4.25*.

4.3.4.3. Determinación de metales

Fundamentos

En el caso de la adsorción de metales, la técnica utilizada ha sido la absorción atómica ya que permite la determinación cuantitativa de la mayoría de los elementos de la tabla periódica en una gran variedad de muestras. La cuantificación se basa en la absorción de la luz por los átomos del metal en estado fundamental. Esta técnica está especialmente indicada para determinar elementos alcalinos, alcalinotérreos y metales pesados presentes en cualquier tipo de muestra previamente disuelta. El rango de análisis está entre tantos por cientos y partes por billón (1 mg/tonelada).

Equipamiento

El equipo utilizado para determinar la cantidad adsorbida de cobre es un sistema de Absorción Atómica Perkin Elmer 3110 (ver *Figura 4.25*) a una longitud de onda de 216.5nm.

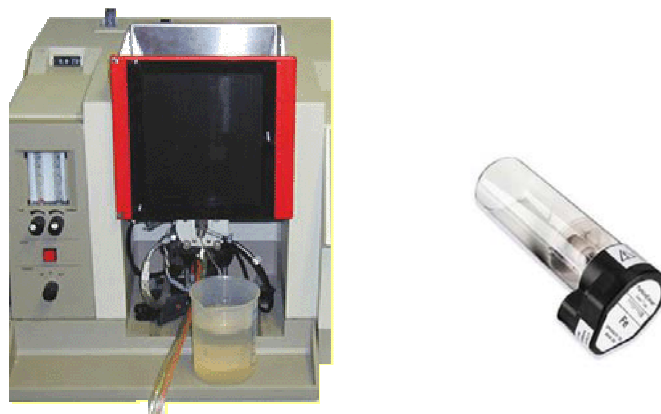


Figura 4.26. Equipo de Absorción Atómica para la determinación de cobre (II) y lámpara específica.

Los experimentos se han realizado en sistemas batch mediante la utilización de 18 erlenmeyers. Cada uno de ellos contiene 150 mg de CA en suspensión con 150 ml de agua desionizada y diferentes cantidades de cloruro de cobre (II), suministrado por Aldrich, se añaden a cada frasco. El pH inicial de cada frasco se ajusta a 5 mediante la adición de NaOH 0.1N y se deja en agitación durante 24 horas a 25°C, tal y como se muestra en la figura siguiente.



Figura 4.27. Sistema de análisis empleado para la adsorción de metales.

La concentración final de cobre se analiza mediante el equipo mencionado y la cantidad adsorbida se calcula por diferencia entre el valor inicial y el final.

4.3.4.4. Determinación de componentes orgánicos

Fundamentos

Por otro lado, también se ha analizado la adsorción^[103] de componentes orgánicos como el fenol^[4, 22, 104-162] y el benceno^[139, 162-164] mediante cromatografía de líquidos. Estos compuestos se han escogido como representantes de los contaminantes orgánicos más comunes en los efluentes industriales. En la actualidad, esta técnica de separación es la más extendida utilizada debido a su versatilidad y amplio campo de aplicación. Los componentes de la muestra, previamente disueltos en un disolvente adecuado (fase móvil), son forzados a atravesar la columna cromatográfica gracias a la aplicación de altas presiones. El material interno de la columna, fase estacionaria, está constituido por un relleno capaz de retener de forma selectiva los componentes de la mezcla. La resolución de esta separación depende de la interacción entre la fase estacionaria y la fase móvil, pudiendo

ser manipulada a través de la elección de diferentes mezclas disolventes y distintos tipo de relleno. Como resultado final los componentes de la mezcla salen de la columna separados en función de sus tiempos de retención en lo que constituye el cromatograma. A través del cromatograma se puede realizar la identificación cualitativa y cuantitativa de las especies separadas.

El campo de aplicación de esta técnica es muy extenso, pudiendo tratar productos farmacéuticos (antibióticos, sedantes, esteroides, analgésicos), bioquímicos (aminoácidos, proteínas, carbohidratos, lípidos), alimentarios (edulcorantes artificiales, antioxidantes, aditivos), contaminantes (plaguicidas, herbicidas, fenoles, PCBs), en química forense (drogas, venenos, alcohol en sangre, narcóticos) y en medicina clínica (ácidos biliares, metabolitos de drogas, extractos de orina, estrógenos).

Equipamiento

En este caso, el análisis se ha llevado a cabo en un cromatógrafo de líquidos de alta precisión Agilent 1100 Series dotado de una columna Hypersil ODS 250 mm y utilizando como fase móvil acetonitrilo/agua en una proporción 65/35. A estas condiciones, los tiempos de residencia de los compuestos orgánicos estudiados son 1.5 minutos para el fenol y 2.5 minutos para el benceno.



Figura 4.28. HPLC: Cromatógrafo de líquidos Agilent 1100 Series.

Adsorción de componentes orgánicos

Para realizar este análisis se ha añadido 10 mg de CA a un bote de cristal con tapón roscado que contenía 10 ml de una disolución de 100 ppm de benceno o fenol preparada con agua ultrapura procedente de un equipo de Milli-Q Millipore alimentado con agua destilada. Cada muestra se preparará por triplicado así como también se preparará por triplicado un blanco sin CA.

Cada frasco se tapa bien y se deja agitando durante 48 horas, tiempo suficiente para alcanzar el equilibrio, a una temperatura constante de 25°C en un baño térmico. Las muestras se colocan perpendicularmente sobre un eje de rotor que gira a una velocidad de 2 rpm. La temperatura se controla mediante un regulador electrónico digital de temperatura P>Selecta modelo Digiterm 100.

Posteriormente, se coge muestra suficiente con ayuda de una jeringuilla y una aguja y se pasa a través de un filtro de celulosa regenerada a un vial de 0.45 μm de tamaño de poro, el cual se tapa y se etiqueta. La medida de la concentración de orgánico se realiza mediante HPLC, donde también se miden los blancos y los patrones. La cantidad adsorbida se calcula por diferencia entre el valor inicial y el final.

Cinéticas de adsorción

Previamente al análisis de adsorción de fenol y benceno, se han realizado estudios cinéticos para determinar el tiempo de adsorción mínimo necesario para alcanzar el equilibrio. La preparación de las muestras se ha llevado a cabo de manera similar a los análisis de adsorción. En este caso, se preparan diferentes botes de cristal que contienen 10 mg de CA y 10 ml de la solución de orgánico recién preparada, tal y como se ha descrito anteriormente.

Todas las muestras se dejan en agitación durante un tiempo determinado hasta un máximo de 7 días y posteriormente la muestra se trata para el análisis, tal y como se ha descrito anteriormente. El equilibrio para el fenol se alcanza en 8 horas mientras que para el benceno, el equilibrio se alcanza a las 2 horas.

Isotermas de adsorción

De igual manera a los análisis de cinética de adsorción, se realizan las isotermas de los dos compuestos orgánicos estudiados. Para ello, diferentes cantidades de adsorbato (1-20 mg) se mezclan con 10 ml de solución contaminante recién preparada de fenol o benceno, a una concentración 100 ppm. Los tubos se tapan y se ponen en agitación durante 8 horas, asegurando así alcanzar el equilibrio establecido mediante los análisis cinéticos, a una velocidad rotatoria de 2 rpm. Una vez transcurrido el tiempo establecido, se toma muestra de cada uno de los botes de cristal y se analiza tal y como se ha realizado anteriormente, en los análisis de adsorción de componentes orgánicos, mediante HPLC.

4.4. Aplicaciones de los carbones activados

Una vez caracterizados, se pueden emplear en el campo de aplicación más adecuado. En este caso, ya que los CA obtenidos son microporosos, se usarán con el objetivo de adsorber metales pesados como el cobre y NOC de efluentes líquidos. Los NOC escogidos han sido fenol y benceno ya que en las últimas décadas la calidad de muchas aguas se ha visto afectadas por la creciente producción de productos químicos tales como pinturas, adhesivos, plásticos, etc. de los que se generan residuos que contaminan, no solo las aguas superficiales, sino también las subterráneas y estos dos componentes son representativos de esta familia de contaminantes.

Por otro lado, el CA también se ha utilizado para obtener membranas poliméricas compuestas, etapa previa a la obtención de reactores de membranas enzimáticos, utilizando el carbón inmovilizado en la matriz polimérica para adsorber enzimas directamente, o a través de un metal (cobre en este caso), considerando como base la técnica de cromatografía de afinidad con ión metálico inmovilizado (IMAC)^[165]. A pesar que existen muchos ámbitos de aplicación para este tipo de membranas, en este trabajo se han utilizado para obtener y separar azúcares de muy bajo peso molecular (cerca al del monómero) a partir de azúcares de tamaño superior.

5. DISCUSIÓN DE RESULTADOS

Una vez preparados y caracterizado los CA (Etapa 1 y 2) se han preparado una serie de artículos que han sido enviados a diferentes publicaciones. Posteriormente, y a partir de la caracterización realizada, los CA preparados en estas dos etapas se emplean en campos determinados, como la adsorción de componentes orgánicos en sistemas líquidos, y en casos más específicos, como por ejemplo, para la obtención de membranas poliméricas donde se retiene un enzima específica.

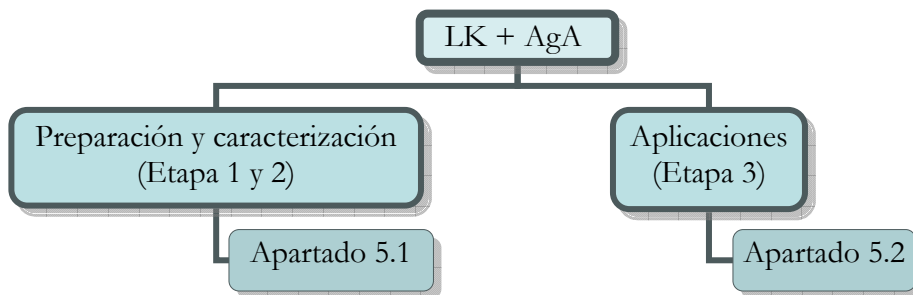


Figura 5.1. Resumen de los reports realizados a partir de la obtención de datos en las etapas 1, 2 y 3.

La lignina Kraft es un material poco utilizado en la preparación de CA, ya que normalmente se utilizan materiales que contienen este polímero pero no por separado. Por esta razón, el estudio de la activación química de la lignina es novedoso y se hace necesario el conocimiento, no tan sólo las características del producto obtenido, sino también por qué tienen lugar y de esta manera prever las características finales del producto con las condiciones de operación necesarias para obtenerlo.

En el caso de la activación química de la lignina Kraft con ácido fosfórico, en primer lugar es necesario conocer los fenómenos que tienen lugar durante la pirólisis y saber qué tipo de porosidad se desarrolla en la obtención de AC-P. En este caso, los estudios en termobalanza son muy útiles y gracias a los datos experimentales obtenidos se ha podido proponer un modelo cinético²⁶ que se ajusta a los escasos datos que se encuentran en la literatura.

Paralelamente al estudio cinético, es necesario conocer como afectan las condiciones de preparación de los AC-P en sus propiedades físico-químicas finales^{27,28}. Este punto es básico para el desarrollo de los objetivos que presenta esta memoria ya que poder prever las condiciones de operación en

²⁶ Montané, D.; Torné-Fernández, V.; Fierro, V.; Activated carbons from lignin: kinetic modelling of the pyrolysis of Kraft lignin activated with phosphoric acid. Chemical Engineering Journal, 2005. 106:p.1-12. (Ver *Apartado 5.1.1*).

²⁷ Fierro, V.; Torné-Fernández, V.; Montané, D.; Celzard, A.; Study of the decomposition of Kraft lignin impregnated with orthophosphoric acid. Thermochimica acta, 2005. 433:p.142-148. (Consultar *Apartado 5.1.2*).

²⁸ Fierro, V.; Torné, V.; Montané, D.; Salvadó, J.; Activated carbons prepared from Kraft lignin by phosphoric acid impregnation. Póster. Carbon. Oviedo (España). 2003. (Ver *Anexo B*).

el proceso de descomposición térmica de la lignina Kraft activada con ácido fosfórico a partir de las propiedades finales deseadas, conlleva un ahorro de tiempo y recursos muy importante. En concreto, parámetros tan importantes como el rendimiento a carbón, el área superficial y la distribución de tamaño de poros²⁹ son aspectos determinantes a la hora de escoger un sólido poroso para una aplicación determinada.

Por otro lado, las características de la materia prima que se utilizan también pueden afectar a las propiedades finales del AC-P³⁰. En concreto, el efecto de las cenizas³¹ que contiene la lignina Kraft, tal y como se suministra, en comparación con el uso de lignina Kraft desmineralizada, es decir, después de proceder a un pretratamiento ácido con el fin de disminuir el contenido en cenizas formadas por sales, afecta a su polimerización y puede reducir la interacción con el agente activante.

En el desarrollo de carbones activados con hidróxido de potasio^{32,33} y sodio³⁴ se ha desarrollado un incremento de interés, por esta razón estudiar la posibilidad de preparar CA microporosos a partir de lignina Kraft desmineralizada e hidróxidos estudiando, como en el caso anterior, el efecto de las condiciones de operación, es importante desde el punto de vista de desarrollar otra vía de producción de CA sin utilizar ácidos.

²⁹ Fierro, V.; Torné-Fernández, V.; Celzard, A.; Kraft lignin as a precursor for microporous activated carbons prepared by impregnation with ortho-phosphoric acid: synthesis and textural characterisation. *Microporous and mesoporous materials*, 2006. 92(1-3):p.243-250. (Consultar *Apartado 5.1.3*).

³⁰ Fierro, V.; Torné-Fernández, V.; Celzard, A.; Montané, D.; Influence of the demineralisation on the chemical activation of Kraft lignin with orthophosphoric acid. Enviado a *Journal of Hazardous Materials* (Mayo 2006). (Consultar *Apartado 5.1.4*).

³¹ Fierro, V.; Torné, V.; Celzard, A.; Influence of the ash content on the microporosity of activated carbons derived from Kraft lignin. Póster. *Carbon*. Corea. 2005. (Ver *Anexo G*).

³² Fierro, V.; Torné-Fernández, V.; Celzard, A.; Highly microporous carbons prepared by activation of Kraft lignin with KOH. *Studies in Surface Science and Catalysis*, 2005. 607-614. (Consultar *Apartado 5.1.5*).

³³ Fierro, V.; Torné-Fernández, V.; Celzard, A.; Highly microporous carbons prepared by activation of Kraft lignin with KOH. Póster. *7th International Symposium on the characterization of porous solids*. Aix-en-Provence (Francia). 2005. (Ver *Anexo E*).

³⁴ Fierro, V.; Torné-Fernández, V.; Celzard, A.; Methodical study of the chemical activation of Kraft lignin with KOH and NaOH. Enviado a *Microporous and Mesoporous Materials*, 2006. (Consultar *Apartado 5.1.6*).

Finalmente, una vez se tienen caracterizados los CA preparados por diferentes métodos, estos se pueden aplicar en el campo más adecuado. La principal aplicación de estos carbones está en la adsorción de diferentes tipos de compuestos contaminantes (componentes metálicos^{35,36,37}, componentes orgánicos de diferente polaridad^{38,39}, etc.) en sistemas líquidos ya que los carbones preparados son básicamente microporosos de áreas superficiales altas.

Sin embargo, estos carbones pueden tener otro campo de aplicación como es el de aditivo en membranas⁴⁰ para la obtención de reactores enzimáticos de membrana (EMR), a partir de una matriz polimérica (polisulfona) y la incorporación de carbón activado, el cual se usa para adsorber la enzima directamente o a partir de un metal, considerando las bases de la técnica IMAC^[165].

Por último, la experiencia ganada en el desarrollo de esta tesis ha permitido trabajar en otros trabajos que han consistido en la caracterización de carbones para la purificación de xilo-oligosacáridos⁴¹. Éste producto tiene

³⁵ Fierro, V.; Torné, V.; Montané, D.; García-Valls, R.; Removal of Cu (II) from aqueous solutions by adsorption on activated carbons prepared from Kraft lignin. Póster. Carbon 2003. 6-10 Julio, Oviedo (España). (Consultar *Apartado 5.2.1*, ver *Anexo C*).

³⁶ Novellon, E.; Fierro, V.; Torné, V.; García-Valls, R.; Montané, D.; Use of Kraft lignin for Cu (II) removal in industrial water. Póster. 9th Mediterranean Congress. Barcelona (Catalunya). 2002. (Ver *Anexo A*)

³⁷ Nastrunisku, G.; Fierro, V.; Torné, V.; García-Valls, R.; Montané, D.; Uptake of Cu (II) and Zn from aqueous solutions by Kraft lignin. Póster. 4th European Congress in Chemical Engineering. Granada (España). 2003. (Ver *Anexo D*).

³⁸ Torné-Fernández, V., Mateo, J. M., Montané, D., Fierro, V.; Optimization of the synthesis of highly microporous carbons by chemical activation of Kraft lignin with NaOH. Enviado a Chemical Engineering Journal, 2006. (Consultar *Apartado 5.2.2*).

³⁹ Torné-Fernández, V., Fierro, V.; Sorption study of organic compounds on highly microporous carbons prepared from Kraft lignin. Enviado al journal Adsorption Science and Technology, 2006. (Consultar *Apartado 5.2.3*).

⁴⁰ Torras, C.; Torné, V.; Fierro, V.; Montané, D.; Garcia-Valls, R. ; Polymeric composite membranes based on carbon/PSf. Journal of membrane science, 2006. 273:p. 38-46. (Consultar *Apartado 5.2.4*, ver *Anexo F*).

⁴¹ Montané, D.; Nabarlantz, D.; Martorell, A.; Torné-Fernández, V.; Fierro, V.; Removal of lignin and associated impurities from xilo-oligosaccharides by activated carbon adsorption. Industrial Engineering Chemistry Research, 2006. 45:p. 2294-2302. (Consultar *Apartado 5.2.5*).

gran importancia ya que deriva de hemicelulosas ricas en xilano que son carbohidratos con un alto potencial en aplicaciones en productos de alimentación y farmacéuticos. Esta metodología pretende ser aplicada en los CA preparados para esta tesis una vez se optimice, debido a la poca cantidad de CA que se obtiene en cada pirólisis.

5.1. Preparación y caracterización de carbones activados

A continuación se presentan seis artículos publicados y enviados a diferentes revistas que tratan de la preparación y caracterización de carbones procedentes de lignina Kraft y activados químicamente con ácido fosfórico, hidróxido de sodio e hidróxido de potasio a diferentes condiciones de operación.

5.1.1. Activated carbons from lignin: kinetic modeling of the pyrolysis of Kraft lignin activated with phosphoric acid

Este artículo se ha publicado en el Chemical Engineering Journal en 2005 en el volumen 106, páginas 1 a 12.



Activated carbons from lignin: kinetic modeling of the pyrolysis of Kraft lignin activated with phosphoric acid

Daniel Montané*, Vanessa Torné-Fernández, Vanessa Fierro

Department of Chemical Engineering-ETSEQ, Rovira i Virgili University, Av. Països Catalans 26, E-43007 Tarragona, Catalunya, Spain

Received 26 April 2004; received in revised form 19 October 2004; accepted 4 November 2004

Abstract

A phenomenological kinetic model has been developed for the pyrolysis at low heating rates of lignin activated with phosphoric acid. The model is based on thermogravimetry (TG) and differential thermogravimetry (DTG) data from pyrolysis experiments and assumes that lignin carbonization proceeds through a set of pseudo-first-order reactions. These reactions are a simplified description of the multiple reactions involved in the process. TG experiments were performed in nitrogen atmosphere for lignin (L) impregnated with 85% phosphoric acid (PA) at mass ratios (PA:L) from 1.0:1.0 to 1.75:1.0, a typical heating rate of 10 °C/min and a maximum carbonization temperature of 650 °C, including isothermal stages at 150 and 300 °C in the temperature programs for some of the experiments. Analysis of the TG and DTG curves led to a kinetic model that includes an initial reaction step between lignin and phosphoric acid, water formation from the dehydration of the excess of phosphoric acid to P₂O₅, pyrolysis of lignin to carbon and volatiles, evaporation of water and P₂O₅ and finally, partial volatilization of the carbon to light gases. Activation energies and the other parameters of the model were adjusted from experimental data. Activation energies were 26.0 kJ/mol for water desorption, 72.0 kJ/mol for the dehydration of phosphoric acid to phosphoric pentoxide, 95.0 kJ/mol for the volatilization of P₂O₅, 47.7 kJ/mol for the carbonization of the activated lignin and 106.3 kJ/mol for the pyrolytic release of light gases from activated carbon. The model provides a good representation of the thermograms regardless of the phosphoric acid to lignin ratio and the temperature profile along the reaction.

© 2004 Elsevier B.V. All rights reserved.

Keywords: Lignin; Activated carbon; Phosphoric acid; Pyrolysis; Kinetics; Thermogravimetric analysis

1. Introduction

Activated carbons are adsorbents that are used industrially in multiple processes for product separation and purification, and for the treatment of liquid and gaseous effluents. Their versatility allows a wide range of uses if their pore size distribution and surface properties are properly tailored, and new applications are being developed in areas such as pollution prevention, supported catalysts and the storage of gaseous fuels such as natural gas and hydrogen. Activated carbons are produced from a wide variety of carbonaceous materials, including wood and agriculture by-products [1], but the expanding market for activated carbons has prompted inter-

est in finding complementary sources of carbonaceous precursors for their manufacture. Using carbonaceous residues and by-products from existing industrial processes as feedstock for producing activated carbons is an attractive strategy that may help reduce costs through process integration. Among several possibilities, lignin, produced as a residual material in the manufacture of cellulose pulps, offers strong potential because it is available in high amounts at low cost. Lignin is the most abundant natural polymer after cellulose. Typically, it represents around 20–30% of the mass of dry wood and is nowadays produced in huge amounts as a by-product in the production of high-quality cellulose pulps, mainly in the Kraft pulping process. In this process, lignin is used as fuel to provide steam for the plant, which also allows the recovery of the pulping chemicals (NaOH and Na₂S). The trend towards larger plant capacities and the op-

* Corresponding author. Tel.: +34 977 559 652; fax: +34 977 558 544.
E-mail address: dmontane@etseq.urv.es (D. Montané).

Table 1
 Lignin analysis (wt. %)

Proximate analysis (wt. %, wet basis)		Ultimate analysis (wt. %, ash and moisture free)	
Moisture	14.45	Carbon	59.46
Ash	9.50	Hydrogen	5.07
Volatile matter	44.93	Nitrogen	0.05
Fixed carbon ^a	31.12	Sulfur	2.15
		Oxygen ^a	33.27

^a Estimated by difference.

timization of the pulping process to improve cost effectiveness have led to the plants producing more by-product lignin than the amount that is needed to cover their energy consumption. Using Kraft lignin as raw material for chemicals has therefore attracted considerable attention. Several applications for the lignin obtained from pulping processes have been considered. One of its main uses so far has been as a phenol substitute in the formulation of phenol–formaldehyde resins and adhesives, but one of the main areas for possible applications for by-product lignin is in the preparation of activated carbons. The physical activation with CO₂ of pyrolyzed lignins [2,3], as well as chemical activation of lignin with ZnCl₂ [4], have been studied, but the use of ZnCl₂ is declining due to its environmental impact [5], and phosphoric acid is the preferred activating agent. However, the activation of lignin with phosphoric acid has not been widely investigated, though maximum surface areas of above 1300 m²/g have been reported [6]. We recently studied the characteristics of the carbons obtained from Kraft lignin activated with phosphoric acid at several process conditions and showed that carbons with high surface areas and good properties can be obtained [7]. In this paper, we study the rates of carbonization of Kraft lignin activated with phosphoric acid in a thermobalance and propose and test a phenomenological kinetic model with the experimental data.

Table 2
 Experimental conditions used for the TGA experiments

Run ID	H ₃ PO ₄ (85%) to lignin mass ratio	Initial temperature (°C)	Heating rate (°C/min)	First stage		Second stage		Third stage	
				T (°C)	Time (min)	T (°C)	Time (min)	T (°C)	Time (min)
Exp #10/3	1.4	25	10	650	120	–	–	–	–
Exp #10/4	1.4	25	10	650	120	–	–	–	–
Exp #10/5	1.4	25	10	650	120	–	–	–	–
Exp #2	1.4	25	10	150	15	650	0	–	–
Exp #3	1.4	25	10	150	30	650	30	–	–
Exp #5	1.4	25	10	150	60	650	120	–	–
Exp #13	1.4	25	10	150	60	650	120	–	–
Exp #18	1.4	25	10	300	60	650	120	–	–
Exp #20	1.4	25	10	150	60	300	60	650	120
Exp #21	1.4	25	10	300	60	500	60	750	60
Exp #24	1.4	150	150	650	120	–	–	–	–
Exp #10 (L/P 1:1.0)	1.0	25	10	650	30	–	–	–	–
Exp #14 (L/P 1:1.4)	1.4	25	10	600	120	–	–	–	–
Exp #18 (L/P 1:1.75)	1.75	25	10	650	120	–	–	–	–

2. Experimental

A sample of Kraft lignin was obtained from Lignotech Ibérica S.A. (Spain) and used to prepare activated carbons as received (see Table 1 for composition). Elemental analysis was performed in a EA1108 Carlo Erba analyzer and the proximate analysis was developed according to ISO standards for moisture (100 °C in air), volatile matter (900 °C in nitrogen atmosphere) and ash (incineration at 815 °C in air).

Phosphoric acid (85% solution, Panreac, Spain) was used as activating agent. Lignin and phosphoric acid were mixed at the desired ratio and the mixture was left for 1 h to allow a complete impregnation of the lignin [8]. A small sample (around 30–50 mg) of the mixture was then transferred to the thermobalance (Perkin-Elmer TGA-7), where pyrolysis was carried out in nitrogen at a constant flow rate of 50 mL/s. Table 2 lists all the other specific conditions for the experiments, which were performed randomly except for a first series, which was performed to establish the reproducibility of the TG results.

3. Results and discussion

Our first set of experiments tested the reproducibility of our experimental procedure. Fig. 1 shows the thermograms (*f* versus *t*) and the differential thermograms (*df/dt* versus *t*) for replicated experiments on the carbonization of a sample of lignin impregnated with a phosphoric acid to lignin mass ratio (PA/L) of 1.4, a heating rate of 10°/min and a final temperature of 650 °C for 120 min (experiments #10/3, #10/4 and #10/5 in Table 2). Since our experiments included isothermal periods, either at the end of the heating ramp or intercalated in it, we preferred time instead of temperature as the independent variable for our calculations. The average value for the final mass fraction was 0.384 ± 0.014 (95% probability level), which shows the good reproducibility of the ex-

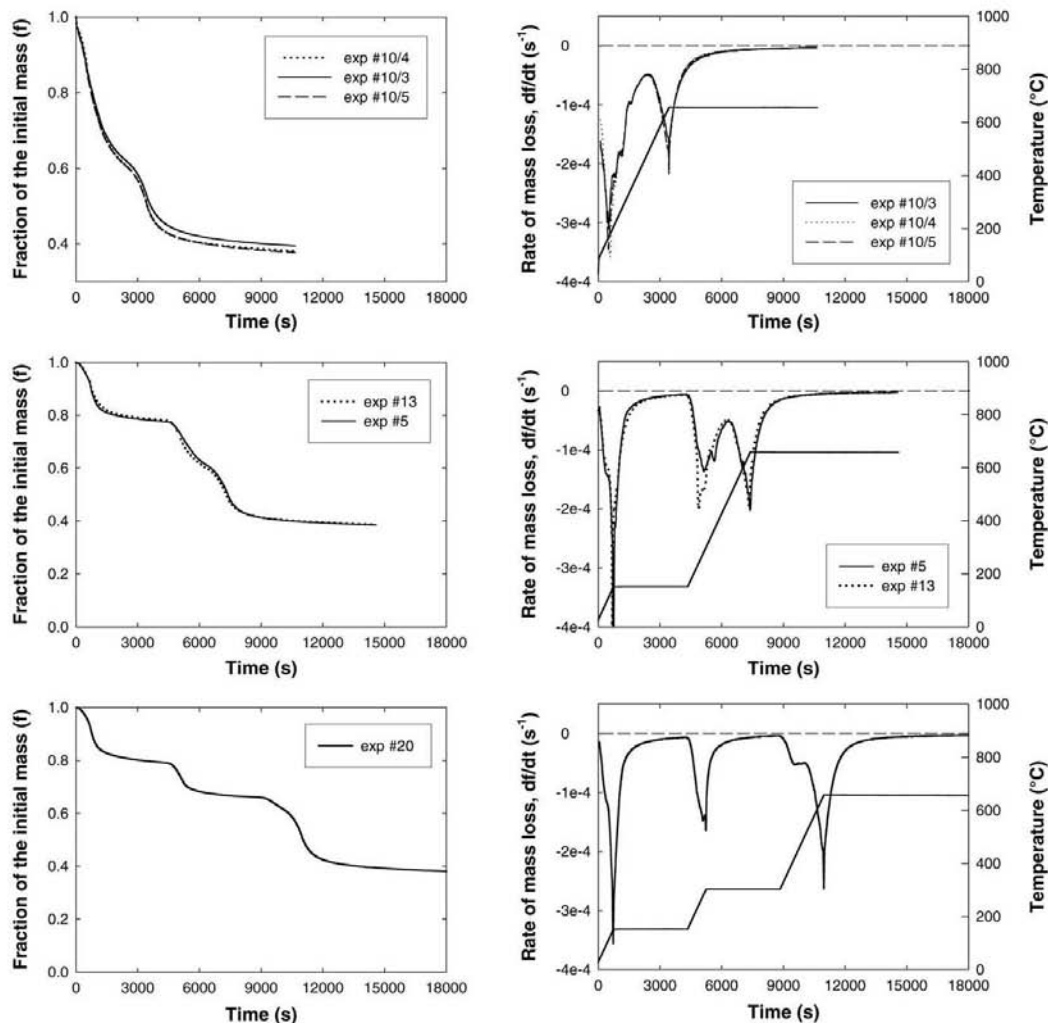


Fig. 1. Effect of the addition of intermediate isothermal stages on the final solid yield and the TG and DTG curves for experiments #5, #10/4 and #20 (experimental conditions listed in Table 2).

periments. The differential thermograms also show excellent agreement among the three experiments throughout the reaction time, since the values of the maximum rates of mass loss and the time at which they are observed are almost identical for the three runs. The differential thermogram shows two peaks for the rate of mass loss. The first starts at low temperature, reaches the maximum rate at around 175–180 °C and extends to 450 °C. The second peak starts at around 500 °C and reaches the maximum rate of mass loss when the isothermal segment at 650 °C starts.

Yoon et al. [9] reported an increase in carbon yield when the sample was maintained at constant temperature for a cer-

tain time once the volatilization of the sample had started. Other studies, however, reported that the carbon yield did not change when intermediate isothermal periods were included during the pyrolysis of viscose rayon cloth [10] and apple pulp [11]. We performed experiments #5 and #13, under the same conditions as #10/3, #10/4 and #10/5 but with an isothermal segment at 150 °C for 60 min. Again, reproducibility was excellent for the TG and DTG curves (Fig. 1). The mass fraction remaining at the end of the experiments was 0.386 ± 0.002 , which is equivalent to that of the experiments without intermediate isothermal period. We may therefore conclude that including isothermal periods does not signif-

icantly changes the final yield of solid. However, including intermediate isothermal stages proved valuable because it revealed that the peaks of the rate of mass loss in the DTG were the result of the superposition of several reactions. For example, if we compare the DTG plots for experiments #10/4 and #5 we can see that the broad peak observed during the heating period in experiment #10/4 splits into two different peaks when an intermediate isothermal period at 150 °C is added. The new peak shows the maximum rate of mass loss at 350–400 °C, but it appears also to be the result of the superposition of two reactions. This is confirmed by experiment #20, which adds two isothermal periods — one at 150 °C for 60 min and another at 300 °C for 60 min — and shows the existence of four maximums in the rate of mass loss along the thermogram. This experiment also had a yield of residual solid of 0.381, which confirmed that including intermediate isothermal stages has no significant effect on the final mass fraction if the same final temperature of carbonization is achieved.

4. Modeling of lignin pyrolysis

Several models are available in the bibliography for the kinetics of the thermal decomposition of biomass and its fractions. The most usual approach starts with the assumption that the components of biomass (cellulose, hemicellulose and lignin) react simultaneously and independently of the others through a set of parallel reactions [12–15]. When applied to lignin activated with phosphoric acid, the model is reduced to two parallel and independent reaction processes: the volatilization of the water present in the sample and the carbonization of the phosphoric acid-activated lignin (PL) into activated carbon and volatiles. Water comes from the phosphoric acid solution and the moisture of lignin. This system is described mathematically by Eqs. (1)–(5), where m_{0LP} and m_{0W} are the initial masses of PL mixture and water, m_{LP} and m_W the actual masses of PL and water at a point along the experiment, m_{∞} the residual mass of solid at the end of the thermogram, f the fraction of the initial mass remaining as solid, f_{LP} and f_W the fractions of the initial mass of phosphoric-activated lignin and water, f_{LP_0} and f_{W_0} the same at the beginning of the experiment, α_{LP} and α_W the degrees of transformation for activated lignin and water, and k_{LP} and k_W Arrhenius rate constants for the volatilization of activated lignin and water.

Water volatilization was assumed to be first-order. Some thermogravimetry studies on lignin pyrolysis propose a first-order reaction process [15–17], but most studies conclude that reaction orders are higher [13,14,18,19]. We therefore assumed that the devolatilization of activated lignin may not be first-order and included the reaction order for activated lignin (α_{LP}) as one of the parameters to be optimized from experimental data, together with the activation energies and the frequency factors. A convenient least-squares objective function to calculate the optimal values of these parameters when

using several thermograms, which may combine isothermal and non-isothermal stages, is presented in Eq. (6) for p thermograms with $n(i)$ data points each. f_{ij}^{exp} are the measured values of f , and f_{ij}^{cal} are those calculated with Eqs. (3)–(5) and numerical integration of Eqs. (1) and (2):

$$\frac{d\alpha_{LP}}{dt} = k_{LP}(1 - \alpha_{LP})^{\alpha_{LP}} \quad \text{with} \quad \alpha_{LP} = \frac{m_{0LP} - m_{LP}}{m_{0LP} - m_{\infty}} \quad (1)$$

$$\frac{d\alpha_W}{dt} = k_W(1 - \alpha_W) \quad \text{with} \quad \alpha_W = \frac{m_{0W} - m_W}{m_{0W}} \quad (2)$$

$$f_{LP} = f_{LP_0} - \alpha_{LP}(f_{LP_0} - f_{\infty}) \quad (3)$$

$$f_W = f_{W_0}(1 - \alpha_W) \quad (4)$$

$$f = f_{LP} + f_W \quad (5)$$

$$F = \sum_{i=1}^p \left(\frac{\sum_{j=1}^{n(i)} (f_{ij}^{cal} - f_{ij}^{exp})^2}{n(i)} \right) \quad (6)$$

Fig. 2 compares the thermograms and the differential thermograms recorded for experiments #10/4, #5 and #20 with those calculated with the best-fit values of the model parameters. The model describes the general trends of the thermograms qualitatively but shows large discrepancies with the experimental results, especially when two intermediate isothermal stages are included in the thermogram (experiment #20). We may therefore conclude that a better description of the interactions between lignin and phosphoric acid has to be incorporated into the model.

Analysis of the TG and DTG plots in Fig. 1 reveals some characteristic trends of the pyrolysis of lignin in the presence of phosphoric acid. Since water will evaporate at the lower temperature, the broad peak observed in the DTG between 100 and 450 °C in experiments #10/3, #4, #5 is not only caused by water evaporation but also by the decomposition of lignin and phosphoric acid. Water comes from the phosphoric acid solution, the moisture in lignin and from reactions of lignin and phosphoric acid at low temperature. In the presence of PA, lignin reacts through cleavage of the aryl-ether bonds, the formation of ketone groups, condensation and dehydration [20]. Pyrolysis of lignin in the presence of phosphoric acid shows that CO and CO₂ begin to evolve as volatile products at a temperature as low as 100 °C [21]. The inclusion of an isothermal stage at 150 °C for 60 min (experiments #5 and #20) shows that only 20% of the initial mass volatilizes at this temperature. This is attributed to the release of water and light compounds from lignin degradation by the action of phosphoric acid. When a second isothermal stage is included at 350 °C for 60 min (experiment #20), the total mass loss reaches 34%. The peak at 240–320 °C in the DTG curve for experiments #5 and #13 is attributed to the release of organic volatiles formed during the carbonization of the activated lignin. This peak is overlapped with the peak of water when no intermediate isothermal stage is used (experiments #10/3, #4, #5). When the sample is heated at 650 °C for 2 h, the final mass loss is around 62% for all experiments. The

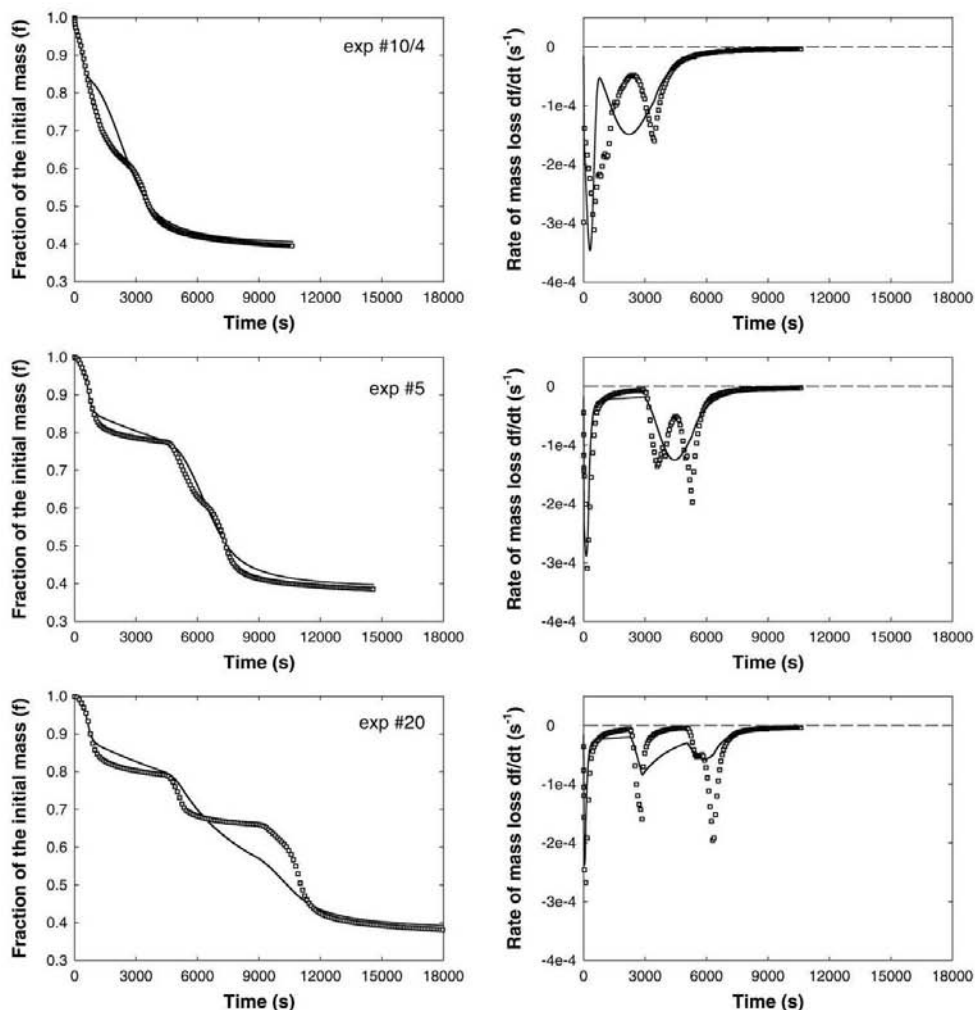


Fig. 2. Comparison between the experimental TG and DTG curves (□) and those calculated with the two parallel reactions kinetic model (–), Eqs. (1)–(5), for experiments #5, #10/4 and #20. (Experimental conditions listed in Table 2. For better visualization, only 1 data point out of 20 is plotted in the experimental TG and DTG curves.)

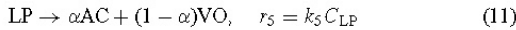
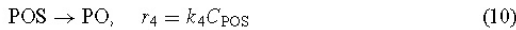
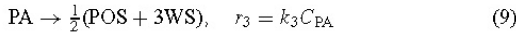
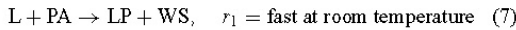
high degree of mass loss between 350 and 650 °C cannot be attributed to volatile matter from lignin alone since the rate of lignin pyrolysis reaches a maximum in the temperature interval from 300 to 370 °C [14,15]. The behavior of phosphoric acid at elevated temperature also has to be accounted for. The experiments presented in Fig. 1 were performed at a phosphoric acid-to-lignin mass ratio of 1.4:1, which exceeds the minimum ratio of 1.0:1.0 required to activate lignin completely [8]. As the temperature of the sample increases, the excess phosphoric acid is converted to pyrophosphoric acid ($H_4P_2O_7$) by condensation and dehydration. Extended heating forms polyphosphoric acid ($H_{n+2}P_nO_{3n+1}$), which

finally decomposes to form P_2O_5 , which sublimates above 300 °C and melts and vaporizes at 580–585 °C [22]. This temperature is very close to the peak observed at 650 °C in the DTG curves, which is therefore attributed to the volatilization of the P_2O_5 .

4.1. Development of a new kinetic model for the pyrolysis of lignin activated with phosphoric acid

Qualitative interpretation of the thermograms leads us to the development of a kinetic model that accounts for the observed phenomena during the pyrolysis of lignin in the pres-

ence of phosphoric acid. The process was modeled with the reaction scheme described by Eqs. (7)–(12). Eq. (7) is the formation of a complex (LP) between lignin (L) and phosphoric acid (PA) through linkage of the phosphoric group to a reactive site in lignin. Based on experimental evidence we determined that this process finishes in 1 h at room temperature [8]. Therefore, this reaction was complete before the thermal treatment was started. Eq. (8) is the drying of the sample through water (WS) evaporation. Eq. (9) accounts for the conversion of the excess phosphoric acid to P_2O_5 (POS) when water is completely removed, and Eq. (10) describes the evaporation of POS. Finally, pyrolysis of the lignin–PA complex yields activated carbon (AC) and volatiles (VO), as described by Eq. (11). The parameter α indicates the mass fraction converted to activated carbon, and $(1 - \alpha)$ indicates the mass fraction converted to volatiles during carbonization. Eq. (12) describes the partial volatilization of the activated carbon through slow pyrolysis to yield light gases (GA). All reaction rates were assumed to be first-order for each reactant.



Assuming that the reacting solid has homogeneous properties, individual mass balances are developed for each component of the solid:

$$\frac{df_{WS}}{dt} = -k_2 f_{WS} + \frac{3}{2} k_3 \frac{MW_{WS}}{MW_{PA}} f_{PA} \quad (13)$$

$$\frac{df_{PA}}{dt} = -k_3 f_{PA} \quad (14)$$

$$\frac{df_{PO}}{dt} = -k_4 f_{PO} + \frac{1}{2} k_3 \frac{MW_{PO}}{MW_{PA}} f_{PA} \quad (15)$$

$$\frac{df_{LP}}{dt} = -k_5 f_{LP} \quad (16)$$

$$\frac{df_{AC}}{dt} = \alpha k_5 f_{LP} - k_6 f_{AC} \quad (17)$$

$$\alpha' = \alpha \frac{MW_{AC}}{MW_{LP}} \quad (18)$$

where f_j denotes the mass fraction of species j referred to the initial mass of the sample (M_0), MW_j is the molar mass of species j , and the rate of decrease of the fraction of the initial mass that remains in the solid (df/dt) is obtained from Eq. (20). All the rate constants were assumed to follow the Arrhenius relationship Eq. (21).

$$f_j = \frac{M_j}{M_0} \quad (19)$$

$$\frac{df}{dt} = \frac{1}{M_0} \sum_{j=1}^5 \frac{dM_j}{dt} \quad (20)$$

$$k_i = k_{0i} \exp\left(-\frac{E_i}{RT}\right) \quad (21)$$

The initial mass-fraction composition of the sample was calculated from the amounts of phosphoric acid and lignin, the moisture content of the latter, and accounting for the water originated through reaction (1) (Eqs. (22)–(24))

$$f_{PA,0} = \frac{\left(\text{mass of anhydrous } H_3PO_4 - \text{mass of dry lignin} \left(\frac{MW_{PA}}{MW_L}\right)\right)}{\text{total mass}} \quad (22)$$

$$f_{LP,0} = \frac{\left(\text{mass of dry lignin} \left(\frac{MW_L + MW_{PA} - MW_W}{MW_L}\right)\right)}{\text{total mass}} \quad (23)$$

$$f_{WS,0} = \frac{\left(\text{mass of water} + \text{mass of dry lignin} \left(\frac{MW_{PA}}{MW_L}\right)\right)}{\text{total mass}} \quad (24)$$

The optimal values for the 12 unknown parameters in the model (k_{0j} , E_j , α' and MW_L) were estimated from the minimization of the least squares objective function F , Eq. (25), where n is the number of thermograms and $p(i)$ is the number of data points recorded for the i th thermogram (time, temperature fraction of the initial mass remaining and rate of mass loss). This objective function was chosen to simultaneously minimize the squared differences in the fraction of the initial mass remaining in the solid and the rate of mass loss. This was needed because it was observed that an objective function that was only based on the fraction of the initial mass gave optimal values that adjusted the data for the isothermal stages correctly, but gave poor results for the non-isothermal stages where the rates of mass loss were higher. Similarly, an objective function based on the rate of mass loss misrepresented the isothermal stages where the rate of mass loss was small.

The fraction of the initial mass remaining predicted by the model, $f(i, k)_{\text{model}}$, was calculated with Eqs. (13)–(21), which were integrated numerically by an explicit Euler method. The temperature recorded at each sampling time along the thermogram was used to calculate the instantaneous rate constants. The rates of mass loss were evaluated numerically from the values of $f(i, k)$. This method provided a sufficient degree of accuracy because, as the thermograms were recorded at a high sampling frequency (typically one data point every 4 s), the time increments used in the calculations were small

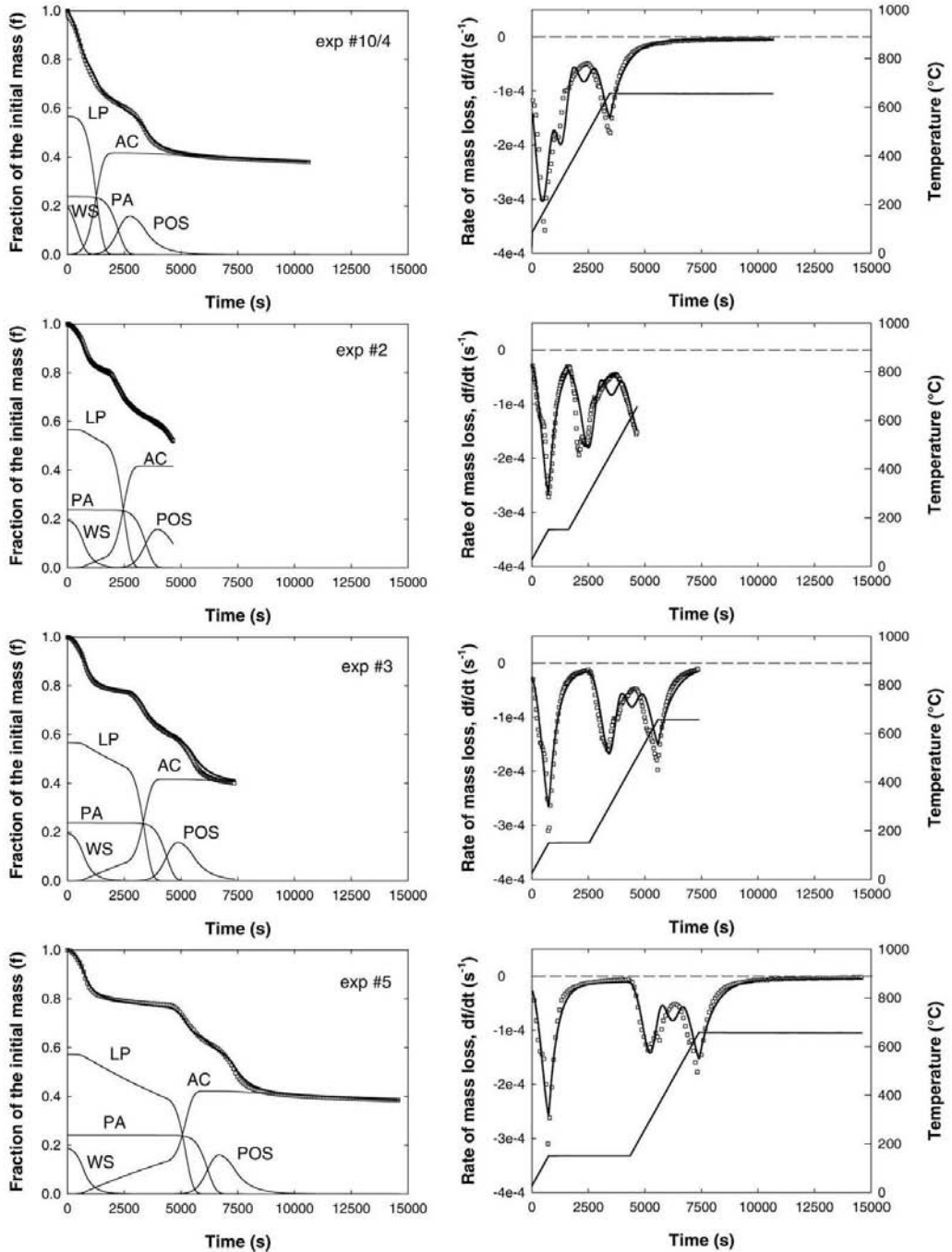


Fig. 3. Comparison between the experimental TG and DTG curves (□) and those calculated with the complete kinetic model (—), Eqs. (13)–(24), for experiments #2, #3, #5 and #10/4. (Experimental conditions listed in Table 2. Continuous thin lines are mass fractions calculated for lignin–phosphoric acid complex (LP), phosphoric acid (PA), water (WS), activated carbon (AC) and P_2O_5 (POS). For better visualization, only 1 data point out of 20 is plotted in the experimental TG and DTG curves.)

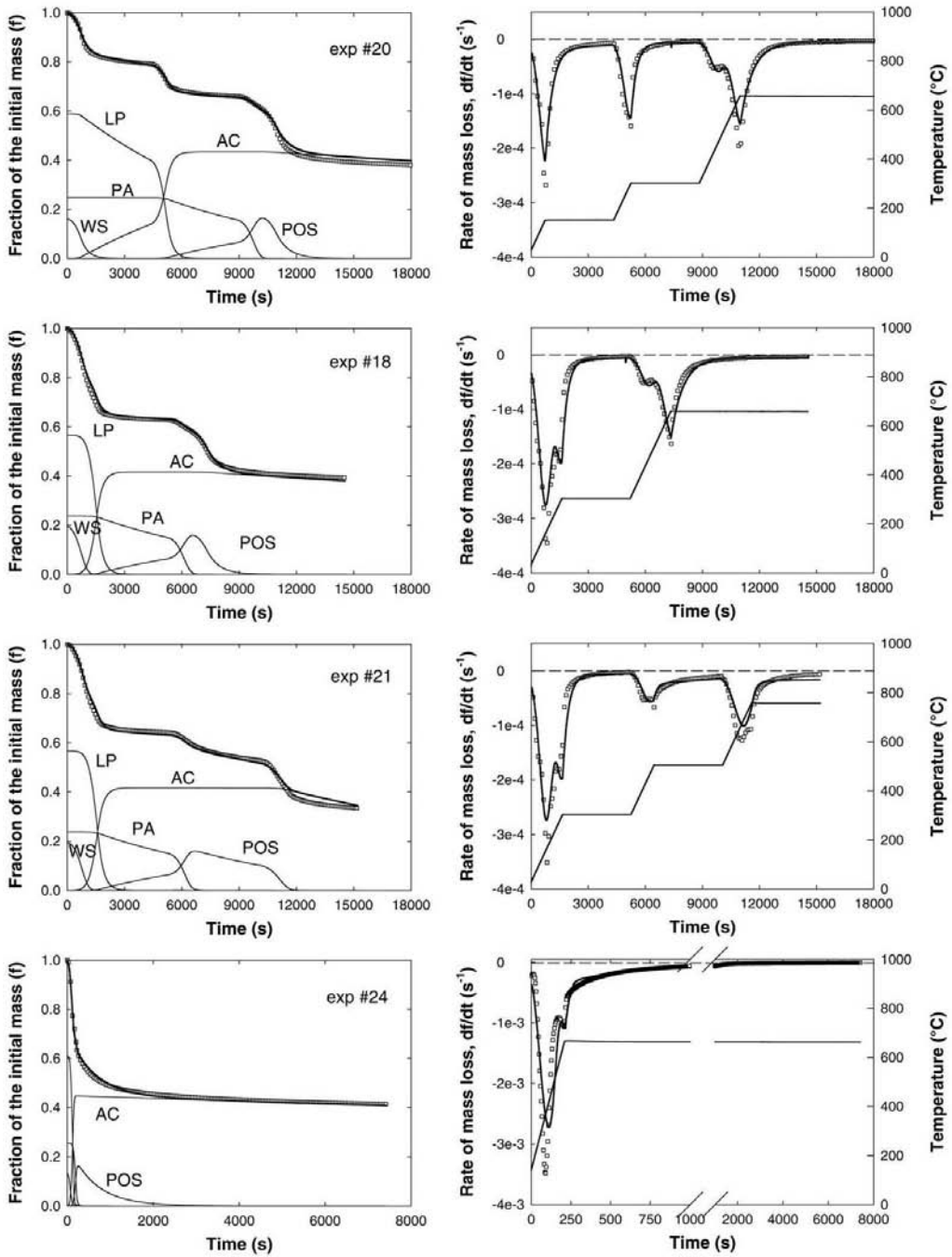


Fig. 4. Comparison between the experimental TG and DTG curves (\square) and those calculated with the two parallel reactions kinetic model (—), Eqs. (13)–(24), for experiments #18, #20, #21 and #24. (Experimental conditions listed in Table 2. Continuous thin lines are mass fractions calculated for lignin–phosphoric acid complex (LP), phosphoric acid (PA), water (WS), activated carbon (AC) and P_2O_5 (POS). For better visualization, only 1 data point out of 20 is plotted in the experimental TG and DTG curves.)

Table 3
 Least-squares best-fit values for the model parameters

Reaction	k_{0j} (s^{-1})	E_j (kJ/mol)	MW_L (g/mol)	α'	Minimum F
(2)	4.20	26.0	135.3	0.736	2.205×10^{-2}
(3)	395.9	72.0			
(4)	326.4	95.0			
(5)	73.9	47.7			
(6)	11.1	106.3			

enough to avoid numerical instability.

$$F = \left(\sum_{i=1}^n \left(\frac{\sum_{k=1}^{p(i)} \left(\frac{f(i,k)_{\text{experimental}} - f(i,k)_{\text{model}}}{f(i,k)_{\text{model}}} \right)^2}{p(i)} \right) \right) \left(\sum_{i=1}^n \left(\frac{\sum_{k=1}^{p(i)} \left(\frac{\left(\frac{df(i,k)}{dt} \right)_{\text{experimental}} - \left(\frac{df(i,k)}{dt} \right)_{\text{model}}}{\left(\frac{df(i,k)}{dt} \right)_{\text{model}}} \right)^2}{p(i)} \right) \right)^{0.5} \quad (25)$$

The optimal values calculated for the activation energies (E_j), the frequency factors (k_{0j}), the stoichiometric coefficient in reaction (5) (α') and the apparent molar mass of lignin (MW_L) are shown in Table 3. Activation energies were 26.0 kJ/mol for water desorption, 72.0 kJ/mol for the dehydration of phosphoric acid to phosphoric pentoxide, 95.0 kJ/mol for the volatilization of P_2O_5 , 47.7 kJ/mol for the carbonization of the activated lignin and 106.3 kJ/mol for the pyrolytic release of light gases from activated carbon. The activation energy for the volatilization of lignin impregnated with phosphoric acid lies in the 35–100 kJ/mol range reported for lignin pyrolysis using several kinetic models [23], and falls below the range of activation energies from 60.6 kJ/mol at 200 °C to 153.6 kJ/mol at 700 °C reported for the pyrolysis of lignin activated with $ZnCl_2$ using a kinetic model based on a continuous distribution of activation energies [24]. Fig. 5 shows a sensitivity analysis for the influence of the model parameters on the least squares objective function F . This analysis shows that the activation energies (E_j), the apparent molar mass of lignin (MW_L) and the stoichiometric coefficient for the carbonization of the activated lignin (α') are evaluated accurately because the error function F is very sensitive to small variations in their individual values. The frequency factors (k_{0j}) that we have calculated are more uncertain due to the low sensitivity of the error function to their value, especially for the frequency factor for the rate constants of phosphoric acid dehydration (k_3) and water volatilization (k_2).

Figs. 3 and 4 compare the thermograms measured for the experiments at an 85% phosphoric acid-to-lignin mass ratio of 1.4:1 (Table 2), and those calculated with the model using the best-fit values of the parameters. Agreement between the model and the experiments is excellent for all the thermo-

grams, regardless of the number of intermediate isothermal stages. The same graphs also show the evolution of the mass fractions of water in the sample (WS), lignin-phosphoric acid complex (LP), phosphoric acid (PA), P_2O_5 (POS) and activated carbon (AC). Analysis of the temporal evolution of the mass fractions computed for each component in the solid mixture shows that drying of the sample (reaction (2)) takes place at the lowest temperature and is completed before the sample reaches 200 °C. Carbonization of the activated lignin (LP) starts at around 100 °C and is completed when the sample reaches 400 °C for the experiments without

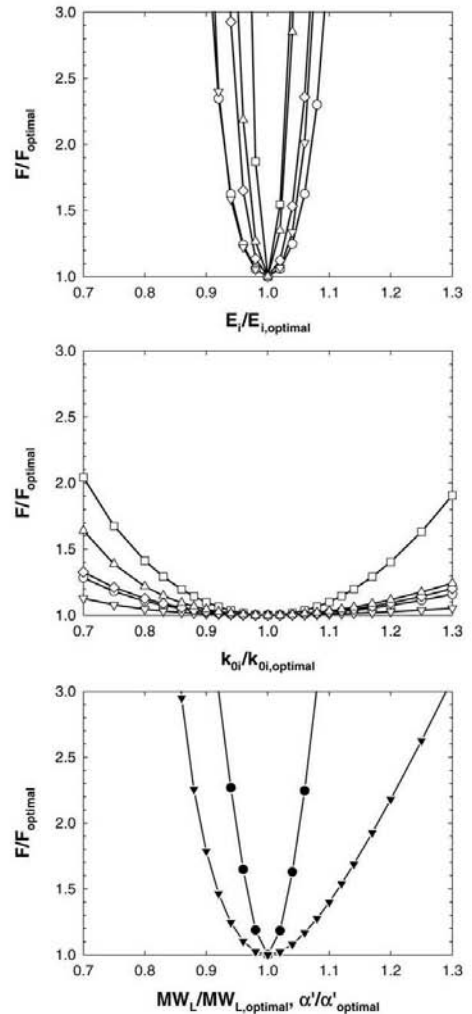


Fig. 5. Sensitivity analysis for the model parameters: activation energies (top), frequency factors (middle), and molar mass of lignin, MW_L , and α' (bottom) (E_1, k_1 : ○; E_2, k_2 : ▽; E_3, k_3 : □; E_4, k_4 : ◇; E_5, k_5 : △; α' : ▼; and MW_L : ●).

intermediate isothermal stages (experiment #10/4), or with an isothermal stage at 150 °C for 60 min (experiment #5), but reaches completion at 300 °C if an isothermal stage at 300 °C for 60 min is included in the temperature program (experiment #18). Decomposition and volatilization of the excess phosphoric acid take place at a higher temperature and are responsible for the mass loss observed above 400 °C. This starts at around 230 °C, which is close to the value of 213 °C reported for pure orthophosphoric acid [22], and is completed at around 550–580 °C. This broad interval of reaction temperature agrees qualitatively with the consecutive

reactions involved in the formation of P₂O₅ from phosphoric acid, which proceeds through the formation of pyrophosphoric acid (H₄P₂O₇), polyphosphoric acid (H_{n+2}P_nO_{3n+1}) and finally P₂O₅. The volatilization of phosphorous pentoxide also happens in a broad interval of temperature. According to the kinetic model, it starts once the sample reaches around 280 °C, which is close to its sublimation temperature of 300 °C, and takes place much faster above 570 °C when vaporization is accelerated due to the melting of P₂O₅ at 580–585 °C [22]. Finally, the residual mass loss during the isothermal stage at 650 °C is caused by the release of light

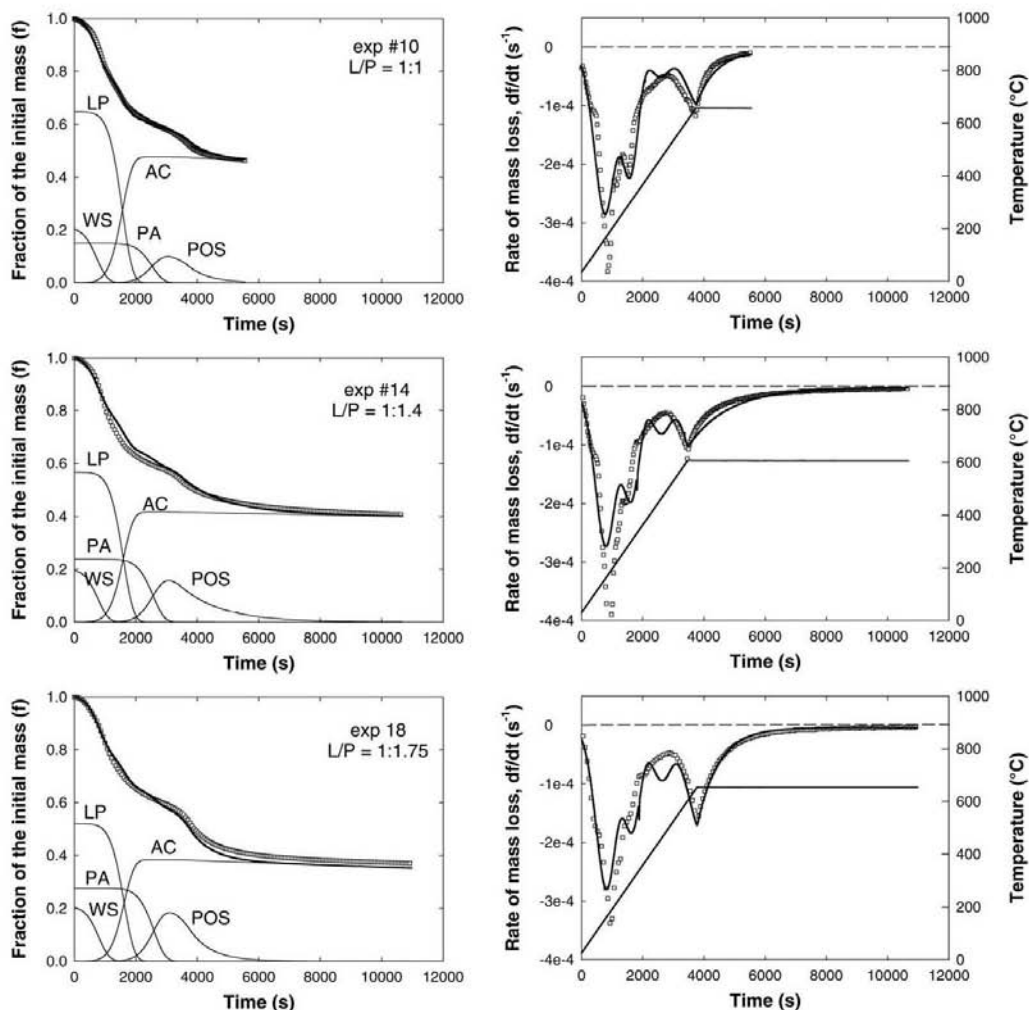


Fig. 6. Comparison between the experimental TG and DTG curves (□) and those calculated with the two parallel reactions kinetic model (—), Eqs. (13)–(24), for experiments #10 L/P 1:1.0, #14 L/P 1:1.4 and #18 L/P 1:1.75. (Experimental conditions listed in Table 2. Continuous thin lines are mass fractions calculated for lignin–phosphoric acid complex (LP), phosphoric acid (PA), water (WS), activated carbon (AC) and P₂O₅ (POS). For better visualization, only 1 data point out of 20 is plotted in the experimental TG and DTG curves.)

gases as the carbon formed at lower temperatures is pyrolyzed to a greater extent.

Analysis of the differential thermograms, also presented in Figs. 3 and 4, shows that the model accurately describes the rate of mass loss for the experiments with one intermediate isothermal stage at 300 °C (#18, #20, #21). Four maximums in the rate of weight loss are observed: the first for water volatilization, the second for the release of volatiles during the formation of activated carbon, the third for the decomposition of phosphoric acid and the fourth for the volatilization of P_2O_5 . For the other experiments there are some discrepancies in the temperature interval from 300 to 500 °C since the model shows the existence of a small maximum on the rate of mass loss at around 450 °C caused by phosphoric acid dehydration to phosphorous pentoxide, which is not observed experimentally. Close examination of the experimental rate of mass loss in this temperature range shows a series of small maximums and inflection points (see experiments #2 and #3, for instance), which point to the existence of a set of simultaneous reactions taking place in the solid. These reactions are probably related to the decomposition of phosphoric acid to P_2O_5 , which in the model has been assumed to proceed through a single reaction step (Eq. (9)), though, as described before, it actually proceeds through a series of consecutive steps (Fig. 5).

The influence of the PA-to-lignin ratio is examined in Fig. 6, which shows the results for experiments performed at PA-to-lignin ratios of 1.0:1.0, 1.4:1.0 and 1.75:1.0 (w:w) using similar temperature profiles throughout the experiment. The model can reproduce the measured thermograms within the limits of the experimental error in all cases, thus proving its robustness. Analysis of the differential thermograms show limitations for the three experiments similar to those noted earlier: the model can describe the general trends in the temporal evolution of the rate of mass loss but there are minor discrepancies in the temperature interval from 300 to 500 °C caused by the complex nature of the reactions involved in phosphoric acid decomposition.

5. Conclusions

A phenomenological kinetic model has been developed for the pyrolysis of lignin activated with phosphoric acid at low heating rates to produce activated carbon. The model is based on TG and DTG data from pyrolysis experiments and it assumes that lignin carbonization proceeds through a set of pseudo-first-order reactions. These reactions are a simplified description of the multiple reaction processes involved in the thermal decomposition of lignin mixed with an excess of phosphoric acid. The model provides a good representation of the thermograms regardless of the phosphoric-acid-to-lignin ratio and the temperature profile along the reaction. The activation energies and other parameters have been calculated from the experimental mass-loss and differential mass-loss curves. The model could be improved if the composition of

the volatile products were analyzed continuously by on-line mass spectrometry to determine the actual rates of volatilization for water, phosphoric acid-derived products (i.e., P_2O_5) and carbon-containing compounds.

Acknowledgements

The authors are indebted to the Catalan Regional Government and the Spanish Government for financial support (projects 2001SGR-00323 and PPQ2002-04201-CO2-02, respectively). Vanessa Torné-Fernández is grateful to the Rovira i Virgili University (URV) for a PhD scholarship.

References

- [1] T. Vemerson, P.R. Bonelli, E.G. Cerrella, A.L. Cukierman, *Arundo donax* cane as precursor for activated carbons preparation by phosphoric acid activation, *Biores. Technol.* 83 (2002) 95–104.
- [2] V.D. del Bagnó, R.L. Miller, J.J. Watkins, On site production of activated carbon from Kraft Black Liquor, US EPA Report 600/2-78-191, 1978.
- [3] J. Rodríguez-Mirasol, T. Cordero, J.J. Rodríguez, Preparation and characterization of activated carbons from eucalyptus kraft lignin, *Carbon* 31 (1993) 87–95.
- [4] E. González Serrano, T. Cordero, J. Rodríguez-Mirasol, J.J. Rodríguez, Development of porosity upon chemical activation of Kraft lignin with $ZnCl_2$, *Ind. Eng. Chem. Res.* 36 (1997) 4832–4838.
- [5] H. Teng, T.S. Yeh, L.Y. Hsu, Preparation of activated carbon from bituminous coal with phosphoric acid activation, *Carbon* 36 (1998) 1387–1395.
- [6] J. Hayashi, A. Kazehaya, K. Muroyama, P. Watkinson, Preparation of activated carbon from lignin by chemical activation, *Carbon* 38 (2000) 1873–1878.
- [7] V. Fierro, V. Torné-Fernández, D. Montané, R. García-Valls, Removal of Cu (II) from aqueous solutions by adsorption on activated carbons prepared from Kraft lignin, in: A. Linares-Solano, D. Cazorla-Amorós (Eds.), *Proceedings of Carbon 2003*, Oviedo, Spain.
- [8] V. Fierro, V. Torné-Fernández, D. Montané, J. Salvadó, Activated carbons prepared from Kraft lignin by phosphoric acid impregnation, in: A. Linares-Solano, D. Cazorla-Amorós (Eds.), *Proceedings of Carbon 2003*, Oviedo, Spain.
- [9] S.H. Yoon, B.C. Kim, Y. Koraí, I. Mochida, Multi-staged carbonization of aramid fibers, in: *Proceedings of the 22nd Biennial Conference on Carbon*, Extended Abstract and Program, San Diego, CA, 1995, p. 218.
- [10] C. Pastor, F. Rodríguez-Reinoso, H. Marsh, M.A. Martínez, Preparation of activated carbon cloths from viscous rayon. Part I. Carbonization procedures, *Carbon* 37 (1999) 1275–1283.
- [11] F. Suárez-García, A. Martínez-Alonso, J.M.D. Tascón, Pyrolysis of apple pulp: effect of operation conditions and chemical additives, *J. Anal. Appl. Pyrolysis* 62 (2002) 93–109.
- [12] G. Varhegyi, M.J. Antal, Kinetics of the thermal decomposition of cellulose, hemicellulose and sugar cane bagasse, *Energy Fuels* 3 (1989) 329–335.
- [13] J.J. Manyà, E. Velo, L. Puigjaner, Kinetics of biomass pyrolysis: a reformulated three-parallel-reactions model, *Ind. Eng. Chem. Res.* 42 (2003) 434–441.
- [14] J.A. Caballero, A. Marcilla, J.A. Conesa, Thermogravimetric analysis of olive stones with sulphuric acid treatment, *J. Anal. Appl. Pyrolysis* 44 (1997) 75–88.
- [15] J.J.M. Órfão, F.J.A. Antunes, J.L. Figueiredo, Pyrolysis kinetics of lignocellulosic materials - three independent reactions model, *Fuel* 78 (1999) 349–358.

- [16] J.J.M. Órfão, J.L. Figueiredo, A simplified method for determination of lignocellulosic materials pyrolysis kinetic from isothermal thermogravimetric experiments, *Thermochim. Acta* 380 (2001) 67–78.
- [17] D. Vamvuka, E. Kakaras, E. Kastanaki, P. Grammelis, Pyrolysis characteristics and kinetics of biomass residuals mixtures with lignite, *Fuel* 82 (2003) 1949–1960.
- [18] V. Cozzani, L. Petarca, L. Tognotti, Devolatilization and pyrolysis of refuse derived fuels: characterization and kinetic modeling by a thermogravimetric and calorimetric approach, *Fuel* 74 (1995) 903–912.
- [19] C.A. Koufopoulos, G. Maschio, A. Lucchesi, Kinetic modeling of the pyrolysis of biomass and biomass components, *Can. J. Chem. Eng.* 67 (1989) 75–84.
- [20] Y.Z. Lai, in: D.N.S. Hon, N. Shirashi (Eds.), *Chemical Degradation in Wood and Cellulose Chemistry*, vol. 10, Marcel Dekker, New York, 1991, p. 455.
- [21] M. Jagtoyen, F. Derbyshire, Activated carbons from yellow poplar and white oak by H_3PO_4 activation, *Carbon* 36 (1998) 1085–1097.
- [22] D.R. Lide (Ed.), *Handbook of Chemistry and Physics*, 72nd ed., CRC Press, Boca Raton, FL, 1991.
- [23] R.K. Sharma, J.B. Wooten, V.L. Baliga, X. Lin, W.G. Chan, M.R. Hajaligol, Characterization of chars from pyrolysis of lignin, *Fuel* (2004) (Corrected proof, available online 25 March).
- [24] E. Gonzalez-Serrano, $ZnCl_2$ —chemical activation of kraft lignin, PhD Dissertation, University of Málaga, Málaga, Spain, 1996.

5.1.2. Study of the decomposition of Kraft lignin impregnated with orthophosphoric acid

Este artículo se ha publicado en el journal *Thermochimica Acta* en 2005 en el volumen 433, páginas 142 a 148.



Study of the decomposition of kraft lignin impregnated with orthophosphoric acid

V. Fierro^{a,*}, V. Torné-Fernández^a, D. Montané^a, A. Celzard^b

^a *Departament de Enginyeria Química, Universitat Rovira i Virgili, Avda dels Països Catalans, 26, 43007 Tarragona, Spain*

^b *Laboratoire de Chimie du Solide Minéral, Université Henri Poincaré—Nancy I, UMR—CNRS 7555, BP 239, 54506 Vandoeuvre-lès-Nancy, France*

Received 9 November 2004; received in revised form 18 February 2005; accepted 18 February 2005
Available online 24 March 2005

Abstract

The aim of this study was to analyze the pyrolysis of Kraft lignin impregnated with orthophosphoric acid by thermogravimetry (TG-DTG). We studied the effect of various parameters on both the char yield and the rate of mass loss: heat treatment temperature up to 650 °C, impregnation time, inclusion of isothermal periods, acid to lignin mass ratio (P/L) and gaseous atmosphere. Decomposition of pure lignin showed two maxima in the mass loss corresponding to evolution of moisture at 92 °C and to lignin decomposition in a broad temperature range from 150 to 650 °C, respectively. When orthophosphoric acid was added, lignin dehydration proceeded to a larger extent, decomposition occurred in a narrower temperature range and decomposition ended at lower temperatures with higher char yields. There was an optimum P/L at values between 0.8 and 1.0, and further increasing P/L had low influence on the decomposition mechanisms. Differential Thermal Analysis (DTA) showed that reactions occurring upon impregnation of lignin with orthophosphoric acid at room temperature are finished after only 1 h, which confirmed the TG-DTG results. Impregnation times longer than 1 h and inclusion of isothermal periods did not affect significantly the subsequent char yield. Concerning the gaseous atmosphere, identical char yield were obtained whether the samples be prepared in nitrogen or in air at 450 °C. However, decomposition in air at 650 °C produced a decrease in the char yield when compared to pyrolysis in nitrogen due to the evaporation of P₂O₅ and the subsequent oxidation of the unprotected carbon.
© 2005 Elsevier B.V. All rights reserved.

Keywords: Lignin; Activated carbon; H₃PO₄; Thermogravimetric analysis

1. Introduction

The kraft method produces black liquor, a residue composed by lignin (30–40%) and other inorganic compounds, that is used as in-house fuel for the recovery of both energy and residual inorganic matter. The trend towards larger plant capacities and the optimization of the pulping process to improve cost effectiveness have led to the plants producing more by-product lignin than the amount that is needed to cover their energy consumption. The separation of lignin after water evaporation of black liquor could be an alternative to its incineration. Lignin is a bountiful and renewable source and could represent an attractive field for future in-

dustrial chemistry (i.e., as a substitute in the formulation of phenol–formaldehyde resins and adhesives). Another interesting option among these potential uses for lignin is the production of activated carbons.

Several authors have reported the use of kraft lignin as activated carbon precursor. Del Bagno et al. [1] investigated char and activated carbon manufacture from black liquors at a pilot-plant scale. Rodríguez-Mirasol et al. [2] prepared activated carbons from carbonization of eucalyptus kraft lignin. The latter research group also studied the chemical activation of this precursor by using ZnCl₂ [3] and obtained microporous activated carbons with a BET surface area as high as 1800 m² g⁻¹. However, the use of ZnCl₂ has declined due to the environmental problems [4] and orthophosphoric acid (PA) is preferred as activating-dehydrating agent.

* Corresponding author. Tel.: +34 977 558546; fax: +34 977 558544.
E-mail address: vanessa.fierro@urv.net (V. Fierro).

PA promotes the bond cleavage in the biopolymers and dehydration at low temperatures [5], followed by extensive cross-linking that bonds volatile matter into the carbon product and so an increase in carbon yield. Benadi et al. [6] showed that the mechanism of PA activation of biomass feedstocks occurs through various steps: cellulose depolymerization, biopolymers dehydration, formation of aromatic rings and elimination of phosphate groups. This allows activated carbons to be prepared with good yields and high surface areas.

The use of PA as activating agent has been reported with various agricultural by-products [7–20], wood [21,22], natural carbons [4,23,24] and synthetic carbons [25,26]. As far as we know, there is only one paper wherein the possibility of chemical activation of kraft lignin with PA among other activating agents has been examined [27]. The authors carried out carbonization over the temperature range of 500–900 °C held for 1 h and under N₂ flow: maximum surface areas of more than 1300 m² g⁻¹ were found at 600 °C.

This paper deals with the thermal decomposition of kraft lignin activated with PA in order to analyze the effect of the operation conditions on the char yield and on the rate of mass loss. The operation conditions studied were the impregnation time, the inclusion of isothermal periods, the PA to lignin mass ratio and the gaseous atmosphere. The role of PA as activating agent but also as inhibitor of carbon oxidation are herein analyzed.

2. Experimental

Kraft lignin was provided by Lignotech Iberica S.A. (Spain). Table 1 shows the proximate and ultimate analysis of lignin. The proximate analysis was carried out according to ISO standards following the weight losses at 100 °C/air (moisture), 900 °C/non-oxidizing atmosphere (volatile matter) and 815 °C/air (ash). An 85 wt.% H₃PO₄ aqueous solution (Panreac, Spain) was used as activating agent. Ultimate analysis was carried out in a EA1108 Carlo Erba Elemental Analyser. Results presented in Table 1 are very similar to those already reported [28].

Table 1
Lignin analysis (wt.%)

Proximate analysis (wt.%, wet basis)	
Moisture	14.5
Ash	9.5
Volatile matter	45.0
Fixed carbon ^a	31.0
Ultimate analysis (wt.%, ash and moisture free)	
Carbon	59.5
Hydrogen	5.1
Nitrogen	0.1
Sulphur	2.2
Oxygen ^a	33.1

^a Estimated by difference.

Lignin was mixed with varying amounts of H₃PO₄ in the range of 0.3–1.8 PA to lignin mass ratio (P/L). The slurry was left for impregnation times from 1 to 22 h at room temperature and under air, then transferred to a Perkin-Elmer TGA 7 thermobalance wherein decomposition was carried out at temperatures up to 650 °C. In this study, approximately 30–50 mg of sample was heated up to a maximum temperature of 650 °C and in a flow rate of 50 cm³ min⁻¹ measured at room temperature and atmospheric pressure.

Experiments were repeated three times to be sure of the reproducibility, which was found to be quite satisfactory. Average data obtained at each set of operation conditions were considered for results and discussion. For comparison purposes between the various activation parameters, we used a sample impregnated for 1 h with a P/L of 1.4 and pyrolyzed with a heating rate of 10 °C min⁻¹ up to 650 °C in nitrogen. The operation conditions were varied with regard to this reference. The effect of impregnation time was studied for samples left for 1 and 22 h at room temperature. The inclusion of isothermal periods was studied holding temperature for 15, 30 or 60 min at 150 °C or for 60 min at 300 °C and heating the sample at 10 °C min⁻¹ up to 650 °C afterwards. The effect of P/L was studied for samples with a P/L of 0.3, 0.6, 0.8, 1.0, 1.4 and 1.8. Finally, the effect of gas atmosphere on decomposition was studied using nitrogen or air and heating the sample to a maximum temperature of either 450 or 650 °C, which temperatures were held for 120 min.

Differential thermal analysis (DTA) was performed by simply recording the voltage drop at both ends of a differential chromel–alumel thermocouple, having one temperature probe embedded within the 1.4 P/L mixture (i.e., the sample), while the other one was inside a fine powder of dry α -alumina (i.e., the reference). The experiment was carried out at room temperature, and the P/L mixture was stirred by the thermocouple probe itself. For that purpose, any part of the experiment (thermocouple, sample and reference), was handled using metallic tongs, in order to avoid parasitic heating due to the fingers of the operator.

3. Results and discussion

Fig. 1(a) and (b) shows thermogravimetric (TG) and differential thermogravimetric (DTG) curves, respectively, for pure lignin, PA and 0.3 P/L mixture when heated at 10 °C min⁻¹ up to a temperature of 650 °C in nitrogen. The three samples were next maintained 2 h long at this latter final temperature. At the initial stage of the thermal treatment, pure lignin losses moisture from room temperature (T_{1a}) to 131 °C (T_{1b}). The dehydration proceeds with a maximum rate at 60 °C (T_{1max}), reaching a constant weight of 87% at 131 °C. Degradation of pure lignin occurs over a broad temperature interval (150–650 °C), with a maximum weight-loss rate between 300 and 370 °C. The decomposition of lignin is highly complex and depends on several factors such as its origin. The occurrence of lignin degradation in a wide range of temperatures

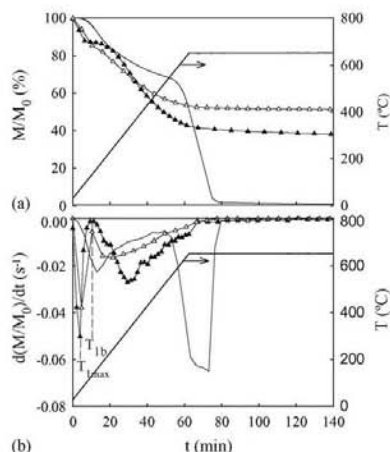


Fig. 1. (a) TG and (b) DTG curves for decomposition of pure lignin (\blacktriangle), PA (—), and the 0.3 P/L mixture (\triangle) in nitrogen. The thermal treatment is also shown on the plot.

has been described by several authors [29,30]. Negligible weight losses were observed while lignin was held 2 h long at 650 °C in nitrogen, hence the x-axis in Fig. 1 was limited to a maximum value of $t = 140$ min.

PA losses water at higher temperatures than pure lignin due to the different nature of the water eliminated. Water from lignin corresponds only to moisture whereas water from PA comes from moisture and the water generated by H_3PO_4 thermal degradation into P_2O_5 . Indeed, when orthophosphoric acid is heated it dehydrates to form pyrophosphoric acid, $H_4P_2O_7$, as a result of the condensation of two phosphoric acid molecules. Continued heating leads to a mixture of orthophosphoric and polyphosphoric ($H_{n+2}P_nO_{3n+1}$) acids called superphosphoric acid. At higher temperatures metaphosphoric acid, HPO_3 , is formed and it decomposes to P_2O_5 [31]. Thus, a maximum weight-loss rate was observed at 170 °C and the sample continued losing weight up to 300 °C, which can be attributed to the successive dehydration reactions to P_2O_5 . As temperature increased above 300 °C, weight loss continued at slower rate due to the sublimation of P_2O_5 that starts at this temperature [31]. Sublimation continued steadily up to $T = 580$ °C where a sharp increase in the weight-loss rate of the sample was observed, due to P_2O_5 melting and evaporation at 580–585 °C [31]. The sample weight when temperature arrived at 650 °C was of 52% and, as the temperature was held for 2 h, the sample was totally evaporated.

The 0.3 P/L mixture showed an intermediate behavior between those shown by lignin and PA. Fig. 2(a) and (b) shows experimental and calculated TG and DTG curves of the 0.3 P/L mixture; the calculation was made on the basis of a weighted combination of the experimental curves of pure PA and pure lignin. Doing so, the calculated carbon yield measured during heating was found to be lower than the

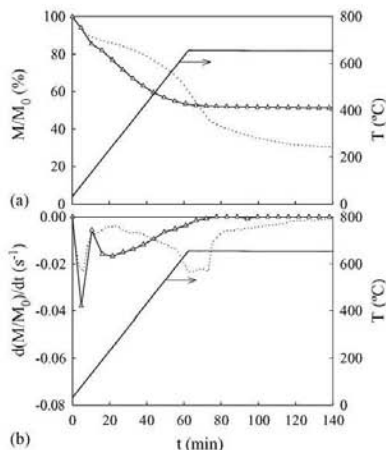


Fig. 2. (a) TG and (b) DTG curves for the decomposition of the 0.3 P/L mixture experimental (\triangle) and calculated (—) assuming a weighted combination of the TG and DTG curves for PA and lignin.

experimental one. However, when temperature was held at 650 °C for 2 h the calculated carbon yield decreased under the experimental one, 29 and 51%, respectively. The experimental weight-loss was higher than that calculated at temperatures lower than 150 °C and between 200 and 450 °C, and the weight of the sample was almost constant at temperatures higher than 600 °C.

These results clearly indicate that lignin reaction with PA during impregnation results in a complex mixed substrate, and that the PA/lignin mixture decomposes according to a reaction path, which is different from that of pure lignin. The PA-impregnated lignin follows a different reaction path during decomposition from that observed in pure lignin. Reaction of lignin with PA starts at room temperature as soon as the components are mixed since, according to the DTA curve given in Fig. 3, the temperature of the P/L sample increases immediately. This observation is in agreement with Lai [32]

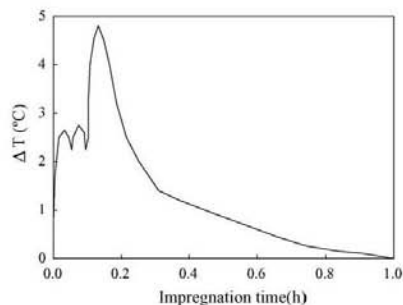


Fig. 3. DTA as a function of the impregnation time of the 1.4 P/L mixture in air and at room temperature. The first two peaks are artefacts only related to the stirring of the formerly inhomogeneous P/L mixture.

who reported the cleavage of aryl ether bonds in accompanied by dehydration, degradation and condensation reactions together with the formation of ketones by hydrolysis of ether linkages at low temperatures. PA promotes dehydration producing an important reordering of the structure and decreasing the volatile compounds emitted during decomposition and so increasing the carbon yield. Therefore, the first weight loss at temperatures lower than 150 °C can be attributed to the increase of dehydration and the higher rate of mass loss between 200 and 450 °C can be attributed to the decomposition of the depolymerized fractions of lignin that degrade at lower temperature than 'pure' lignin. The mass loss rate calculated as the weighted combination of the curves for PA and lignin is very different from the experimental one at temperatures higher than 500 °C (see Fig. 2). Whereas the weight of the sample remained approximately constant at 51% the calculated weight decreases steadily up to 29% due to P₂O₅ evaporation at temperatures above 580 °C. This result agrees with the total reaction of PA with lignin once they are mixed with a P/L of 0.3.

3.1. Effect of the impregnation time

In order to study the effect of the impregnation time, two samples with a P/L = 1.4 and impregnation times of 1 and 22 h were pyrolysed with a heating rate of 10 °C min⁻¹ up to 600 °C in nitrogen. TG curves showed nearly the same evolution with temperature. The char yield at 600 °C was of 56 and 55% for the samples with 1 and 22 h of impregnation time, respectively. This little difference is within the uncertainties of the method and it is difficult to conclude from these results that impregnation time has a real effect on the char yield.

Fig. 3 shows a DTA curve of a sample during the impregnation time with a P/L = 1.4 in air and at room temperature. The temperature difference between the sample and the reference is seen to be almost zero after 1 h impregnation time, evidencing that no chemical reaction still occurs after that time. Therefore, the expected differences, if there are, will be of minor importance for carbons prepared with impregnation times longer than 1 h. In that sense, DTA results are in good agreement with TG-DTG analysis and hence the effect of the other operating conditions can be studied using only 1 h impregnation time.

3.2. Effect of intermediate isothermal periods

Yoon et al. [33] reported an increase of char yield by maintaining the sample at constant temperature for a certain period of time at the beginning of the weight loss. Therefore, we have studied the effect of including isothermal periods at 150 and 300 °C, temperatures at which maximum weight-loss rates in PA-lignin mixtures were observed.

The PA-lignin decomposition was studied for a sample with a P/L = 1.4 and an impregnation time of 1 h, intercalating isothermal periods of 15, 30 and 60 min at 150 °C. Fig. 4 shows the mass loss of these samples and that of the ref-

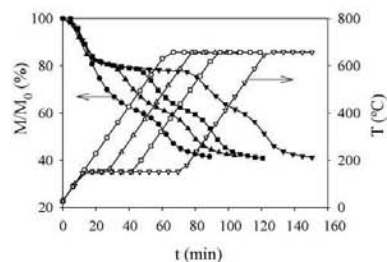


Fig. 4. TG curves of the 1.4 P/L mixture in nitrogen when intercalating isothermal periods at 150 °C (●) 0 min-reference, (▲) 15 min, (■) 30 min, (▼) 60 min). The thermal treatment is also shown on the plot ((○) 0 min-reference, (△) 15 min, (□) 30 min, (▽) 60 min).

erence sample without including isothermal periods. Except for the step at 150 °C, the shape of the curves was essentially the same with a slight variation in the slope of the mass loss between 250 and 400 °C due to the higher extent of lignin degradation with longer isothermal periods. Thus, the differences observed at the end of the isothermal period at 150 °C were small 81, 79 and 77% after 15, 30 and 60 min, respectively. However, once the temperature arrived to 650 °C and after holding for 30 min the char yield was of 42, 41 and 41% for the same samples, respectively, and also of 41% for the reference sample. Therefore, intercalating isothermal periods does not produce changes in the char yield.

Although the differences of char yield upon addition of an isothermal period at 150 °C were not very important, including an isothermal step at this temperature can be of practical interest. Biomass is usually ground and pelletized before carbonization for commercial purposes. As the maximum weight-loss rate corresponding to moisture vaporization during the decomposition of lignin takes place at approximately 150 °C, the rapid water vaporization could crack-up the pellet. Carbonization of lignin in pellets indeed evidenced that intercalating an isothermal period between 100 and 150 °C allows a steady vaporization of lignin moisture, finally leading to pellets free of cracks.

We also studied the PA-lignin decomposition with a P/L = 1.4 and with the inclusion of isothermal periods of 1 h at 150 or 300 °C. The inclusion of an isothermal period of 1 h at 150 °C or at 300 °C did not produce any change in the char yield that was about 41% after holding for 30 min once the temperature arrived to 650 °C. These results are in agreement with the works of Rodríguez-Reinoso et al. [34] and Tascón et al. [35] who found no change in carbon yield with inclusion of intermediate isothermal periods during the course of decomposition of viscose rayon cloth and apple pulp, respectively.

3.3. Effect of phosphoric acid to lignin mass ratio (P/L)

Fig. 5 shows the DTG curves of PA-lignin mixtures, varying P/L from 0.3 to 1.8. As the P/L increased, the tempera-

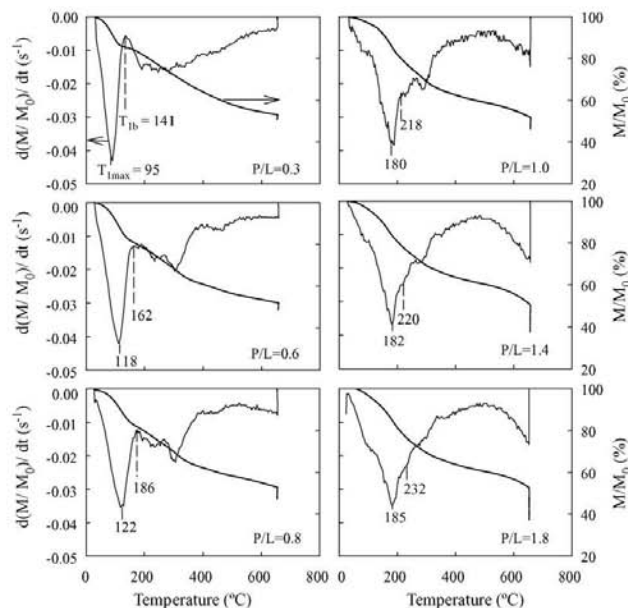


Fig. 5. TG and DTG curves of the decomposition of PA/lignin mixtures, varying P/L from 0.3 to 1.8, heating at $10\text{ }^{\circ}\text{C min}^{-1}$ up to $650\text{ }^{\circ}\text{C}$ and holding the final temperature for 2 h.

ture at which the rate of weight loss was maximal raised up to $P/L = 1.0$. At $P/L \geq 1.0$, $T_{1\text{max}}$ remains practically unchanged at a temperature of around $180\text{--}185\text{ }^{\circ}\text{C}$. We can also observe in the figure that increasing P/L from 0.3 to 0.8 makes the lignin to be completely degraded at decreasingly lower temperatures, from 620 to about $400\text{ }^{\circ}\text{C}$. By contrast, $P/L \geq 1.0$ lead to almost identical end of degradation temperatures, lower than $400\text{ }^{\circ}\text{C}$.

Jagtøyen and Derbyshire [21] reported that CO_2 and CO begin to evolve from biomass in presence of PA just below about $100\text{ }^{\circ}\text{C}$ and their production increases sharply to achieve a maximum at about $200\text{ }^{\circ}\text{C}$. In Fig. 5, it may be observed that $T_{1\text{max}}$ becomes higher than the temperature of maximal rate for PA dehydration ($170\text{ }^{\circ}\text{C}$) and so there is not a clear difference between dehydration of the PA-lignin mixture, dehydration of the PA in excess and lignin degradation with increasing P/L. However, it seems clear that there is a P/L value where PA totally reacts with lignin and so higher P/L should not produce any effect on the decomposition of lignin. In order to confirm the existence of this optimum P/L, the inflexion point of the TG curve after $T_{1\text{max}}$ was assumed to mark the end of the dehydration peak, and hence to correspond to the limiting temperature $T_{1\text{b}}$ between dehydration and decomposition. The percentage of mass loss due to the reaction of PA with lignin, $\%ML_{P/L}$, could thus be quantified, and was calculated as follows:

$$\%ML_{P/L} = \frac{ML_{T_{1b}} - [X_P ML_P + X_L ML_L]}{ML_{T_{1b}}} \times 100$$

where $ML_{T_{1b}}$ is the percentage of mass loss at the inflexion point of the curve, T_{1b} , for a mixture PA-lignin. ML_P and ML_L stand for the water loss of PA and lignin respectively when pyrolyzed independently. X_P and X_L are the weight fraction of PA and lignin in the PA-lignin mixture at a given P/L.

Fig. 6 shows the $\%ML_{P/L}$ calculated as defined above as a function of P/L. The mass loss due to the addition of PA increases nearly linearly between a P/L of 0 and 0.8 and remains approximately constant for $P/L \geq 1.0$ within the error in the estimation of $ML_{T_{1b}}$. This figure confirms that it exits a maximum of acid that can react with lignin. Using $P/L \geq 1.0$ does not increase dehydration: the acid in excess degrades

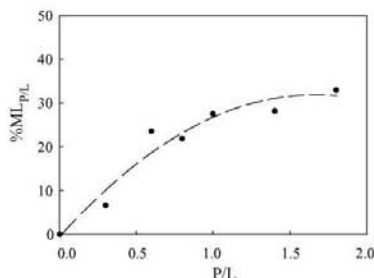


Fig. 6. Percentage of mass loss due to the reaction of PA with lignin as a function of P/L.

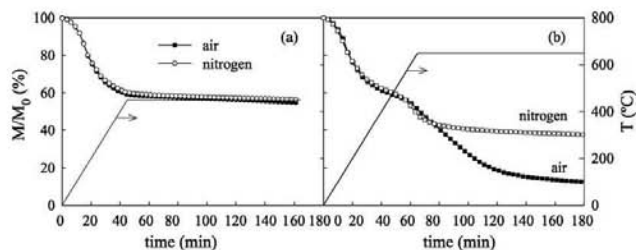


Fig. 7. TG curves of the 1.4 P/L mixture in nitrogen and air when heating at $10^{\circ}\text{C min}^{-1}$ up to (a) 450°C and (b) 650°C , and holding the final temperature for 2 h.

up to P_2O_5 and evolves, which is confirmed by the weight loss produced at $\text{P/L} \geq 1.0$ and at temperatures higher than 550°C observed in Fig. 5.

It may be seen from Fig. 5 that, at $\text{P/L} = 0.3$, the plateau indicating that no more reaction takes place while the material is heated (i.e., the lignin degradation is finished), occurs near 600°C . Increasing P/L makes the end of the degradation occur at decreasing temperatures as far as P/L remains below 1.0. The DTG curves for $\text{P/L} \geq 1.0$ evidenced the same behavior, i.e., the lignin degradation took place at lower ($<400^{\circ}\text{C}$) and almost identical temperatures, and the weight-loss rate was nearly constant at temperatures from 450 to 550°C . The melting and vaporization of P_2O_5 of the unreacted PA could explain the increase in weight-loss rate from 550 to 650°C . This observation supports the hypothesis of an optimum on P/L at values between 0.8 and 1.0 as argued above. It seems clear that since PA reacts with lignin, the optimum P/L will depend on the lignin origin.

3.4. Effect of the gaseous atmosphere

Materials impregnated with PA are usually pyrolyzed in nitrogen. However, earlier studies have shown that chemical activation with PA in air produced carbons with the greatest total number of functional groups when compared with activation under nitrogen flow [25,36,37]. Therefore, excluding obvious economical concerns, activation in air is an interesting option when activated carbons are used for the removal of metals in water treatment because metal uptake appears to be directly correlated with the number of functional groups [36].

To study the effect of the gaseous atmosphere in the process, a sample of PA-impregnated lignin was heated at $10^{\circ}\text{C min}^{-1}$ up to 450 or 650°C in air and in nitrogen and both final temperatures were held for 2 h. Fig. 7(a) shows TG curves of PA-lignin decomposition with $\text{P/L} = 1.4$ in nitrogen and air when heating at $10^{\circ}\text{C min}^{-1}$ up to 450°C . The TG curves for these two experiments exhibit exactly the same shape, i.e., the sample losses weight in the same way and independently of the atmosphere used. Moreover, there was no significant weight loss for 2 h once the temperature of the sample arrived to 450°C .

Fig. 7(b) shows the same as in Fig. 7(a) but the final temperature was 650°C , held 2 h long. Again, the TG curves for both nitrogen and air atmospheres exhibit exactly the same shape up to 650°C . However, if temperature was held at 650°C for a longer time, the samples behaved differently in air and in nitrogen. The sample pyrolyzed in nitrogen showed a sharp decrease in the weight from 51 to 43% during the first 15 min and afterwards the weight remained approximately constant with time. On the contrary, the sample pyrolyzed in air showed a continuous decrease during 80 min reaching a mass percentage of 14.5% meaning the total combustion of the sample. Indeed, due to the phosphatation of the ashes, a residual mass higher than that given in Table 1, 9.5%, was recovered. The low mass variation (8%) of the sample pyrolyzed in nitrogen can be attributed to the P_2O_5 vaporization whereas the low char yield in air is the result of the P_2O_5 vaporization of the PA used in excess and the combustion of unprotected carbon. Examining Fig. 7, one can extract a conclusion of practical and economical importance: char yield is nearly independent of the gaseous atmosphere at moderate temperatures and with the adequate P/L.

4. Conclusions

When lignin and PA are mixed together, they react completely in less than 1 h and longer impregnation times or inclusion of isothermal periods do not have any influence on the char yield. The product of the reaction between PA and lignin pyrolyses following a reaction path different from that of pure lignin. PA acts on lignin increasing dehydration and anticipating its complete degradation at temperatures as low as 400°C . There exists an optimum P/L at values between 0.8 and 1.0 that allows the complete reaction of lignin, and further increases in P/L do not produce changes on the pyrolysis process. H_3PO_4 in excess dehydrates progressively into P_2O_5 which finally melts and evaporates. P_2O_5 protects carbon from oxidation and once evaporated at temperatures higher than 580°C the carbon is totally oxidized in air whereas the char yield in nitrogen remains constant. Char yield is nearly independent of the gaseous atmosphere at moderate decomposition temperatures as long as lignin has reacted completely with PA.

Acknowledgements

This research was made possible in part by financial support from MCYT (project PPQ2002-04201-CO02) and DURSI (2001SGR00323). V. Fierro acknowledges the MCYT and the Universitat Rovira i Virgili (URV) for the financial support of her 'Ramón y Cajal' research contract. V. Torné-Fernández acknowledges the URV for her PhD grant.

References

- [1] V.D. del Bagno, R.L. Miller, J.J. Watkins, On site production of activated carbon from Kraft Black Liqueur, U.S. EPA Report no. 600/2-78-191 (1978).
- [2] J. Rodríguez-Mirasol, T. Cordero, J.J. Rodríguez, *Carbon* 31 (1993) 87–95.
- [3] E. Gonzalez Serrano, T. Cordero, J. Rodríguez-Mirasol, J.J. Rodríguez, *Ind. Eng. Chem. Res.* 36 (1997) 4832–4838.
- [4] H. Teng, T.S. Yeh, L.Y. Hsu, *Carbon* 36 (1998) 1387–1398.
- [5] M. Jagtoyen, F. Derbyshire, *Carbon* 31 (1993) 1185–1192.
- [6] H. Benadi, D. Legras, J.N. Rouzaud, F. Béguin, *Carbon* 36 (1998) 306–309.
- [7] J. Laine, A. Calafat, M. Labady, *Carbon* 27 (1989) 191–195.
- [8] M. Molina-Sabio, F. Rodríguez-Reinoso, F. Caurila, M.J. Sellés, *Carbon* 34 (1996) 457–462.
- [9] B.S. Girgis, A.A. El-Hendawy, *Micropor. Mesopor. Mater.* 52 (2002) 105–117.
- [10] A.A. El-Hendawy, S.E. Samra, B.S. Girgis, *Colloid Surf. A* 180 (2001) 209–221.
- [11] B.S. Girgis, M.F. Ishak, *Mater. Lett.* 39 (1999) 107–114.
- [12] F. Suárez-García, A. Martínez-Alonso, J.M.D. Tascón, *J. Anal. Appl. Pyrolysis* 63 (2002) 283–301.
- [13] F. Suárez-García, A. Martínez-Alonso, J.M.D. Tascón, *Carbon* 39 (2001) 1111–1115.
- [14] M.C. Baquero, L. Giraldo, J.C. Moreno, F. Suárez-García, A. Martínez-Alonso, J.M.D. Tascón, *J. Anal. Appl. Pyrolysis* 70 (2003) 779–784.
- [15] B.S. Girgis, S.S. Yunis, A.M. Soliman, *Mater. Lett.* 57 (2002) 164–172.
- [16] T. Vemersson, P.R. Bonelli, E.G. Cerrella, A.L. Cukiernan, *Bioreour. Technol.* 83 (2002) 95–104.
- [17] J. Guo, A.C. Lua, *Sep. Purif. Technol.* 30 (2003) 265–273.
- [18] R.A. Shawabkeh, D.A. Rockstraw, R.K. Ehada, *Carbon* 40 (2002) 781–786.
- [19] Y. Diao, W.P. Walawender, L.T. Fan, *Bioreour. Technol.* 81 (2002) 45–52.
- [20] C.A. Toles, W.E. Marshall, M.M. Johns, L.H. Wartelle, A. McAloon, *Bioreour. Technol.* 71 (2000) 87–92.
- [21] M. Jagtoyen, F. Derbyshire, *Carbon* 36 (1998) 1085–1097.
- [22] H. Benaddi, T.J. Bandoz, J. Jagiello, J.A. Schwarz, J.N. Rouzaud, D. Legras, F. Béguin, *Carbon* 38 (2000) 669–674.
- [23] C. Toles, S. Rimmer, J.C. Hower, *Carbon* 34 (1996) 1419–1426.
- [24] F. Carrasco-Marín, M.A. Alvarez-Merino, C. Moreno-Castilla, *Fuel* 75 (1996) 966–970.
- [25] A.M. Puziy, O.I. Poddubnaya, A. Martínez-Alonso, F. Suárez-García, J.M.D. Tascón, *Appl. Surf. Sci.* 200 (2002) 196–202.
- [26] A.M. Puziy, O.I. Poddubnaya, B. Gawdzik, M. Sobiesiak, D. Dziadko, *Appl. Surf. Sci.* 196 (2002) 89–97.
- [27] J. Hayashi, A. Kazehaya, K. Muroyama, A.P. Watkinson, *Carbon* 38 (2000) 1873–1878.
- [28] J. Rodríguez-Mirasol, T. Cordero, J.J. Rodríguez, *Carbon* 34 (1996) 43–52.
- [29] J.A. Caballero, A. Marcilla, J.A. Conesa, *J. Anal. Appl. Pyrol.* 44 (1997) 75–88.
- [30] J.J.M. Órfão, F.J.A. Antunes, J.L. Figueiredo, *Fuel* 78 (1999) 349–358.
- [31] *Handbook of Chemistry and Physics*, 72nd ed., CRC press, Boca Raton, Florida, 1985, p. B-119.
- [32] Y.Z. Lai, in: D.N.S. Hon, N. Shirashi (Eds.), *Wood and Cellulosic Chemistry*, 10, Marcel Dekker, New York, 1991, p. 455.
- [33] S.H. Yoon, B.C. Kim, Y. Korai, I. Mochida, *Proceedings of the 22nd Biennial Conference on carbon. Extended Abstract and Program*, San Diego, California, 1995, p. 218.
- [34] C. Pastor, F. Rodríguez-Reinoso, H. Marsh, M.A. Martínez, *Carbon* 3 (1999) 1275–1283.
- [35] F. Suárez-García, A. Martínez-Alonso, J.M.D. Tascón, *J. Anal. Appl. Pyrolysis* 62 (2002) 93–109.
- [36] C.A. Toles, W.E. Marshall, M.M. Johns, *Carbon* 37 (1999) 1207–1214.
- [37] C.A. Toles, W.E. Marshall, M.M. Johns, *J. Chem. Technol. Biotechnol.* 72 (1998) 255–263.

5.1.3. Kraft lignin as a precursor for microporous activated carbons prepared by impregnation with orto-phosphoric acid: synthesis and textural characterisation

Este artículo se ha publicado en el journal *Microporous and Mesoporous Materials* en 2006 en el volumen 92, páginas 243 a 250.



Kraft lignin as a precursor for microporous activated carbons prepared by impregnation with ortho-phosphoric acid: Synthesis and textural characterisation

V. Fierro ^{a,*}, V. Torné-Fernández ^a, A. Celzard ^b

^a *Departament de Enginyeria Química, Universitat Rovira i Virgili, Avda dels Països Catalans, 26, 43007 Tarragona, Spain*

^b *Laboratoire de Chimie du Solide Minéral, Université Henri Poincaré—Nancy I, UMR—CNRS 7555, BP 239, 54506 Vandoeuvre-lès-Nancy, France*

Received 25 October 2005; received in revised form 12 January 2006; accepted 19 January 2006

Available online 3 March 2006

Abstract

Activated carbons were prepared by activation of Kraft lignin with ortho-phosphoric acid at various temperatures (400–650 °C), weight ratios of ortho-phosphoric acid to lignin (P/L = 0.7–1.75) and impregnation times (1–48 h). The resulting carbons were characterised by elemental analysis, N₂ adsorption at 77 K and SEM. The results indicate that the pyrolysis of lignin impregnated with ortho-phosphoric acid produces essentially microporous carbons, with a percentage of the total micropore volume approximately constant (80%), whatever the carbonisation temperature. The fraction of ultramicropores decreases with increasing temperature whereas that of supermicropores reaches a maximum at 600 °C. The maximum surface area (1305 m²/g) and pore volume (0.67 cm³/g) are reached at 600 °C, while pyrolysis of acid-impregnated lignin at temperatures higher than 600 °C produces a significant reduction of both pore volume and BET surface area due to: (i) the shrinkage of the material caused by the degradation of the phosphate and polyphosphate bridges and (ii) the oxidation of the carbon caused by the loss of the protecting P₂O₅. Increasing the P/L ratio increases the carbon yield and involves changes in the total volume of pores, the pore size distribution and the BET surface area. There exists an optimum P/L ratio which probably depends on the activation temperature, an excess of ortho-phosphoric acid beyond this optimum value reducing the surface area and the pore volume of the resultant activated carbon. Increasing the impregnation time, the surface area and the pore volume are lowered, and such an effect is more severe at higher activation temperatures.

© 2006 Elsevier Inc. All rights reserved.

Keywords: Activated carbon; Ortho-phosphoric acid activation; Porosity; Surface area

1. Introduction

The conversion of wood chips to pulp for manufacturing paper generates huge quantities of by-product lignins. Various processes can be used to remove and isolate lignin. The Kraft process produces black liquor, a residue composed of lignin (30–40%) and other inorganic compounds. This residue is used as in-house fuel for the recovery of

energy and of the remaining inorganic reactants. As progress has been taken to maximise production, the recovery furnaces in an ever-increasing number of mills have become overloaded; the result is that all the by-product lignin can no longer be used in its traditional role as a fuel. Unfortunately the necessary capital investment usually precludes construction of a new recovery furnace so that there is little prospect of rectifying the situation in the majority of recovery-loaded mills. The separation of lignin and its use as precursor for activated carbons (ACs) could be an alternative to incineration.

ACs have already been synthesised by physical activation of eucalyptus Kraft lignin by CO₂ partial gasification [1] and by chemical activation of this precursor using zinc

* Corresponding author. Present address: Laboratoire de Chimie du Solide Minéral, Université Henri Poincaré—Nancy I, UMR—CNRS 7555, BP 239, 54506 Vandoeuvre-lès-Nancy, France. Tel.: +33 383684000; fax: +33 383684619.

E-mail address: Vanessa.Fierro@lcsm-uhp.nancy.fr (V. Fierro).

chloride [2]. Chemical activation of Kraft lignin with $ZnCl_2$ within the thermal range 400–500 °C allowed obtaining high surface area ACs with predominantly microporous structure. At 500 °C and impregnation ratio $ZnCl_2$ /lignin of 2.3 w:w, the maximum of mesoporosity ($0.59 \text{ cm}^3/\text{g}$) and microporosity ($1.04 \text{ cm}^3/\text{g}$) and a corresponding BET surface area of $1800 \text{ m}^2/\text{g}$ were obtained. However, the use of $ZnCl_2$ has declined due to environmental problems [3], and ortho-phosphoric acid is preferred as activating-dehydrating agent.

The use of ortho-phosphoric acid as activating agent has been reported for various agricultural by-products [4–17], wood [18,19], natural [20,21,3] and synthetic [22,23] carbons. The ortho-phosphoric acid impregnating the material plays a double role according to Jagtoyen and Derbyshire [18]: (i) it produces the hydrolysis of the lignocellulosic matters and the subsequent extraction of some components, thus weakening the material, which swells and (ii) the acid occupies a volume which inhibits the contraction of the material during the heat treatment, by forming phosphate and polyphosphate bridges that connect and cross-link biopolymer fragments, thus leaving a porosity when it is extracted by washing after carbonisation.

To the best of our knowledge, there is only one paper [24] in which the possibility of chemical activation of Kraft lignin with H_3PO_4 , among other activating agents, has been examined. The authors carried out carbonisation at a temperature held for 1 h within the range 500–900 °C, under N_2 flow. Maximum surface areas of more than $1300 \text{ m}^2 \text{ g}^{-1}$ were reached at 600 °C.

Our previous studies, dealing with the analysis of the thermal decomposition of Kraft lignin impregnated with ortho-phosphoric acid, were carried out using thermogravimetry (TG–DTG) [25,26]. In these papers, we got significant insight in the activation process and in the role of P_2O_5 , up to its evaporation at 580 °C, in protection against carbon oxidation. Thus, ortho-phosphoric acid was found to increase the carbon yields in two ways: (i) increase of dehydration and promotion of a structural rearrangement of the solid, which also reduces the emission of volatile compounds and (ii) prevention of combustion in the air atmosphere.

In this paper, the preparation at a larger scale and the characterisation of the ACs derived from Kraft lignin (KL), using chemical activation with ortho-phosphoric acid in air, are reported. Our purpose was to examine the influence of preparation conditions (activation temperature, ortho-phosphoric/lignin weight ratio and impregnation time) on carbon yield, surface area and pore size distribution.

2. Experimental

2.1. Starting materials

Kraft lignin (KL) was provided by Lignotech Iberica S.A. The proximate analysis was carried out according to

ISO standards, following the weight losses of the material at 100 °C in air (moisture, ISO-589-1981), at 900 °C in a non-oxidising atmosphere (volatile matter, ISO-5623-1974) and at 815 °C in air (ashes, ISO-1171-1976). An 85 wt.% H_3PO_4 solution (Panreac, Spain) was used as activating agent. The ultimate analysis of the pristine lignin was carried out in an EA1108 Carlo Erba Elemental Analyser.

2.2. Preparation and characterisation of the ACs

Lignin was mixed with various amounts of H_3PO_4 in the range of 0.7–1.75 acid to lignin weight ratio (P/L) on a wet basis. The slurry was left for impregnation times varying from 1 to 48 h at room temperature in air, and then transferred to a furnace DUM Model 10CAF where carbonisation was carried out under air atmosphere. The furnace was heated at $10 \text{ }^\circ\text{C min}^{-1}$, up to 150 °C, which temperature was held for 1 h to allow free evolution of water. Afterwards the oven was heated at $10 \text{ }^\circ\text{C min}^{-1}$ up to the final carbonisation temperature, ranging from 400 to 650 °C, which was held for 2 h. To remove the excess of H_3PO_4 after carbonisation, the activated carbon was extensively washed with distilled water until a neutral pH was met (a CyberScan PC 510 pH-meter with a Hamilton-electrode ‘Fluhtrode’ was used). Then, the samples were dried overnight in an oven at 105 °C.

C, H, S and N contents of the ACs were measured using an EA1108 Carlo Erba Elemental Analyser. P content was determined by scanning electron microscopy (SEM) with a JEOL JSM-6400 equipped with an energy dispersive X-ray (EDX) microanalyser. Oxygen was calculated by difference.

Surface area and pore size distributions were determined from the corresponding nitrogen adsorption–desorption isotherms obtained at 77 K with an automatic instrument (ASAP 2020, Micromeritics). The samples were previously outgassed at 523 K for several hours. N_2 adsorption data at relative pressures ranging from 10^{-5} to 0.99 (in a set of values previously fixed) were analysed according to: (i) the BET method [27] for calculating the apparent surface area, S_{BET} and (ii) the α_s method [28] (using Carbopack F Graphitised Carbon Black as reference material [29]) for calculating the micropore volume, $V_{\alpha\text{micro}}$, and the ultramicropore volume, $V_{\alpha\text{ultra}}$. The total pore volume, $V_{0.99}$, was calculated from nitrogen adsorption at a relative pressure of 0.99. ACs were examined by scanning electron microscopy (SEM) operating at magnifications of $\times 400$ and $\times 7000$.

3. Results and discussion

3.1. Characterisation of the raw material

Table 1 shows the proximate and ultimate analyses of lignin. The high sulfur content (2.2%) in KL is originated both from the Kraft or sulfate process, based on the action of NaOH and Na_2S for separating cellulose from the other

Table 1
 Lignin analyses (wt.%)

Proximate (wt.%, humid basis)		Elemental (wt.%, ash and moisture free)	
Moisture	14.45	Carbon	59.46
Ash	9.50	Hydrogen	5.07
Volatile matter	44.93	Nitrogen	0.05
Fixed carbon ^a	31.12	Sulfur	2.15
		Oxygen ^a	33.27

^a Estimated by difference.

wood constituents, and from organically bound sulfur (up to 1.5%) [30].

Fig. 1 shows SEM images of KL at different magnifications. KL particles are small, and have a rounded (even spherical) shape with widely open volumes inside. Such morphology is probably due to the concentration process of lignin from black liquors, which is done by evaporation; due to their surface tension, the particles take a spherical—thermodynamically more stable form. A more detailed observation reveals that the surface of the KL particles is very rough.

We observed that reaction of lignin with ortho-phosphoric acid starts at room temperature, and as soon as the components are mixed together, the temperature of the vessel increases [25]. Lai [31] indeed reported the cleavage of aryl ether bonds accompanied by dehydration, degradation and condensation reactions together with the formation of ketones by hydrolysis of ether linkages at low temperatures.

In order to understand the effect of the preparation conditions on the ACs produced by activation of KL with ortho-phosphoric acid, activation temperature (400–650 °C), weight ratio of acid to lignin (P/L = 0.7–1.75) and impregnation time (1–48 h) were systematically varied.

3.2. Effect of the activation temperature

The effect of activation temperature was studied from 400 to 650 °C using KL impregnated with ortho-phosphoric acid for 1 h and with a P/L ratio of 1.4.

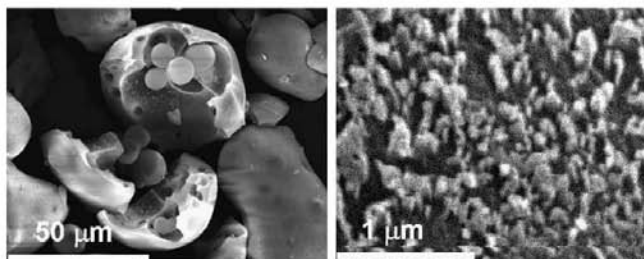


Fig. 1. SEM images of Kraft lignin at different magnifications.

Fig. 2 shows the variation of carbon yield with activation temperature. Increasing the temperature, the carbon yield decreases from 49% at 400 °C to 8% at 650 °C. There are two sharp decreases in carbon yield, one from 400 to 450 °C and the other between 550 and 650 °C, whereas the slope is lower between 450 and 550 °C. The corresponding weight loss mechanisms were explained in our previous studies [25,26] carried out in a thermogravimetric device. The first sharp weight loss corresponds to the loss of most of the volatile matter. The second one would correspond: (i) to the volatilisation of the P₂O₅ coming from the H₃PO₄ in excess and (ii) to the resultant carbon combustion once the formerly protecting P₂O₅ is lost.

Table 2 shows the elemental analysis of the ACs prepared according to the experimental conditions used in this study. As temperature is increased up to 550 °C, there is an increase in C and a decrease in O and H contents, due to an increasing degree of aromaticity. At activation temperatures higher than 550 °C, the C/H ratio remains nearly constant, indicating no further changes in the chemical composition, which again confirms the aforementioned process explaining the variations of carbon yield. The P content in the ACs decreases with temperature, indicating a degradation of the phosphate and polyphosphate groups.

Fig. 2 also shows the BET apparent surface area of the ACs prepared at different activation temperatures. The BET surface area increases between 400 and 600 °C up to

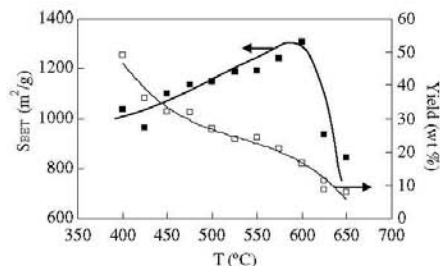


Fig. 2. BET surface area and carbon yield of the activated carbons as a function of the activation temperature (P/L = 1.4 and 1 h impregnation time).

Table 2
 Activation conditions and elemental analysis of the resultant ACs

Activation conditions			Elemental analysis						
T (°C)	P/L (w/w)	t _i (h)	C (%)	H (%)	C/H	N (%)	S (%)	P (%)	O ^a (%)
400	1.4	1	76.19	2.03	37.53	0.12	0.65	n.d.	n.d.
425	1.4	1	76.26	1.84	41.45	0.16	0.73	n.d.	n.d.
450	1.4	1	78.03	1.59	49.08	0.20	1.08	1.20	17.90
475	1.4	1	78.02	1.58	49.38	0.22	0.98	n.d.	n.d.
525	1.4	1	79.54	1.41	56.41	0.23	0.68	0.80	17.34
550	1.4	1	79.97	1.29	61.99	0.20	0.66	n.d.	n.d.
575	1.4	1	80.51	1.35	59.64	0.27	0.88	n.d.	n.d.
600	1.4	1	80.82	1.27	63.64	0.29	0.79	0.60	16.23
625	1.4	1	79.06	1.40	56.47	0.46	0.66	n.d.	n.d.
650	1.4	1	78.14	1.24	63.02	0.59	0.85	0.60	18.58
450	0.7	1	77.23	2.02	38.23	0.25	0.80	1.10	18.60
450	1.0	1	77.83	1.78	43.72	0.25	1.20	0.9	18.04
450	1.2	1	77.95	1.92	40.60	0.19	0.66	1.3	17.98
450	1.75	1	76.23	1.91	39.91	0.19	0.77	2.3	18.60
450	1.4	48	78.25	1.66	47.14	0.20	0.54	n.d.	n.d.
600	1.4	2	80.42	1.41	57.04	0.31	0.42	n.d.	n.d.
600	1.4	6	79.9	1.19	67.16	0.32	0.89	n.d.	n.d.
600	1.4	48	78.75	1.23	64.02	0.36	1.04	n.d.	n.d.

^a Estimated by difference; n.d. not determined.

a maximum value of 1305 m² g⁻¹ observed at 600 °C and the surface areas are considerably reduced at higher temperatures. These results are consistent with the two sharp decreases in carbon yield observed previously. The steady increase of surface area with temperature up to 600 °C would correspond to the evolution of compounds produced from the cross-linking reactions. The latter preserve the structure of the polymer at the same time as the BET surface area and the porosity increase up to 600 °C. At higher temperatures, the degradation of the phosphate and polyphosphate bridges, already observed by the decrease of P content in the ACs with temperature [25,26], would weaken the structure; the resultant collapse would then lower both the BET surface area and the pore volume. Moreover, the loss of the protecting P₂O₅ and the combustion of the carbon could also explain this reduction in the surface and the porosity. Hayashi et al. [24] also reported that 600 °C is the optimum temperature for surface development in ACs prepared by ortho-phosphoric acid activation of KL, in good agreement with our results.

Fig. 3 shows adsorption isotherms of N₂ at 77 K measured on ACs prepared at different temperatures from 400 to 650 °C. All the isotherms are of type I. That of the carbon prepared at 400 °C has a very small upward bending at the highest pressures, indicating an essentially microporous character with some contribution of wider pores (meso- and macropores). As activation temperature increases, the knee of the isotherm widens and the plateau is not clearly reached, indicating pore widening. The isotherm of the carbon prepared at 650 °C shows the lowest N₂ adsorption capacity, due to the reduction of both its surface and its pore volume.

Fig. 4 shows the application of the α_s method to the N₂ isotherms of the ACs prepared at 400, 500, 600 and 650 °C, which allows to calculate V_{αmicro} and V_{αultra}. Fig. 5 shows

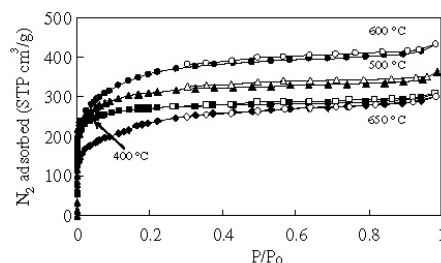


Fig. 3. Nitrogen adsorption (full symbols) and desorption (empty symbols) isotherms of activated carbons prepared at different temperatures (P/L = 1.4 and 1 h impregnation time).

the evolution of V_{0.99}, V_{αmicro} and V_{αultra} as a function of activation temperature. V_{αultra} always decreases with increasing temperature whereas the volume of supermicropores, calculated as the difference between V_{αmicro} and V_{αultra}, reaches a maximum at 600 °C. At temperatures higher than 600 °C, there is a reduction of all the pore volumes. This reduction in the total porosity would be due to: (i) the collapse of the structure produced by the loss of phosphate and polyphosphate bridges and the resultant weakening of the structure at temperatures higher than 600 °C and (ii) the oxidation of the carbon caused by the volatilisation of the protecting P₂O₅.

SEM photographs of the ACs prepared at different temperatures, with a constant P/L ratio of 1.4 and an impregnation time of 1 h, are shown in Fig. 6. This figure shows well-defined macropores and the presence of small grains at the surface; these grains are more hardly seen in the AC prepared at 650 °C, which also presents a smoother surface. It can be observed that increasing activation temperature, the small grains agglomerate, or soften, to form

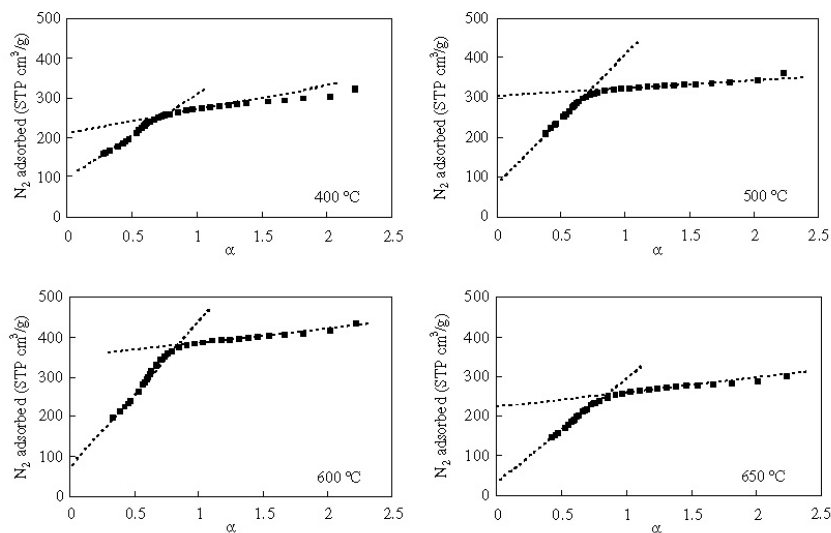


Fig. 4. α_c plots of N_2 adsorption at 77 K on ACs prepared at: (a) 400, (b) 500, (c) 600 and (d) 650 °C (P/L = 1.4 and 1 h impregnation time).

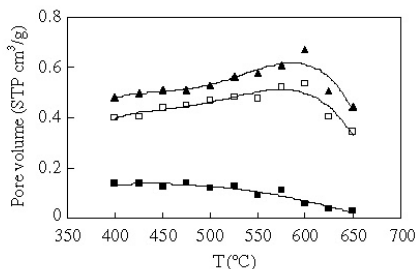


Fig. 5. Effect of the activation temperature on the pore volumes: $V_{0.99}$ (\blacktriangle), $V_{\alpha\text{micro}}$ (\square) and $V_{\alpha\text{ultra}}$ (\blacksquare) of the ACs.

bigger spheres until becoming nearly undistinguished with the surface at 650 °C. This finding is consistent with a lowering of the surface area at high temperatures.

3.3. Effect of the impregnation ratio

Porosity is generated with ortho-phosphoric acid remaining intercalated in the internal structure of the biopolymer material in the form of phosphate and polyphosphate compounds [32], hindering the shrinkage. As P/L increases, it is reasonable to expect, on one hand, an increase in the volume filled by polyphosphate compounds as long as ortho-phosphoric acid can react with lignin, but also, on the other hand, a weakening of the structure due to the attack of the excess acid. The effect of the P/L ratio was studied using carbons impregnated during 1 h at five differ-

ent P/L ratios, ranging between 0.7 and 1.75, and activated at 450 °C.

Fig. 7(a) shows the variation of carbon yield with the P/L ratio. The carbon yield increases from 21% at P/L = 0.7–32% at P/L = 1.4. The latter value of carbon yield is nearly identical to the amount of fixed carbon determined in Table 1, once more confirming the protecting role of the phosphoric acid against carbon oxidation in air at the experimental activation temperatures. It was found that P/L values higher than 1.4 do not produce further increase of carbon yield at 450 °C. The P/L ratio not only affects the char yield but also the apparent surface area and the pore size distribution. Fig. 7(a) also shows the variation of the apparent surface areas with the P/L ratio. The highest value is reached at P/L = 1.2–1.4, and further increases in the P/L ratio produces a decrease in the BET surface area.

Nitrogen adsorption isotherms measured on ACs prepared at several P/L ratios are of type I, just like those already presented in Fig. 3. At P/L = 0.7, the activated carbons are essentially microporous with some contribution of wider pores (meso- and macropores). Increasing the P/L ratio produces the development of porosity in the mesoporous region, evidenced by the widening of the knee of the isotherms. Fig. 7(b) shows the variation of $V_{0.99}$, $V_{\alpha\text{micro}}$ and $V_{\alpha\text{ultra}}$ of the ACs with the P/L ratio used for activation. The highest micropore to total volume ratio is found at the lowest P/L ratio used. As P/L ratio increases up to P/L = 1.4, the $V_{0.99}$ and $V_{\alpha\text{micro}}$ increases but the $V_{\alpha\text{ultra}}$ decreases. Within the inherent error in the N_2 adsorption measurements and despite the heterogeneity of the AC samples, a P/L ratio between 1.2 and 1.4 seems to be an optimum when carbonisation is carried out at 450 °C.

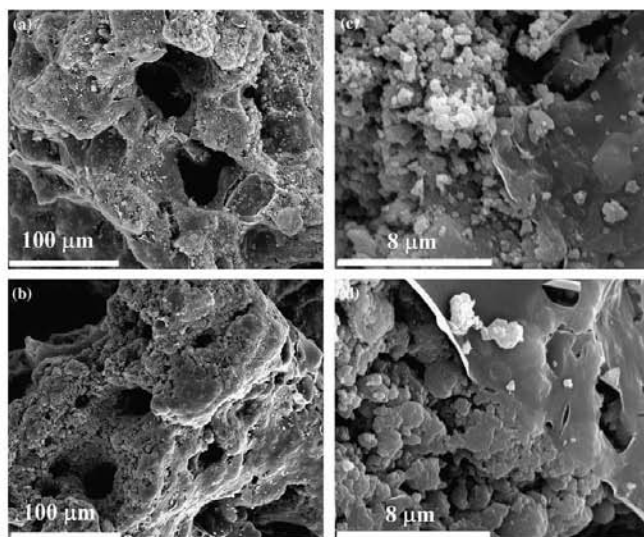


Fig. 6. SEM images of the activated carbons prepared at 450 (a, c) and 650 °C (b, d) at different magnifications (P/L = 1.4 and 1 h impregnation time).

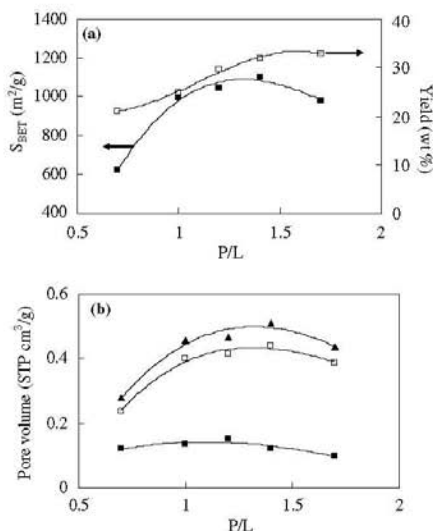


Fig. 7. Effect of the P/L ratio: (a) on the BET surface area and the carbon yield; (b) on the pore volumes $V_{0.99}$ (▲), V_{micro} (□) and V_{ultra} (■) of the ACs prepared at 450 °C and 1 h impregnation time.

P/L between 1.2 and 1.4 allowed to obtain carbons with high surface areas ($S_{BET} = 1049$ and $1101 \text{ m}^2 \text{ g}^{-1}$, respectively) and total pore volumes ($V_{0.99} = 0.469$ and $0.511 \text{ cm}^3 \text{ g}^{-1}$, respectively). Higher P/L ratios reduce the total pore volume and in a similar extent in the entire pore diameter interval.

It has been shown above that the use of P/L ratios in the range 1.2–1.4 allows obtaining ACs with high surface areas and porosity. The use of lower P/L ratios produces ACs having a higher contribution of micropores to the total porosity but also lower surface areas. The use of P/L = 1.75 reduces the total porosity and surface area, probably by the attack of the structure by the acid in excess. Thus, an optimum amount of ortho-phosphoric acid that can react exists, and higher P/L ratios produce an extensive breaking of biopolymer bonds, the shrinkage of the structure and consequently the reduction of the surface area and the total volume of pores.

Fig. 8 shows SEM photographs of the ACs prepared at 450 °C, with P/L = 0.7 and 1.75 and 1 h impregnation time at different magnifications, that can be compared with Fig. 6(a) and (c) corresponding to the AC prepared at P/L = 1.4 and 450 °C. The aspects of the surface of the ACs prepared with P/L ratios of 0.7 and 1.75 are very similar to each other, both at $\times 400$ and at $\times 7000$ magnification, with little grains agglomerated in bigger particles. The use of intermediate P/L ratios (see Fig. 6(a) and (c)) gives ACs with rough surfaces where small individual grains can be observed at $\times 7000$ magnification. These SEM observations agree well with the analysis done by N_2 adsorption.

Increasing the temperature or the P/L ratio seems to have the same effect on the pore texture. V_{ultra} always decreases with increasing activation temperature and P/L ratio, and there is an optimum value for both variables, allowing to obtain high surface areas and pore volumes. If the temperature or the P/L ratio are higher than their respective optimum, the surface area and the pore volume decrease, probably because of the collapse of the porous

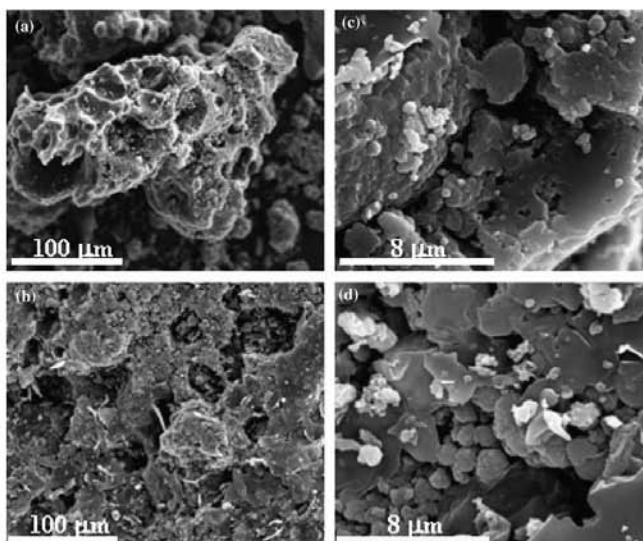


Fig. 8. SEM images of the activated carbons prepared at P/L = 0.7 (a, c) and 1.75 (b, d) at different magnifications ($T = 450\text{ °C}$ and 1 h impregnation time).

structure by the weakening of the phosphate bridges or by the excessive attack of the polymeric matrix, respectively.

3.4. Effect of the impregnation time

ACs were prepared within the range 450–600 °C with P/L = 1.4 and impregnation times ranging from 1 to 48 h. There was no significant difference in the carbon yield with impregnation time, although a very small decrease of carbon yield with increasing impregnation time was observed.

Fig. 9 shows the variation of the BET surface area for carbons prepared with different impregnation times at 450, 525 and 600 °C. Higher impregnation times lead to lower BET surface areas, the magnitude of this lowering being more important as the temperature increases. The

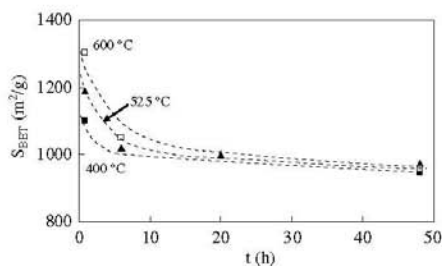


Fig. 9. Effect of the impregnation time on the BET surface area for carbons prepared at 450, 525 and 600 °C.

apparent surface area decreases from 1305 to 956 $\text{m}^2\text{ g}^{-1}$ from 1 to 48 h impregnation time, respectively, for ACs prepared at 650 °C. These changes in surface area and porosity are of less importance at low temperatures, and so the surface area is only reduced by 150 $\text{m}^2\text{ g}^{-1}$ at 450 °C when the impregnation time is extended from 1 to 48 h. The effect of time seems to be more important at the first moments of the impregnation of lignin with phosphoric acid, since BET surface areas values are nearly constant after 6 h impregnation time. Higher impregnation times promote the diffusion of ortho-phosphoric acid in the material and its role in the cross-linking reactions. Since KL is a powder, the ortho-phosphoric acid reacts rapidly with it, but it seems that it could also damage the polymeric structure at impregnation times higher than 1 h, thus leading to lower pore volumes and lower surface areas.

4. Conclusions

In the present study, activated carbon was produced by chemical activation of Kraft lignin, using H_3PO_4 as the activating agent. The results evidenced that pyrolysis of Kraft lignin impregnated with ortho-phosphoric acid produces essentially microporous ACs with high apparent surface areas and reasonable carbon yields.

Increasing the temperature of activation from 400 to 600 °C leads to the decrease of the volume of ultramicropores but to the increase of the total microporosity. The optimum temperature for porosity development in lignin-derived ACs was found to be 600 °C. Temperatures higher than 600 °C reduce both the volume of pores and the BET

surface areas due to the shrinkage and the oxidation of the material.

The ortho-phosphoric acid to lignin (P/L) ratio strongly affects the pore structure. Low impregnation ratios, i.e., P/L = 0.7, promote the creation of micropores whereas P/L ratios equal to or higher than 1.2 slightly affect the pore size distribution. P/L ratios higher than 1.4 decrease the surface area and the total volume of pores, possibly due to the attack of the polymeric matrix by the excess of ortho-phosphoric acid. The value of the P/L ratio has a clear effect on the total volume of pores: there is an optimum P/L = 1.2–1.4 for the development of porosity when the activation temperature is 450 °C.

Increasing the impregnation time lowers the BET surface area and the total pore volume. Moreover, impregnation time also affects the pore size distribution of the ACs. The effect of impregnation time is more important at higher temperatures, due to the decomposition of phosphate and polyphosphate bridges cross-linking parts of the carbon structure.

Acknowledgements

This research was made possible in part by financial support from the Spanish Government (MCYT, project PPQ2002-04201-CO02), the Catalan Regional Government (DURSI, 2001SGR00323 and 2002AIRE) and the ALFA Program of the E.U. (project ALFA II 0412 FA FI). V.F. acknowledges the MCYT and the Universitat Rovira i Virgili (URV) for the financial support of her 'Ramón y Cajal' research contract. V.T.F. acknowledges the URV for her PhD grant. The authors are grateful to Lignotech Iberica S.A. for supplying the Kraft lignin.

References

[1] J. Rodríguez-Mirasol, T. Cordero, J.J. Rodríguez, *Carbon* 31 (1993) 87.
[2] E. Gonzalez Serrano, T. Cordero, J. Rodríguez-Mirasol, J.J. Rodríguez, *Ind. Eng. Chem. Res.* 36 (1997) 4832.
[3] H. Teng, T.S. Yeh, L.Y. Hsu, *Carbon* 36 (1998) 1387.
[4] J. Laine, A. Calafat, M. Labady, *Carbon* 27 (1989) 191.

[5] M. Molina-Sabio, F. Rodríguez-Reinoso, F. Caturla, M.J. Sellés, *Carbon* 34 (1996) 457.
[6] B.S. Girgis, A.N.A. El-Hendawy, *Micropor. Mesopor. Mater.* 52 (2002) 105.
[7] A.N.A. El-Hendawy, S.E. Samra, B.S. Girgis, *Coll. Surf. A: Physicochem. Eng. Asp.* 180 (2001) 209.
[8] B.S. Girgis, M.F. Ishak, *Mater. Lett.* 39 (1999) 107.
[9] F. Suárez-García, A. Martínez-Alonso, J.M.D. Tascón, *J. Anal. Appl. Pyrol.* 63 (2002) 283.
[10] F. Suárez-García, A. Martínez-Alonso, J.M.D. Tascón, *Carbon* 39 (2001) 1111.
[11] M.C. Baquero, L. Giraldo, J.C. Moreno, F. Suárez-García, A. Martínez-Alonso, J.M.D. Tascón, *J. Anal. Appl. Pyrol.* 70 (2003) 779.
[12] B.S. Girgis, S.S. Yunis, A.M. Soliman, *Mater. Lett.* 57 (2002) 164.
[13] T. Vernersson, P.R. Bonelli, E.G. Cerrella, A.L. Cukierman, *Bioreour. Technol.* 83 (2002) 95.
[14] J. Guo, A.C. Lua, *Sep. Purif. Technol.* 30 (2003) 265.
[15] R.A. Shawabkeh, D.A. Rockstraw, R.K. Bhada, *Carbon* 40 (2002) 781.
[16] Y. Diao, W.P. Walawender, L.T. Fan, *Bioreour. Technol.* 81 (2002) 45.
[17] C.A. Toles, W.E. Marshall, M.M. Johns, L.H. Wartelle, A. McAloon, *Bioreour. Technol.* 71 (2000) 87.
[18] M. Jagtoyen, F. Derbyshire, *Carbon* 36 (1998) 1085.
[19] H. Benaddi, T.J. Bandosz, J. Jagiello, J.A. Schwarz, J.N. Rouzaud, D. Legras, F. Béguin, *Carbon* 38 (2000) 669.
[20] C. Toles, S. Rimmer, J.C. Hower, *Carbon* 34 (1996) 1419.
[21] F. Carrasco-Marín, M.A. Alvarez-Merino, C. Moreno-Castilla, *Fuel* 75 (1996) 966.
[22] A.M. Puziy, O.I. Poddubnaya, A. Martínez-Alonso, F. Suárez-García, J.M.D. Tascón, *Appl. Surf. Sci.* 200 (2002) 196.
[23] A.M. Puziy, O.I. Poddubnaya, B. Gawdzik, M. Sobiesiak, D. Dziadko, *Appl. Surf. Sci.* 196 (2002) 89.
[24] J. Hayashi, A. Kazehaya, K. Muroyama, A.P. Watkinson, *Carbon* 38 (2000) 1873.
[25] V. Fierro, V. Torné-Fernández, D. Montané, A. Celzard, *Thermo. Acta.* 433 (2005) 142.
[26] D. Montané, V. Torné-Fernández, V. Fierro, *Chem. Eng. J.* 106 (2005) 1.
[27] S. Brunauer, P.H. Emmett, E. Teller, *J. Am. Chem. Soc.* 60 (1938) 309.
[28] K.S.W. Sing, *Carbon* 27 (1989) 5.
[29] M. Kruk, Z.J. Li, M. Jaroniec, W.R. Betz, *Langmuir* 15 (1999) 1435.
[30] C.H. Hoyt, D.W. Goheen, in: K.V. Sarkanen, C.H. Ludwig (Eds.), *Lignins*, Wiley-Interscience, New York, 1971, p. 833 (Chapter 20).
[31] Y.Z. Lai, in: D.N.S. Hon, N. Shirashi (Eds.), *Wood and Cellulosic Chemistry*, vol. 10, Marcel Dekker, New York, 1991, p. 455.
[32] M. Jagtoyen, F. Derbyshire, *Carbon* 31 (1993) 1185.

5.1.4. Influence of the demineralisation on the chemical activation of Kraft lignin with orthophosphoric acid

Este artículo ha sido enviado al Journal of Hazardous Materials durante el año 2006.

Influence of the demineralisation on the chemical activation of Kraft lignin with orthophosphoric acid

V. Fierro^{1*◇}, V. Torné-Fernández¹, A. Celzard², D. Montané¹

¹*Departament de Enginyeria Química, Universitat Rovira i Virgili, Avda dels Països Catalans, 26, 43007 Tarragona, Spain*

²*Laboratoire de Chimie du Solide Minéral, Université Henri Poincaré - Nancy I, UMR - CNRS 7555, BP 239, 54506 Vandoeuvre-lès-Nancy, France*

Abstract

Preparation of activated carbons (ACs) produced from the thermal decomposition of mixtures of orthophosphoric acid (PA) and either as-received Kraft lignin, KL, or demineralised one, KL_d, has been investigated. Activation with PA has been studied for a PA/lignin ratio of 1 (daf basis) and 1h carbonisation time at final temperatures of 400, 500 and 600 °C. The yield, surface area, porosity and surface chemistry (acidic and basic groups) have been determined. All ACs were found to be essentially microporous, with surface areas higher than 800 m²/g and a maximum value of nearly 1200 m²/g for the carbon prepared at 600 °C from KL. In order to study the influence of temperature on yield, surface area, porosity and functional groups of the ACs prepared from KL and KL_d, the latter precursors were analysed by Fourier transform infrared spectroscopy (FT-IR), scanning electron microscopy (SEM) and X-ray diffraction (XRD). We have concluded that the very different characteristics of the ACs obtained from KL and KL_d are due to the presence or absence of mineral matter during carbonisation, but mainly to the demineralisation process itself, which produces a polymerisation of the raw lignin.

Keywords: Kraft Lignin; Activated carbon; H₃PO₄; demineralisation

1. Introduction

The Kraft method produces black liquor, a residue comprising lignin (30 - 40 %) and other inorganic compounds, which is used as in-house fuel for the recovery of both energy and residual inorganic matter. An interesting alternative is the production of activated carbons by physical [1] or chemical activation [2-4].

Kraft lignin has a high content of inorganic/mineral matter that usually ranges between 6 and 15% on dry ash-free (daf) basis. Since the mineral matter does not directly contribute to the specific surface area and porosity of the resultant active carbons it can be considered as an inert material, which decreases the adsorption capacity per unit mass. The demineralisation and/or abatement of inorganic compounds from carbonaceous precursors are thus thought to be necessary for the production of porous carbons with high surface areas [5]. This is particularly true for biomass, having higher inorganic contents than other precursors like synthetic polymers, and being recognised as a good feedstock for the production of cheap porous carbon materials. Thus, commercial activated carbons with low ash contents are prepared either by acid washing of the products, or by a suitable selection of the raw precursors [6]. Hence, in the case of precursors loaded with mineral matter, it may be wondered if the ashes should be removed before (i.e., in the precursor) or after (i.e., in the product) carbonisation and activation.

Indeed, it is well established that the presence of alkaline and alkaline earth elements in coal affects the reactivity of chars, and that the catalytic effect of inorganic matter depends on their concentration, dispersion and chemical form in the coal matrix [7]. It is also the case with biomass, since Fengel and

Wegener [8] suggested that the inorganic species naturally occurring in wood catalyse its pyrolysis. Since well-dispersed cations like sodium or calcium are good for activation of carbon by steam or CO₂ [9-10] and are abundant in lignin [11], a demineralisation pre-treatment would be *a priori* harmful for obtaining efficient adsorbents.

It has been reported that sodium promotes demethoxylation, demethylation and dehydration of lignin [12-13], and so the non-existence of these reactions could affect the final char yield. Furthermore, it has been recently shown [14] that when lignin is demineralised from 5.7 to 1% and afterwards pyrolysed at 300 °C, the char yield decreases from ca. 71 to 51% (on a daf basis), respectively. Authors indicated that the partial removal of sodium and potassium enhanced the de-volatilisation of lignin at the expense of char formation. DeGroot and Shafizadeh [15] observed a similar decrease in the char yield of wood after the latter was acid-washed. However, the presence of inorganic matter in lignin was found to be useful in reducing its plasticity and hindering its swelling in the carbonisation stage when pyrolysed under N₂ atmosphere [1].

The growing interest in the conversion of woods and its derivatives for producing alternative fuels, chemicals and products of high added value, as activated carbons are, requires a fundamental understanding of the processes involved. Lignin as a precursor of activated carbons is the subject of an increasing number of papers [4, 16-19] and, due to the high content of ashes in lignin, their effect on the pyrolysis process and on the product of carbonisation is worth studying. In this work, the physico-chemical properties of activated carbons produced from the thermal decomposition of mixtures of orthophosphoric acid (PA) and either as-received Kraft lignin, KL, or demineralised one, KL_d, were investigated.

2. Experimental

2.1 Precursor materials

Kraft lignin (KL) was supplied by Lignotech Iberica S.A. (Spain) in the form of fine dark brown particles. The removal of the inorganic matter of KL was achieved as follows: batches of 100 gr were introduced in 2 L of water, leading to black suspensions of pH 9.5. Lignin was precipitated by adding H_2SO_4 until the pH decreased to 1. The precipitate was gently washed with distilled until the pH of the rinse remained constant and close to 6, and finally dried overnight at 105 °C. The lignin prepared in this way ~~is~~ was nearly mineral-free and was termed demineralised Kraft lignin (KL_d).

2.2 Active carbon preparation

An 85 wt. % H_3PO_4 aqueous solution (Panreac, Spain) was used as activating agent. The weight ratio PA/precursor of all mixtures was 1.0 on a daf basis. The slurry was left for 1h impregnation time at room temperature in air, then transferred into a furnace DUM Model 10CAF where carbonisation was carried out under air atmosphere. The furnace was heated at 10 °C min⁻¹, up to 150 °C which temperature was held for 1h to allow free evolution of water. Next, the oven was heated at 10 °C min⁻¹ up to the carbonisation temperatures: 400, 500 and 600 °C, which were maintained for 1h. The excess of H_3PO_4 was removed after carbonisation by thorough washing with distilled water. As shown below, the resultant activated carbons were nearly free of ashes.

2.3 Characterisation of lignins and ACs

2.3.1 Proximate and ultimate analysis

Analysis of C, H, S and N content in the activated carbons (ACs) was done using a Carlo Erba EA-1108 instrument and oxygen was calculated by difference. The proximate analysis was carried out by thermogravimetric analysis in a Perkin-Elmer TGA 7 microbalance equipped with a 273–1273 K programmable temperature furnace, upon following the weight losses at 110 °C/air (moisture), 900 °C/non-oxidising atmosphere (volatile matter), 900 °C/air (fixed carbon); ash content was obtained by difference.

2.3.2 FTIR analysis

Infrared spectra of KL, KL_d and their derived ACs were recorded in the near IR region (4000–600 cm⁻¹) with a spectral resolution of 4 cm⁻¹, a scan speed of 2 mm/s and after 200 scans. The equipment used was a Fourier transform infrared (FTIR) spectrophotometer JASCO FT/IR-680 equipped with a diamond-composite attenuated total reflectance (ATR) cell.

2.3.3 SEM analysis

The surface morphology of KL and KL_d was studied by scanning electron microscopy (SEM) with a JEOL JSM-6400. The microscope was equipped with an energy dispersive X-ray (EDX) microanalyser that was used to observe the dispersion of the mineral matter in KL and KL_d.

2.3.4 Surface area and porosity

Surface area and porosity were determined from the corresponding nitrogen adsorption–desorption isotherms obtained at 77 K with an automatic instrument (ASAP 2020, Micromeritics). The samples were previously outgassed at 523 K for several hours. N₂ adsorption was studied within two pressure ranges. First, for P/P₀ lower than 10⁻³, N₂ were dosed to the sample in fixed amount of 3 cm³/g and the corresponding values of P/P₀ at equilibrium were recorded. The Horvath–Kawazoe (HK) model was applied to the adsorption data in order to obtain the micropore size distribution. Next, N₂ adsorption data for P/P₀ ranging from 10⁻⁵ to 0.99 (in a set of values previously fixed) were analysed according to: (i) the BET method for calculating the specific surface area, A_{BET} ; (ii), the Dubinin-Radushkevich (DR) for calculating the micropore volume, V_{DR} , the characteristic energy of N₂ with respect to carbon, E_0 , and the average width of the slit-shaped micropores, L_0 ; and (iii) the α_s method [20-21] for calculating the the ultramicropore volume, $V_{\alpha,\text{ultra}}$ and the micropore volume, $V_{\alpha,\text{micro}}$. The total pore volume, $V_{0.99}$, was calculated from nitrogen adsorption at a relative pressure of 0.99. The mesopore volume, V_{mp} was calculated as the difference between $V_{0.99}$ and V_{DR} .

3. Results and discussion

3.1 Characterization of KL and KL_d

Table I shows the proximate and ultimate analyses of KL and KL_d. It may be seen that the initial ash content of KL (11.1 % dry basis) was nearly totally removed (0.2 % dry basis) after the treatment with H₂SO₄. The high sulphur

content (2.2 %) in KL originates both from the Kraft or sulphate process, based on the action of NaOH and Na₂S for separating cellulose from the other wood constituents, and from organically bound sulfur (up to 1.5 %) [22]. XRD studies of lignin evidenced the presence of the phase Na₂CO₃ · 2 Na₂SO₄, further confirmed by microprobe analysis. The demineralisation of lignin produced a decrease of both S (down to 0.5 %) and O (from 33.3 to 27.8 %) contents. This finding is not surprising since both sodium carbonate and sulphate are very soluble in aqueous solutions. Analysis by SEM-EDX showed that S and Na are uniformly distributed in the polymeric matrix before and after the demineralisation treatment.

Figure 1 shows the IR spectra of KL and KL_a. The two lignins show a broad band at 3000 – 3600 cm⁻¹, attributed to the hydroxyl groups in phenolic and aliphatic structures, and bands centered around 2975-2945 cm⁻¹, predominantly arising from CH stretching in aromatic methoxyl groups and in methyl and methylene groups of side chains. Both bands decrease after acid treatment. The very weak bands centered near 2300 cm⁻¹ are assigned to carbon–oxygen groups due to ketene [23].

The most characteristic infrared bands of lignin are found at about 1510 and 1600cm⁻¹ (aromatic ring vibrations) and between 1470 and 1460 cm⁻¹ (C-H deformations and aromatic ring vibrations). [24]. The intensity of these bands, however, is strongly influenced by neighbouring functional groups. The band centred at 1585 cm⁻¹ in KL spectrum is the result of the aromatic ring vibrations at 1600 cm⁻¹ and coordinated carbonates [25], already evidenced by XRD analysis. Low absorption around 1650 cm⁻¹ in KL spectrum, resulting in the asymmetry and broadening of the more intense band at 1600 cm⁻¹, may originate from both carbohydrates impurities and water associated with lignin. [26]. The higher intensity of the 1510 cm⁻¹ band compared with the 1600 cm⁻¹ band in the spectra indicates that KL comes

from softwood. The intensive bands of the carbonyl groups appear in the range between 1660 and 1725 cm^{-1} . The exact position of the bands depends on whether the C=O groups are in conjunction with the aromatic ring (position below 1700 cm^{-1}) or not (position above 1700 cm^{-1}). After acid-washing, the carbonates are completely removed from lignin; as a consequence, the intensity of the 1585 cm^{-1} band decreased and was shifted to 1600 cm^{-1} . The KL_d spectrum also exhibits an intense band centered at 1729 cm^{-1} , which indicates C=O (ketones, aldehydes or carboxyl groups) not associated with aromatic rings.

The spectral region below 1400 cm^{-1} is more difficult to analyse, since most bands are complex, with contribution from various vibration modes. However, this region contains vibrations that are specific to the different monolignol units and allows the structural characterisation of lignins. The spectra of both samples show the characteristic vibrations of the guaiacyl unit (1269 cm^{-1} : guaiacyl ring breathing and C=O stretching; 1140 cm^{-1} : C-H in-plane deformation; 860 and 824 cm^{-1} : C-H out-of-plane vibrations in position 2, 5 and 6 of guaiacyl units) but the intensities of the bands vary significantly with the samples. The importance of guaiacyl characteristic vibrations increased after acid washing.

Both spectra also show a weak band at 1369 cm^{-1} originated by phenolic OH and aliphatic C-H in methyl groups and a strong vibration at 1215–1220 cm^{-1} that can be associated with C-C plus C-O plus C=O stretching. The aromatic C-H deformation at 1031 cm^{-1} appears as a complex vibration associated with the C-O, C-C stretching and C-OH bending in polysaccharides. Carbohydrates that remained in KL could be also the origin of the vibrations in the spectral region 1000–1300 cm^{-1} [26].

In summary, the most important changes introduced by acid-washing is the reduction of the amount of hydroxyl groups with the concomitant increase of the number of C=O functions, as well as the elimination of carbonates.

According with these findings, Yasuda et al.[27-28] demonstrated that the acid treatment of lignin produces its cross-linking, an increase of the phenol / aliphatic hydroxyl fraction, and a decrease of the total hydroxyl content of the lignin fractions.

Figure 2 shows SEM images of KL and KL_d at different magnifications. Differences in particle shapes and sizes may be observed. KL particles are smaller, and have a rounded (even spherical) shape with widely open volumes inside. Such morphology is probably due to the concentration process of lignin from black liquors, which is done by evaporation; due to their surface tension, particles take a spherical - thermodynamically more stable - form. After acid washing, KL_d particles are much bigger and sharp, and look broken. A more detailed observation reveals that the surface of KL particles is rough, whereas that of the KL_d is nearly smooth. Such different morphologies between KL and KL_d are probably due to the method used for lignin separation (evaporation or sedimentation-filtration) although changes in the polymer structure due to demineralisation process can not be excluded.

3.2 Characterisation of the activated carbons produced

3.2.1 Carbon yield and elemental composition

Table II shows the carbon yield (daf basis) and the proximate and ultimate analyses of the carbons. Carbon yields of KL were always higher, ranging from 66.2 to 87.6 %, than those obtained from KL_d, ranging from 61.3 to 80.9 %. Although the differences in carbon yield for Kl and KL_d are of the same order of magnitude, their evolution with temperature is not the same.

Increasing temperature from 400 to 500 °C makes the carbon yield decrease by 2.6% and 7.6 % for KL and KL_d, respectively. On the contrary, within the range 500– 600 °C, the carbon yield decreases much more for KL (19.3 %) than for KL_d (12.0 %).

PA promotes dehydration, producing an important reordering of the structure [29], decreasing the volatile compounds emitted during decomposition and hence increasing the carbon yield. Our previous works also [30-31] showed that the PA-impregnated lignin follows during decomposition a reaction path, which is different from that observed with pure lignin, and that the carbon yield is higher. PA promotes bond cleavage in the biopolymers and dehydration at low temperatures [32] followed by extensive cross-linking that binds volatile matter into the carbon product and so increase the carbon yield. Consequently, activated carbons may be prepared with good yields and high surface areas using chemical activation with PA. As demineralisation decreases the hydroxyl content of lignin, the reaction of PA with lignin, hence the subsequent cross-linking are clearly lowered, and consequently the aromatisation of the activated carbons and the carbon yield would be also reduced.

Figure 3 shows the Van Krevelen diagram plotting H/C vs O/C ratios, for activated carbons derived from KL and KL_d within the temperature range of this study. The ACs become increasingly more aromatic when the temperature increases, but the variation of H/C vs O/C ratios depends on the precursor. At constant pyrolysis temperature, ACs derived from KL have lower H/C and O/C ratios than those from KL_d, suggesting a higher aromatic nature that increases with temperature. The Van Krevelen diagram confirms the lower aromaticity of the ACs prepared from KL_d. Furthermore,

it is not excluded that the acid pretreatment could form new polymeric structures that would be thermally less resistant, resulting in a decrease of the carbon yield.

3.2.2 *Surface area and porosity*

Table III shows the apparent surface area and porosity of the carbons produced from KL and KL_d at 400, 500 and 600 °C. The apparent surface areas determined by the BET method are always higher than 800 m²/g, but the observed temperature dependences are very different for carbons prepared from KL and KL_d. The data obtained by the application of the BET, DR and α_s methods to the isotherms at high N₂ relative pressures confirm the trends already observed in the micropore region. The surface areas increase with temperature for KL-based carbons while the opposite is observed for those prepared from KL_d. The maximum surface area determined in this work, 1189 m²/g, corresponds to the carbon prepared from KL at 600 °C. The trend observed for the evolution with temperature of the surface areas of both kinds of carbons is also that of the variation of V_{DR} and $V_{\alpha_{micro}}$. However, the volume of pores smaller than 0.7 nm determined by the α_s method, $V_{\alpha_{ultra}}$, decreases with increasing temperatures for all the carbons prepared. $V_{\alpha_{ultra}}$ is always the highest for carbons prepared from KL, and its decrease with temperature (from 0.18 to 0.11 cm³/g) is less than that observed for carbons prepared from KL_d (from 0.12 to 0.04 cm³/g) when increasing temperatures from 400 to 600 °C. Finally, the average micropore width derived from the DR method, L_o , increases with the temperature, whatever the material, although higher values were found with KL_d.

Figure 4 shows the micropore size distribution of the 6 active carbons, for pores narrower than 0.9 nm, obtained by the application of the HK method. The maximum of the micropore size distribution is always found for a pore diameter lower than 0.4 nm whatever the precursor and the activation temperature. Carbons prepared from KL always showed the highest amount of pores smaller than 0.4 nm. Carbons prepared from KL_d showed wider pore diameters and a dramatic decrease of the pores smaller than 0.4 nm was observed for carbons prepared at 600 °C. These results are in good agreement with those obtained by application of the α_s method.

The results of the present study show that, on average, the adsorbents made from KL have better characteristics (higher areas and pore volumes) than those derived from KL_d. Such differences between KL and KL_d may be explained by the ability of PA to react with lignin. KL can react more extensively with PA due to its higher phenolic content. Moreover, the deashed lignin is less reactive (much more compact, as revealed by SEM, and with much less hydroxyl groups with which PA can react, as revealed by IR spectra), due to an acid-induced cross-linking of the macromolecules. PA can penetrate easily the texture of KL, producing an increasingly high number of small micropores when the temperature increases. Additionally, phosphate and polyphosphate bridges connect cross-linked biopolymer fragments, avoiding pore collapse. On the contrary, PA hardly penetrates KL_d, and cannot prevent pore collapse; hence, the activation mainly occurs at the surface of the grains, producing wider pores (higher L_0 and lower E_0 than for KL). Finally, a catalytic effect of cations improving the activation at constant temperature is also possible.

3.2.3 *Surface chemistry of the activated carbons*

Figure 5 shows the IR spectra of the ACs-derived from KL and KL_d prepared in this study. Bands between 3200 and 3600 cm⁻¹ are typically ascribed to hydroxyl groups; the bands around 2900–2800 and 1500–1400 cm⁻¹ are caused by -CH₂- groups; the band around 1300–1000 cm⁻¹ is attributed to C=O stretch. The band around 1700 cm⁻¹ is usually caused by the stretching vibration of C=O in ketones, aldehydes, lactones, and carboxyl groups; and the band around 1600 cm⁻¹ is ascribed to aromatic ring stretching vibration. The intensities of these two bands show that the aromatization extent and the content of carbonyl-containing groups. The band around 1230 cm⁻¹ is usually attributed to a C-O bond; while, for carbons activated by H₃PO₄, the bands at 1300–900 cm⁻¹ could be caused by phosphorus-containing groups [33].

Spectra of ACs prepared from KL_d were much smoother than those of ACs prepared from KL, which pointed up a lesser amount of functional groups that were present in these carbons. It can be also observed the reduction in the intensity of the bands characteristic of the different functional groups with increasing temperature for both types of carbons. In a recent study [18], it has been demonstrated that the acidic surface groups on carbons prepared from Kraft lignin consist of temperature-sensitive and temperature-insensitive. The temperature-sensitive groups consist of primarily carbonyl-containing groups of varying acidic strength; while the temperature-insensitive groups are mainly phosphorus-containing. Thus, the functional groups of the ACs prepared from KL would be essentially temperature sensitive whereas those prepared from KL_d would include temperature-sensitive and temperature-insensitive groups, phosphorus-containing, due to

the more extensive reaction of PA with KL. These findings are in good agreement with the hypothesis of lower reaction extent of PA with KL_d.

4. Conclusions

The objective of this work was to study the effect of the ash content of Kraft lignin on the physicochemical properties of the activated carbons produced by activation with H₃PO₄ (PA). SEM observations and IR studies suggested that the demineralisation process produces lignin polymerisation and reduces its ability to react with PA.

The results have shown that carbon yield, surface area, porosity and surface chemistry are affected by the removal of the mineral matter. The carbon yield and the aromaticity are the highest for activated carbons derived from the raw Kraft lignin (KL). The activated carbons prepared by activation of KL and KL_d, were essentially microporous with surface areas higher than 800 m²/g, the highest one being close to 1200 m²/g and corresponding to the AC prepared from KL at 600 °C. The surface area increased with temperature for ACs prepared from KL but the opposite evolution was observed for those prepared from KL_d. The functional groups decreased with increasing temperature and their concentration was much more significant in ACs prepared from KL probably because there are more phosphorus-containing groups, which have been recently described as temperature-insensitive groups.

In other words, it may be concluded that the very different characteristics of the ACs obtained may clearly be attributed to the demineralisation process itself. However, a favourable catalytic effect of the ashes on the activation process could not be discarded. The main conclusion of this work is then the following: since better active carbons are produced from raw lignin, the demineralisation – if required – should be carried out on the products and not on the precursors.

Acknowledgements

This research was partly made possible by financial support from MCYT (project PPQ2002-04201-CO02), DURSI (2001SGR00323) and the European Commission through the ALFA program (project LIGNOCARB-ALFA II 0412 FA FI). V. Fierro acknowledges the MCYT and the Universitat Rovira i Virgili (URV) for the financial support of her 'Ramón y Cajal' research contract. V. Torné-Fernández acknowledges the URV for her PhD grant.

References

- [1] J. Rodríguez-Mirasol, T. Cordero and J. J. Rodríguez Carbon 31 1 (1993) 87-95.
- [2] E. González-Serrano, T. Cordero, J. Rodríguez-Mirasol and J.J. Rodríguez, Development of porosity upon chemical activation of kraft lignin with $ZnCl_2$. Ind Eng Chem Res 36 (1997) 4832–4838.
- [3] J. Hayashi, A. Kazehaya, K. Muroyama, A. Paul Watkinson Carbon 38 (2000) 1873-1878.
- [4] V. Fierro, V. Torné-Fernández, A. Celzard, D. Montané, microporous and mesoporous materials 92 (2006) 243-250.
- [5] M.V. Rivera-Utrilla, López-Ramón, F. Carrasco-Marín, F.J. Maldonado-Hódar, C. Moreno-Castilla, Carbon 34 (1996) 917–921.
- [6] C. Bansal, J.B. Donnet and H.F. Stoeckli. Active carbon Marcel Dekker, New York (1988).
- [7] F. Kapteijn, H. Porre, J. A. Moulijn AIChE J. (1986) 691-695.
- [8] D. Fengel and G. Wegener. Wood: chemistry ultrastructure, reactions, Walter de Gruyter, New York (1984) 132–181.
- [9] J.G. Spreigh. Chemistry and technology of coal Marcel Dekker, New York (1994)
- [10] D.W. van Krevelen. Coal Elsevier, Amsterdam (1993)
- [11] M. Kleen, G. Gellerstedt, J Anal Appl Pyrol 35 (1995) 15-41.
- [12] E. Jakab, O. Faix, F. Till. J Anal Appl Pyrol 40 (1997) 171-186.
- [13] J.C. Rio, A. Gutierrez, J. Romero, M.J. Martinez, T. Martinez. J Anal Appl Pyrol 58–59 (2001) 425-439.

- [14] R. K. Sharma, J. B. Wooten, V. L. Baliga, X. Lin, W. G. Chan, M. R. Hajaligol *Fuel* 83 (2004) 1469-1482.
- [15] W.F. DeGroot, F.J. Shafizadeh. *J Anal Appl Pyrol* 6 (1984) 217-232.
- [16] L. Khezami, A. Chetouani, B. Taouk and R. Capart *Powder Technology* 157, (2005) 48-56.
- [17] E. Gonzalez-Serrano, T. Cordero, J. Rodriguez-Mirasol, L. Cotoruelo and J. J. Rodriguez; ; *Water Research* 3 (2004) 3043-3050.
- [18] Y. Guo, D. A. Rockstraw *Carbon*, Volume 44 (2006) 1464-1475.
- [19] J. Rodriguez-Mirasol, J. Bedia, T. Cordero, J. J. Rodriguez. *Sep. Sci. & Tech.* 40 (2005) 3113-3135.
- [20] F. Rouquerol, J. Rouquerol, K.S.W. Sing *Adsorption by Powders and Porous Solids. Principles, Methods and Applications*, Academic Press, San Diego, CA (1999).
- [21] N. Setoyama, T. Suzuki, K. Kaneko *Carbon* 36 (1998) 1459–1467.
- [22] C.H. Hoyt, D.W. Goheen, in: K.V Sarkanen, C.H. Ludwig (Eds.), *Lignins*, Wiley-Interscience, New York, 1971, Chapter 20 833.
- [23] E. Papirer, E. Guyon, N. Perol. *Carbon* 16 (1978) 133-140.
- [24] D. Fengeland, G. Wegener, Wood. *Chemistry ultrastructure reactions*. De Gruyter (Eds.), 1989: 143-164.
- [25] Socrates, G. *Infrared characteristic group frequencies*, ed. L. John Wiley & Sons. (Eds.), 1980.
- [26] C. G. Boeriu, D. Bravo, R. J. A. Gosselink, J. E. G. van Dam *Industrial Crops and Products*, 20 (2004) 205-218.
- [27] S. Yasuda, N. Terashima, T. Ito, *Mokuzai Gakkaishi* 26 (1980) 552–557.

- [28] S. Yasuda, K. Hayashi, T. Ito, N. Terashima, *Mokuzai Gakkaishi* 27 (1991) 478–483.
- [29] Y.Z. Lai, in *Wood and Cellulosic Chemistry*, Vol. 10, Eds. D.N.S. Hon and N. Shirashi. Marcel Dekker, New York, 1991, 455
- [30] D. Montané, V. Torné-Fernández, V. Fierro *Chem. Eng. JI*, 106 (2005) 1-12.
- [31] V. Fierro, V. Torné-Fernández, D. Montané, A. Celzard. *Thermo. Acta* 433 (2005) 142-148.
- [32] M. Jagtoyen, F. Derbyshire, *Carbon* 31(1993) 1185-1192.
- [33] M. Puizy, O.I. Poddubnaya, A. Martínez-Alonso, F. Suárez-García and J.M.D. Tascón, *Carbon* 40 (2002) 1493–1505.

Captions of the figures

- Figure 1** IR spectra of KL (grey line) and KL_d (black line).
- Figure 2** SEM images of KL (a, c and e) and KL_d (b, d and f) at different magnifications.
- Figure 3** Van Krevelen diagram for ACs prepared from KL (full symbols) and KL_d (open symbols) at 400, 500 and 600 °C.
- Figure 4** Micropore size distribution of ACs prepared from KL (black line) and KL_d (grey line) at 400, 500 and 600 °C (a, b and c respectively) from the application of the HK method.
- Figure 5** IR spectra of ACs prepared from KL and KL_d at 400, 500 and 600 °C.

Influence of the demineralisation on the chemical activation of Kraft lignin with orthophosphoric acid

V. Fierro, V. Torné-Fernández, A. Celzard and D.Montané

Table I

Proximate and ultimate analyses of KL and KL_d (wt.%)

	Proximate Analysis (wt %, dry basis)			Ultimate Analysis (wt %, daf)				
	Fixed Carbon	Volatile matter	Ash	C	H	N	S	O*
KL	36.4	52.5	11.1	59.5	5.1	0.1	2.2	33.3
KL _d	39.7	60.1	0.2	65.8	5.9	0.0	0.5	27.8

* Estimated by difference

Influence of the demineralisation on the chemical activation of Kraft lignin with orthophosphoric acid

V. Fierro, V. Torné-Fernández, A. Celzard and D.Montané

Table II

Carbon yield on daf basis, and ultimate analyses of the ACs prepared.

T (°C)	Yield ^a	Proximate Analysis (wt %, dry basis)			Ultimate Analysis (wt %, daf)				
		Volatile matter	Fixed Carbon	Ash	C	H	N	S	O
<i>KL</i>									
400	87.6	36.23	63.26	0.52	65.3	1.2	0.0	1.0	32.5
500	85.0	32.30	67.11	0.59	70.2	1.1	0.0	1.1	27.6
600	65.7	40.90	58.15	0.95	72.7	0.5	0.0	1.2	25.6
<i>KL_d</i>									
400	80.9	33.80	68.85	0.35	61.4	1.2	0.0	1.0	36.4
500	73.3	35.42	62.03	2.55	62.7	1.1	0.0	0.7	35.5
600	61.3	38.13	59.81	2.05	63.5	0.8	0.0	0.6	35.1

^a dry ash free basis.

Influence of the demineralisation on the chemical activation of Kraft lignin with orthophosphoric acid

V. Fierro, V. Torné-Fernández, A. Celzard and D.Montané

Table III

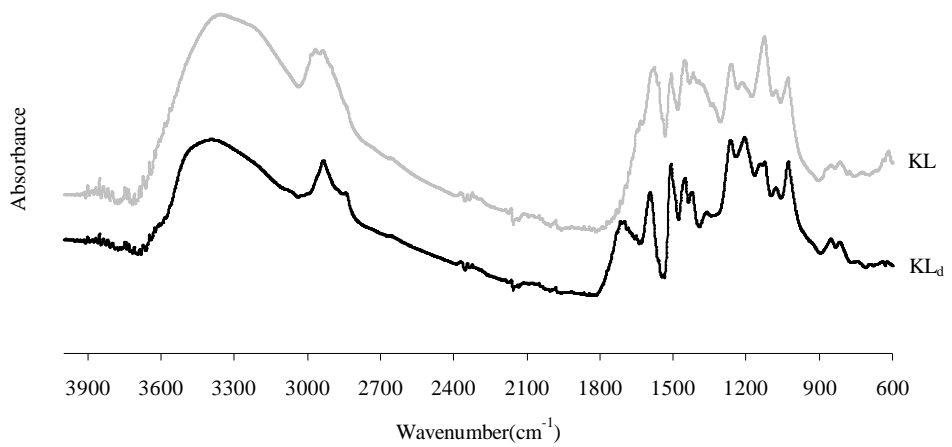
Textural parameters deduced from N₂ adsorption at 77K on activated carbons prepared from KL and KL_d

T (°C)	A _{BET} (m ² g ⁻¹)	V _{0.99} (cm ³ g ⁻¹)	DR equation			α _s method	
			V _{DR} (cm ³ g ⁻¹)	E ₀ (kJmol ⁻¹)	L ₀ (nm)	V _{α,micro} (cm ³ g ⁻¹)	V _{α,ultra} (cm ³ g ⁻¹)
<i>KL as carbon precursor</i>							
400	815	0.40	0.38	22.2	1.0	0.34	0.18
500	1004	0.49	0.45	19.7	1.3	0.43	0.13
600	1189	0.59	0.51	18.9	1.5	0.49	0.11
<i>KL_d as carbon precursor</i>							
400	1008	0.47	0.45	19.1	1.4	0.45	0.12
500	960	0.46	0.40	17.9	1.7	0.38	0.05
600	890	0.44	0.37	17.6	1.7	0.35	0.04

Influence of the demineralisation on the chemical activation of Kraft lignin with orthophosphoric acid

V. Fierro, V. Torné-Fernández, A. Celzard and D.Montané

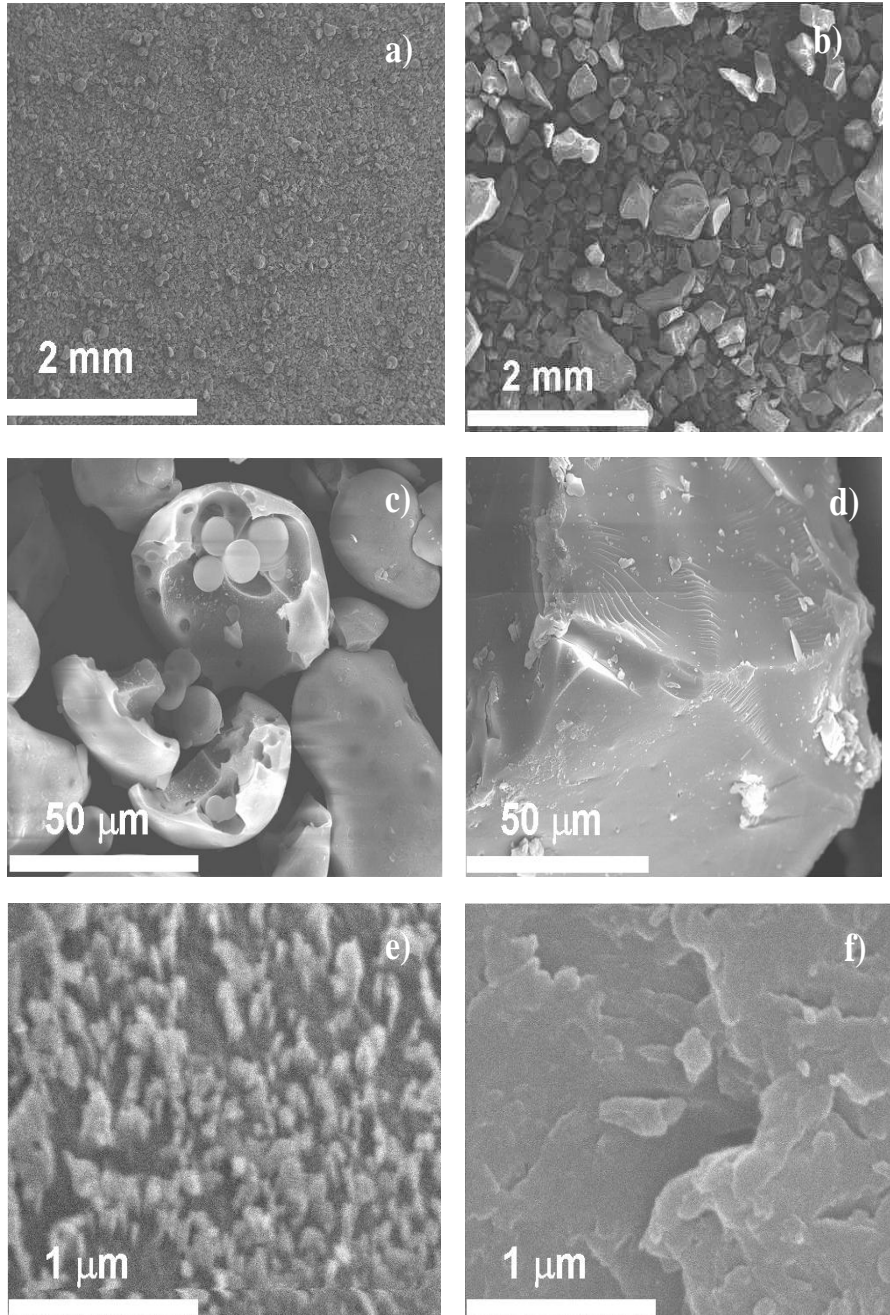
Figure 1



Influence of the demineralisation on the chemical activation of Kraft lignin with orthophosphoric acid

V. Fierro, V. Torné-Fernández, A. Celzard and D. Montané

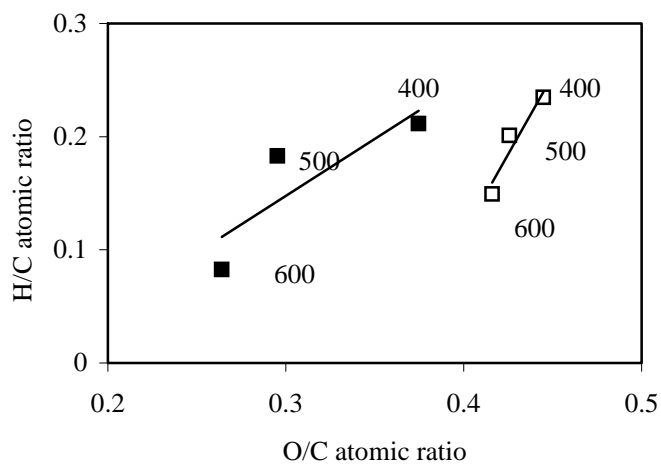
Figure 2



Influence of the demineralisation on the chemical activation of Kraft lignin with orthophosphoric acid

V. Fierro, V. Torné-Fernández, A. Celzard and D. Montané

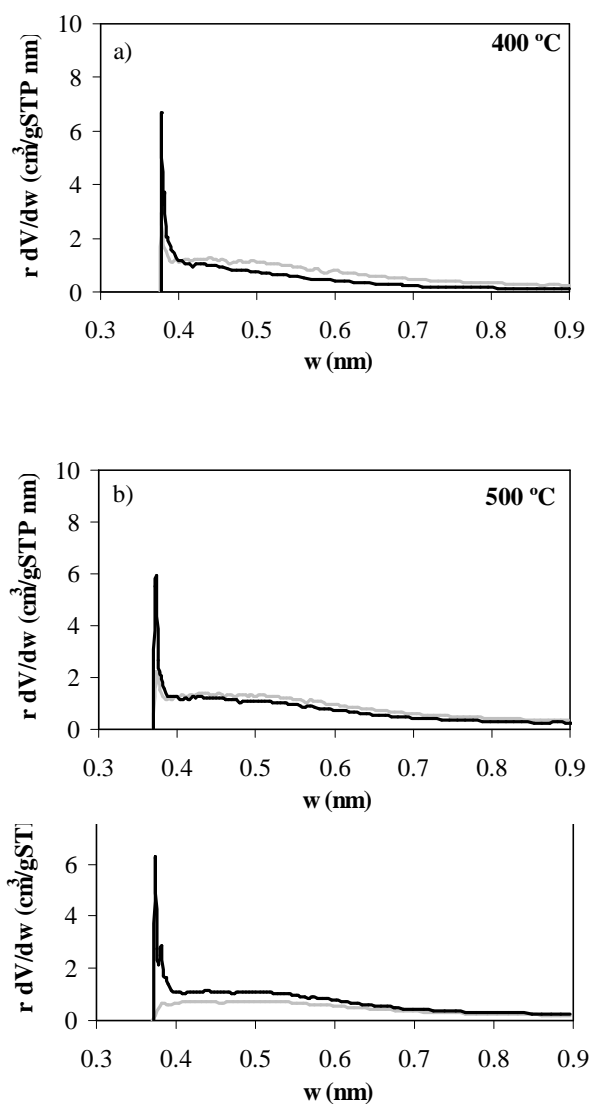
Figure 3



Influence of the demineralisation on the chemical activation of Kraft lignin with orthophosphoric acid

V. Fierro, V. Torné-Fernández, A. Celzard and D. Montané

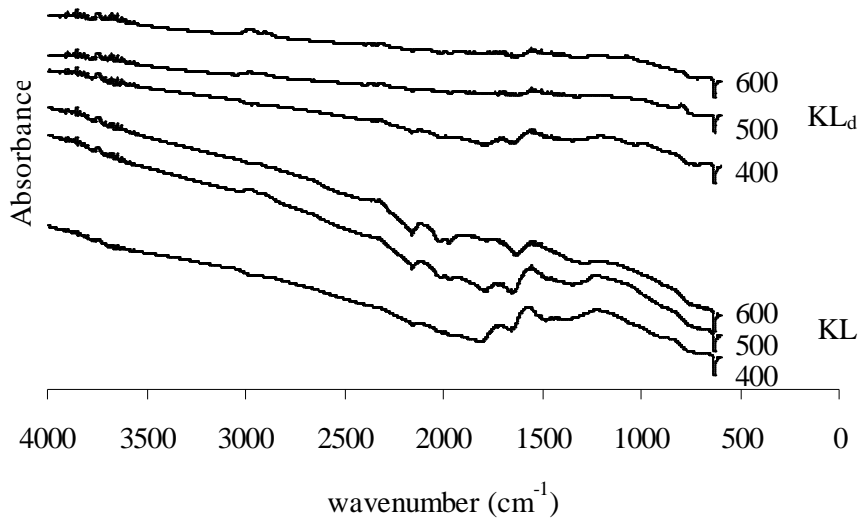
Figure 4



Influence of the demineralisation on the chemical activation of Kraft lignin with orthophosphoric acid

V. Fierro, V. Torné-Fernández, A. Celzard and D. Montané

Figure 5



5.1.5. Highly microporous carbons prepared by activation of kraft lignin with KOH

Este artículo ha sido enviado al journal *Studies in Surface Science and Catalisys* durante el año 2006.

Otros trabajos relacionados se presentan en el anexo B donde se presenta el póster “Highly microporous carbons prepared by activation of Kraft lignin with KOH” publicado en el congreso 7th Internacional symposium on the characterization of porous solids.

Highly microporous carbons prepared by activation of Kraft lignin with KOH

V. Fierro^a, V. Torné-Fernández^a and A. Celzard^b

^a Departament d'Enginyeria Química, Universitat Rovira i Virgili, Campus Sescelades, Av. dels Països Catalans 26, 43007 Tarragona, Spain.

^b Laboratoire de Chimie du Solide Minéral, UMR CNRS 7555, Université Henri Poincaré, 54506 Vandoeuvre-lès-nancy Cédex, France.

Highly microporous carbon materials with high apparent surface areas (up to $\sim 3000 \text{ m}^2 \text{ g}^{-1}$) were obtained by heat treatment of mixtures of demineralised kraft lignin (KL_d) and KOH. The effects of five parameters: temperature of activation (500-900 °C), KOH/ KL_d ratio (1-5), time of activation (0.5-2h), heating rate (5 and 10 °C min^{-1}) and nitrogen flow rate (200-800 $\text{cm}^3 \text{min}^{-1}$) on carbon yield, surface area, pore volume and pore size distribution were investigated. An increase in the activation degree of KL_d produced a gradual enhancement in the volume of total micropores. Highly activated samples also presented noteworthy mesoporosity. Too high activation temperature resulted in the burn-off of carbon structures and widening of micropores to mesopores.

1. INTRODUCTION

The term lignin refers to a group of phenolic polymers accounting for the strength and the rigidity of the vegetal cell walls. The objective of any chemical pulping process is to remove enough lignin to separate cellulosic fibres from each other, producing a suitable pulp for the manufacture of paper and other related products. In terms of industrial chemical modification of lignin, the kraft pulping process is the main one. The kraft method produces black liquor, a residue composed of lignin (30 - 40 %) and other inorganic compounds, which is used as in-house fuel for the recovery of both energy and residual inorganic matter. Several alternatives to combustion have been considered. One of the main possible applications of by-product kraft lignin (KL) consists in preparing activated carbons. Recently, the chemical activation of KL impregnated with H_3PO_4 was reported [1,2]. The activated carbons produced were essentially microporous with surface areas as high as $1300 \text{ m}^2/\text{g}$.

The literature evidences a growing interest in alkaline hydroxide activation process, and KOH has been found to be one of the most effective compounds for that purpose [3-7]. High surface areas and pore volumes are reported for lignocellulosic materials, carbons and chars activated by KOH. However, controlling the mean pore size and the pore size distribution is necessary for using such materials in a given application. The present study shows the possibility of producing highly microporous carbons by activation of KL_d with KOH. The effects of five experimental parameters: activation temperature, KOH/ KL_d ratio, time of activation, heating rate and nitrogen flow rate on surface area and pore size distribution were investigated.

2. EXPERIMENTAL

2.1. Demineralisation of KL

KL was supplied by Lignotech Iberica S.A. (Spain), and was presented in the form of a fine dark brown powder. The removal of the inorganic matter from KL was achieved as follows: batches of 100 g were introduced in 2 l of water, leading to dark brown suspensions of pH 9.5, and lignin was precipitated by adding H_2SO_4 until the pH decreased to 1. The precipitate was gently washed with distilled water until the pH of the rinse was constant, and finally dried overnight at 105 °C. The lignin prepared this way was nearly mineral-free and was termed demineralised Kraft lignin (KL_d).

2.2. Preparation of carbons

KOH lentils (Scharlau) were ground and physically mixed with KL_d according to various KOH/ KL_d mass ratios ($R = 1:1, 2:1, 3:1, 4:1$ or $5:1$). The carbonisation was carried out in a horizontal furnace and the samples were heated ($r = 5$ or 10 °C/min) from room temperature up to the final carbonization temperature ($T_{carb} = 500, 600, 700, 800$ or $900^\circ C$) in different nitrogen flows ($f_{N_2} = 200, 400, 600$ or 800 ml/min). Samples were kept at the final temperature for different carbonisation times ($t_{carb} = 0.5, 1$ or 2 h) before cooling down under nitrogen.

During the experiments, both metallic potassium (produced by the reduction of KOH by carbon at high temperature) and KOH were partly transported in the vapour phase, and could be observed at the outlet of the reactor. Metallic potassium mixed with potassium carbonate was also present inside the crucible; therefore the latter was submitted to atmospheric humidity for two days, during which the alkaline metal slowly oxidised. Finally, the

activated carbon was washed with extreme care, first with 1M HCl, and finally with distilled water until the pH of the rinse remains constant and close to 6. After drying in an oven during 24 h, a very light activated carbon was obtained.

2.3. Characterisation of lignin and carbons

Proximate and ultimate analyses. Elemental analysis of C, H, S and N content in lignins and activated carbons was done using a Carlo Erba EA-1108 instrument. Oxygen was calculated by difference. The proximate analysis was carried out by thermogravimetric analysis in a Perkin-Elmer TGA 7 microbalance equipped with a 273–1273 K programmable temperature furnace following the weight losses at 110°C/air (moisture), 900°C/non-oxidising atmosphere (volatile matter), 900°C/air (fixed carbon); ash content was obtained by difference.

SEM studies. The surface morphology of KL and KL_d was studied by scanning electron microscopy (SEM) with a JEOL JSM-6400. The microscope was equipped with an energy dispersive X-ray (EDX) microanalyser that was used for observing the dispersion of the mineral matter in KL and KL_d.

Surface area and porosity. Surface area and porosity were determined from the corresponding nitrogen adsorption–desorption isotherms obtained at 77 K with an automatic instrument (ASAP 2020, Micromeritics). The samples were previously outgassed at 523 K for several hours. N₂ adsorption data for P/P₀ from 10⁻⁵ to 0.99 (in a set of values previously fixed) were analysed according to: (i) the BET method [8] for calculating the specific surface area, S_{BET} ; and

(ii) the α_s method [9] (using Carbopack F Graphitised Carbon Black as reference material [10] for calculating the micropore volume, $V_{\alpha_{\text{micro}}}$, and the supermicropore volume, $V_{\alpha_{\text{super}}}$. The total pore volume, $V_{0.99}$, was calculated from nitrogen adsorption at a relative pressure of 0.99.

3. RESULTS AND DISCUSSION

Table 1 shows the proximate and ultimate analyses of KL and KL_d. KL has a high ash content (11.1 % on dry ash-free (daf) basis) which is nearly removed (0.2 % on daf basis) after the treatment with H₂SO₄. The high S content (2.2 %) in KL is due to both the Kraft or sulphate process, which consists in a treatment with NaOH and Na₂S to separate the cellulose from the other wood constituents, and to organically bound sulphur (up to 1.5 %) [11]. XRD analysis of lignin showed that Na is found combined with S and C inside the phase Na₂CO₃ · 2 Na₂SO₄. Lignin demineralisation produced a decrease of S content (down to 0.5 %) and of O content (from 33.3 to 27.8 %). Analysis by SEM-EDX showed that S and Na are uniformly distributed in the polymeric matrix before and after the demineralisation treatment.

Table 1. Proximate and ultimate analyses of KL and KL_d (wt. %)

	Proximate Analysis (wt %, dry basis)			Ultimate Analysis (wt %, daf)				
	Fixed Carbon	Volatile matter	Ash	C	H	N	S	O*
KL	36.4	52.5	11.1	59.5	5.1	0.1	2.2	33.3
KL _d	39.7	60.1	0.2	65.8	5.9	0.0	0.5	27.8

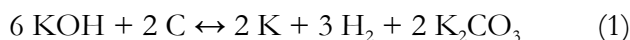
* Estimated by difference.

The effect of the experimental parameters considered in this study is discussed below.

3.1. Effect of the temperature of activation

Figure 1 a) shows the variation of carbon yield with the temperature of activation. Increasing the activation temperature produces the decrease of the carbon yield due: (i) to the pyrolysis of lignin up to 600°C; (ii) to the activation by KOH and K₂CO₃ that starts at 450-500°C. The dissociation of the two phenomena, pyrolysis and activation, is impossible because lignin have already reacted with KOH in some extent before pyrolysis finishes.

Activation with KOH involves the oxidation of C and the production of K metal, H₂ and K₂CO₃ according to the main reaction :

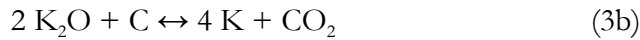


However, reaction (1) is certainly not the only one, since various molecules like CO, CO₂, H₂ and H₂O originating from the thermal decomposition of lignin are also present. Thus, K₂CO₃ produced by reaction of KOH with CO₂ also acts as an efficient activating agent. Hayashi and coworkers [12] showed that high surface areas of nearly 1700 and 2000 m²/g can be obtained by activation of KL with K₂CO₃ for R=2 at 700 and 800 °C, respectively. Moreover, carbons prepared by K₂CO₃ activation showed higher surfaces than those prepared by KOH activation at temperatures higher than 600°C. Hayashi has also worked with different raw materials: husks [13], nutshells [14] or formaldehyde resins [15] reaching very high surfaces even at 700°C. McKee [16] studied the gasification of graphite

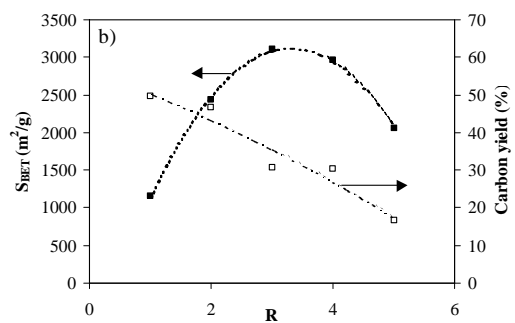
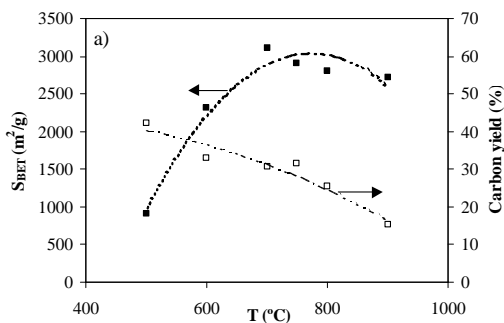
powder by a serie of alkali metal salts and found that K_2CO_3 was reduced in inert atmosphere by carbon as follows:



The decomposition of K_2CO_3 to CO_2 and K_2O could also lead to activation by the two latter products, according to:



Nevertheless, CO_2 and K_2O individually are not expected to be activating agents until high temperatures (above 800 °C) are reached. Hence, the other most efficient activant is rather the water vapour evolved from lignin pyrolysis, and giving the following reaction:



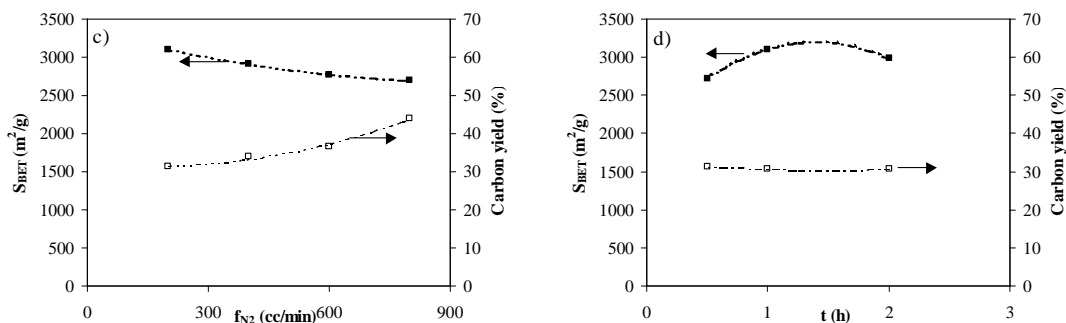


Figure 1. Variation of the S_{BET} (■) and carbon yield (□) with: a) temperature of activation ($R= 3$, $f_{N_2}= 200$ cc/min, $r= 5^{\circ}\text{C}/\text{min}$, $t_{\text{carb}}= 1$ h); b) R ($T= 700$ °C, $f_{N_2}= 200$ cc/min, $r= 5^{\circ}\text{C}/\text{min}$, $t_{\text{carb}}= 1$ h); c) N_2 flow ($T= 700$ °C, $R= 3$, $r= 5$ °C/min, $t_{\text{carb}}= 1$ h); d) activation time ($T= 700$ °C, $R= 3$, $f_{N_2}= 200$ cc/min, $r= 5$ °C/min).

Figure 2 a) shows the adsorption-desorption isotherms of N_2 at 77 K of the activated carbons prepared at 500, 600, 700, 800 and 900 °C. All the isotherms are of type I (Langmuir), characterising microporous solids. The carbon prepared at 500 °C presents an extensive plateau in the range of medium to high relative pressures, indicating an essentially microporous character. As carbonization temperature increases the knee of the isotherms widens and the width of the plateau decreases, indicating a widening of the pores. Thus, the material prepared at 900 °C shows a hysteresis loop, evidencing a well-developed mesoporosity. The decrease of carbon yield is accompanied by an increase of both surface area and microporosity up to the temperature of 750 °C, above which these properties decrease as seen in Figure 1 a).

Figure 3 a) shows the total pore, micropore and ultramicropore volumes. The total pore volume always increases with activation temperature but at temperatures higher than 750°C there is a widening of micropores to create mesopores. Figure 3 b) shows the corresponding pore size distributions calculated by application of the Horwatz-Kawazoe method; the maximum is always centered in the micropore region but, as the temperature increases the contribution of wider pores is more important, in agreement with the results of Figures 2a) and 3a).

3.2. Effect of the KOH/KLd weight ratio (R)

At constant temperature (700 °C), the value of R has a marked effect on both the carbon yield and the BET surface area S_{BET} . Figure 1b) shows that there is a linear decrease of carbon yield with R whereas a maximum of the S_{BET} can be observed at R values around 3. Figure 2 b) shows that an increase of R from 1 to 3 produces a great enhancement of N_2 adsorption capacity at 77 K but higher values of R reduce it. The micropore volumes are also reduced for $R \geq 3$ (see Figure 3 c) with the concomitant increase of the fraction of wider pores (see Figure 3 d).

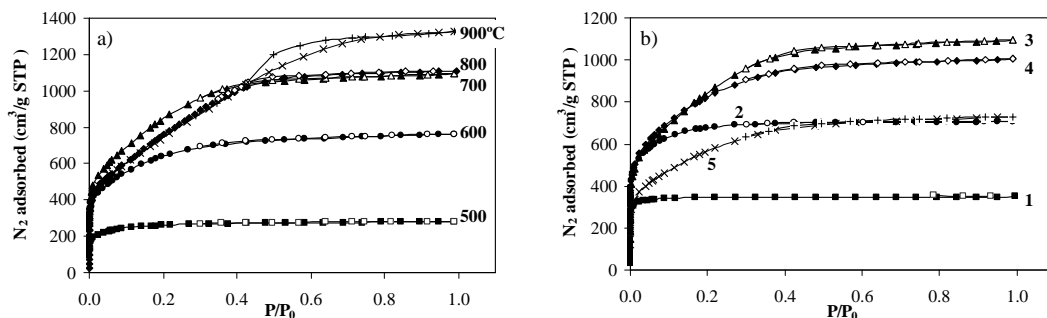


Figure 2. Adsorption-desorption isotherms of N₂ at 77 K on the activated carbons derived from KL_d: a) effect of T and b) effect of R (open symbols and x: adsorption isotherms; full symbols and +: desorption isotherms).

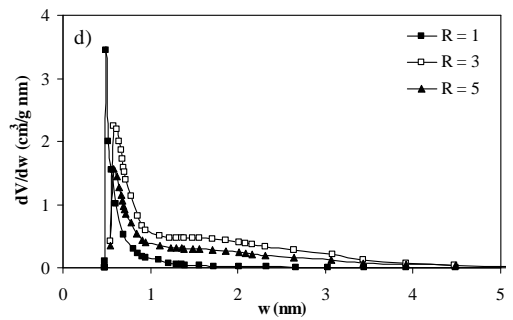
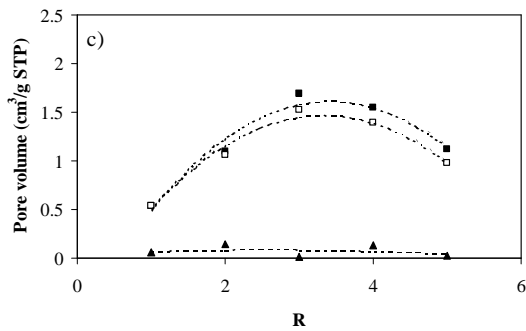
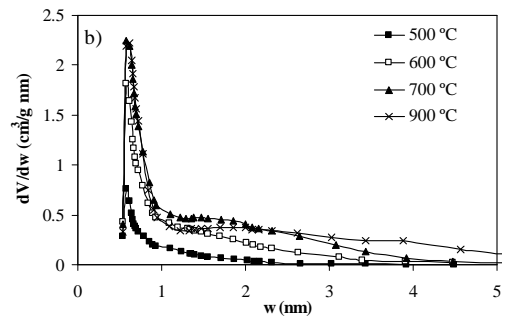
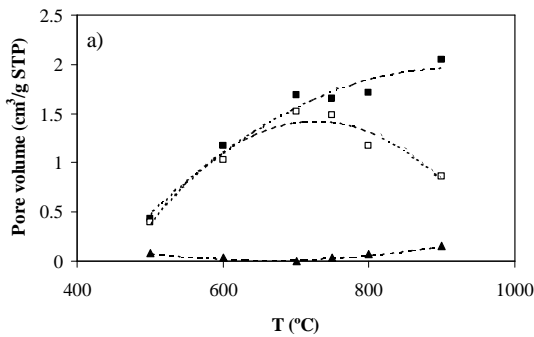
3.3. Effect of the N₂ flow

The flow of N₂ removes the gaseous reaction products but also a part of the activating agent as it was observed in this study. Figure 1 c) shows that the increase in the N₂ flow rate from 200 to 800 cc/min produces an increase of carbon yield because the activating agent is increasingly swept out.

Such a decrease of the activation efficiency may be explained both by a lower contact time of KOH vapour with the solid matter, and by the removal of other possible activating agents: CO₂ (either as such, or as K₂CO₃ after its reaction with KOH), and H₂O.

S_{BET} and the porosity, in the whole pore diameter range, decrease with increasing N₂ flow rate as it is shown in Figures 1c) and 3 e) respectively. These results are different from those found by Linares-Solano and

coworkers who found that N_2 flow enhances the activation of the carbon [6]. However, it is obvious that the different nature of the precursor has an effect on the activation process and so on the activated carbon produced. These results, apparently opposed, could not be contradictory. When pyrolysis and activation take place simultaneously, as for biomass precursors, the co-activation by water vapour evolved during pyrolysis could be important as suggested above.



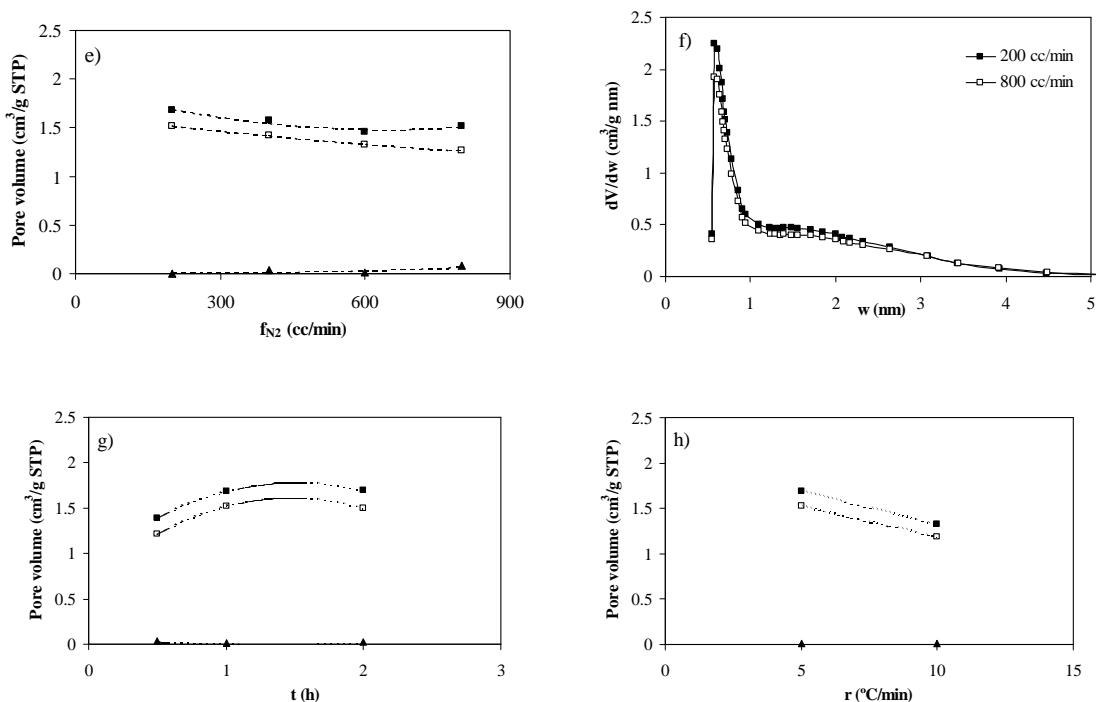


Figure 3. Variation of the $V_{0.99}$ (■), $V_{\alpha_{\text{micro}}}$ (□) and $V_{\alpha_{\text{ultra}}}$ (▲) with: a) temperature of activation ($R = 3$, $f_{\text{N}_2} = 200$ cc/min, $r = 5^\circ\text{C}/\text{min}$, $t_{\text{carb}} = 1$ h); c) R ($T = 700^\circ\text{C}$, $f_{\text{N}_2} = 200$ cc/min, $r = 5^\circ\text{C}/\text{min}$, $t_{\text{carb}} = 1$ h); e) N_2 flow rate ($T = 700^\circ\text{C}$, $R = 3$, $r = 5^\circ\text{C}/\text{min}$, $t_{\text{carb}} = 1$ h); g) activation time ($T = 700^\circ\text{C}$, $R = 3$, $f_{\text{N}_2} = 200$ cc/min, $r = 5^\circ\text{C}/\text{min}$); h) heating rate ($T = 700^\circ\text{C}$, $R = 3$, $f_{\text{N}_2} = 200$ cc/min, $t_{\text{carb}} = 1$ h). Evolution of the pore size distribution of the carbons with: b) temperature of activation (experimental conditions as in Fig. 3 a); d) R (experimental conditions as in Fig. 3 c).

Figure 3 f) shows the PSD of two activated carbons prepared with a N_2 flow of 200 or 800 cc/min. Increasing the N_2 flow does not change the PSD but decreases the pore volume (S_{BET} and $V_{0.99}$ decrease). Since the size of the

pores is the same, finding a lower pore volume should be related to a lower number of pores. Therefore, the effect of the N₂ flow is very different from that of R, even is the latter is more noticeable.

3.4. Effect of the activation time

The duration of activation at a given temperature does not seem to affect neither the carbon yield nor the elemental composition, since differences in both analyses are very small. Figure 1 d) and 3 g) show that there is an optimum in the activation time, between 1 and 2 h, to get the highest surface area and microporosity. The S_{BET} decreases from 3105 to 2990 m²/g when increasing activation time from 1 to 2h respectively.

3.5 Effect of the heating rate

An increase of the heating rate from 5 to 10 °C/min produces a lowering of the S_{BET} from 3105 to 2493 m²/g (see figure 3h). Actual technical limitations do not allow using higher heating rates but our results agree with previous findings [6]. During the heating process the hydroxide melts, then, it is reasonable that a lower heating rate allows a longer contact time between carbon and liquid hydroxide, and hence a better impregnation, before the reaction temperature is reached.

4. CONCLUSIONS

The present exploratory study evidenced the possibility of preparing highly microporous active carbons from demineralised Kraft lignin, using KOH in suitable experimental conditions. The most relevant parameters were found to be activation temperature and mass ratio KOH/lignin, while the other ones (flow of inert gas, duration time, heating rate) were found to have minor effects within the corresponding range of values investigated. Thus, the best materials (surface area $\sim 3000 \text{ m}^2/\text{g}$, micropore volumes $\sim 1.5 \text{ cm}^3/\text{g}$) were obtained at $700 \text{ }^\circ\text{C}$ and $\text{KOH}/\text{KL}_d = 3$. Such results are very close to those already reported for anthracites, which are known to lead to very good adsorbents when prepared in similar conditions [17]. Furthermore, modifying the experimental conditions easily leads to a range of active carbons, from almost purely microporous to mesoporous. Hence, even if the detailed mechanisms are still unclear, chemical activation now appears to be a valuable (rapid, simple and cheap) process for the valorization of lignin.

ACKNOWLEDGEMENTS

This research was made possible in part by financial support from MCYT (project PPQ2002-04201-CO02), DURSI (2001SGR00323 and 2002AIRE) and ALFA Program (project ALFA II 0412 FA FI). V. Fierro acknowledges the MCYT and the Universitat Rovira i Virgili (URV) for the financial support of her 'Ramón y Cajal' research contract. V. Torné-Fernández acknowledges the URV for her PhD grant.

REFERENCES

- [1] V. Fierro, V. Torné-Fernández, D. Montané and J. Salvadó, 'Activated Carbons Prepared from Kraft Lignin by Phosphoric Acid Impregnation', In proceedings of Carbon'03, Oviedo (Spain) 2003.
- [2] V. Fierro, V. Torné-Fernández, D. Montané and A. Celzard, *Thermochim. Acta*, 433 (2005) 153.
- [3] A. Ahmadpour and DD. Do, *Carbon*, 34 (1996) 471.
- [4] T. Otowa, Y. Nojima, T. Miyazaki, *Carbon*, 35 (1997) 1315.
- [5] C. Liang, Z. Wei, Q. Xin and C. Li, *Appl. Catal. A*, 208 (2001) 193.
- [6] D. Lozano-Castelló, M.A. Lillo-Ródenas, D. Cazorla-Amorós and A. Linares-Solano, *Carbon*, 39 (2001) 741.
- [7] E. Frackowiak and F. Beguin, *Carbon*, 40 (2002) 1775.
- [8] F. Rouquerol, J. Rouquerol and K.S.W. Sing Adsorption by Powders and Porous Solids. Principles, Methods and Applications, Academic Press, San Diego, CA (1999).
- [9] N. Setoyama, T. Suzuki and K. Kaneko, *Carbon*, 36 (1998) 1459.
- [10] M. Kruk, Z.J. Li, M. Jaroniec, W.R. Betz, *Langmuir*, 15 (1999) 1435.
- [11] C.H. Hoyt, D.W. Goheen, in: K.V Sarkanen, C.H. Ludwig (Eds.), *Lignins*, Wiley-Interscience, New York, 1971, Chapter 20, p. 833.
- [12] J. Hayashi, A. Kazehaya, K. Muroyama, A.P. Watkinson, *Carbon*, 38 (2000) 1873.
- [13] J. Hayashi, T. Horikawa, K. Muroyama, V.G. Gomes, *Micropor. Mesopor. Mat.*, 55 (2002) 63.
- [14] J. Hayashi, T. Horikawa, I. Takeda, K. Muroyama, F.N. Ani *Carbon*, 40 (2002) 2381.
- [15] J. Hayashi, M. Uchibayashi, T. Horikawa, K. Muroyama, V.G. Gomes, *Carbon*, 40 (2002) 2747.

[16] D.W. McKee, *Carbon*, 20 (1982) 59.

[17] A. Celzard and V. Fierro, *Energy and Fuels*, 19 (2005) 573.

5.1.6. Methodical study of the chemical activation of Kraft lignin with KOH and NaOH

Este artículo ha sido enviado al journal Microporous and Mesoporous Materials durante el año 2006.

Methodical study of the chemical activation of Kraft lignin with KOH and NaOH

V. Fierro¹, V. Torné-Fernández² and A. Celzard^{3*}

¹*Laboratoire de Chimie du Solide Minéral, UMR CNRS 7555,
Nancy-Université, BP 239,
54506 Vandœuvre-lès-Nancy, France*

²*Departament de Enginyeria Química,
Universitat Rovira i Virgili,
Avda dels Països Catalans,
43007 Tarragona, Spain*

³*Laboratoire de Chimie du Solide Minéral, UMR CNRS 7555,
Nancy-Université, ENSTIB
27 rue du Merle Blanc, BP 1041, 88051 Épinal Cedex 9, France*

* Corresponding author.

postal address : ENSTIB, 27 rue du Merle Blanc, BP 1041

Laboratoire de Chimie du Solide Minéral, UMR CNRS 7555,
88051 Épinal Cedex 9, France

fax number : 33 (0) 3 29 29 61 38

e-mail : Alain.Celzard@enstib.uhp-nancy.fr

Abstract

A commercially available Kraft lignin was chemically activated with two alkaline hydroxides, viz NaOH and KOH, using different preparation conditions. The activation was made at various temperatures, mass ratios hydroxide / lignin, activation times, flow rates of inert gas, and heating rates. The resulting active carbons were characterised in terms of BET surface area, total, micro and meso-pore volumes, average pore width, carbon yield and packing density. The influence of each parameter of the synthesis on the properties of the active carbons is discussed, and the efficiencies of each activating agent are methodically compared. It is the first time that so many preparation parameters and so many pore texture characteristics are simultaneously considered for two closely related activating agents of the same lignin precursor. Whatever the preparation conditions, it is shown that KOH is the one leading to the most microporous materials, which is in agreement with some early works. However, the surface areas and the micropore volumes obtained in the present study are much higher than in previous studies. The thorough study of the way each preparation parameter influences the properties of the final materials brings insight into the activation mechanisms. Each time it was possible, the results of lignin chemically activated with hydroxides were compared with those obtained with anthracites: explanations of similarities and differences were systematically looked for.

1. Introduction

Lignin is a waste mass-produced from the paper industry and as such, is generally used for its fuel value. However, an ever-growing number of research works are carried out in order to bring added value to this material. Lignin is becoming frequently accepted as a suitable chemical reagent for formulating new adhesives [1-5], as filler in polymer mixtures [6], and as promising precursor of carbonaceous materials [7-14]. Other possible applications are reviewed in [15]. Concerning the preparation of carbons, lignin is particularly advantageous because of its high phenolic content, leading to higher carbon yields than those obtained from the two other main macromolecular compounds of biomass: cellulose and hemicellulose [16,17]. Hence, getting almost pure lignin is really interesting for preparing carbons and, especially active carbons.

In the present work, the activating efficiency of two alkaline hydroxides classically used for chemical activation of various precursors was investigated thoroughly with one kind of commercially available Kraft lignin, once the latter was demineralised. All the parameters of the active carbon synthesis which could be varied were investigated, namely activation temperature, mass ratio hydroxide / lignin, flow rate of inert gas, activation time and heating rate. The influence of each of them was systematically correlated to the pore structure of the corresponding activated carbons. From this work, the suitable preparation conditions of the material having given desired porous characteristics can be identified, while insights into the activation mechanisms may be derived.

The first section of the present paper deals with the intrinsic features of the lignin, and with the experimental conditions by which it was demineralised and activated; the way the resultant active carbons were characterised is then described. The pore volumes and the related properties: mean pore size, surface area, and also the carbon yield and the packing density obtained with both activating agents are systematically compared and discussed in section 2.

2. Experimental

2.1. Kraft lignin and activating agents

The Kraft lignin (KL) was supplied by Lignotech Iberica S.A (Spain) in the form of a fine dark brown powder. The proximate analysis was carried out according to ISO standards, following the weight losses of the material at 100 °C in air (moisture, ISO-589-1981), at 900 °C in a non-oxidising atmosphere (volatile matter, ISO-5623-1974) and at 815 °C in air (ashes, ISO-1171-1976). The ultimate analysis was carried out in an EA1108 Carlo Erba Elemental Analyser.

The removal of the inorganic matter from KL was achieved as follows: batches of 100 g were introduced in 2 L of water, leading to dark brown suspensions of pH 9.5, and lignin was precipitated by adding carefully concentrated H₂SO₄ until the pH decreased to 1. The precipitate was gently washed with distilled water until the pH of the rinse was constant, and finally dried overnight at 105 °C. The lignin prepared this way was nearly mineral-free and was termed demineralised Kraft lignin (KL_d). It should be stressed

that the activated carbons discussed in the following were all prepared from KL_d , never from the pristine commercial lignin (KL). As a remark, it can be added that such a deashed lignin is somewhat different from the original material, since the acid treatment is known to modify the physico-chemical properties and the structural features of the polymer (see [18,19] for example). Consequently, the properties of the activated carbons obtained from KL_d are different from those derived from raw KL; a paper to be published soon was devoted to this subject [20].

KOH lentils on one hand, and NaOH lentils on the other hand (Scharlau) were ground and physically mixed with KL_d according to various hydroxide / KL_d mass ratios, R. The purity of both activating agents was higher than 99 %. Activated carbons were then obtained by heat-treatment in inert atmosphere of the hydroxide – lignin mixtures (see below). It should be stressed that such an activation mode is different from the two ones generally employed. The first widely used method indeed consists in: (i) a preliminary pyrolysis of the biomass; (ii) the impregnation of the char with a concentrated aqueous solution of the activating agent; (iii) the subsequent drying at temperatures slightly above 100 °C; and finally (iv) the heat-treatment of the dry hydroxide – char mixture (see for example [21-23]). The second well known protocol consists in a direct impregnation of the biomass in aqueous solution, followed by a drying and a heat-treatment (see for example [11,24,25]). However, as shown below, the activation method proposed here is very efficient, probably because of the low melting point of KOH and NaOH (ca 360 and 318 °C, respectively) compared with the synthesis temperatures used in this work (above 400 °C).

2.2. *Active carbon synthesis*

The carbonisation of the hydroxide – KL_d mixtures was carried out in a horizontal furnace flushed with nitrogen. The samples were heated ($r = 5$ or 10 °C/min) from room temperature up to the final carbonisation temperature ($400 \leq T \leq 900^\circ\text{C}$) in different nitrogen flows ($50 \leq f \leq 800$ mL/min). Samples were kept at the final temperature for different carbonisation times ($0.5 \leq t \leq 4$ h) before cooling down under nitrogen.

Only one of the aforementioned synthesis parameters was varied while the others were kept constant. A reference sample was defined as the one prepared in the following condition: $T = 700^\circ\text{C}$; $R = 3$; $t = 1$ h; $f = 200$ mL min^{-1} ; $r = 5$ °C min^{-1} . This means that if, for example, T was varied, the values of R , t , f and r were constant and equal to 3, 1, 200 and 5, respectively.

During the experiments, both the metallic alkaline elements produced by the reduction of NaOH or KOH by carbon at high temperature, and the hydroxides themselves were partly transported in the vapour phase, and could be observed at the outlet of the reactor. Metallic sodium or potassium mixed with sodium or potassium carbonate, respectively, were also present inside the sample-holder. Such phenomena were also observed upon activating anthracites with NaOH [26,27]. Therefore, whatever the activating agent, the sample-holder was submitted to atmospheric humidity for two days, during which the alkaline metals slowly oxidised. At last, the resulting activated carbon was washed with extreme care, first with 1M HCl, and finally with distilled water until the pH of the rinse remains constant and

close to 6. After drying in an oven during 24 h, a light, pure, activated carbon was obtained.

2.3. Active carbon characterisation

Surface area and pore volumes were determined from the corresponding nitrogen adsorption–desorption isotherms obtained at 77 K with an automatic instrument (ASAP 2020, Micromeritics). The samples were previously outgassed at 523 K for several hours. N₂ adsorption data at relative pressures ranging from 10⁻⁵ to 0.99 (in a set of values previously fixed) were analysed according to: (i) the BET method [28] for calculating the apparent surface area, S_{BET}, (ii) the α_s method [29] (using Carbopack F Graphitised Carbon Black as reference material [30]) for calculating the total micropore volume, V_{micro}, and (iii) the Dubinin-Radushkevich method [31], leading to the micropore volume V_{DR}. The values of V_{micro} and V_{DR} should have been close to each others, however, as usual, discrepancies were observed, and we have preferred to present both values. The total pore volume, V_{0.99}, was calculated from nitrogen adsorption at a relative pressure of 0.99, and the mesopore volume, V_{meso}, was obtained according to V_{meso} = V_{0.99} - V_{micro}.

The average pore size, L₀, was calculated according to the widely accepted equation:

$$L_0 \text{ (nm)} = \frac{10.8 \text{ (nm kJ mol}^{-1}\text{)}}{E_0 - 11.4 \text{ (kJ mol}^{-1}\text{)}} \quad (1)$$

in which E_0 is the characteristic adsorption energy of probe molecules, see [32] and references therein. E_0 was derived from the nitrogen adsorption isotherms at 77 K, applying the Dubinin-Radushkevich method.

The carbon yield was simply defined as the weight ratio: final active carbon / initial demineralised lignin. The packing density was determined by pouring, as reproducibly as possible, the activated carbon into a plastic tube (inner diameter 1.4 cm) until a given height, and calculating the ratio: sample weight / sample volume. When KOH was used, the material obtained after the activation was in a powder form (a phenomenon also systematically observed for KOH activation of olive stones [33]), hence no milling was done before measuring the packing density. By contrast, NaOH-activated carbons were most of times aggregated, hence the packing density of such material was ill-defined. The blocks should have been crushed in order to obtain a powder, but doing this would have modified the shape of the carbon grains, and thus the packing density itself. Consequently, the latter was not measured for activated carbons derived from NaOH activation.

3. Results and discussion

3.1. *Pristine and demineralised Kraft lignin*

Table 1 shows the proximate and ultimate analyses of KL and KL_d. KL has a high ash content (11.1 % on dry ash-free (daf) basis), which is nearly removed (0.2 % on daf basis) after the treatment with H₂SO₄. The high S content (2.2 %) in KL is due to both the Kraft or sulphate process, which consists in a treatment with NaOH and Na₂S to separate the cellulose from

the other wood constituents, and to organically bound sulphur (up to 1.5 %) [34]. XRD analysis of lignin showed that Na is found combined with S and C inside the phase Na_2CO_3 , $2 \text{Na}_2\text{SO}_4$. Lignin demineralisation produced a decrease of S content (down to 0.5 %) and of O content (from 33.3 to 27.8 %). Analysis by SEM-EDX showed that S and Na are uniformly distributed in the polymeric matrix before and after the demineralisation treatment [20].

3.2. Characteristics of the activated carbons

3.2.1. BET surface area

Figure 1 presents the variations of the BET surface area when each synthesis parameter is individually varied with respect to the reference preparation condition ($T = 700 \text{ }^\circ\text{C}$; $R = 3$; $t = 1 \text{ h}$; $f = 200 \text{ mL min}^{-1}$; $r = 5 \text{ }^\circ\text{C min}^{-1}$). It can be seen that, whatever the way the preparation conditions may vary, KOH is the activating agent leading to the highest specific area, in agreement with a previous work [11]. However, to our knowledge, BET values close to $3000 \text{ m}^2 \text{ g}^{-1}$ are the highest ever published so far for a lignin-derived activated carbon. The curves show that, most of times, an optimum may be observed for the parameters corresponding to our reference, i.e., for $T = 700 \text{ }^\circ\text{C}$, $R = 3$, etc. In other words, the reference material is the one obtained from the (already optimised) conditions leading to the most microporous active carbons. This is especially true for the ones obtained using KOH, while those made from NaOH have similar but not identical optimal preparation conditions. However, the curves clearly show that NaOH can not allow obtaining surface areas as high as those derived from KOH, while the opposite was found in the activation of anthracites, as far as the activating agent and the precursor were physically mixed together (the results being

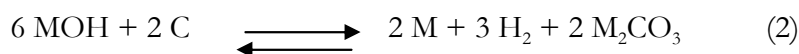
different with the more classical wet impregnation technique) [35]. This fact could be explained as follows. KOH has higher dehydrating and oxidising efficiency than NaOH, hence a higher activating activity for biomass. But anthracites are already ultramicroporous high-rank coals, with closed narrow porosity that can be open through the oxidising character of both KOH and NaOH; Na^+ being smaller than K^+ , it can penetrate more deeply the carbon structure and develop a higher number of smaller pores than K^+ can do. Anthracites activated with NaOH thus present higher surface areas than those prepared with KOH using the same protocol [35]. Thus, because the mechanisms of chemical activation of lignin and coal are different, the optimal preparation parameters are not the same.

Values of T , R and t lower than 700, 3 and 1, respectively, lead to an insufficiently activated carbon (i.e., there are a few narrow pores, hence the surface area is low), while higher values lead to materials in which the pores are too wide (i.e., there are less micropores and more mesopores, hence the surface area is also lower). Indeed, increasing the values of these parameters improve the activation phenomenon, by which the porosity is both open and widened. This effect of the activation temperature was already observed with chemically activated anthracites [26]. The existence of optimal values is thus readily explained, since the narrowest pores are those which most contribute to the surface area, provided that their number is high enough (low values of T , R and t), while these narrow pores become wider and scarcer at high values of T , R and t , leading to decreasing surface areas.

It should be emphasised that the mass ratio hydroxide / lignin, R , is the parameter having the strongest influence. This finding agrees with previous results dealing with the activation of anthracites with NaOH [36]. It is thus not surprising to find surface areas much higher than those already published

so far, for with values of R were lower than 3 [11,24]. For a given constant value of R (e.g., $R = 3$), T is the second most important parameter, while the activation time t has the lowest influence on the surface area. The heating rate r also has a low effect; for KOH, increasing r makes the BET area decrease, while the latter keeps almost constant with NaOH. This may be explained by the fact that the activation of lignin already begins during the heating step. Increasing the heating rate for a given activation time (which is defined only once the carbonisation temperature is reached) finally has a similar effect as reducing the activation time (although it will be shown below that the effects of t and r are not exactly the same in the case of NaOH). For example, assuming that the kinetics of activation is non negligible above 500 °C (which was clearly evidenced in [37]), 40 min are required for increasing the temperature from 500 up to 700 °C at 5 °C min⁻¹, while only 20 min are necessary at 10 °C min⁻¹. 40 min are indeed important when compared to an activation time of 1 h, and decreasing to 20 min logically decreases the surface area of KOH-activated carbons. Since the effect of the activation time was low on the BET area of NaOH-activated carbons, so is the effect of the heating rate.

The influence of the flow rate of inert gas is now considered. For both NaOH and KOH, an optimum is again observed. This fact is very different from what was found with anthracites activated with the same hydroxides in the same conditions, for which the higher the nitrogen flow rate, the higher was the surface area [35,38]. The behaviour of anthracites submitted to similar nitrogen flow was explained on the basis of the following chemical reaction [37,39]:



in which M is either the element K or Na. Such a reaction indeed explains how the equilibrium may be displaced towards the formation of more reaction products if dihydrogen and alkaline vapours are evacuated. However, observing completely opposite behaviour in the present work proves that Equation (2) is, as expected, not suitable to lignin. Lignin is a macromolecule which can not be compared with a coal, and whose heat-treatment produces a number of volatile matters, like CO, CO₂ and H₂O [12], among others. The presence of an optimum in the case of lignin activation may be explained by the competition between the favourable removal of gaseous reaction products and the unfavourable removal of activating agents in the gas phase. Indeed, it is expected that the volatility of both hydroxides is non negligible at the activation temperatures, and their presence at the outlet of the reactor was observed, proving that they are transported in the gas phase. However, the strongest effect might not be due to the removal of the hydroxide vapours, but to that of both water vapour and carbon dioxide necessary formed during the activation process, in which both charring and dehydration phenomena occur. CO₂ and H₂O are indeed well known activating agents of carbons, and they might induce a substantial co-activation of the char, since several hundreds of m² g⁻¹ can be easily gained or lost by simply changing the flow rate of inert gas.

It is nevertheless not clear, so far, if CO₂ should be considered or not as a possible co-activating agent, because: (i) CO₂ usually requires higher temperatures than steam to react with the char, and (ii) CO₂ causes the carbonation of the hydroxides, thus producing carbonates. On one hand, carbonation of NaOH was shown to lead to poorly microporous carbons [37] (because the activity of Na₂CO₃ is low, which was confirmed in the case of lignin activation [11]) and, on the other hand, K₂CO₃ was found to be a very effective activating agent of lignin [11]. The role of CO₂ in the co-

activation of lignin – hydroxides mixtures is thus unclear, while that of steam is more likely.

3.2.2. Pore textures

The pore volumes (total: $V_{0.99}$; micro: V_{DR} and V_{micro} ; meso: V_{meso}) are given in Figure 2. For the sake of clarity, the results concerning the carbons activated with KOH and NaOH are presented in separate plots, gathered in Figure 2(a) and 2(b), respectively. As expected, given the preceding findings about the BET surface area, the activated carbons prepared with KOH are those having the highest total pore and micropore volumes, confirming the higher activating activity of KOH on lignin.

The optima shown on the curves are nearly the same as those already observed for the surface area, as far as micropores are concerned. This finding is readily explained by the fact that the narrowest pores most contribute to the specific surface area. Thus, in the case of NaOH-activated carbons for example, the maximum of S_{BET} at $f = 400 \text{ mL min}^{-1}$ exactly coincides with that of V_{DR} and V_{micro} , while the total pore volume (hence including mesopores, with a low influence on S_{BET}) has its maximum at $f = 200 \text{ mL min}^{-1}$. In [38], it was argued that a high nitrogen flow rate could be compared to a low heating rate, since both lead to a lower concentration of the gaseous reaction products, influencing the chemical equilibria occurring during the activation process. Such arguments could not be extended to the case of lignin activation, since high flow rates of inert gas led to lower BET surface area and pore volumes, while low heating rates led to the opposite situation. These facts prove once more that the chemical reactions of lignin and anthracites are different, even if, as shown all through the present paper,

many similarities may be found between the resulting activated carbons. Concerning now the effect of the heating rate, r , the micropore volume of KOH-activated carbons decreases with r , and this may be explained as follows. A lower heating rate corresponds to a longer impregnation of the lignin with melted KOH, leading to better development of the porosity; the same is found for NaOH.

The mesopore volume, obtained as the difference $V_{0.99} - V_{\text{micro}}$ is worth studying because information about the way the chemical activation of lignin is achieved may be obtained. Concerning KOH first, it can be seen that V_{meso} increases with the activation temperature, and a stronger increase above 750 °C coincides with the drop of the micropore volume. This finding may be accounted for by the conversion of micropores into mesopores at high activation temperatures. In other words, increasing T mainly induces the widening of the pores, which is a phenomenon already clearly evidenced for the chemical activation of anthracites [26,36]. By contrast, the mesopore volume remains low and increases very slightly with the mass ratio KOH / lignin; above $R = 3$, the micropore volume decreases, however no additional mesopores are created. This means that the influences on the pore texture of T on one hand, and R on the other hand, are really different. Lignin being less and less activated at increasingly high values of R may be explained by the fact that KOH produces pores but also weakens and progressively destroys the incipient carbon structure. More and more matter is consumed when R increases, as shown by the coke yield and suggested by the packing density (see below), but no additional porosity is formed. Getting the highest amount of micropores thus really requires finding the optimum value of R , otherwise average characteristics are obtained (see the results published in [17,24] for example). The mesopore volume is the lowest at a flow rate of 200 mL min⁻¹, while the micropore volume is the highest, confirming that the

parameter f is suitably optimised for the activation of lignin with KOH. Finally, the influence of t and r on the mesopore volume is very low.

Concerning now NaOH, the mesopore volume exhibits a maximum close to 700 °C, just like does the micropore volume. The widening of the pores can thus no longer be invoked as in the case of KOH, since the total porosity decreases above 800 °C. This finding may be explained by the closure of the porosity at such high temperatures, which is a well-known mechanism in heat-treated carbon materials (see for example [12,40,41] and references therein), but also in lignin activated with H₃PO₄ [13]. This quite common phenomenon, occurring during charring and / or collapsing of the incipient carbon structure due to an excessive chemical attack, was also observed with KOH used in a different preparation condition, especially $R = 1$ in [11]. Such a low value of R indeed probably favoured charring upon activation, while an optimised value of R (3, in the present work) did not lead to the same effect (i.e., the process is rather governed by activation). The influence of the mass ratio NaOH / lignin is very similar to what was observed with KOH, hence the conclusion is identical: too much activating agent consumes the material rather than forming porosity. Concerning the flow rate of inert gas, a maximum of mesopore volume is obtained at $f = 200$, while the greatest micropore volume is obtained at 400 mL min⁻¹. This finding corroborates the fact that $f = 200$ is not the optimal value of this parameter as far as NaOH is used as activating agent. Obtaining the most microporous carbons is thus achieved at 400 mL min⁻¹, which value was also the best for activating anthracites with NaOH [36]. Activation time has, again, a low impact on the mesopore volume. Finally, increasing the heating rate produces more micropores and less mesopores. It was assumed in § 3.2.1 that a higher heating rate could be nearly equivalent to a shorter full activation process. However, Figure 2(b) evidences that a shorter activation time leads to lower

micropore volumes and higher mesopore volumes, while the opposite is observed for a higher heating rate. Consequently, a high heating rate and a short activation process are not identical. During the heating of the lignin – hydroxide mixture, charring and activation occur simultaneously; increasing the heating rate indeed probably favours the charring since it may be assumed that the dehydrating action of the hydroxide requires time, while charring is a very fast process just depending on the temperature. This is especially true with NaOH, which activating efficiency is lower than that of KOH, Na⁺ being indeed less oxidising than K⁺ (this fact may also explain the lower activation by NaOH in terms of surface area and pore volumes). Moreover, KOH indeed activates anthracites more rapidly than NaOH and at lower temperatures: 400 °C and 550 °C for KOH and NaOH, respectively [37]. Additionally, the reactions occur at even lower temperatures when the rank of the coal is low; it is thus expected that activation of lignin begins since 200 °C [39]. With NaOH, the charring is achieved at a much higher rate than the activation itself, leading to more char formed. A higher heating rate thus leads to a material characterised by more narrow pores and less wider pores, since the activation with NaOH of carbon structures is the one leading to the narrowest pores (compare the results given in [27] for NaOH and [42] for KOH).

3.2.3. Mean pore size

The dependence of the mean pore size, L_0 , on the process parameters is shown in Figure 3. The presented values are close to what was already calculated for a lignin and for fir wood both activated with KOH [17,23]. L_0 is an average characteristic of the pore texture closely related to both the surface area and the pore volumes. Since the data presented are either above,

or only slightly below, 2 nm, mesopores widely contribute to the values of L_0 . Thus, analogies between the dependence of L_0 and that of the total pore volume presented in Figure 2 can be evidenced. Whatever the activating agent, the same kinds of maxima are indeed recovered for nearly identical values of T , R , f and t . Increasing the heating rate decreases the average pore size, just like the total pore volume is decreased for both NaOH and KOH. It should finally be emphasised that the values of L_0 were derived only from the characteristic adsorption energy (see Equation (1)), therefore in an independent way from the pore volumes. Finding completely consistent variations of total pore volume on one hand, and of mean pore size on the other hand, supports the accuracy and the relevance of both kinds of results.

3.2.4. Carbon yield

The carbon yields of lignin activated with both hydroxides in different experimental conditions are presented in Figure 4. All the results are below 50 %; they are lower than what can be obtained with H_3PO_4 [13,25] or $ZnCl_2$ [10] activation, but only slightly below what is found for pure charring of lignin at the same temperatures [12,43], especially in the case of KOH. It can indeed be seen that, most of times and whatever the preparation conditions of the corresponding activated carbons, KOH leads to the highest carbon yields. This is a very interesting result, and also rather surprising, given that KOH was the hydroxide leading to the highest pore volumes and surface areas. This means that KOH is definitely the best activating agent, since the resulting materials are not only more microporous, but more lignin is transformed into active carbon during the process.

Examining now the effect of the individual preparation conditions, it can be observed that the carbon yield decreases with both T and R , whatever the hydroxide, in agreement with an enhanced activation when these parameters increase. However, as shown above in section 3.2.2, enhanced activation does not necessarily mean higher pore volumes, and mass ratios hydroxide / lignin higher than 3 are then more prone to destroy the incipient carbon structure than to create a narrow porosity inside.

Finding that the carbon yield is an increasing function of the flow rate of inert gas confirms the assertion suggested in section 3.1.1, according to which flushing the reactor with nitrogen removes the activating agents: either the hydroxide vapour itself, or the reaction products (H_2O and also possibly CO_2) acting as co-activating agents, or both. KOH being more volatile and more oxidising (hence producing more reaction products) than NaOH, its activating efficiency is also more sensitive to the flow of inert gas removing the vapours. The materials are thus less activated with higher flow rates of nitrogen, and the carbon yield progressively tends towards that of pure charring at high flow rates. The dehydrating and hence the cross-linking activities of KOH being higher than those of NaOH, a higher coke yield is obtained.

The effect of activation time and heating rate on the carbon yield is rather small, probably within the experimental uncertainty, and hence it is better not trying to describe them.

3.2.5. *Packing density*

The packing density is a property of the material in the powder form. For this reason, it does not only depend on the density of the particles themselves, but also on the way these particles are packed (see [44] for a full description of the packing of carbon particles). Assuming that the shape of the grains does not vary from one experiment to another, and assuming that the pouring of the powder into a given vessel is fully reproducible, are the required conditions to state that the packing density is representative of the density of the constitutive grains. It reads:

$$\textit{packing density} = \textit{particle density} \times \textit{filling factor of the vessel} \quad (3)$$

The filling factor is supposed to be constant (except for the NaOH-activated materials, whose results are not worth discussing and are not given, as explained in section 2.3), the packing density therefore gives an idea on the porosity of the active carbon grains.

The packing densities shown in Figure 5 are rather low, though values with which they could be compared are few in the literature. Only packing densities of activated carbons powders made from crops, fruit stones or nut shells may be found, but such values are strongly dependent on the amount of macroscopic voids already present in the precursor and which are retained during the pyrolysis – activation process. A list of values may be found in [44] and [45], giving values ranging from 0.3 to 0.5 g cm⁻³ for typical activated carbons, suggesting that the materials made from lignin activation are light indeed.

The density of the grains decreases with the activation temperature, in agreement with the increasing total pore volume (see Figure 2(a)). By contrast, the density increases with the mass ratio hydroxide / lignin, R , and even much faster above $R = 3$. This finding corroborates the fact that less porosity is created at high values of R , because the carbon is formed as ever-smaller grains, instead of developing inner porosity. Additionally, this agrees with what was also concluded in [33], where it was assumed that for medium-to-high impregnation ratio, the KOH does not reach the interior of the char particles, remaining on the external surface. Thus, materials obtained at low R are very lights; however, their micro- and meso-porosity is poor, and large visible bubbles, inefficient for adsorption, are present inside the grains. Higher R allows obtaining higher micro- and meso-porosity, with less and less macroscopic voids. Thus, there is no contradiction between higher activation level and higher density.

The packing density increases also with the flow rate of inert gas, but for a completely different reason, i.e., because the activation level decreases, as suggested in the previous sections. The effect of the activation time is low; maybe a swallow minimum is observed at $t = 1.5$ h, i.e., coinciding with the maxima of pore volumes, L_0 , and surface area. Finally, the density increases with the heating rate, in agreement with the previously observed decrease of the activation level.

4. Conclusions

The characteristics of porous carbons made from the activation of demineralised lignin by either KOH or NaOH were described as a function of their preparation conditions. It has been shown that similar variations shall sometimes be interpreted in different ways, and this is the reason why all the characteristics presented in this work were methodically measured. Some of them are of crucial importance for the applications of the activated carbon (surface area, pore texture, average pore size), others are useful for understanding the activation mechanisms or are of practical use (carbon yield, packing density). The effect of all the synthesis parameters on the properties of the resulting activated carbons are summarised below.

Increasing the activation temperature raises the activation level; all kinds of pores are simultaneously open and widened, with subsequent increase of the total pore volumes (induced by the development of mesopores) and decrease of both carbon yield and density. Due to the widening of the micropores and their conversion into mesopores, maxima of surface area and micropore volumes are observed, showing that an optimal activation temperature exists.

Increasing the amount of activating agent has another effect; the activation level is also increased, but the resulting pore textures are different. The total pore volume presents a maximum, above which the micropores become less and less abundant. Since the carbon yield decreases while the density raises, this means that the lignin is still converted into carbon, but into a less and less porous one at high hydroxide / lignin ratios. Again, an optimum ratio exists.

The flow rate of inert gas has a lower effect, as compared with the 2 preceding parameters. The competition between the removal of useless reaction products and that of potential activating agents in the vapour phase again leads to the observation of an optimum. High flow rates decrease the efficiency of the activation, giving less micropores and a lower surface area, while a denser carbon is obtained in higher proportion (higher carbon yield and density).

Activation time and heating rates are the parameters to which the final properties are the less sensitive. Hence, only little improvement of the carbon characteristics can be achieved through their variation. Increasing these parameters may lead to higher or lower micropore volumes, depending on the hydroxide and the other preparation conditions.

The last essential conclusion is that, whatever the way the activated carbons were prepared from lignin, KOH is undoubtedly the best activating hydroxide for obtaining highly microporous adsorbents. This result is different from what can be found for the activation of carbon materials like anthracites, for which NaOH is more efficient, whatever the experimental conditions. The present work also stressed the fact that the weight ratio: activating agent / precursor is of highest importance, so poor adsorption properties may be obtained if this parameter is not optimised through a systematic investigation.

References

- [1] A. Pizzi, A. Stephanou, *Holzforschung*, 47 (1993) 439.
- [2] A. Pizzi, A. Stephanou, *Holzforschung*, 47 (1993) 501.
- [3] P. Truter, A. Pizzi, H.V. Ermaas, *J. Appl. Polymer Sci.*, 51 (1994) 1319.
- [4] N. El Mansouri, A. Pizzi, J. Salvado, *Holz. Roh. Werkstoff*, (2006) in press.
- [5] N. El Mansouri, A. Pizzi, J. Salvado, *J. Appl. Polymer Sci.*, (2006) in press.
- [6] D. Feldman, in: T.Q. Hu (Ed.), *Modification, Properties and Usage of Lignin*, Kluwer Academic, New York, 2002, p. 81.
- [7] J. Rodríguez-Mirasol, T. Cordero, J.J. Rodríguez, *Carbon*, 31 (1993) 87.
- [8] J. Rodríguez-Mirasol, T. Cordero, J.J. Rodríguez, *Carbon*, 31 (1993) 53.
- [9] J. Rodríguez-Mirasol, T. Cordero, J.J. Rodríguez, *Carbon*, 34 (1996) 43.
- [10] E. Gonzalez-Serrano, T. Cordero, J. Rodríguez-Mirasol, J.J. Rodríguez, *Ind. Eng. Chem. Res.*, 36 (1997) 4832.
- [11] J. Hayashi, A. Kazehaya, K. Muroyama, A.P. Watkinson, *Carbon*, 38 (2000) 1873.
- [12] R.K. Sharma, J.B. Wooten, V.L. Baliga, X. Lin, W.G. Chan, M.R. Hajaligol, *Fuel*, 83 (2004) 1469.
- [13] V. Fierro, V. Torné-Fernández, A. Celzard, *Micropor. Mesopor. Mater.*, 92 (2006) 243.
- [14] V. Fierro, V. Torné-Fernández, A. Celzard, *Stud. Surf. Sci. Catal.* 160 (2005) 607.
- [15] T.Q. Hu (Ed.), *Modification, Properties and Usage of Lignin*, Kluwer Academic, New York, 2002.
- [16] D.M. Mackay, P.V. Roberts, *Carbon*, 20 (1982) 87.

- [17] L. Khezami, A. Chetouani, B. Taouk, R. Capart, *Powder Technol.*, 157 (2005) 48.
- [18] R.C. Sun, J. Tomkinson, J. Bolton, *Polym. Degrad. Stab.*, 63 (1999) 195.
- [19] C. Pouteau, B. Cathala, P. Dole, B. Kurek, B. Monties, *Ind. Crops. Prod.*, 21 (2005) 101.
- [20] V. Fierro, V. Torné-Fernández, A. Celzard, D. Montané, J. *Hazardous Mater.*, submitted.
- [21] M. Olivares-Marín, C. Fernández-González, A. Macías-García, V. Gómez-Serrano, *Appl. Surf. Sci.*, 252 (2006) 5980.
- [22] R. Ubago-Pérez, F. Carrasco-Marín, D. Fairén-Jiménez, C. Moreno-Catilla, *Micropor. Mesopor. Mater.*, 92 (2006) 64.
- [23] F.C. Wu, R.L. Tseng, *J. Coll. Interf. Sci.*, 294 (2006) 21.
- [24] J. Hayashi, K. Muroyama, V.G. Gomes, A.P. Watkinson, *Carbon*, 40 (2002) 617.
- [25] Y. Guo, D.A. Rockstraw, *Carbon*, 44 (2006) 1464.
- [26] A. Perrin, A. Celzard, A. Albiniak, J. Kaczmarczyk, J.F. Marêché, G. Furdin, *Carbon*, 42 (2004) 2855.
- [27] A. Perrin, A. Celzard, A. Albiniak, M. Jasienko-Halat, J.F. Marêché, G. Furdin, *Micropor. Mesopor. Mater.*, 81 (2005) 31.
- [28] S. Brunauer, P.H. Emmett, E. Teller, *J. Am. Chem. Soc.*, 60 (1938) 309.
- [29] K.S.W. Sing, *Carbon*, 27 (1989) 5.
- [30] M. Kruk, Z.J. Li, M. Jaroniec, W.R. Betz, *Langmuir*, 15 (1999) 1435.
- [31] J.W. Patrick (Ed.), *Porosity in Carbons*, Wiley, 1995.
- [32] F. Stoeckli, A. Slasli, D. Hugi-Cleary, A. Guillot, *Micropor. Mesopor. Mater.*, 51 (2002) 197.
- [33] M. Molina-Sabio, F. Rodríguez-Reinoso, *Coll. Surf. A: Physicochem. Eng. Aspects*, 241 (2004) 15.

- [34] C.H. Hoyt, D.W. Goheen, in: K.V Sarkanen, C.H. Ludwig (Eds.), *Lignins*, Wiley-Interscience, New York, 1971, p. 833.
- [35] M.A. Lillo-Ródenas, D. Lozano-Castelló, D. Cazorla-Amorós, A. Linares-Solano, *Carbon*, 39 (2001) 751.
- [36] A. Celzard, V. Fierro, *Energy & Fuels*, 19 (2005) 573.
- [37] M.A. Lillo-Ródenas, D. Cazorla-Amorós, A. Linares-Solano, *Carbon*, 41 (2003) 267.
- [38] D. Lozano-Castelló, M.A. Lillo-Ródenas, D. Cazorla-Amorós, A. Linares-Solano, *Carbon*, 39 (2001) 741.
- [39] M.A. Lillo-Ródenas, J. Juan-Juan, D. Cazorla-Amorós, A. Linares-Solano, *Carbon*, 42 (2004) 1371.
- [40] A. Celzard, J.F. Maréché, F. Payot, D. Bégin, G. Furdin, *Carbon*, 38 (2000) 1207.
- [41] M.S. Solum, R.J. Pugmire, M. Jagtoyen, F. Derbyshire, *Carbon*, 33 (1995) 1247.
- [42] D. Lozano-Castelló, D. Cazorla-Amorós, A. Linares-Solano, D.F. Quinn, *Carbon*, 40 (2002) 989.
- [43] J. Li, B. Li, X. Zhang, *Polym. Degrad. Stab.*, 78 (2002) 279.
- [44] A. Celzard, J.F. Maréché, F. Payot, G. Furdin, *Carbon*, 40 (2002) 2801.
- [45] A. Ahmadpour, D.D. Do, *Carbon*, 35 (1997) 1723.

Table 1. Proximate and ultimate analyses of KL and KL_d (wt. %)

	Proximate Analysis			Ultimate Analysis				
	(wt %, dry basis)			(wt %, daf)				
	Fixed Carbon	Volatile matter	Ash	C	H	N	S	O*
KL	36.4	52.5	11.1	59.5	5.1	0.1	2.2	33.3
KL _d	39.7	60.1	0.2	65.8	5.9	0.0	0.5	27.8

* Estimated by difference

Figure captions

Figure 1: Dependence of the BET surface area of the activated carbons on their synthesis parameters. Empty symbols = NaOH; full symbols = KOH. Curves are just guides for the eye.

Figure 2: Dependence of the pore volumes of (a) the KOH-activated carbons (full symbols) and (b) the NaOH-activated ones (empty symbols), on their synthesis parameters. Triangles = V_{DR} ; Circles = $V_{0,99}$; Squares = V_{micro} ; Diamonds = V_{meso} . Curves are just guides for the eye.

Figure 3: Dependence of the mean pore size of the activated carbons on their synthesis parameters. Empty symbols = NaOH; full symbols = KOH. Curves are just guides for the eye.

Figure 4: Dependence of the carbon yield on the activation parameters. Empty symbols = NaOH-activated carbons; full symbols = KOH-activated carbons. Curves are just guides for the eye.

Figure 5: Dependence of the packing density of the KOH-activated carbons on their synthesis parameters. Curves are just guides for the eye.

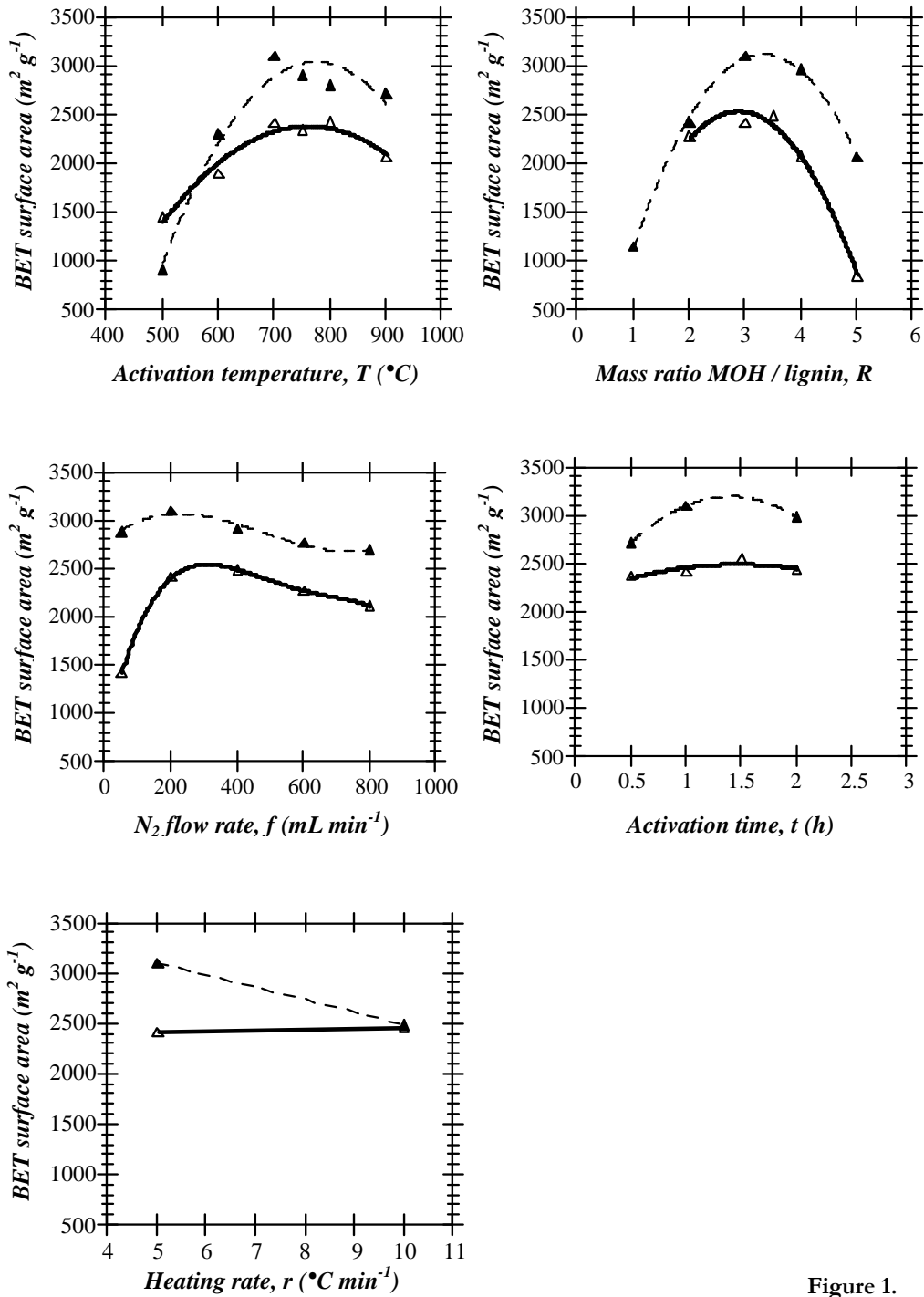


Figure 1.

V. Fierro et al.

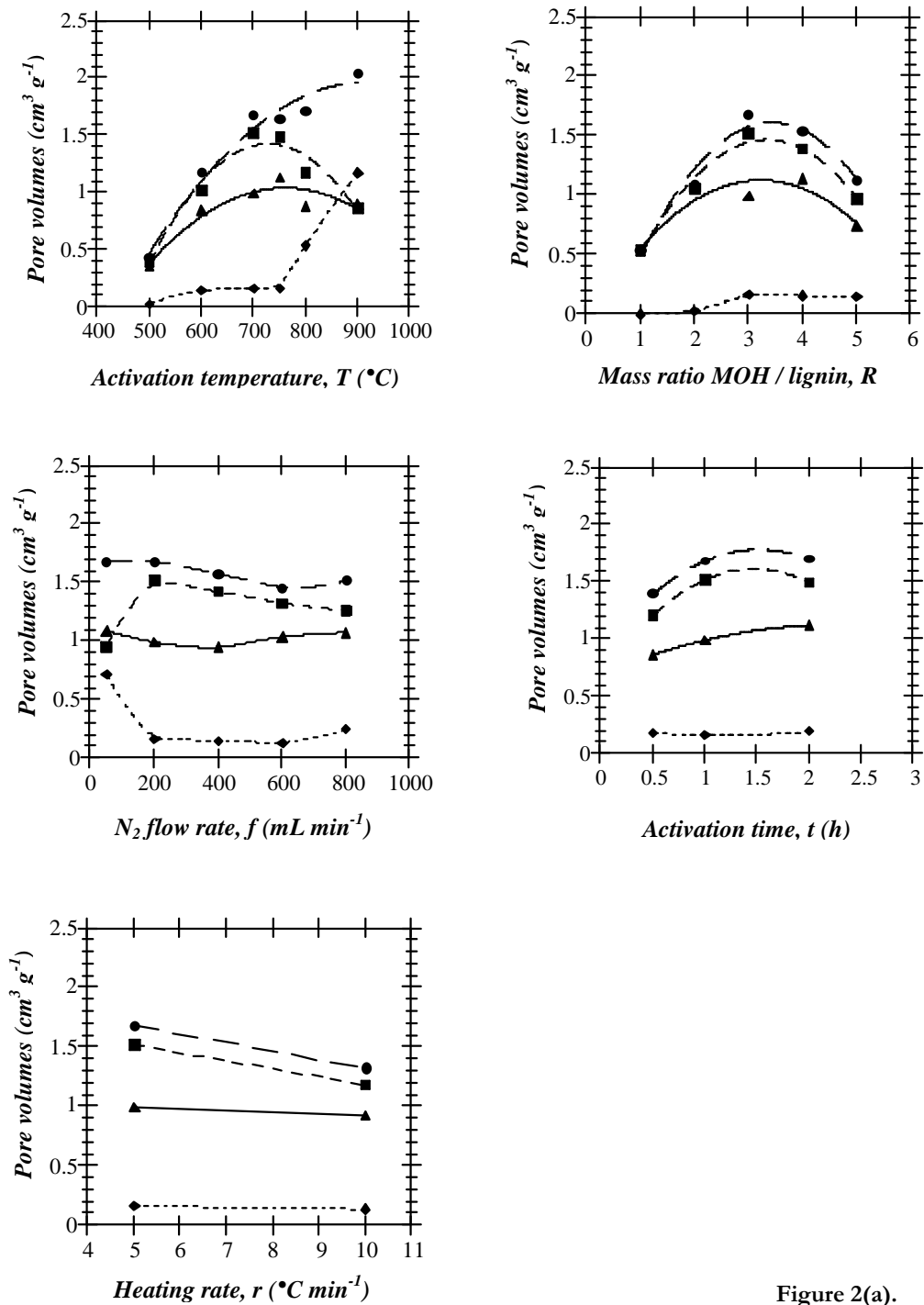


Figure 2(a).

V. Fierro et al.

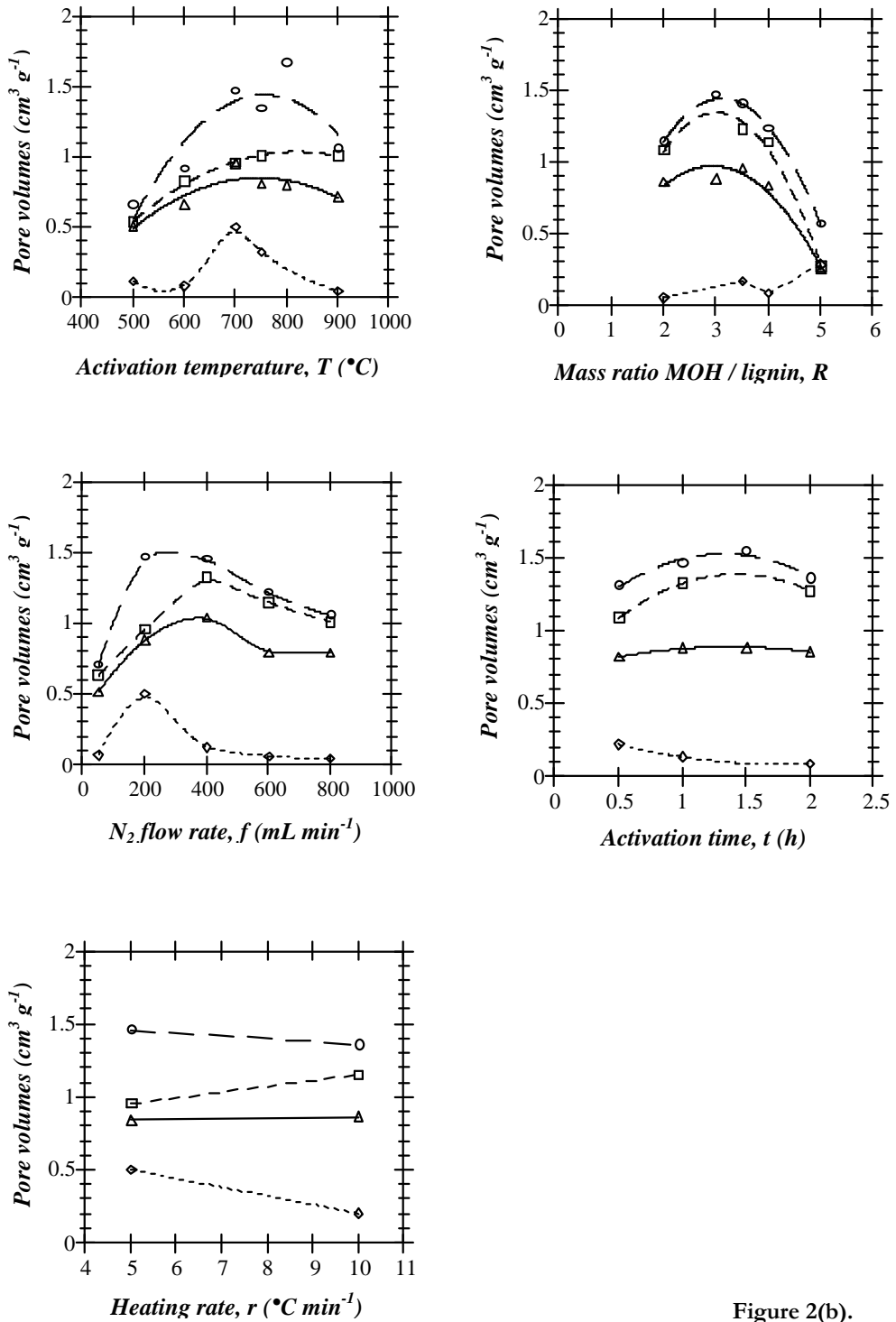


Figure 2(b).

V. Fierro et al.

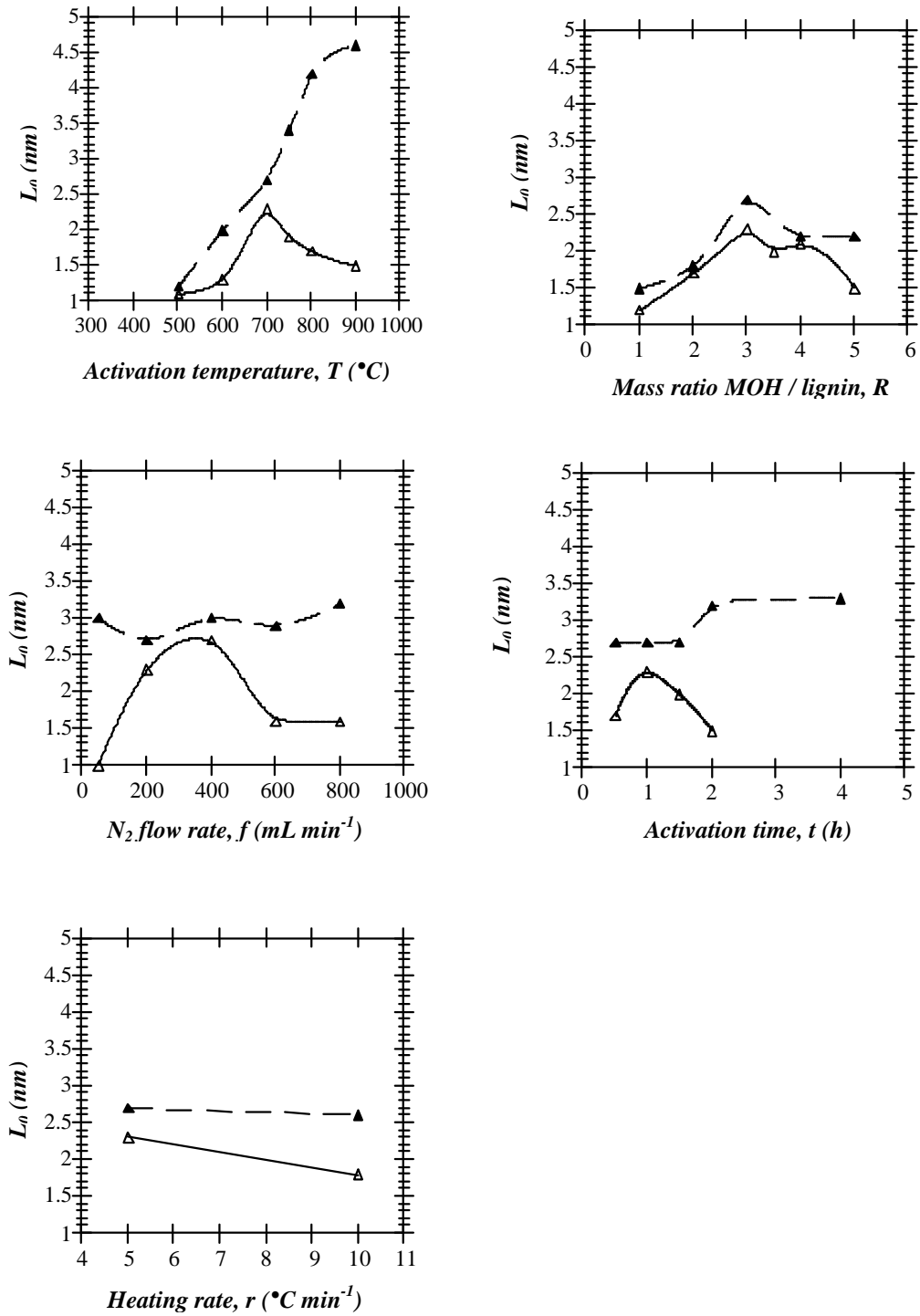


Figure 3.

V. Fierro et al.

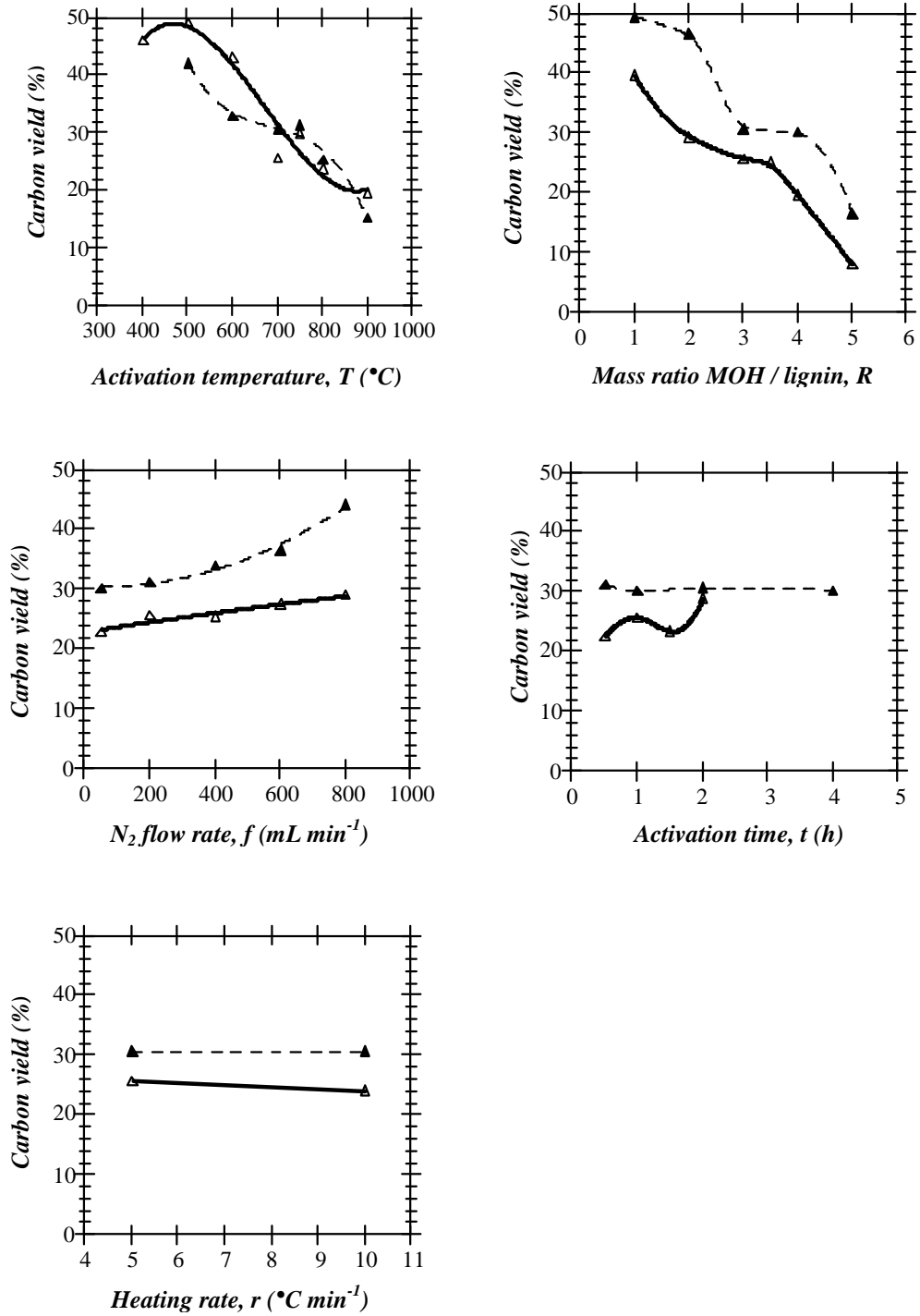


Figure 4.
V. Fierro et al.

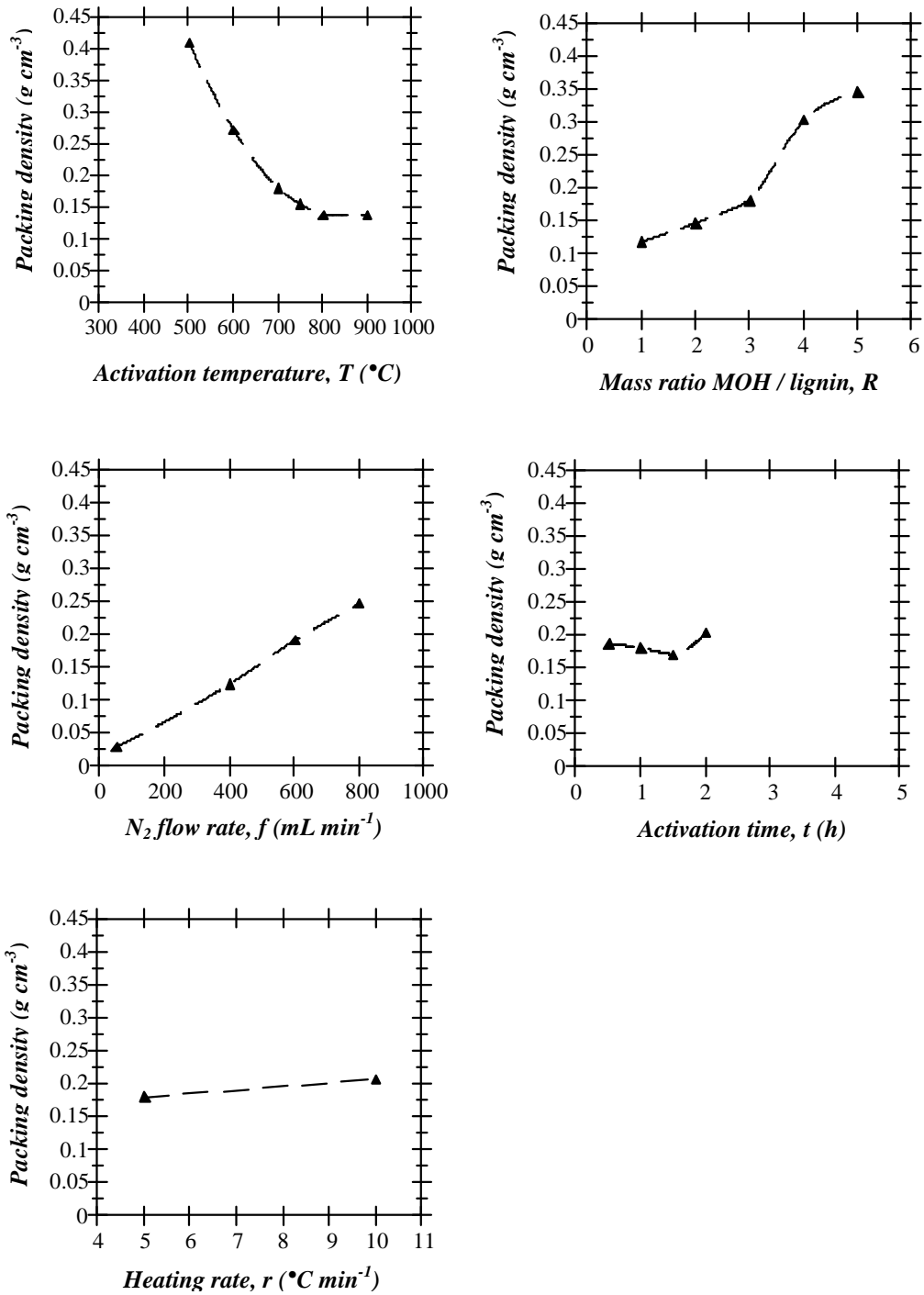


Figure 5.
V. Fierro et al.

5.2. Aplicaciones de carbones activados

Tal y como se ha mostrado, es posible obtener CA esencialmente microporosos a partir de gñina Kraft. Así pues, básicamente su aplicación se restringe a la eliminación de contaminantes en efluentes líquidos. Sin embargo, a continuación también se muestran la participación en trabajos específicos en el campo de los reactores de membrana y en la purificación de xylo-oligosacáridos.

5.2.1. Removal of Cu (II) from Aqueous Solutions by Adsorption on Activated Carbons Prepared from Kraft Lignin

Este artículo se presentó en forma de póster en el congreso internacional Carbon 2003 (consultar Anexo C).

Otros trabajos relacionados se presentan en los anexos A y D donde se presentan dos pósters: “Use of Kraft lignin for Cu (II) removal in industrial water” y “Uptake of Cu (II) and Zn from aqueous solution by Kraft lignin” publicados en los congresos 9th Mediterranean congress y 4th European Congress in Chemical Engineering, respectivamente.

Removal of Cu (II) from Aqueous Solutions by Adsorption on Activated Carbons Prepared from Kraft Lignin

V. Fierro*, V. Torne, D. Montané and R. Garcia-Valls

Departament d'Enginyeria Química, ETSEQ, Universitat Rovira i Virgili, Avinguda dels Països Catalans 26, Campus Sescelades, Tarragona 43007, Spain

Abstract

Activated carbons were prepared by phosphoric acid activation of Kraft lignin varying carbonization temperature (400-650°C) and the weight ratio of phosphoric acid to lignin (P/L=0.7-1.75). As a result of the different pyrolysis conditions, activated carbons with various pore size distribution, surface area and surface acidic groups were obtained. The results showed the significant importance of carbonization temperature on the adsorption capacity for removal of copper. A maximum in the copper adsorption was found for carbons prepared at a carbonization temperature between 450 and 550°C. Increasing temperature acidic groups were degraded but increasing mesoporosity and surface area favored diffusion and adsorption. Increasing P/L ratio did not influence significantly on adsorption capacity of the activated carbons once lignin had completely reacted with phosphoric acid. P/L ratios higher than 1.2 did not modify the pore size distribution but it reduced the total volume of pores.

Keywords: activated carbon, phosphoric activation, porosity, surface properties, metal removal

* vfierro@etscq.urv.es

Tel: +34 977 55 85 46
Fax: +34 977 55 85 44

1. INTRODUCTION

The term lignin refers to a group of phenolic polymers that confer strength and rigidity to the woody cell wall of plants. Lignin is separated from wood during pulp and paper making operations, where it serves primarily as in-house fuel required for the recovery of chemicals. The separation of Kraft lignin could be an alternative to incineration since lignin is a bountiful and renewable resource and represents an attractive field for future industrial chemistry. One of the potential uses is the production of activated carbon.

Lignin can be used as precursor for activated carbon as it has been reported on physical activation of eucalyptus Kraft lignin by CO₂ partial gasification¹ and on chemical activation of this precursor by using zinc chloride². However, the use of ZnCl₂ has declined due to the environmental problems³ and phosphoric acid is preferred as activating-dehydrating agent.

Activated carbons are high porosity, high surface area materials used in industry for environmental remediation, purification and chemical recovery operations. While most activated carbons are used for adsorption of organic compounds, previous studies have shown that many activated carbons can uptake metal ions from solutions.

This work was undertaken to study the feasibility of the utilization of activated carbon produced from Kraft lignin by chemical activation with phosphoric acid for the removal of heavy metal cations from water solutions. For this study, we chose copper as monitor of metal uptake, since copper is a ubiquitous metal in plating and jewelry manufacturing wastewaters. The influence of carbonization temperature and phosphoric acid to lignin weight ratio on Cu adsorption are analyzed.

2. EXPERIMENTAL

2.1 Materials

Kraft lignin was provided by Lignotech Iberica S.A. Table 1 shows the ultimate and elemental analyses of lignin. Elemental analysis was carried out in a EA1108 Carlo Erba Elemental Analyzer. The proximate analysis was carried out following ISO standards following the weight losses at 100°C/air (moisture), 900°C/non-oxidizing atmosphere (volatile matter) and 815°C/air (ash).

A 85% H₃PO₄ solution (Panreac, Spain) was used as activating agent.

2.2 Preparation and characterization of the activated carbons

Lignin was mixed with varying amounts of H₃PO₄ in the range of 0.7 to 1.75 phosphoric acid to lignin weight ratio (P/L) in wet basis. The slurry was left for 1h at room temperature and under air atmosphere, then transferred to a furnace DUM Model 10CAF where carbonization was carried out under air atmosphere. The oven was heated at 10°C min⁻¹, up to 150°C where temperature was hold to allow free evolution of water. Afterwards the oven was heated at 10°C min⁻¹ to the final carbonization temperature (from 400 to 650°C) it was hold for 2h. In order to remove the excess of H₃PO₄ after carbonization, the cooled mass was extensively washed with distilled water until a neutral pH was attained (a CyberScan PC 510 pH-meter with a Hamilton-electrode 'Flushtrode', special for deionized water, was used). Then, the samples were dried in an oven at 110°C overnight.

Surface area and pore size characterization were performed using a Micromeritics ASAP2000 gas adsorption surface area analyzer. The specific

surface area of the samples was determined from the nitrogen isotherms at -196°C and by using the BET equation. Micropore volume was determined using t-plot, mesopore volume using the BJH equation and total volume of pores was calculated at a relative pressure (p/p^0) of 0.99.

2.4 *Cation-exchange capacity (CEC)*

A weighed amount of adsorbent was placed into an Erlenmeyer flask. A volume of 50ml of 0.1M NaOH was added. To attain equilibrium the flasks were shaken for 24h. After equilibration the NaOH concentration was measured by titration with HCl. The quantity of NaOH consumed was converted to CEC and expressed in meq g⁻¹.

2.5 *Copper uptake from aqueous solutions*

Experiments were done in batches with 18 Erlenmeyer flasks containing 150 mg of activated carbon and 150 ml of deionized water. Varying amounts of Cu(II) chloride (p.a. quality from Aldrich) were added to each flask. The initial pH of the solution was adjusted at pH=5 by adding 0.1N NaOH solution. The flasks were sealed to avoid evaporation and stirred for 24h at 25°C. The resulting Cu(II) concentration was analyzed by atomic absorption spectrophotometry (AAS) with a Perkin Elmer 3110 model. The amounts of adsorbed copper were obtained by calculating the difference of each concentration before and after adsorption. Several activated carbons prepared at different carbonization temperature and acid phosphoric to lignin ratio (P/L) were tested.

3. RESULTS AND DISCUSSION

3.1 Surface area and porosity

Table 2 shows BET surface area and pore volume distribution of the activated carbons prepared from Kraft lignin by phosphoric acid impregnation at different temperatures and P/L ratios.

The surface areas increased between the temperature of 400 and 600°C and the maximum surfaces of more than 1200 m²g⁻¹ was observed at 600°C. At temperatures higher than 600°C, the surface areas were considerably reduced. The isotherms approached type I (Langmuir), indicating an essentially microporous character with some contribution of wider pores (meso- and macropores) depending on the carbonization temperature. At 400°C, the activated carbon showed the highest value of microposity. Increasing the carbonization temperature produced the development of porosity in the mesoporous region. The activated carbons prepared at 550°C exhibited a high contribution of the mesoporous region with a considerably reduced microposity. At these temperatures there is a reduction in the total volume of pores due to shrinkage of the material.

The highest BET surface area was attained at P/L=1.2 and further increases in the P/L ratio produced a decrease in the BET surface area. The highest micropore to total volume ratio was found for the carbon prepared with the lowest P/L ratio. As P/L ratio increased up to P/L=1.2, the micropore volume also increased but in a lower extent than the mesoporous volume. Higher values of the P/L ratio reduced the total pore volume and affected to the micro and mesopore volume in a similar extent. Moreover, the relative importance of the volume of macropores increases with the P/L ratio. The

use of a P/L ratio of 1.2 yields a carbon with the highest surface area at 450°C ($S_{\text{BET}}=1036 \text{ m}^2\text{g}^{-1}$) and total pore volume ($V_p = 0.6 \text{ cm}^3\text{g}^{-1}$).

Detailed discussion of these results and on the effect of phosphoric acid on surface area and pore size distribution is given elsewhere⁴.

3.2 *Cation-exchange capacity*

The acidic groups covering the carbon surface are usually quantified by using the Boehm's method⁵. NaHCO_3 can detect only strong acids as the carboxylic group. Na_2CO_3 can detect the carboxylic groups, lactones and lactoles. NaOH , in addition of the aforementioned groups, is capable of detecting phenols.

Benadi et al.⁶ analyzed phosphoric acid activated carbons produced from wood precursors using potentiometric titration and identified peaks corresponding to phosphonic acids ($-\text{PO}_3\text{H}_2$; pK_a 7-9), phosphonous acids ($-\text{PO}_2\text{H}_2$; pK_a 3-4.5), and phosphines ($-\text{PR}_3$; pK_a 3-6.5, 8-9).

In this work, we used modified method based on Bohem's method to measure the cation-exchange capacity (CEC) of the carbons⁷. Using NaOH , the total amount of acidic groups is quantified: carboxylic groups, lactones, lactoles, phenol and phosphorous-containing acids.

Figure 1 shows that CEC decreases with carbonization temperature. The decrease in the functional groups determined by NaOH titration is possibly due to degradation of phosphorous compounds. As temperature increases phosphate and polyphosphate bridges acting as crosslinking parts of the carbon structure decompose^{8,9} and it also could affect to surface phosphorous compounds that are degraded. Dastgheib and Rockstraw¹⁰ working on pecan shell activated carbons found a linear decrease in the

functional groups detected by NaOH. These authors quantified functional groups by Boehm's method and concluded that temperature mainly affected to phenolic and/or phosphonic groups.

Figure 2 shows CEC for carbons prepared at different P/L ratio between 0.7 and 1.75. CEC increases with P/L ratio but the value remains proximately from P/L=1.0. As H₃PO₄ reacts with the hydroxyl groups of lignin it would exist a maximum in the P/L ratio and so a maximum in the phosphorous-containing acids attached to the surface. In a previous work¹¹ carried out in a thermogravimetric device, we have shown that phosphoric acid is in excess at P/L ratios higher than 1.0.

3.3 Copper adsorption isotherms

Langmuir isotherm was applied for adsorption equilibrium.

$$C_e/q_e = 1/(Q_0 b) + C_e/Q_0$$

where C_e is the equilibrium concentration (mg l⁻¹), q_e is the amount absorbed at equilibrium (mg g⁻¹), Q_0 and b are the Langmuir constants related to adsorption capacity and energy of adsorption. The linear plot of C_e/q_e versus C_e showed that the adsorption obeyed the Langmuir model. Here we study the variation of Q_0 with carbonization temperature and P/L ratio taking into account CEC, surface area and pore size distribution of the activated carbons.

Figure 3 shows the variation of the Cu adsorption capacity with the carbonization temperature. Comparing this plotting with the data showed in Figure 1 it can be clearly seen that the adsorption capacity of the activated carbons can not be directly correlated with the CEC. Although the lower the

temperature of preparation the higher the determined CEC, it must be taken into account the surface area and the pore size distribution.

Figure 3 also shows the evolution of BET surface area with temperature. The highest CEC was determined at 400°C but also the surface area was low and most of the pore size distribution (75%) are micropores (with diameters less than 2nm). Considering the diameter of copper ion in aqueous solutions as 1.2 nm¹², a portion of micropores is not accessible to the hydrated copper ion. On the one hand, as temperature of carbonization increased up to 600°C the surface area and the ratio of meso- and macropore volumes to total volume ratio also increased. On the other hand, CEC decreased with temperature as seen above. These two factors could explain the existence of a maximum in Cu adsorption for activated carbons prepared at temperatures between 450 and 550°C. At temperatures higher than 600°C, the shrinkage of the structure together with the decreasing tendency of CEC with temperature would explain the Cu adsorption observed.

Figure 4 shows the evolution of the Cu adsorption capacity and the BET surface area with the P/L ratio. Cu adsorption increased with P/L ratio according with the higher CEC determined. However, the differences observed in Cu adsorption at low P/L ratios can not only be explained by the moderate variation of CEC for P/L values between 0.7 and 1.75. There was also a strong variation of the surface area and pore size distribution with the P/L ratio. At P/L=0.7, the activated carbon had a surface area of 603 m²g⁻¹ and 75% of the total pore volume corresponded to microporosity, therefore diffusional limitations could be expected. Increasing the P/L ratio microporosity decreased and remained proximately constant at 66% of the total pore volume even at the highest P/L=1.75 where surface decreased considerably. We think that the high CEC together with the no existence of diffusional limitations in carbons at P/L=1.75 could be the reason of the

slight decrease in copper adsorption even if the surface area decreased greatly from $959 \text{ m}^2\text{g}^{-1}$ at $P/L=1.4$ to $704 \text{ m}^2\text{g}^{-1}$ at $P/L=1.75$.

4. CONCLUSIONS

This study showed that activated carbons produced from Kraft lignin can be tailored to have a high surface concentration of acidic groups and a pore size distribution favorable for adsorption of metallic ions from solutions.

Carbonization temperature strongly affects to metal adsorption by changing porosity distribution and degrading phosphorous-acidic groups. The P/L ratio does not influence the amount of copper adsorbed if the added phosphoric acid is enough to allow the complete reaction of lignin.

Thus, pyrolysis of lignin with phosphoric at temperatures about 500°C and P/L ratio of 1.0 produces activated carbons with a favorable pore size distribution and enough surface acidic groups for removal of copper ions.

ACKNOWLEDGEMENTS

V. Fierro acknowledges the “Ministerio de Ciencia y Tecnología” and the “Universitat Rovira i Virgili” for the financial support of her “Ramón y Cajal” contract. V. Torné acknowledges the “Universitat Rovira i Virgili” for her PhD grant.

REFERENCES

- [1] J. Rodríguez-Mirasol, T. Cordero, J.J. Rodríguez Carbon 31 (1993) 87-95.
- [2] E. Gonzalez Serrano et al. Ind Eng. Chem. Res., 36 (1997) 4832-4838.
- [3] H. Teng, T.S. Yeh, L.Y. Hsu, Carbon 36 (1998) 1387-1395
- [4] V. Fierro, V. Torné, D. Montané, J. Salvadó in proceedings of Carbon'03. Oviedo (Spain) 2003.
- [5] H.P. Boehm Advances in catalysis, New York: Academic Press, 1966, 179-274.
- [6] H. Benadi, T.J. Bandosz, J.Jagiello, J.A. Schwarz, J.N. Rouzaud, D. Legras, F. Beguin Carbon 38 (2000) 669-674.
- [7] F. Suárez-García, A. Martínez-Alonso, J. M. D. Tascón J. Anal. Appl. Pyrolysis 63 (2002) 283-301.
- [8] M. Jagtoyen, F. Derbyshire, Carbon 31(1993) 1185-1192.
- [9] M. Molina-Sabio, F. Rodríguez-Reinoso, F. Caturla, M. J. Sellés Carbon, 33 (1995) 1105-1113.
- [10] S. A. Dastgheib, D. A. Rockstraw, Carbon 39 (2001) 1849-1855.
- [11] V. Fierro, D. Montané submitted for publication
- [12] J. Laine, A. Calafat, M. Labady Carbon 27 (1987) 191-195.

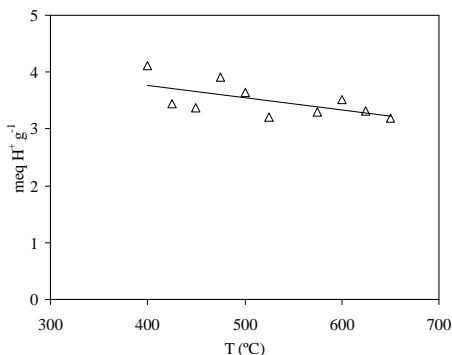


Fig. 1. Variation of the CEC of the activated carbons with the carbonization temperature. (P/L=1.4)

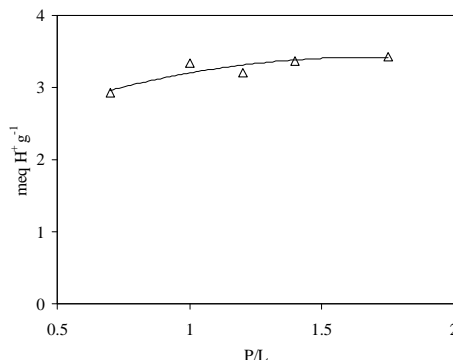


Fig. 2. Variation of the CEC of the activated carbons with the P/L ratio. (T=450°C)

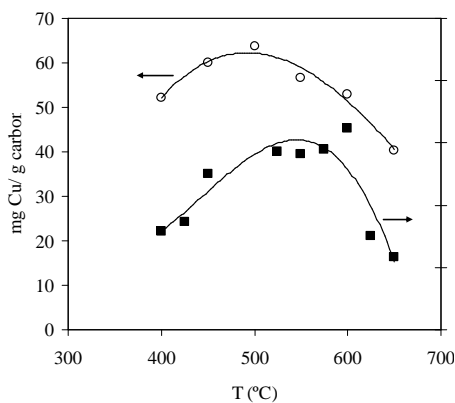


Fig. 3. Variation of the Cu adsorbed and of the BET surface area with the carbonization temperature. (P/L=1.4)

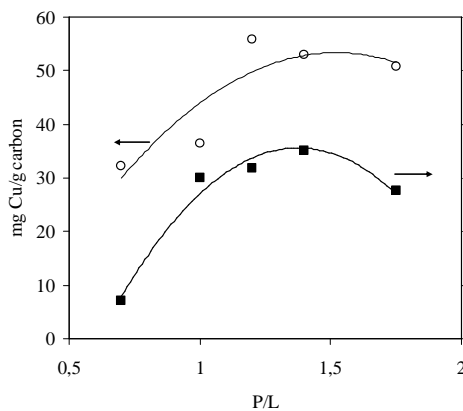


Fig. 4. Variation of the Cu adsorbed and of the BET surface area with the P/L ratio. (T=450°C)

Table 1 Lignin Analyses (wt.%)

	Proximate (wt.%, humid basis)		Elemental (wt.%, ash and moisture free)
Moisture	14.45	Carbon	59.46
Ash	9.50	Hydrogen	5.07
Volatile matter	44.93	Nitrogen	0.05
Fixed carbon ^a	31.12	Sulfur	2.15
		Oxygen ^a	33.27

^a Estimated by difference

Table 2 Surface area and porosity of the activated carbons

T (°C)	P/L	S _{BET} (m ² /g)	V _{total} (cm ³ /g)	V _{micro} (cm ³ /g)	V _{meso} (cm ³ /g)	V _{macro} (cm ³ /g)
400	1.4	917	0.48	0.34	0.11	0.03
425	1.4	944	0.50	0.27	0.18	0.05
450	1.4	1101	0.54	0.33	0.01	0.20
525	1.4	1173	0.60	0.29	0.08	0.22
550	1.4	1163	0.58	0.31	0.14	0.13
575	1.4	1178	0.59	0.30	0.05	0.25
600	1.4	1245	0.67	0.24	0.10	0.33
625	1.4	901	0.51	0.15	0.08	0.28
650	1.4	834	0.46	0.10	0.09	0.27
450	0.7	541	0.30	0.20	0.02	0.09
450	1.0	998	0.50	0.30	0.10	0.10
450	1.2	1036	0.51	0.31	0.10	0.10
450	1.8	950	0.46	0.28	0.07	0.12

5.2.2. Optimization of the synthesis of highly microporous carbons by chemical activation of Kraft lignin with NaOH

Este artículo ha sido enviado al Chemical Engineering Journal durante el año 2006.

OPTIMIZATION OF THE SYNTHESIS OF HIGHLY MICROPOROUS CARBONS BY CHEMICAL ACTIVATION OF KRAFT LIGNIN WITH NAOH

V. Torné-Fernández^{1*}, J.M. Mateo¹, D. Montané¹, V. Fierro^{1,2}

¹Departament d'Enginyeria Química, Universitat Rovira i Virgili, Campus
Sescelades, Av. dels Països Catalans 26, 43007 Tarragona, Spain.

²Laboratoire de Chimie du Solide Minéral. Université Henri Poincaré –Nancy I.
UMR CNRS 7555, BP 239, F 54506 Vandoeuvre-lés-Nancy, France.

*Corresponding author: vanessa.torne@urv.cat. FAX: +00 34 977 559667

Abstract

Highly microporous carbon materials with high apparent surface areas (up to 2400 m²/g) were obtained by heat treatment of mixtures of demineralised kraft lignin (KL_d) and NaOH. Application of a statistical tool, the response surface methodology, was used to determine the optimum operation conditions for preparing activated carbons able to adsorb phenol. For that purpose, three parameters were varied: temperature of activation, NaOH/KL_d percent mass ratio and nitrogen flow rate. This carbon was tested for the adsorption of methylene blue, obtaining adsorptions of 93.9 g/100 g AC. It has a high microporosity (0.997 cm³/g that corresponds with more than 74% of the total porosity) and specific surface area of 2400 m²/g. This best activated carbon was prepared at 783°C, 26.4% of Kraft lignin and 200 cm³ N₂/min.

Key words: activated carbon, methylene blue, phenol, adsorption capacity, response surface methodology.

1. INTRODUCTION

Lignin is an abundant bio-polymer that is obtained in large quantities during chemical pulping of wood and annual plants for the production of cellulose pulps. Several kinds of technical lignins are identified depending on the pulping process, such as Kraft lignin, lingsulfonates, and organosolv lignin, the first being the most extended. The established use of lignin in the Kraft process is as in-house fuel to supply energy to the process, which also allows the simultaneous regeneration of the pulping chemicals. However, the enormous amount of lignin that is processed through the Kraft pulping-plants yearly has prompted interest on finding higher value applications for this material. Some uses that have been explored are as binder for animal fodder, to prepare lubricants for oil well drilling, in soil stabilization, as substitute for phenol in adhesives, and as precursor for the manufacture of activated carbon. The latter is currently a favored application, since the demand of carbonaceous adsorbents is growing worldwide driven by stricter environmental regulations, which force improvement in separation techniques and intensive processing of waste streams to reduce the emissions of gas and liquid contaminants. Activated carbons and carbon molecular sieves are used in several industrial processes such as gas separation, gas storage, purification or catalyzed reactions [1-3]. The properties of the carbonaceous adsorbent depend on the pore volume distribution, the kind of pores present, and on the surface chemistry. All those factors are direct consequence of the nature of the precursor material and, most important, on the activation agent and reaction conditions [4-9].

In recent studies on the chemical activation of Kraft lignin with H_3PO_4 [10, 11], we obtained microporous activated carbons with surface areas as high as

1300 m²/g, although higher specific surfaces may be obtained with other activating agents. There is a growing interest in alkaline hydroxide activation process, and KOH has been found to be one of the most effective compounds for that purpose [9, 12-15]. High surface areas and pore volumes are reported for lignocellulosic materials, carbons and chars activated by KOH with surface areas up to 3000 m²/g [16]. Exploratory studies evidenced the possibility of preparing highly microporous carbons from Kraft lignin using NaOH and KOH as activating agent in suitable experimental conditions [16].

There are several parameters that influence the activation process [4-9]. Make a complete study of each one to observe its effect entails a large number of experiments. Conventional and classical methods of studying a process by maintaining other factors involved at an unspecified constant level does not depict the combined effect of all the factors involved. Thus, a parameter alone has not a significant effect but it can affect to others parameters. To study all this interactions and the effect of each parameter separately a statistical tool can be used, the response surface methodology [17-25]. In this case, this method also requires time, depending on the number of parameters studied, but this optimization tool studies the effect of the parameters in a collectively way reducing the number of experiments.

The aim of the present work was to develop a systematic study to optimize the manufacture of carbons activated from Kraft lignin by activation with NaOH. A statistical study based on the surface-response method [17-25] has been developed using the adsorption of methylene blue as dependent variable, since it serves as a model compound for the most usual organic

pollutants [16, 25-39]. We have used the methylene blue adsorption capacity as response variable to choose the best AC.

Methylene blue can serve as a model for the adsorption of organic pollutants [25], as several works has demonstrated [16, 26-39]. These compounds destroy the ozone stratospheric layer, are the precursors of photochemical oxidants, produce acid rain, affect to the nervous system and are carcinogenic and mutagenic agents [40]. For this reason, a big number of studies about the elimination of these compounds have been published [40-42] using different methods for treating them.

2. EXPERIMENTAL

2.1. Materials

KL was supplied by Lignotech Ibérica S.A. (Spain), and was presented in the form of a fine dark brown powder. Ash content of the lignin was 9.5% on reception, and lignin was demineralised prior to the preparation of the carbons. To remove the inorganic matter from KL, batches of 100 g were introduced in 2 l of water leading to dark brown suspensions of pH 9.5, and lignin was then precipitated by adding H₂SO₄ until the pH decreased to 1. The precipitate was gently washed with distilled water until constant pH and it was dried overnight at 105 °C. The lignin prepared this way was nearly mineral-free and was labelled demineralised Kraft lignin (KL_d).

Extra pure methylene blue chloride (MB) powder was supplied by Scharlau. It was diluted in distilled water to obtain a solution of 3.2 mM of

concentration. Sodium hydroxide (NaOH) of 99% purity was purchased in the form of lentils from Scharlau.

2.2. Preparation of carbons

Sodium hydroxides lentils were ground and physically mixed with KL_d at KL_d to total mix mass ratios between 18% and 32%. The carbonisation was carried out in a horizontal tubular furnace, where the samples were heated in a crucible at $5^\circ\text{C}/\text{min}$ from room temperature to a nominal carbonisation temperature (T_{carb}) of between 700°C and 869°C . Flows of N_2 (f) of between 200 and $500\text{ cm}^3/\text{min}$ were used, and the samples were kept at the nominal carbonization temperature for one hour before cooling them down under nitrogen atmosphere.

During the experiments, both metallic sodium and NaOH were transported by the vapours and could be observed at the outlet of the reactor. Metallic sodium mixed with sodium carbonate was also present inside the crucible. Therefore, the latter was submitted to atmospheric humidity for two days to oxidise sodium metal slowly. Finally, the activated carbon was washed with extreme care, first with 1 M HCl, and finally with distilled water until a constant pH of around 6. After drying in an oven during 24 h, a very light activated carbon was obtained.

The effectiveness of the carbons prepared from Kraft lignin for methylene blue adsorption was compared with that of three commercial AC (CAC1, CAC2 and CAC3), which were kindly provided by Norit Americas Inc. These carbons are prepared by physical activation with steam [37] and their main properties are shown in Table 1. CAC1 and CAC3 are mainly microporous

with high surface areas of more than 1000 m²/g. CAC2 has a lower surface area and less than 30% of microporous (0.185 cm³/g in microporous volume respect a total volume of 0.637 cm³/g). All of them have an acidic surface character.

2.3. Response surface methodology (RSM)

The experiments were planned using a response surface methodology, which was based on a central factorial design established around a central point located in the expected optimal zone [43, 44]. Methylene blue adsorption was the dependent variable, and the independent variables were the proportion of NaOH, the carbonisation temperature and the flow-rate of nitrogen inside the carbonization tube [16].

This technique develops a two or three dimension surface obtained from several experimental data [43, 44]. As we can see in Figure 1, this methodology is based on a central factorial design established in a central point that is determined in a theoretical optimum zone. From this point, some deviations of a controlled size are made and if it is necessary, more equidistant axial points from the central one can be added to complete the experimental table, called the compost central factorial design. Figure 2 shows the algorithm followed in the RSM.

The analysis of the surface response determined the significance of the effect of the independent variables and their interactions. The design was expanded with a second set of experiments into a compost central factorial design (see Figure 2) to locate the optimum more precisely.

In the presented work, the central point was established at a carbonisation temperature of 770°C, a mass ratio of 25% of KL₄, and a nitrogen flow of 350 cm³/min, according to the available literature [45-50]. The variations performed were ±70°C in the temperature, ±5% in the mass ratio, and ±150 cm³/min in the nitrogen flow.

2.4. Characterisation of the activated carbons

2.4.1. Surface area and porosity

Surface area and porosity were determined from the nitrogen adsorption–desorption isotherms obtained at 77 K with an automatic instrument (ASAP 2020, Micromeritics). The samples were previously degassed at 523 K for several hours. N₂ adsorption data for P/P₀ from 10⁻⁵ to 0.99 (in a set of values previously fixed) were analysed according to: (i) the BET method [51] for calculating the specific surface area, S_{BET} ; and (ii) the α_s method [52] for calculating the micropore volume, $V_{\alpha, \text{micro}}$, and the ultramicropore volume, $V_{\alpha, \text{ultra}}$, using Carboxen 1000 as reference material [53]. The total pore volume, $V_{0.99}$, was calculated from nitrogen adsorption at a relative pressure of 0.99.

2.4.2. Methylene blue (MB) adsorption tests

MB serves as a model compound for adsorption of organic contaminants from aqueous solution and is used as a primary indicator of the adsorption capacity of activated carbons [25]. The adsorption test of MB is based on a

one point adsorption isotherm. The analysis was performed mixing 33.7 mg of AC in a topped plastic bottle with 50 ml of a solution of 3.2 mM of MB. This suspension remained under mechanical agitation for 24 hours. Afterwards, a sample of the solution was extracted and analysed in a UV-VIS in an 8500 Dinko Instruments spectrophotometer, equipped with a tungsten lamp operated at 664.8 nm. The MB adsorption capacity (q_{AM}) was calculated by the difference between the initial and the final concentrations, and expressed as grams of MB per 100g of AC (g MB/100g AC).

2.4.3. *Surface functionality*

Modified Boehm titration [54] was used to identify and quantify the acid and basic surface functionality of the AC. For this, 25 mg of dry sample were mixed with 25 ml of NaOH 0.1 N, Na_2CO_3 0.1 N, $NaHCO_3$ 0.1 N, sodium ethoxide 0.1 N and HCl 0.05 N. The first four solutions determine the acidic surface sites whereas the latter is used to measure the total basic sites. NaOH is used to quantify carboxylic, lactone and phenol groups, Na_2CO_3 for carboxylics and lactones; $NaHCO_3$ determines carboxylics and sodium ethoxide for the total acidic sites. By difference between them, it is possible to calculate the quantity of each surface group. The suspensions of AC were stirred for 48 hours to complete contact between the surface groups and the reagent in the solution. Afterwards, the suspension was filtered and samples of 5 ml were titrated with HCl or NaOH depending on the solution. The adsorbed quantity was calculated by the difference between the initial and the final valours and expressed in terms of miliequivalents per gram of AC (meq/g AC).

3. RESULTS AND DISCUSSION

3.1. Application of RSM to optimize adsorption capacity

A preliminary study with activated carbons prepared with LK_d and potassium hydroxide [16] dealing with the effect of the experimental conditions on the characteristics of the activated carbons was carried out in order to determine the most relevant ones. The latter were found to be activation temperature T_{carb} , mass ratio of lignin R and N₂ flow rate f , while the activation time and heating rate were found to have minor effects within the corresponding range of values investigated. For this reason, activation time and heating rate were fixed at one hour and 5 °C/min, respectively.

3.1.1. First screening experiments

According to the central factorial design, seventeen AC were prepared under the conditions detailed in Table 3. The central point was: $T_{\text{carb}} = 770$ °C, $R = 25\%$ and $f = 350$ cm³/min. Table 4 shows the values of the statistical parameter, p-value, that represent the error existing in the linear and quadratic approximations for the RSM. The error level has been established in 5% so a p-value above 0.050 means that this parameter has not a significant influence on the dependent variable. Application of a linear approximation gives information about the influence of temperature, mass ratio and nitrogen flow within the MB adsorption. Table 4 shows that the three parameters have p-values above 0.050, which means that these parameters have not a significant linear effect in the adsorption of the MB, but comparing among them temperature and the mass ratio are more

significant than nitrogen flow. The quadratic approximation of the central factorial design, shows two important facts: i) first, the influence of each parameter alone and the combined effect of each pair in the adsorption of MB (for instance, the combined effect of the temperature and mass ratio in the elimination of MB); ii) second, if the experiments are well represented by the quadratic approximation or not, from the value of the parameter $T_{carb}^2+R^2+f^2$. The latter is important because the quadratic approximation gives a surface area where an optimum can be located. If we are not working in this zone, we do not find the maximum.

Table 4 shows that the quadratic approximation corroborates the results obtained from the application of the linear approximation. The influence of temperature and mass ratio is not strictly significant on the adsorption of MB at 95% probabilities but their p-values, 0.085 and 0.078 for the temperature and the mass ratio respectively, are very close to 0.05. Probably, the election of a new central point should result in a clearer determination of the true effects of temperature and mass ratio, which is supported by the p-value of the combined effect of temperature and mass ratio, which is below 0.050. In contrast, the nitrogen flow and the combination of this parameter with temperature and mass ratio give p-values bigger than 0.300, and in consequence, the nitrogen flow was determined not to be a significant parameter for the study. Finally, the value of $T^2+R^2+f^2$ was 0.039 which shows that we are working with a quadratic surface that with a better central point should give us the optimum conditions for the preparation of ACs, with adsorption of MB. It was necessary to expand the study with a maximum a compost central factorial design by adding experiments 12 to 17.

From these results, we can conclude that we are working near the optimum zone but the central point must be improved. In summary, the effect of the

nitrogen flow and its interaction with T_{carb} and R were not significant. Therefore, a constant value of $f = 200 \text{ cm}^3 \text{ N}_2/\text{min}$, that is a typical value [49, 50, 55], was maintained for the remaining experiments. On the other hand, when the temperature was below 750°C , the MB adsorption capacity decreased with the mass ratio, but above that temperature the dependence with the mass ratio was the opposite. The mass ratio increased the MB adsorption capacity, and it also increased with the temperature for all the mass ratios studied until 777°C , where a maximum exists, and from where the adsorption decreases. This phenomenon occurs because at higher temperatures and mass ratios, the structure of the AC begins to collapse caused by an excessive effect of the activation [16] producing the reduction of the specific surface area that is the main responsible for the MB adsorption.

3.1.2. Experiments with the refined central point

The results of the first screening experiments demonstrated that nitrogen flow-rate was not significant, but the significance of temperature and mass ratio was not clearly established, nor was the optimum located. Therefore a second set of experiments was conducted according to a new design around a new central point, which used smaller variations. The central point was fixed at 777°C with a content of lignin of 23% within variations of $\pm 30^\circ\text{C}$ and $\pm 2\%$. Fourteen new samples of AC were prepared at the conditions detailed in Table 5.

The experiments realised in this second zone gave the p-values for the quadratic approximation of the temperature and mass ratio shown in Table 6. In this case, it is not necessary to study the linear approximation since we are

working with only two parameters, temperature and mass ratio. The significant influence of both parameters was clear, since the p-values were below 0.050. The combined effect of temperature and mass ratio had also significance. Values for T^2 and R^2 , 0.002 and 0.017 respectively, show that the quadratic surface should give the optimum conditions to prepare an AC with maximum adsorption of MB.

3.1.3. Integration of the first-step experiments

Figure 3 shows the response surface modelled from all the experimental data, the first and the second sets of experiments. A maximum MB adsorption of 96.4 g MB/100g AC was predicted at 783°C, 26.4% in KL_d content and 200 $\text{cm}^3 \text{N}_2/\text{min}$. The activated carbon prepared at those conditions gave a MB adsorption of 93.9 g MB/100g AC. Table 7 shows the characterisation of the AC prepared at the optimum conditions. The carbon had a specific surface of 2400 m^2/g , and it was highly microporous (more than 65% of the total porosity), and its surface was predominantly basic, with 15.8 meq/g of basic groups and only 10.5 meq/g of acidic groups.

3.2. Other characteristics of the activated carbons

In general, the MB adsorption capacity of an activated carbon is closely related to the specific surface area, as shown in Figure 4 for activated carbons prepared by chemical and physical activation. Carbons obtained by chemical activation include our own results on ACs from Kraft lignin activated with H_3PO_4 [35], KOH [16] and NaOH, and bibliographic data on carbons prepared by activation with H_3PO_4 [32], KOH [26-31, 33] and steam [38, 39].

Three commercial carbons are also included [37]. MB adsorption capacity for the activated carbons prepared in this study range from 38.7 g MB/100g AC to 98.2 g MB/100g AC, in good agreement with the results reported by several authors [26-31, 33] for carbons prepared from different types of raw materials (olive stone, petroleum coke, pistachio shells, wood, etc.) by KOH activation, which ranged from 26.3 g MB/100g AC to 110.0 g MB/100g AC which lay in the same range of values than for NaOH carbons. The very large porosities and surface areas of the activated carbons prepared with NaOH and KOH facilitates the adsorption of large quantities of adsorbates and thus carbons can find application in removing organic and inorganic molecules from contaminated streams, efficiently [26, 27, 29, 32, 34]. In contrast, activated carbons prepared from Kraft lignin by phosphoric acid activation have more limited MB adsorption capacities, about 38.9 g MB/100g AC [32], which is caused by the lower specific surfaces. Finally, carbons activated with steam [38, 39] and the three commercial activated carbons tested in this study have adsorption capacities similar to those of phosphoric acid carbons.

Due to the size of the MB molecule, around 15 Å, this compound is adsorbed only in the larger micropores or supermicropores (13-20 Å), and the mesopores (>20 Å) [34]. Figures 5 and 6 show the variation of the MB adsorption capacity with the micropore and the supermicropore and mesopore volumes. These figures confirm that MB is adsorbed on the supermicropores and mesopores.

On the other hand, in some cases where the surface area and the porosity is less developed, the MB adsorption capacity is greater than the expected and it is caused by the surface chemistry [31, 56]. MB is a dye with basic character and when is put in contact with a strong acid surface charge, electrostatic

interactions acts between the delocalised π electron of the carbon surface and the free electrons of the dye molecule presents in aromatic rings principally [56]. In Figures 7 and 8, the effect of the acid and basic surface chemistry is presented, respectively. In general, a better correlation between the MB adsorption capacities exists with the acidity surfaces (Figure 7). However, due to the fact that the porosity is well developed in the AC studied (Table 1 and 7), the surface chemistry does not play an important role collaborating in the adsorption phenomena.

4. CONCLUSIONS

The aim of this study was to optimize the preparation of carbons activated with NaOH for the purification of water polluted with organic compounds, and to study the interaction between the experimental variables by using a statistical method for the design of experiments.

The statistical method selected, the Response Surface Methodology, has been showed to provide the optimum conditions for prepare an AC that adsorb more MB and phenol than de commercials carbons used for comparison.

In the first step of the experimental application of the RSM, the effect of the nitrogen flow and its interaction with T_{carb} and R were not significant and does not affect the finally properties of the AC, especially the adsorption of MB. A typical constant value of $f = 200 \text{ cm}^3 \text{ N}_2/\text{min}$ was set for the remaining experiments centered in a second central point.

Integration of the first-step and the second-step experiments allowed selecting the optimum AC where the maximum MB adsorption take place is

achieved at 783°C, 26.4% in KL_d content and 200 cm³ N₂/min with a MB adsorption capacity of 93.9 mg/100g AC. These adsorption capacities are well correlated with the supermicropore and mesopore volume and also with the acidic groups of the surface due to the character of the basic dye employed.

ACKNOWLEDGEMENTS

Funding for this work was provided by the Spanish Ministry of Science and Technology (MCYT, project PPQ2002-04201-CO2-02, partially funded by the FEDER program of the European Union), and the Catalan Regional Government (Project 2005SGR-00580). This research was also partly made possible by financial support from the European Commission through the ALFA program (project LIGNOCARB-ALFA II 0412 FA FI). V. Torné-Fernández acknowledges the URV for her PhD grant. V. Fierro acknowledges the MCYT and the Universitat Rovira i Virgili (URV) for the financial support of her 'Ramón y Cajal' research contract.

REFERENCES

1. Activated carbon compendium. A collection of papers from the journal Carbon 1996-2000. 1^a ed, ed. H. Marsh. 2001, North Shields (UK): Elsevier.
2. Lin, S.Y., Jr., S.E. Lebo, and Lignotech USA, Inc., Lignin, in Kirk-Othmer Encyclopedia of Chemical Technology. 2000.
3. Lin, S. Y. and Lin, I. S., Lignin. Ullmann's Encyclopedia of industrial chemistry, ed. S.H. Barbara Elvers, Gail Schulz. Vol. A15. 1990, New York. 305-315.
4. Ahmad, A.L., Loh, M.M., and Aziz, J.A., Preparation and characterization of activated carbon from oil palm wood and its evaluation on Methylene blue adsorption. Dyes and Pigments. In Press, Corrected Proof.
5. Duran-Valle, Carlos J., Gomez-Corzo, Manuel, Gomez-Serrano, Vicente, et al., Preparation of charcoal from cherry stones. Applied Surface Science, 2006. 252(17): p. 5957-5960.
6. Ganan, J., González, J.F., González-García, C.M., et al., Air-activated carbons from almond tree pruning: Preparation and characterization. Applied Surface Science, 2006. 252(17): p. 5988-5992.
7. Lillo-Rodenas, M. A., Lozano-Castelló, D., Cazorla-Amorós, D., et al., Preparation of activated carbons from Spanish anthracite: II. Activation by NaOH. Carbon, 2001. 39(5): p. 751-759.
8. Lozano-Castello, D., Cazorla-Amoros, D., Linares-Solano, A., et al., Influence of pore size distribution on methane storage at relatively low pressure: preparation of activated carbon with optimum pore size. Carbon, 2002. 40(7): p. 989-1002.

9. Lozano-Castello, D., Lillo-Rodenas, M. A., Cazorla-Amoros, D., et al., Preparation of activated carbons from Spanish anthracite: I. Activation by KOH. *Carbon*, 2001. 39(5): p. 741-749.
10. Fierro, V., Torné-Fernández, V., Montané, D., et al. Activated Carbons Prepared from Kraft Lignin by Phosphoric Acid Impregnation. in *Carbon'03*. 2003. Oviedo (Spain).
11. Fierro, V., Torné-Fernández, V., Montané, D., et al., Study of the decomposition of kraft lignin impregnated with orthophosphoric acid. *Thermochimica Acta*, 2005. 433(1-2): p. 142-148.
12. Ahmadpour, A. and Do, D. D., The preparation of active carbons from coal by chemical and physical activation. *Carbon*, 1996. 34(4): p. 471-479.
13. Otowa, T., Nojima, Y., and Miyazaki, T., Development of KOH activated high surface area carbon and its application to drinking water purification. *Carbon*, 1997. 35(9): p. 1315-1319.
14. Liang, C., Wei, Z., Xin, Q., et al., Ammonia synthesis over Ru/C catalysts with different carbon supports promoted by barium and potassium compounds. *Applied Catalysis A: General*, 2001. 208(1-2): p. 193-201.
15. Frackowiak, Elzbieta and Beguin, Francois, Electrochemical storage of energy in carbon nanotubes and nanostructured carbons. *Carbon*, 2002. 40(10): p. 1775-1787.
16. Fierro, V., Torné-Fernández, V., and Celzard, A., Highly microporous carbons prepared by activation of Kraft lignin with KOH. *Studies in Surface Science and catalysis*, 2005: p. 607-614.
17. Veglio', F. and Beolchini, F., Removal of metals by biosorption: a review. *Hydrometallurgy*, 1997. 44(3): p. 301-316.

18. Ravikumar, K., Krishnan, S., Ramalingam, S., et al., Optimization of process variables by the application of response surface methodology for dye removal using a novel adsorbent. *Dyes and Pigments*, 2007. 72(1): p. 66-74.
19. K., Ravikumar, S., Ramalingam, S., Krishnan, et al., Application of response surface methodology to optimize the process variables for Reactive Red and Acid Brown dye removal using a novel adsorbent. *Dyes and Pigments*, 2006. 70(1): p. 18-26.
20. Karacan, F., Ozden, U., and Karacan, S., Optimization of manufacturing conditions for activated carbon from Turkish lignite by chemical activation using response surface methodology. *Applied Thermal Engineering*. In Press, Corrected Proof.
21. Azargohar, R. and Dalai, A.K., Production of activated carbon from Luscar char: Experimental and modeling studies. *Microporous and Mesoporous Materials*, 2005. 85(3): p. 219-225.
22. Ravikumar, K., Deebika, B., and Balu, K., Decolourization of aqueous dye solutions by a novel adsorbent: Application of statistical designs and surface plots for the optimization and regression analysis. *Journal of Hazardous Materials*, 2005. 122(1-2): p. 75-83.
23. Ravikumar, K., Pakshirajan, K., Swaminathan, T., et al., Optimization of batch process parameters using response surface methodology for dye removal by a novel adsorbent. *Chemical Engineering Journal*, 2005. 105(3): p. 131-138.
24. Goel, Jyotsna, Kadirvelu, K., Rajagopal, C., et al., Removal of mercury(II) from aqueous solution by adsorption on carbon aerogel: Response surface methodological approach. *Carbon*, 2005. 43(1): p. 197-200.

25. Bacaoui, A., Dahbi, A., Yaacoubi, A., et al., Experimental Design To Optimize Preparation of Activated Carbons for Use in Water Treatment. *Environ. Sci. Technol.*, 2002. 36(17): p. 3844-3849.
26. Stavropoulos, G.G. and Zabaniotou, A.A., Production and characterization of activated carbons from olive-seed waste residue. *Microporous and Mesoporous Materials*, 2005. 82(1-2): p. 79-85.
27. Stavropoulos, G.G., Precursor materials suitability for super activated carbons production. *Fuel Processing Technology*, 2005. 86(11): p. 1165-1173.
28. Tseng, Ru-Ling and Tseng, Szu-Kung, Pore structure and adsorption performance of the KOH-activated carbons prepared from corncob. *Journal of Colloid and Interface Science*, 2005. 287(2): p. 428-437.
29. Wu, Feng-Chin, Tseng, Ru-Ling, and Juang, Ruey-Shin, Comparisons of porous and adsorption properties of carbons activated by steam and KOH. *Journal of Colloid and Interface Science*, 2005. 283(1): p. 49-56.
30. Wu, Feng-Chin, Tseng, Ru-Ling, and Hu, Chi-Chang, Comparisons of pore properties and adsorption performance of KOH-activated and steam-activated carbons. *Microporous and Mesoporous Materials*, 2005. 80(1-3): p. 95-106.
31. El-Hendawy, Abdel-Nasser A., Surface and adsorptive properties of carbons prepared from biomass. *Applied Surface Science*, 2005. 252(2): p. 287-295.
32. Girgis, Badie S., Yunis, Samya S., and Soliman, Ashraf M., Characteristics of activated carbon from peanut hulls in relation to conditions of preparation. *Materials Letters*, 2002. 57(1): p. 164-172.
33. Khezami, L., Chetouani, A., Taouk, B., et al., Production and characterisation of activated carbon from wood components in powder: Cellulose, lignin, xylan. *Powder Technology*, 2005. 157(1-3): p. 48-56.

34. Lei, S., Miyamoto, J.-I., Kanoh, H., et al., Enhancement of the methylene blue adsorption rate for ultramicroporous carbon fiber by addition of mesopores. *Carbon*, 2006. In Press, Corrected Proof.
35. Fierro, V., Torné-Fernández, V., and Celzard, A., Kraft lignin as a precursor for microporous activated carbons prepared by impregnation with ortho-phosphoric acid: Synthesis and textural characterisation. *Microporous and Mesoporous Materials*, 2006. 92(1-3): p. 243-250.
36. Torné-Fernández, V., Fierro, V., Mateo, J. M., et al., Highly microporous carbons from chemical activation of lignin with hydroxides: optimization of preparation conditions., in 10th Mediterranean congress. 2005: Barcelona.
37. Inc., Norit Americas, www.norit-americas.com.
38. Warhurst, A. Michael, Mcconnachie, Gordon L., and Pollard, Simon J. T., Characterisation and applications of activated carbon produced from *Moringa oleifera* seed husks by single-step steam pyrolysis. *Water Research*, 1997. 31(4): p. 759-766.
39. Wu, Feng-Chin, Tseng, Ru-Ling, and Juang, Ruey-Shin, Pore structure and adsorption performance of the activated carbons prepared from plum kernels. *Journal of Hazardous Materials*, 1999. 69(3): p. 287-302.
40. Lillo-Rodenas, M.A., Cazorla-Amorós, D., and Linares-Solano, A., Behaviour of activated carbons with different pore size distributions and surface oxygen groups for benzene and toluene adsorption at low concentrations. *Carbon*, 2005. 43(8): p. 1758-1767.
41. Dimotakis, E. D., Cal, M. P., Economy, J., et al., Chemically Treated Activated Carbon Cloths for Removal of Volatile Organic Carbons from Gas Streams: Evidence for Enhanced Physical Adsorption. *Environmental Science and Technology*, 1995. 29(7): p. 1876-1880.

42. Benkhedda, J., Jaubert, J.-N., Barth, D., et al., Experimental and Modeled Results Describing the Adsorption of Toluene onto Activated Carbon. *J. Chem. Eng. Data*, 2000. 45(4): p. 650-653.
43. Montgomery, D. C., Design and analysis of experiments. 5th ed. 2000, New York: John Wiley & Sons cop.
44. Prat, A., Tort-Martorell, X., and Pozueta, L., Métodos estadísticos. Control y mejora de la calidad. 1997, Barcelona: UPC.
45. Guo, Y. P., Qi, J. R., Yang, S. F., et al., Adsorption of Cr(VI) on micro- and mesoporous rice husk-based active carbon. *Materials Chemistry and Physics*, 2002. 78(1): p. 132-137.
46. Guo, Y. P., Yang, S. F., Yu, K. F., et al., The preparation and mechanism studies of rice husk based porous carbon. *Materials Chemistry and Physics*, 2002. 74(3): p. 320-323.
47. Guo, Y. P., Zhang, H., Tao, N. N., et al., Adsorption of malachite green and iodine on rice husk-based porous carbon. *Materials Chemistry and Physics*, 2003. 82(1): p. 107-115.
48. Guo, Y. P., Yu, K. F., Wang, Z. C., et al., Effects of activation conditions on preparation of porous carbon from rice husk. *Carbon*, 2000. 41(8): p. 1645-1648.
49. Lillo-Rodenas, M. A., Cazorla-Amoros, D., and Linares-Solano, A., Understanding chemical reactions between carbons and NaOH and KOH. An insight into the chemical activation mechanisms. *Carbon*, 2003. 41(2): p. 267-275.
50. Lillo-Rodenas, M. A., Lozano-Castello, D., Cazorla-Amoros, D., et al., Preparation of activated carbons from Spanish anthracite II. Activation by NaOH. *Carbon*, 2001. 39(5): p. 751-759.
51. Rouquerol, F., Rouquerol, J., and Sing, K. S. W., Adsorption by Powders and Porous Solids. Principles, Methods and Applications. 1999, San Diego: Academic Press.

52. Setoyama, Norihiko, Suzuki, Takaomi, and Kaneko, Katsumi, Simulation study on the relationship between a high resolution [alpha]-plot and the pore size distribution for activated carbon. *Carbon*, 1998. 36(10): p. 1459-1467.
53. Kruk, M., Li, Z., Jaroniec, M., et al., Nitrogen Adsorption Study of Surface Properties of Graphitized Carbon Blacks. *Langmuir*, 1999. 15(4): p. 1435-1441.
54. Boehm, H. P., Chemical Identification of surface groups. *Advances in catalysis*, 1966. 16: p. 179-225.
55. Amarasekera, G., Scarlett, M.J., and Mainwaring, D.E., Development of microporosity in carbons derived from alkali digested coal. *Carbon*, 1998. 36(7-8): p. 1071-1078.
56. Pereira, Manuel Fernando R., Soares, Samanta F., Orfao, Jose J. M., et al., Adsorption of dyes on activated carbons: influence of surface chemical groups. *Carbon*, 2003. 41(4): p. 811-821.

Optimization of the synthesis of highly microporous carbons by chemical activation of kraft lignin with NaOH

V. Torné-Fernández, J.M. Mateo, D. Montané, V. Fierro

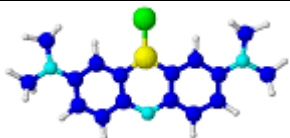
Table 1. Physical properties of the commercial AC used.

	S_{BET} (m^2/g)	$V_{\alpha,\text{micro}}$ (cm^3/g)	$V_{\alpha,\text{ultra}}$ (cm^3/g)	$V_{0.99}$ (cm^3/g)	Acidic Groups ($\text{meq H}^+/\text{gAC}$)	Basic Groups ($\text{meq OH}^-/\text{gAC}$)
CAC1	1350	0.458	0.139	0.713	2.6	0.5
CAC2	620	0.185	0.085	0.637	7.9	1.2
CAC3	1020	0.334	0.152	0.625	5.0	2.1

Optimization of the synthesis of highly microporous carbons by chemical activation of kraft lignin with NaOH

V. Torné-Fernández, J.M. Mateo, D. Montané, V. Fierro

Table 2. Properties of adsorptive molecule.

Molecule	Structure	MW ^a (g/mol)	Tb ^b (°C)	Solubility (%) w/w	Size (Å) ^a
MB		319.9	Decompose	100.0	15

MW^a. Molecular weight.

Tb^b. Normal boiling point.

Size^c. Size calculated with ACDLABS 8.0.

Optimization of the synthesis of highly microporous carbons by chemical activation of kraft lignin with NaOH

V. Torné-Fernández, J.M. Mateo, D. Montané, V. Fierro

Table 3. Points studied in the first-step experiments.

Experiment	Real Values			Statistical Values			q_{AM} (g/100 g AC)
	T_{carb} (°C)	R (%)	f (cm ³ /min)	T_{carb} (°C)	R (%)	f (cm ³ /min)	
1	700	20	200	-1	-1	-1	79.2
2	840	20	500	1	-1	1	38.7
3	770	25	350	0	0	0	86.7
4	840	30	200	1	1	-1	85.1
5	700	30	500	-1	1	1	62.6
6	770	25	350	0	0	0	98.2
7	840	30	500	1	1	1	82.2
8	700	30	200	-1	1	-1	83.6
9	770	25	350	0	0	0	91.8
10	840	20	200	1	-1	-1	49.8
11	700	20	500	-1	-1	1	87.0
Axial Points:							
12	770	32	350	0	1.4	0	91.5
13	869	25	350	-1.4	0	0	91.9
14	770	25	350	0	0	0	96.1
15	770	25	350	0	0	0	94.7
16	671	25	350	1.4	0	0	77.0
17	770	18	350	0	-1.4	0	83.4

Optimization of the synthesis of highly microporous carbons by chemical activation of kraft lignin with NaOH

V. Torné-Fernández, J.M. Mateo, D. Montané, V. Fierro

Table 4. Statistic p-value for the analysis in the first-step experiments, linear and quadratic approximations.

		T_{carb}	R	f	$T_{\text{carb}} \cdot R$	$T_{\text{carb}} \cdot f$	R · f	$T_{\text{carb}}^2 + R^2 + f^2$
Central factorial design	Linear approximation	0.298	0.282	0.606	-	-	-	-
	Quadratic approximation	0.085	0.078	0.309	0.021	0.977	0.423	0.039
Compost central factorial design	Quadratic approximation	0.822	0.230	-	0.059	-	-	0.153

Optimization of the synthesis of highly microporous carbons by chemical activation of kraft lignin with NaOH

V. Torné-Fernández, J.M. Mateo, D. Montané, V. Fierro

Table 5. Points studied in the second-step experiments.

Experiment	Real Values			Statistical Values			q_{AM} (g/100 g AC)
	T_{carb} (°C)	R (%)	f (cm ³ /min)	T_{carb} (°C)	R (%)	f (cm ³ /min)	
18	807	25	200	1	1	-	97.2
19	747	21	200	-1	-1	-	94.3
20	777	23	200	0	0	-	96.2
21	807	21	200	1	-1	-	91.9
22	747	25	200	-1	1	-	94.1
23	777	23	200	0	0	-	93.6
24	777	23	200	0	0	-	93.9
Axial Points:							
25	777	20	200	0	-1.4	-	95.1
26	777	26	200	0	1.4	-	88.0
27	777	23	200	0	0	-	97.4
28	777	23	200	0	0	-	93.2
29	777	23	200	0	0	-	95.7
30	819	23	200	1.4	0	-	90.3
31	735	23	200	-1.4	0	-	95.6

Optimization of the synthesis of highly microporous carbons by chemical activation of kraft lignin with NaOH

V. Torné-Fernández, J.M. Mateo, D. Montané, V. Fierro

Table 6. Statistic p-value for the variables, quadratic approximation.

	T_{carb}	R	$T_{\text{carb}} \cdot R$	T_{carb}^2	R^2
Quadratic approximation	0.057	0.016	0.008	0.002	0.017

Optimization of the synthesis of highly microporous carbons by chemical activation of kraft lignin with NaOH

V. Torné-Fernández, J.M. Mateo, D. Montané, V. Fierro

Table 7. Properties of the optimum AC for the adsorption of MB.

S_{BET} (m^2/g)	$V_{\alpha,\text{micro}}$ (cm^3/g)	$V_{\alpha,\text{super}}$ (cm^3/g)	$V_{0.99}$ (cm^3/g)	Acidic Groups ($\text{meq H}^+/\text{g AC}$)	Basic Groups ($\text{meq OH}^-/\text{g AC}$)
2400	0.964	0.090	1.472	10.5	15.8

Optimization of the synthesis of highly microporous carbons by chemical activation of kraft lignin with NaOH

V. Torné-Fernández, J.M. Mateo, D. Montané, V. Fierro

Table 8. MB (q_{MB}) adsorption capacity of the optimum AC and the commercial ones.

q_{MB}	AC-optimum	CAC1	CAC2	CAC3
g/100 g AC	93.9	41.5	31.5	21.7

Captions of the figures

Figure 1. Scheme of experimental points for the RSM development in two dimensions.

Figure 2. Response Surface Methodology basic steps.

Figure 3. Variation of the quantity of MB adsorbed depending on the temperature (T) and the KL_d quantity (R) a) in three dimensions and b) in two dimensions.

Figure 4. Specific surface area in front of MB adsorption capacity for AC obtained by activation with: \diamond H_3PO_4 (our AC), \blacklozenge H_3PO_4 from bibliography, \square KOH (our AC), \blacksquare KOH from bibliography, Δ NaOH, \circ commercial carbons and \bullet steam activation from bibliography. Continuous line show the general data tendency.

Figure 5. Microporous volume in front of MB adsorption capacity for AC obtained by activation with: \diamond H_3PO_4 , \square KOH, \blacksquare KOH from bibliography, Δ NaOH and \circ commercial AC. Continuous line show the general data tendency.

Figure 6. Supermicroporous and mesoporous volume in front of MB adsorption capacity for different AC obtained by activation with: \diamond H_3PO_4 (our AC), \square KOH (our AC), Δ NaOH and \circ commercial carbons. Continuous line show the general data tendency.

Figure 7. Acidic surface chemistry influence with the MB adsorption capacity for different AC obtained by activation with: \diamond H_3PO_4 (our AC), \square KOH (our AC), \triangle NaOH and \circ commercial carbons. Continuous line show the general data tendency.

Figure 8. basic surface chemistry vs. MB adsorption capacity for different AC obtained by activation with: \diamond H_3PO_4 (our AC), \square KOH (our AC), \triangle NaOH and \circ commercial carbons. Continuous line show the general data tendency.

Optimization of the synthesis of highly microporous carbons by chemical activation of kraft lignin with NaOH

V. Torné-Fernández, J.M. Mateo, D. Montané, V. Fierro

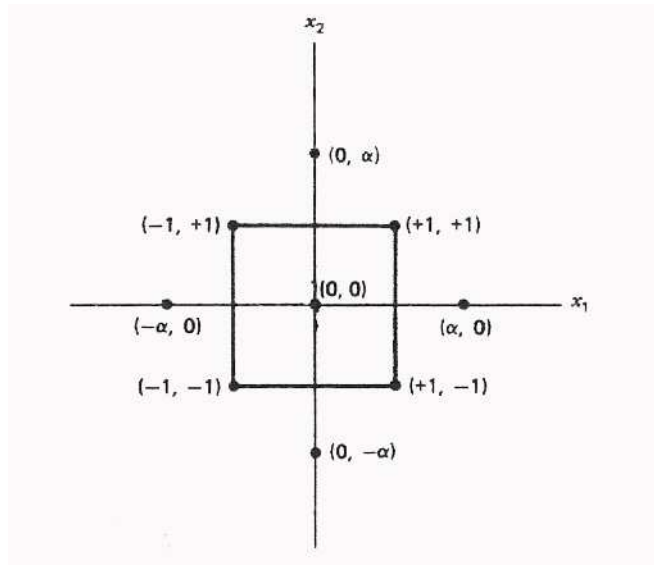


Figure 1
Torné-Fernández, V., et.al

Optimization of the synthesis of highly microporous carbons by chemical activation of kraft lignin with NaOH

V. Torné-Fernández, J.M. Mateo, D. Montané, V. Fierro

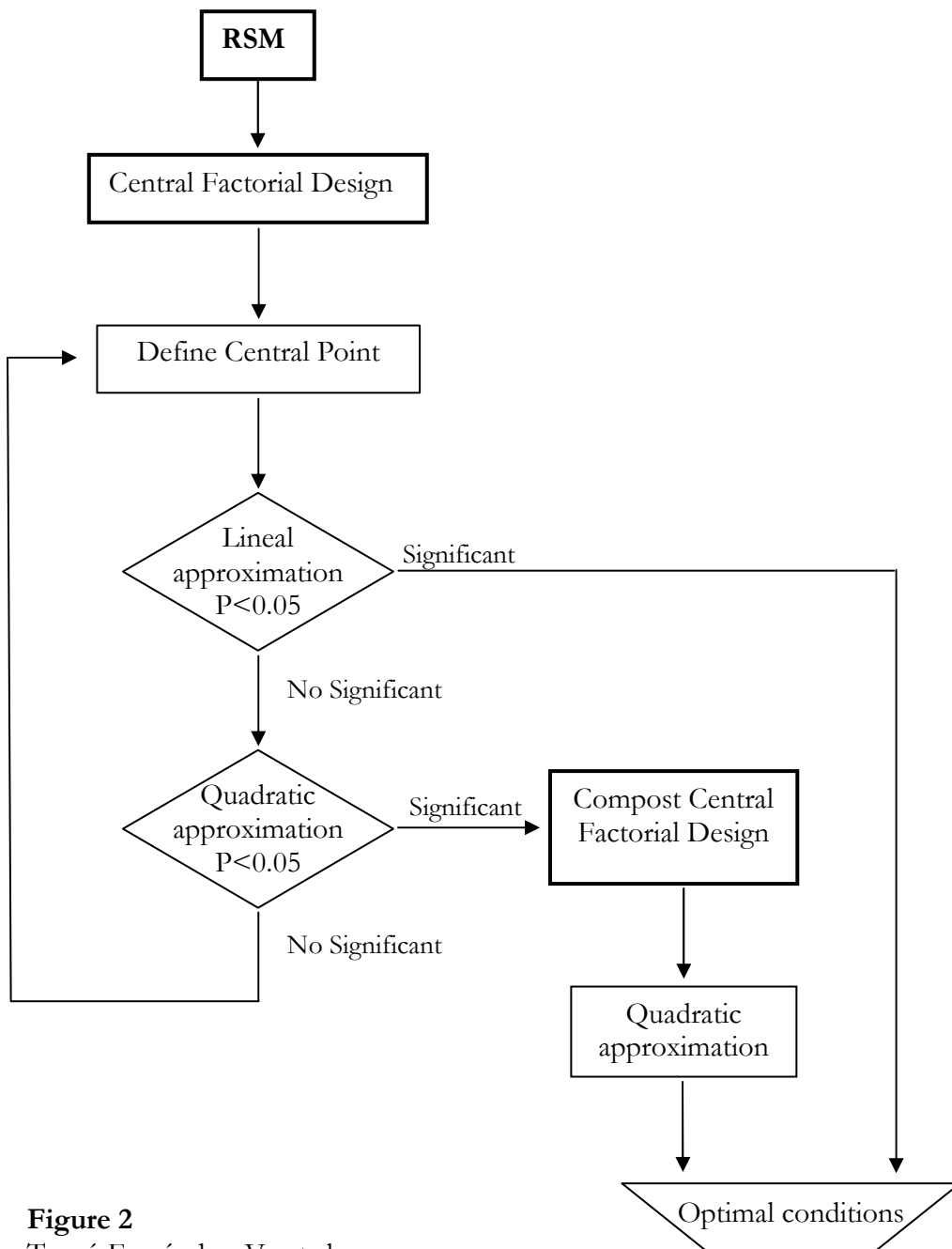


Figure 2
Torné-Fernández, V., et.al

Optimization of the synthesis of highly microporous carbons by chemical activation of kraft lignin with NaOH

V. Torné-Fernández, J.M. Mateo, D. Montané, V. Fierro

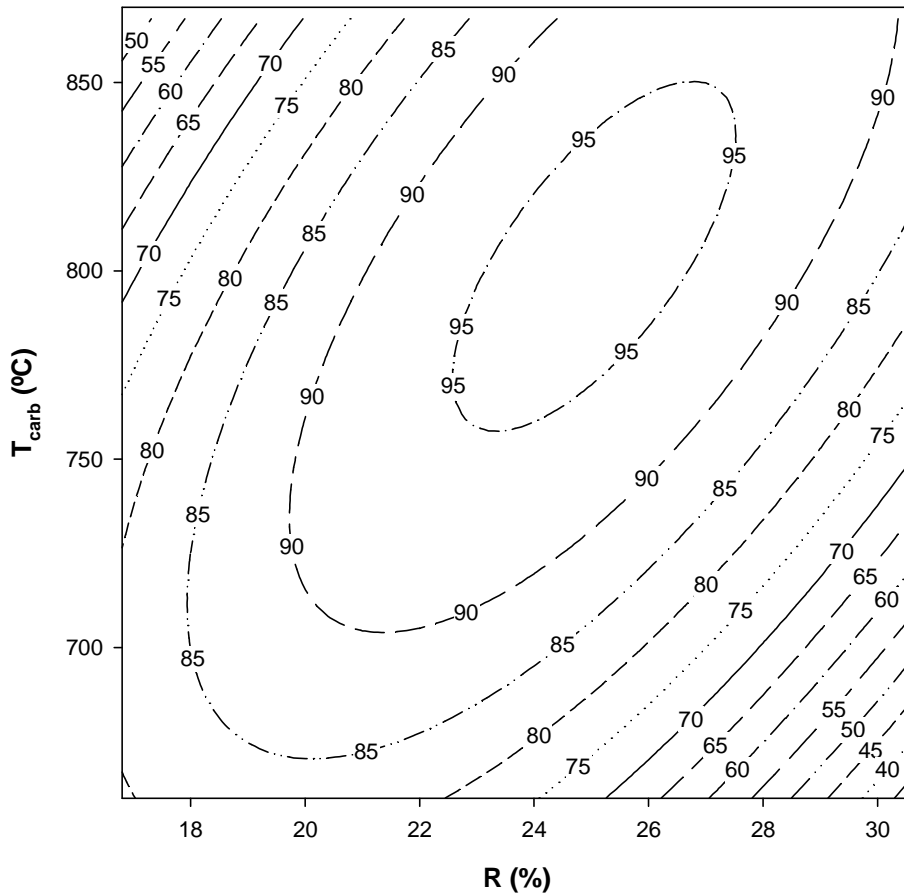


Figure 3
Torné-Fernández, V., et.al

Optimization of the synthesis of highly microporous carbons by chemical activation of kraft lignin with NaOH

V. Torné-Fernández, J.M. Mateo, D. Montané, V. Fierro

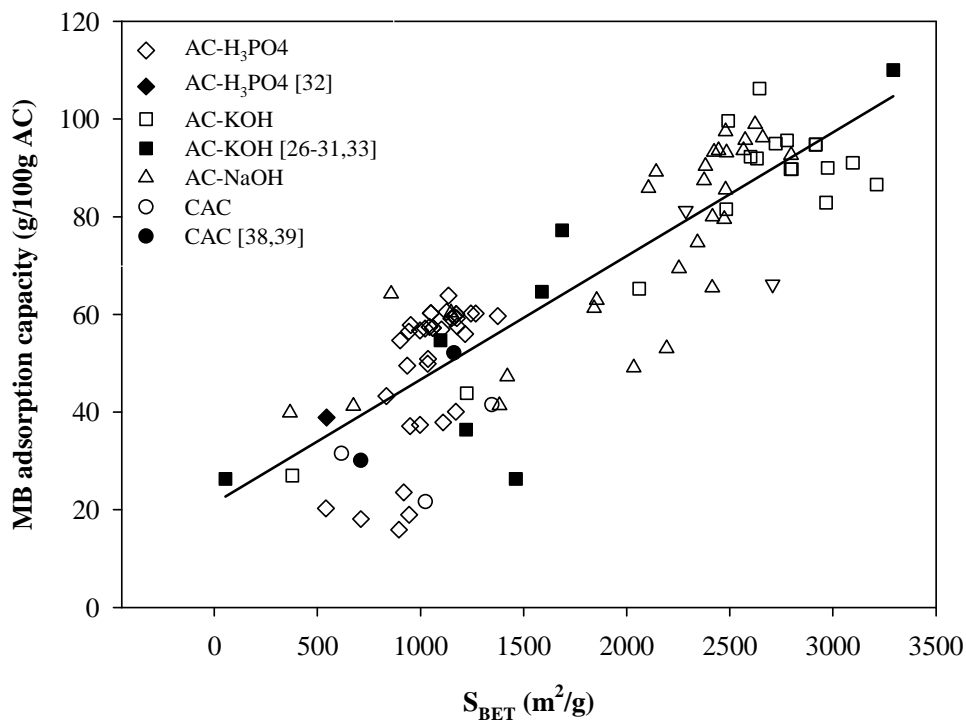


Figure 4
Torné-Fernández, V., et.al

Optimization of the synthesis of highly microporous carbons by chemical activation of kraft lignin with NaOH

V. Torné-Fernández, J.M. Mateo, D. Montané, V. Fierro

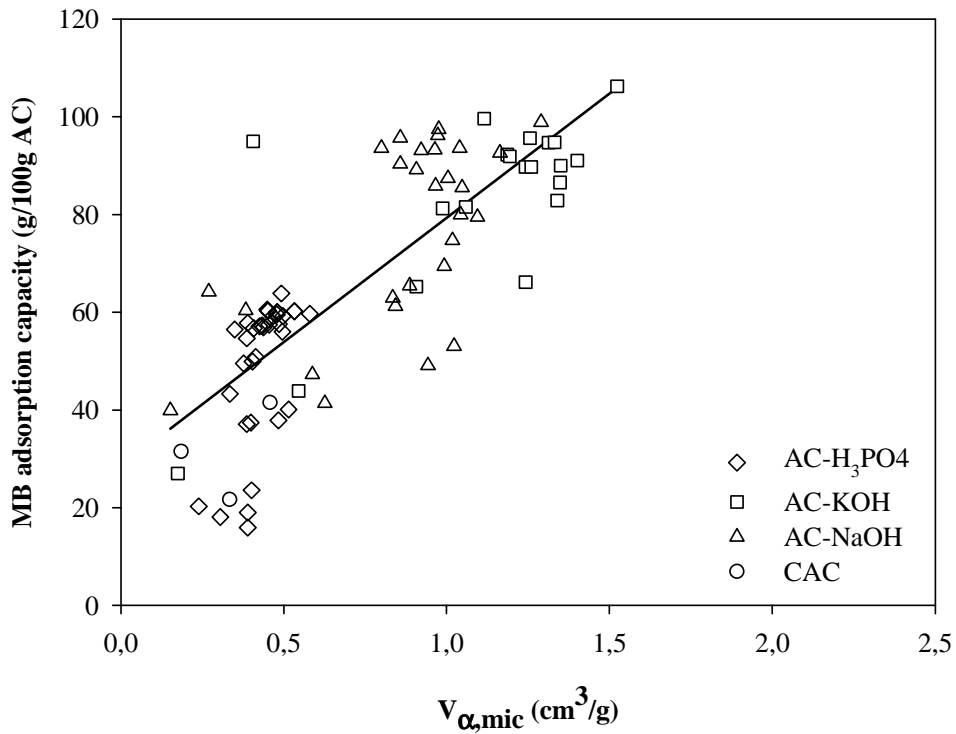


Figure 5
Torné-Fernández, V., et.al

Optimization of the synthesis of highly microporous carbons by chemical activation of kraft lignin with NaOH

V. Torné-Fernández, J.M. Mateo, D. Montané, V. Fierro

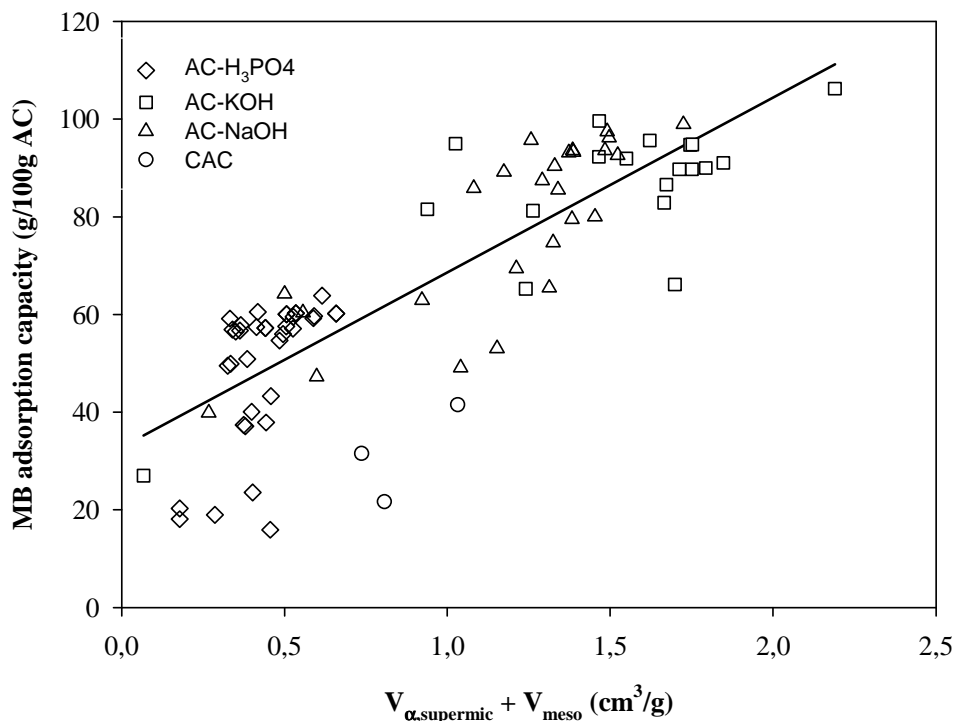
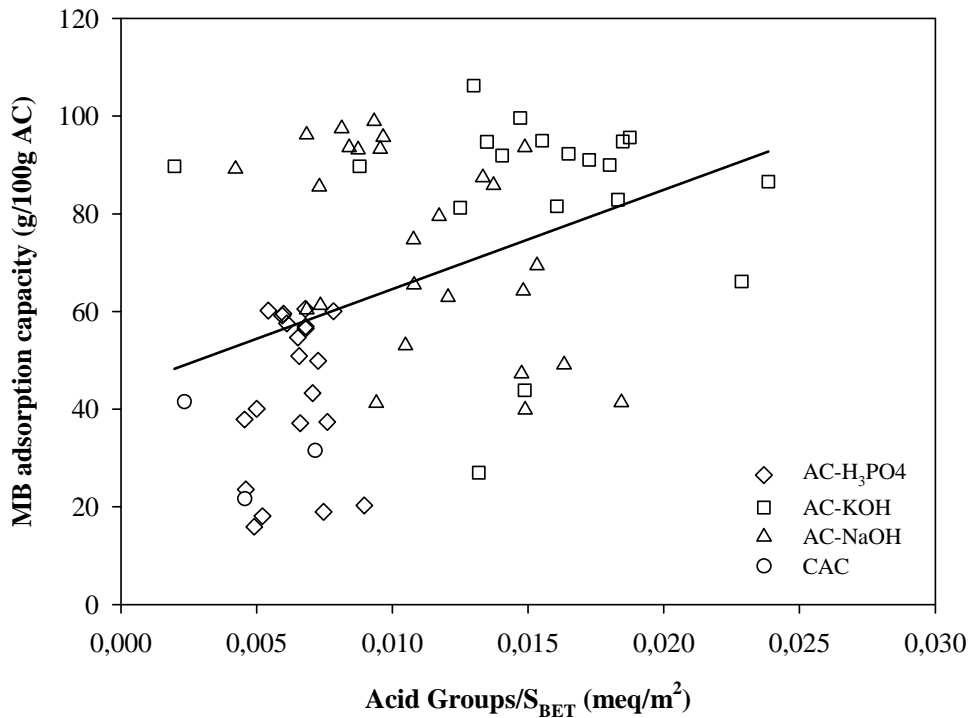


Figure 6
Torné-Fernández, V., et.al

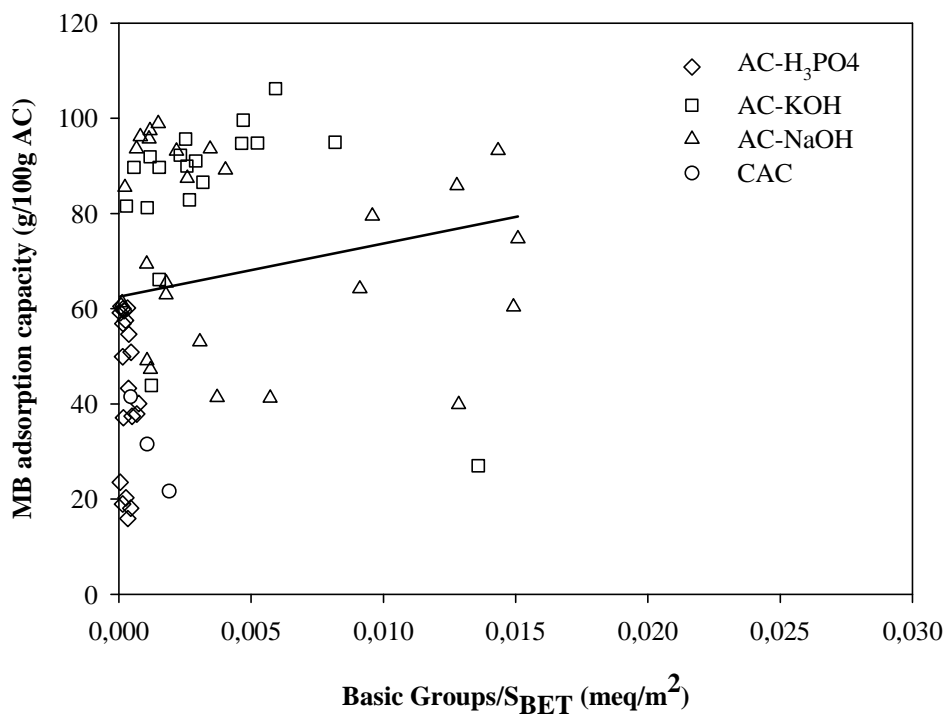
Optimization of the synthesis of highly microporous carbons by chemical activation of kraft lignin with NaOH

V. Torné-Fernández, J.M. Mateo, D. Montané, V. Fierro



Optimization of the synthesis of highly microporous carbons by chemical activation of kraft lignin with NaOH

V. Torné-Fernández, J.M. Mateo, D. Montané, V. Fierro



5.2.3. Sorption study of organic compounds on highly microporous carbons prepared from Kraft lignin

Este artículo ha sido enviado al journal Adsorption Science and Technology durante el año 2006.

SORPTION STUDY OF ORGANIC COMPOUNDS ON HIGHLY MICROPOROUS CARBONS PREPARED FROM KRAFT LIGNIN

V. Torné-Fernández^{1*}, V. Fierro^{1,2}

¹ Departament d'Enginyeria Química, Universitat Rovira i Virgili, Campus
Sescelades, Av. dels Països Catalans 26, 43007 Tarragona, Spain.

² Laboratoire de Chimie du Solide Minéral. Université Henri Poincaré –
Nancy I. UMR CNRS 7555, BP 239, F 54506 Vandoeuvre-lés-Nancy,
France.

*Corresponding author: vanessa.torne@urv.cat. FAX: +00 34 977 559667

Abstract

Activated carbons obtained from Kraft lignin by chemical activation with sodium hydroxide, potassium hydroxide or phosphoric acid are highly microporous carbon materials with high apparent surface areas up to 2900 m²/g. Carbonaceous microporous adsorbates have been used for the adsorption of organic contaminants in aqueous phase. Thus, three different types of activated carbons derived from Kraft lignin are used for this purpose and large amounts of adsorbed pollutants are achieved with values between 100 and 240 mg g⁻¹ for phenol and 185 and 235 mg g⁻¹ for benzene. A kinetic study was done and phenol and benzene adsorption data obtained fit well a pseudo-second-order reaction, as it is described in the literature.

Key words: activated carbon, phenol, benzene, adsorption capacity, liquid phase.

1. INTRODUCTION

Kraft lignin is obtained from the treatment of black liquors originating of paper production. This black liquor is a residue composed principally of cellulose, hemicellulose and lignin. This last one, the second most abundant component in wood in a proportion until 24%.

The preparation of activated carbons (AC) from Kraft lignin [1-6] is a novel usage of this raw material, which is mainly used as in-house fuel for the recovery of both energy and residual inorganic matter, and also others employments [7-14] as animal feed binding, oil well drilling, soil stabilization, protein precipitation or board additives are of minor importance.

We have recently reported the chemical activation of KL impregnated with H_3PO_4 [6, 15], NaOH [5, 16] and KOH [16] obtaining AC essentially microporous with surface areas as high as $1300\text{ m}^2/\text{g}$ for the activation with H_3PO_4 and $2400\text{ m}^2/\text{g}$ for alkaline hydroxides. Activation with potassium hydroxide (KOH) has gained a growing interest as activating agent since it has been found to be one of the most effective compounds for that purpose [17-21]. High surface areas and pore volumes are reported for lignocellulosic materials, carbons and chars activated by KOH with surface areas up to $3000\text{ m}^2/\text{g}$ [5].

ACs are used in several industrial processes such as gas separation, gas storage, purification or catalyzed reactions [7, 22, 23]. The aim of the present study is to examine the capability of a series of AC developed from the chemical activation of Kraft lignin with phosphoric acid, sodium hydroxide and potassium hydroxide impregnation to adsorb organic compounds from

low concentration wastewater. These organic components are common contaminants in industrial waters since they are used as intermediates in the synthesis of dyes, pesticides, explosives, insecticides, and also they constitute priority pollutants [24]. These waters are generally treated with chlorine, used as disinfectant and it reacts with phenol and form chlorophenols. This derived compound from phenol is a big problem since it is one of the most toxic pollutants found in industrial wastewaters. For these reasons, benzene and phenol in dilute aqueous solution were chosen as representative model compounds for adsorption assessment.

As it is presented in Table 1, phenol is commonly used in this sense [25-92] but only few experimental aqueous-phase adsorption isotherm data are available in the literature for benzene [24, 36, 53, 93-96] and toluene [24, 36, 49, 53, 70, 93-95, 97] compared with the large quantity of tests in gas phase [98]. The importance of the study of this kind of compounds is based on the fact that they destroy the ozone stratospheric layer, are the precursors of photochemical oxidants, produce acid rain, affect to the nervous system and are carcinogenic and mutagenic agents [98]. For this reason, a big number of studies about the elimination of these compounds have been published [98-100] using different methods for treating it.

2. EXPERIMENTAL

2.1. Materials

KL was supplied by Lignotech Ibérica S.A. (Spain), and was presented in the form of a fine dark brown powder. The removal of the inorganic matter from KL was achieved as follows: batches of 100 g were introduced in 2 l of

water, leading to dark brown suspensions of pH 9.5, and lignin was precipitated by adding H_2SO_4 until the pH decreased to 1. The precipitate was gently washed with distilled water until the pH of the rinse was constant and finally dried overnight at 105 °C. The lignin prepared this way was nearly mineral-free and was termed demineralised Kraft lignin (KL_d).

Two activating agents were used with KL_d : sodium hydroxide (NaOH) with a 99% purity and potassium hydroxide (KOH) with 85% of purity, both provided by Scharlau as lentils. Another activating agent was used with KL_d , an 85% solution of phosphoric acid (H_3PO_4) supplied by Panreac Spain.

For the adsorption tests, phenol (Ph) crystals and benzene solution were supplied by Aldrich with more than 99% of purity. Both organic compounds were solved in ultrapure water from a Milli-Q Millipore equipment for preparing 100 ppm solutions that were kept in crystal bottles under a temperature of 6°C.

2.2. Preparation of carbons

For the preparation of AC with NaOH (AC-Na), sodium hydroxides lentils were ground and physically mixed with KL_d according to a NaOH/ KL_d mass ratio of 3/1. The carbonisation was carried out in a horizontal furnace and the samples were heated from room temperature to 750°C in a N_2 flow of 200 cm^3/min . This sample was kept at the final temperature for a carbonisation time of one hour before cooling down under nitrogen. The heat rate was established in 5°C/min. Afterwards, the sample was submitted to atmospheric humidity for two days, during which the alkaline metal remaining slowly oxidised. Finally, the activated carbon was washed with

extreme care, first with 1 M HCl, and finally with distilled water until the pH of the rinse remains constant and close to 6 (a CyberScan PC 510 pH-meter with a Hamilton-electrode “Flushtrode” was used). After drying in an oven during 24 hours, a very light activated carbon was obtained.

The preparation of AC with KOH (AC-K) was made following the same methodology explained before but with different activating conditions: 700°C of carbonisation temperature, a KOH/ KL_d mass ratio of 3/1 and a 400 cm³ N₂/min.

In the chemical activation with H₃PO₄ (AC-P), the procedure was different. KL was mixed with H₃PO₄ a 1.4 acid to lignin weight ratio (P/L) on a wet basis. The slurry was left for an impregnation time of 48 hours at room temperature in air, and then transferred to a furnace DUM Model 10CAF where carbonization was carried out under air atmosphere. The furnace was heated at 10 °C min⁻¹, up to 150 °C, which temperature was held for 1 h to allow free evolution of water. Afterwards the oven was heated at 10 °C min⁻¹ up to the final carbonisation temperature, 450°C, which was held for 2 h. To remove the excess of H₃PO₄ after carbonisation, the activated carbon was extensively washed with distilled water until a neutral pH was met (a CyberScan PC 510 pH-meter with a Hamilton-electrode “Flushtrode” was used). Then, the samples were dried overnight in an oven at 105 °C.

To compare with these activated carbons, three commercial AC was used, called CAC1, CAC2 and CAC3. These AC are prepared by physical activation with steam [101] and are provided from Norit Americas Inc. The properties of all these carbons are shown in Table 2. AC-Na, AC-K, AC-P, CAC1 and CAC3 are highly microporous AC with high surface area between 900 m²/g and 2900 m²/g. CAC2 has less surface area with less than 30% of

microporous ($0.185 \text{ cm}^3/\text{g}$ in microporous volume respect a total volume of $0.637 \text{ cm}^3/\text{g}$). All these AC have a high acidic surface character although AC-Na has also a large quantity of basic groups.

2.3. Characterisation of adsorbates

Surface area and porosity were determined from the corresponding nitrogen adsorption–desorption isotherms obtained at 77 K with an automatic instrument (ASAP 2020, Micromeritics). The samples were previously outgassed at 523 K for several hours. N_2 adsorption data for P/P_0 from 10^{-5} to 0.99 (in a set of values previously fixed) were analysed according to: (i) the BET method [102] for calculating the specific surface area, S_{BET} ; and (ii) the α_s method [103] (using Carbo-pack F Graphitised Carbon Black as reference material [104] for calculating the micropore volume, $V_{\alpha_{\text{micro}}}$, and the ultramicropore volume, $V_{\alpha_{\text{ultra}}}$. The total pore volume, $V_{0.99}$, was calculated from nitrogen adsorption at a relative pressure of 0.99.

2.4. Phenol (Ph) and Benzene (B) adsorption

Adsorption of phenol and benzene was studied with the six AC presented before. The properties of these organic molecules used in the adsorption tests onto the different AC are present in the table 3. As it is showed, both compounds are very similar in molecular weight and size but the presence of an OH group in the phenol structure gives different polarity compared with benzene. From this property, benzene presents a highest volatility and less

solubility in comparison with phenol. Thus, this both components represent good models for this type of tests.

2.4.1. Kinetic study

For the determination of the time needed for achieve the adsorption equilibrium, 10 mg of AC was mixed with 10 ml of a 100 ppm solution of phenol or benzene in several well topped glass flasks. The mixing step took place for a determined time until a maximum of 7 days to ensure the equilibrium state at a constant temperature of 25°C. The tubes were attached perpendicularly with clamps to a horizontal revolving shaft that had a rotating speed of 2 rpm and the temperature was controlled with an electronic digital regulator P-Selecta Digiterm-100. Afterwards, 3 ml of sample were taken and filtered in a regenerated cellulose filter of 0.45 μm of pore size to a vial topped. The concentration of the organic compound was obtained by liquid chromatography in an 1100 Series Agilent chromatograph with a Hypersil ODS 250 mm column. The dynamic phase was acetonitrile/water in a relation of 65/35. The adsorbed quantity (q) was calculated by the difference between the initial and the final valour.

2.4.2. Adsorption isotherms

For the preparation of the adsorption isotherms, different quantities of adsorbate (between 1 and 20 mg) were mixed with 10 ml of a 100 ppm solution of phenol or benzene in several well topped glass flasks. The sample granulometry was between 63 and 500 μm of diameter particle. The tubes were capped and placed in a water bath at 25°C, attached perpendicularly

with clamps to the horizontal revolving shaft for 8 hours to ensure the equilibrium. Afterwards, 3 ml of sample were taken and filtered in a regenerated cellulose filter of 0.45 μm of pore size to a vial topped. The concentration of the organic compound was obtained by HPLC, as it has been explained before.

The adsorbed quantity (q_t) was calculated by the difference between the initial and the final valour.

The acidic surface of the AC used in this report provides low pH during the tests for the AC activated with KOH and H_3PO_4 and not high variations for the rest of AC. The initial pH of the phenol adsorption test was proximally 7 but due to the acidity character of AC the final pH varies to between 4 (AC-K and AC-P) and ~ 6.7 (AC-Na, CAC1, CAC2 and CAC3) depending on the adsorbate used. In the benzene adsorption tests, the behaviour is quite similar. The initial pH is 7.7 and the free evolution of the pH goes to 4 (AC-K and AC-P) and ~ 6.5 (AC-Na, CAC1, CAC2 and CAC3).

At lows pH, the acidic compounds prevails in the nonionized form, that have higher adsorption capacity of organic species than when is present in the ionized form [24]. This phenomena occurs because the reduction of repulsions interactions that improve the organic adsorption capacity.

3. RESULTS AND DISCUSION

Experimental adsorption tests realised with phenol and benzene present similar results. Figure 1 and 2 present the experimental data obtained for ACs prepared from lignin and the commercial carbons for phenol and benzene

adsorption, respectively. As it can be appreciated, in both cases the maximum adsorption capacity is achieved in less than 2 hours. Results presented only correspond to the first 10 hours of experiments, when the stability is achieved.

3.1. Kinetic of the adsorption processes

The dependence of the reaction rate on the concentration of the species present, in form of quantity adsorbed, must be determined by experimental observation. Although, the functional dependence must be obtained from the theory and corroborated with the experimental data. One of the most common general form [105] of the dependence of organic adsorption on the adsorbate is

$$-r_t = k \cdot (q_e - q_t)^n \quad (1)$$

Where $-r_t$ is the reaction rate that can be expressed as the variation of the adsorption capacity respect to the time (dq_t/dt); k is the adsorption rate constant expressed in terms of mass phenol or benzene adsorbed per adsorbate mass unit and time ($\text{g} \cdot \text{mg}^{-1} \cdot \text{min}^{-1}$); q_e and q_t are the equilibrium and instantaneous mass amount of the organic compound adsorbed per carbon mass unit (mg/g), respectively; t is the contact time (minutes); and n is the reaction order. The reaction order refers to the powers to which the concentration is raised in the kinetic rate law and gives an idea about how fast the reaction take place.

Equation 1 can be rearranged as:

$$\frac{dq_t}{(q_e - q_t)^n} = k \cdot dt \quad (2)$$

Integrating the general form of Eq. (2) for the boundary conditions $t = 0$ to $t=t$ and $q_t = 0$ to $q_t = q_t$ gives:

$$\log(q_e - q_t) = \log(q_e) + \frac{1}{1-n} \{ \log(t) + \log[k \cdot (n-1)] \} \quad (3)$$

Linear plot of $\log(q_e - q_t)$ against $\log(t)$ gives values of the global reaction order, n , and kinetic constant, k , presented in Table 4. As it is showed, the reaction order of the adsorption process is quite similar to a second order chemical reaction with good correlations ($r^2 > 0.930$) of the data for phenol and benzene adsorptions on the AC studied. For this reason, a pseudo-second order (equation 4) can be applied for this process, as is well cited in the literature [24, 54, 64], providing very similar results for constant rates, k and k' .

$$\frac{t}{q_t} = \frac{1}{k' \cdot q_e^2} + \frac{1}{q_e} \cdot t \quad (4)$$

The adsorption rate constant points to a faster adsorption rates for phenol than for benzene in the AC derived from lignin except for CAC2 and CAC3 that are very similar. The AC derived from lignin presents better adsorptions capacities compared with the commercial carbons in both experiments, with phenol and benzene.

Phenol and benzene are small organic molecules with a size of 6 Å and 5 Å respectively and it is well known that they are adsorbed essentially in micropores, as previous studies have shown for other organic compounds [106]. The highest phenol adsorption capacity corresponds with the maximum benzene adsorption capacity that is achieved for AC-Na and AC-K. Both ACs have the maximum volume of mesopores (0.428 cm³/g and 0.384 cm³/g, respectively) and micropores (1.018 cm³/g and 1.332 cm³/g, respectively). Figure 3 shows the adsorption of phenol and benzene on each AC studied as a function of their microporosity. It can be seen that the organic adsorption capacity linearly increases with the micropore volume.

3.2. Isotherm tests

From the experimental data presented in Figures 1 and 2, it is possible to obtain the equilibrium isotherms for the adsorption of phenol or benzene on the AC studied. Adsorption isotherm is important to describe the interaction between the solute and the adsorbate and is very important to optimize the use of adsorbents.

Figure 4 shows the relation between the amounts of phenol adsorption capacity versus the equilibrium concentration at 25°C. Figure 5 shows the same data as in Figure 4 but using benzene as solute. In the experimental data, there is a general agreement that the adsorption isotherms of phenol and benzene on AC are L-shaped [63]. However, there are many attempts in the literature to fit the adsorption isotherms to some kind of model. For this data, three well-known empirical equations were proposed. The first one is the Freundlich model [38, 54, 63, 73] (Equation 5) that is normally used for

high concentrations. This method is based on adsorptions variations with the pressure and considers the decrease of the affinity with the surface saturation, giving best fit at high concentrations.

$$q_e = k_f \cdot C_e^{1/n} \quad (5)$$

where q_e is the mass amount of the organic compound adsorbed per carbon mass unit (mg/g), k_f is the Freundlich constant related with the adsorption capacity (mg g^{-1}), C_e is the concentration of adsorbate in solution at equilibrium (mg l^{-1}) and n is the empirical parameter that represents the heterogeneity of the site energies (dimensionless).

The second model is the Langmuir equation [24, 38, 54, 60, 63, 72, 90]. Generally, this model is better than the Freundlich model but not all the adsorptions fit well with this isotherm (Equation 6) due to the formation of a monomolecular layer in the adsorbate surface. The fit is better at low concentrations.

$$\frac{C_e}{q_e} = \frac{1}{Q_0 \cdot b} + \frac{C_e}{Q_0} \quad (6)$$

where C_e and q_e are the same parameters as in the Freundlich isotherm. Q_0 is maximum amount of adsorbate adsorbed per carbon mass unit (mg/g) and b is the Langmuir constant related with the adsorption energy (l mg^{-1}).

This isotherm is the relation between the recovery degree of the solute particles and the pressure and is based on the velocity of the decrease of intermolecular interactions with the increase of the distance between the

adsorptive molecules and the adsorbate. This isotherm consider several factors: the adsorption is localized, all the active sites on the surface are power equivalents, there is not interaction between adsorbed molecules and the limiting reaction step is the surface reaction as in the heterogeneous catalytic reaction.

The efficiency of adsorption process can be predicted by the dimensionless equilibrium parameter R_L , which is defined by the following equation:

$$R_L = \frac{1}{1+b \cdot C_o} \quad (7)$$

where b is the Langmuir constant ($l \cdot mg^{-1}$) and C_o the initial concentration of phenol and benzene compounds ($mg \cdot l^{-1}$). When $R_L > 1$, the isotherm is considered to be unfavourable, linear when $R_L = 1$, favourable when $0 > R_L > 1$ or irreversible when $R_L = 0$.

The last model is the Tempkin isotherm [27, 107-110]. The main difference between these three models is in the variation of the heat of adsorption with the surface coverage. Langmuir model assumes uniformity, Freundlich isotherm assumes logarithmic decrease and Tempkin model assumes linear decrease in heat of adsorption with surface coverage.

$$q_e = k_1 \cdot \ln(k_2) + k_1 \cdot \ln(C_e) \quad (8)$$

where k_1 is the Tempkin isotherm energy constant ($l \text{ mg}^{-1}$) and k_2 is the dimensionless Tempkin isotherm constant.

The results of the fitted parameters to the adsorption isotherms are summarised in Table 5. In general, the experimental data are well correlated for all the equations. According to the fits obtained, none of those two equations can be postulated as definitely better to reproduce the equilibrium data, particularly in the case of phenol. Langmuir fitted well with all the phenol and benzene data with regression coefficients higher than 0.91. Freundlich isotherm are quite well related with for all the data except for the phenol adsorption onto AC-Na ($r^2 = 0.88$) and benzene adsorption on CAC2 ($r^2 = 0.83$). Tempkin gives goods adjustments for all the data except for the phenol adsorption on CAC1 ($r^2 = 0.89$).

The maximum adsorption capacity achieve was 33.84 mg g^{-1} for phenol in CAC3 and 21.20 mg g^{-1} in AC-Na, as it is showed in Table 5. For benzene, the maximum are 38.30 mg g^{-1} in CAC3 and 17.02 mg g^{-1} in AC-Na. These values also correspond with ones of the highest energetic heterogeneity. Respect the results obtained with the Langmuir isotherm, the maximum adsorption capacity for benzene and phenol are achieved for the AC-Na (238 mg g^{-1} and 233 mg g^{-1} , respectively). These values are all quite similar with values detailed in Table 1, presented before as a summary of the liquid adsorption test realised by several authors.

4. CONCLUSIONS

AC obtained with Kraft lignin and chemical activation with sodium hydroxide, potassium hydroxide or phosphoric acid gives as result, essentially microporous AC that adsorb larger amounts of phenol and benzene, compared with the data available in the literature.

The phenol or benzene adsorption data obtained for the AC studied correspond to a pseudo-second-order reaction with good correlations. The adsorption rate constant points to faster adsorption rates for phenol than for benzene in the AC derived from lignin except for CAC2 and CAC3 that are very similar. The AC derived from lignin presents better adsorptions capacities compared with the commercial carbons in both experiments, with phenol and benzene.

The experimental data are well correlated with the three models presented, Freundlich, Langmuir and Tempkin. According to the fits obtained, none of those three equations can be postulated as definitely better to reproduce the equilibrium data, particularly in the case of phenol. Langmuir fitted well the phenol and benzene data adsorption on all the ACs. Freundlich isotherm is quite well related with for all the data except for the phenol adsorption onto AC-Na and benzene adsorption on CAC2. Tempkin gives goods adjustments for all the data except for the phenol adsorption on CAC1.

Maximum adsorption capacity for benzene and phenol are achieved for the AC-Na (238 mg g^{-1} and 233 mg g^{-1} , respectively) that are good values compared with the ones available in the literature. The AC-K and AC-P also showed high adsorption capacities with values greater than 213 mg g^{-1} and

106 mg g⁻¹, respectively, for phenol and 213 mg g⁻¹ and 185 mg g⁻¹, respectively, for benzene.

ACKNOWLEDGEMENTS

Funding for this work was provided by the Spanish Ministry of Science and Technology (MCYT, project PPQ2002-04201-CO2-02, partially funded by the FEDER program of the European Union), and the Catalan Regional Government (Project 2005SGR-00580). This research was also partly made possible by financial support from the European Commission through the ALFA program (project LIGNOCARB-ALFA II 0412 FA FI). V. Torné-Fernández acknowledges the URV for her PhD grant. V. Fierro acknowledges the MCYT and the Universitat Rovira i Virgili (URV) for the financial support of her 'Ramón y Cajal' research contract.

REFERENCES

1. Gonzalez-Serrano, E., Cordero, T., Rodríguez-Mirasol, J., et al., Development of Porosity upon Chemical Activation of Kraft Lignin with ZnCl₂. *Industrial & Engineering Chemical Research*, 1997. 36(11): p. 4832-4838.
2. Rodríguez-Mirasol, J., Cordero, T., and Rodríguez, J.J., Preparation and characterization of activated carbons from eucalyptus kraft lignin. *Carbon*, 1993. 31(1): p. 87-95.
3. Guo, Y. and Rockstraw, D.A., Physical and chemical properties of carbons synthesized from xylan, cellulose, and Kraft lignin by H₃PO₄ activation. *Carbon*, 2006. 44(8): p. 1464-1475.
4. Fierro, V., Torné-Fernández, V., and Celzard, A., Kraft lignin as a precursor for microporous activated carbons prepared by impregnation with ortho-phosphoric acid: Synthesis and textural characterisation. *Microporous and Mesoporous Materials*, 2006. 92(1-3): p. 243-250.
5. Fierro, V., Torné-Fernández, V., and Celzard, A., Highly microporous carbons prepared by activation of Kraft lignin with KOH. *Studies in Surface Science and catalysis*, 2005: p. 607-614.
6. Fierro, V., Torné-Fernández, V., Montané, D., et al. Activated Carbons Prepared from Kraft Lignin by Phosphoric Acid Impregnation. in *Carbon'03*. 2003. Oviedo (Spain).
7. Lin, S.Y. and Lin, I.S., Lignin. *Ullmann's Encyclopedia of industrial chemistry*, ed. S.H. Barbara Elvers, Gail Schulz. Vol. A15. 1990, New York. 305-315.
8. Adler, E., Lignin chemistry-Past, Present and Future. *Wood Science Technology*, 1977. 11: p. 169-218.

9. Northey, R.A. Low-Cost Uses of Lignin, Emerging Technology of Materials and Chemicals from Biomass. in ACS Symposium Series 476. 1992. Washington D.C.
10. Sarkanen, K.V. and Ludwig, C.H., Lignins: Occurrence, Formation, Structure and Reactions. 1971, New York: Wiley-Interscience.
11. Ballerini, A., Ewert, R., and Solís, M., Utilización de Ligninas en la formulación de adhesivos para tableros contrachapados. Maderas: Ciencia y Tecnología, 1998. 1(1).
12. Crawford, D.L., Pometto, A.L., and Crawford, R.L., Production of useful modified lignin polymers by bioconversion of lignocellulose with *Streptomyces*. Biotechnology Advances, 1984. 2(2): p. 217-232.
13. Goheen, D.W. and Hoyt, C.H., Lignin. Third Edition ed. Kirk-Othmer Encyclopedia of Chemical Technology, ed. I. John Wiley & Sons. Vol. 14. 1981, New York: Wiley-Interscience. 294-313.
14. Mansilla, H., Lizama, C., Gutarra, A., et al., Tratamiento de residuos líquidos de la industria de celulosa y textil.
15. Fierro, V., Torné-Fernández, V., Montané, D., et al., Study of the decomposition of kraft lignin impregnated with orthophosphoric acid. Thermochemica Acta, 2005. 433(1-2): p. 142-148.
16. Fierro, V., Torné-Fernández, V., and Celzard, A., Methodical study of the chemical activation of Kraft lignin with KOH and NaOH. Microporous and Mesoporous Materials, 2006. Submitted.
17. Ahmadpour, A. and Do, D.D., The preparation of active carbons from coal by chemical and physical activation. Carbon, 1996. 34(4): p. 471-479.
18. Otowa, T., Nojima, Y., and Miyazaki, T., Development of KOH activated high surface area carbon and its application to drinking water purification. Carbon, 1997. 35(9): p. 1315-1319.

19. Liang, C., Wei, Z., Xin, Q., et al., Ammonia synthesis over Ru/C catalysts with different carbon supports promoted by barium and potassium compounds. *Applied Catalysis A: General*, 2001. 208(1-2): p. 193-201.
20. Lozano-Castelló, D., Lillo-Rodenas, M.A., Cazorla-Amorós, D., et al., Preparation of activated carbons from Spanish anthracite: I. Activation by KOH. *Carbon*, 2001. 39(5): p. 741-749.
21. Frackowiak, E. and Beguin, F., Electrochemical storage of energy in carbon nanotubes and nanostructured carbons. *Carbon*, 2002. 40(10): p. 1775-1787.
22. Activated carbon compendium. A collection of papers from the journal *Carbon* 1996-2000. 1^a ed, ed. H. Marsh. 2001, North Shields (UK): Elsevier.
23. Lin, S.Y., Jr., S.E.L., and LignoTech USA, I., Lignin, in *Kirk-Othmer Encyclopedia of Chemical Technology*. 2000.
24. Basso, M.C. and Cukierman, A.L., Arundo donax - Based activated carbons for aqueous-phase adsorption of volatile organic compounds. *Industrial Engineering Chemical Research*, 2005. 44: p. 2091-2100.
25. Alvarez, P.M., Garcia-Araya, J.F., Beltran, F.J., et al., Ozonation of activated carbons: Effect on the adsorption of selected phenolic compounds from aqueous solutions. *Journal of Colloid and Interface Science*, 2005. 283(2): p. 503-512.
26. Ariyadejwanich, P., Tanthapanichakoon, W., Nakagawa, K., et al., Preparation and characterization of mesoporous activated carbon from waste tires. *Carbon*, 2003. 41(1): p. 157-164.
27. Ayranci, E. and Duman, O., Adsorption behaviors of some phenolic compounds onto high specific area activated carbon cloth. *Journal of Hazardous Materials*, 2005. 124(1-3): p. 125-132.

28. Bae, S.-D., Sagehashi, M., and Sakoda, A., Activated carbon membrane with filamentous carbon for water treatment. *Carbon*, 2003. 41(15): p. 2973-2979.
29. Brasquet, C., Rousseau, B., Estrade-Szwarckopf, H., et al., Observation of activated carbon fibres with SEM and AFM correlation with adsorption data in aqueous solution. *Carbon*, 2000. 38(3): p. 407-422.
30. Chen, X., Jeyaseelan, S., and Graham, N., Physical and chemical properties study of the activated carbon made from sewage sludge. *Waste Management*, 2002. 22(7): p. 755-760.
31. de Oliveira Pimenta, A.C. and Kilduff, J.E., Oxidative coupling and the irreversible adsorption of phenol by graphite. *Journal of Colloid and Interface Science*, 2005. In Press, Corrected Proof.
32. El-Hendawy, A.-N.A., Influence of HNO₃ oxidation on the structure and adsorptive properties of corncob-based activated carbon. *Carbon*, 2003. 41(4): p. 713-722.
33. El-Hendawy, A.-N.A., Surface and adsorptive properties of carbons prepared from biomass. *Applied Surface Science*, 2005. 252(2): p. 287-295.
34. Furuya, E.G., Chang, H.T., Miura, Y., et al., A fundamental analysis of the isotherm for the adsorption of phenolic compounds on activated carbon. *Separation and Purification Technology*, 1997. 11: p. 69-78.
35. Galiatsatou, P., Metaxas, M., Arapoglou, D., et al., Treatment of olive mill waste water with activated carbons from agricultural by-products. *Waste Management*, 2002. 22(7): p. 803-812.
36. Ghiaci, M., Abbaspur, A., Kia, R., et al., Equilibrium isotherm studies for the sorption of benzene, toluene, and phenol onto organo-zeolites and as-synthesized MCM-41. *Separation and Purification Technology*, 2004. 40(3): p. 217-229.

37. Girgis, B.S. and El-Hendawy, A.-N.A., Porosity development in activated carbons obtained from date pits under chemical activation with phosphoric acid. *Microporous and Mesoporous Materials*, 2002. 52(2): p. 105-117.
38. Gonzalez-Serrano, E., Cordero, T., Rodriguez-Mirasol, J., et al., Removal of water pollutants with activated carbons prepared from H₃PO₄ activation of lignin from kraft black liquors. *Water Research*, 2004. 38(13): p. 3043-3050.
39. Hsieh, C.-T. and Teng, H., Liquid-Phase Adsorption of Phenol onto Activated Carbons Prepared with Different Activation Levels. *Journal of Colloid and Interface Science*, 2000. 230(1): p. 171-175.
40. Hsieh, C.-T. and Teng, H., Influence of mesopore volume and adsorbate size on adsorption capacities of activated carbons in aqueous solutions. *Carbon*, 2000. 38(6): p. 863-869.
41. Hu, Z. and Srinivasan, M.P., Preparation of high-surface-area activated carbons from coconut shell. *Microporous and Mesoporous Materials*, 1999. 27(1): p. 11-18.
42. Hu, Z., Srinivasan, M.P., and Ni, Y., Novel activation process for preparing highly microporous and mesoporous activated carbons. *Carbon*, 2001. 39(6): p. 877-886.
43. Juang, R.-S., Lin, S.-H., and Cheng, C.-H., Liquid-phase adsorption and desorption of phenol onto activated carbons with ultrasound. *Ultrasonics Sonochemistry*, 2005. In Press, Corrected Proof.
44. Juang, R.-S., Wu, F.-C., and Tseng, R.-L., Adsorption Isotherms of Phenolic Compounds from Aqueous Solutions onto Activated Carbon Fibers. *J. Chem. Eng. Data*, 1996. 41(3): p. 487-492.

45. Juang, R.-S., Wu, F.-C., and Tseng, R.-L., Mechanism of Adsorption of Dyes and Phenols from Water Using Activated Carbons Prepared from Plum Kernels. *Journal of Colloid and Interface Science*, 2000. 227(2): p. 437-444.
46. Juang, R.-S., Wu, F.-C., and Tseng, R.-L., Characterization and use of activated carbons prepared from bagasses for liquid-phase adsorption. *Colloids and Surfaces A: Physicochemical and Engineering Aspects*, 2002. 201(1-3): p. 191-199.
47. Katoh, M., Takao, H., Abe, N., et al., Adsorption Selectivity of FSM-16 for Several Organic Compounds. *Journal of Colloid and Interface Science*, 2001. 242(2): p. 294-299.
48. Khan, A.R., Al-Bahri, T.A., and Al-Haddad, A., Adsorption of phenol based organic pollutants on activated carbon from multi-component dilute aqueous solutions. *Water Research*, 1997. 31(8): p. 2102-2112.
49. Khan, A.R., Ataullah, R., and Al-Haddad, A., Equilibrium Adsorption Studies of Some Aromatic Pollutants from Dilute Aqueous Solutions on Activated Carbon at Different Temperatures. *Journal of Colloid and Interface Science*, 1997. 194(1): p. 154-165.
50. Khezami, L., Chetouani, A., Taouk, B., et al., Production and characterisation of activated carbon from wood components in powder: Cellulose, lignin, xylan. *Powder Technology*, 2005. In Press, Corrected Proof.
51. Klimenko, N., Winther-Nielsen, M., Smolin, S., et al., Role of the physico-chemical factors in the purification process of water from surface-active matter by biosorption. *Water Research*, 2002. 36(20): p. 5132-5140.
52. Koh, M. and Nakajima, T., Adsorption of aromatic compounds on CxN-coated activated carbon. *Carbon*, 2000. 38(14): p. 1947-1954.

53. Koh, S.-M. and Dixon, J.B., Preparation and application of organo-minerals as sorbents of phenol, benzene and toluene. *Applied Clay Science*, 2001. 18(3-4): p. 111-122.
54. Kumar, A., Kumar, S., and Kumar, S., Adsorption of resorcinol and cathecol on granular activated carbon: equilibrium and kinetics. *Carbon*, 2003. 41: p. 3015-3025.
55. Laszlo, K., Bota, A., Nagy, L.G., et al., Porous carbon from polymer waste materials. *Colloids and Surfaces A: Physicochemical and Engineering Aspects*, 1999. 151(1-2): p. 311-320.
56. Laszlo, K., Bota, A., and Nagy, L.G., Characterization of activated carbons from waste materials by adsorption from aqueous solutions. *Carbon*, 1997. 35(5): p. 593-598.
57. Laszlo, K. and Szucs, A., Surface characterization of polyethyleneterephthalate (PET) based activated carbon and the effect of pH on its adsorption capacity from aqueous phenol and 2,3,4-trichlorophenol solutions. *Carbon*, 2001. 39(13): p. 1945-1953.
58. Lee, K.M. and Lim, P.E., Bioregeneration of powdered activated carbon in the treatment of alkyl-substituted phenolic compounds in simultaneous adsorption and biodegradation processes. *Chemosphere*, 2005. 58(4): p. 407-416.
59. Leng, C.-C. and Pinto, N.G., Effects of surface properties of activated carbons on adsorption behavior of selected aromatics. *Carbon*, 1997. 35(9): p. 1375-1385.
60. Moreno-Castilla, C., Rivera-Utrilla, J., López-Ramón, M.V., et al., Adsorption of some substituted phenols on activated carbons from a bituminous coal. *Carbon*, 1995. 33(6): p. 845-851.
61. Nakagawa, K., Namba, A., Mukai, S.R., et al., Adsorption of phenol and reactive dye from aqueous solution on activated carbons derived from solid wastes. *Water Research*, 2004. 38(7): p. 1791-1798.

62. Namane, A., Mekarzia, A., Benrachedi, K., et al., Determination of the adsorption capacity of activated carbon made from coffee grounds by chemical activation with $ZnCl_2$ and H_3PO_4 . *Journal of Hazardous Materials*, 2005. 119(1-3): p. 189-194.
63. Nevskaia, D.M., Castillejos-Lopez, E., Guerrero-Ruiz, A., et al., Effects of the surface chemistry of carbon materials on the adsorption of phenol-aniline mixtures from water. *Carbon*, 2004. 42(3): p. 653-665.
64. Nevskaia, D.M., Santianes, A., Munoz, V., et al., Interaction of aqueous solutions of phenol with commercial activated carbons: an adsorption and kinetic study. *Carbon*, 1999. 37(7): p. 1065-1074.
65. Nevskaia, D.M., Santianes, A., Muñoz, V., et al., Interaction of aqueous solutions of phenol with commercial activated carbons: an adsorption and kinetic study. *Carbon*, 1999. 37: p. 1065-1074.
66. Okolo, B., Park, C., and Keane, M.A., Interaction of Phenol and Chlorophenols with Activated Carbon and Synthetic Zeolites in Aqueous Media. *Journal of Colloid and Interface Science*, 2000. 226(2): p. 308-317.
67. Otero, M., Rozada, F., Calvo, L.F., et al., Elimination of organic water pollutants using adsorbents obtained from sewage sludge. *Dyes and Pigments*, 2003. 57(1): p. 55-65.
68. Otero, M., Zabkova, M., and Rodrigues, A.E., Adsorptive purification of phenol wastewaters: Experimental basis and operation of a parametric pumping unit. *Chemical Engineering Journal*, 2005. 110(1-3): p. 101-111.
69. Podkoscielny, P., Dabrowski, A., and Marijuk, O.V., Heterogeneity of active carbons in adsorption of phenol aqueous solutions. *Applied Surface Science*, 2003. 205(1-4): p. 297-303.

70. Rio, S., Faur-Brasquet, C., Coq, L.L., et al., Experimental design methodology for the preparation of carbonaceous sorbents from sewage sludge by chemical activation--application to air and water treatments. *Chemosphere*, 2005. 58(4): p. 423-437.
71. Roostaei, N. and Tezel, F.H., Removal of phenol from aqueous solutions by adsorption. *Journal of Environmental Management*, 2004. 70(2): p. 157-164.
72. Sabio, E., González-Martín, M.L., Ramiro, A., et al., Influence of the regeneration temperature on the phenols adsorption on activated carbon. *Journal of Colloid and Interface Science*, 2001. 242: p. 31-35.
73. Salame, I.I. and Bandosz, T.J., Role of surface chemistry in adsorption of phenol on activated carbons. *Journal of Colloid and Interface Science*, 2003. 264(2): p. 307-312.
74. San Miguel, Guillermo, Fowler, G.D., and Sollars, C.J., A study of the characteristics of activated carbons produced by steam and carbon dioxide activation of waste tyre rubber. *Carbon*, 2003. 41(5): p. 1009-1016.
75. Shu, H.-T., Li, D., Scala, A.A., et al., Adsorption of small organic pollutants from aqueous streams by aluminosilicate-based microporous materials. *Separation and Purification Technology*, 1997. 11(1): p. 27-36.
76. Singh, B., Madhusudhanan, S., Dubey, V., et al., Active carbon for removal of toxic chemicals from contaminated water. *Carbon*, 1996. 34(3): p. 327-330.
77. Streat, M., Patrick, J.W., and Perez, M.J.C., Sorption of phenol and para-chlorophenol from water using conventional and novel activated carbons. *Water Research*, 1995. 29(2): p. 467-472.
78. Tai, H.-S. and Jou, C.-J.G., Application of granular activated carbon packed-bed reactor in microwave radiation field to treat phenol. *Chemosphere*, 1999. 38(11): p. 2667-2680.

79. Tamon, H., Atsushi, M., and Okazaki, M., On Irreversible Adsorption of Electron-Donating Compounds in Aqueous Solution. *Journal of Colloid and Interface Science*, 1996. 177(2): p. 384-390.
80. Tancredi, N., Medero, N., Moller, F., et al., Phenol adsorption onto powdered and granular activated carbon, prepared from Eucalyptus wood. *Journal of Colloid and Interface Science*, 2004. 279(2): p. 357-363.
81. Tanthapanichakoon, W., Ariyadejwanich, P., Japthong, P., et al., Adsorption-desorption characteristics of phenol and reactive dyes from aqueous solution on mesoporous activated carbon prepared from waste tires. *Water Research*, 2005. 39(7): p. 1347-1353.
82. Terzyk, A.P., Molecular properties and intermolecular forces--factors balancing the effect of carbon surface chemistry in adsorption of organics from dilute aqueous solutions. *Journal of Colloid and Interface Science*, 2004. 275(1): p. 9-29.
83. Tryba, B., Morawski, A.W., and Inagaki, M., Application of TiO₂-mounted activated carbon to the removal of phenol from water. *Applied Catalysis B: Environmental*, 2003. 41(4): p. 427-433.
84. Tseng, R.-L., Wu, F.-C., and Juang, R.-S., Liquid-phase adsorption of dyes and phenols using pinewood-based activated carbons. *Carbon*, 2003. 41(3): p. 487-495.
85. Villacanas, F., Pereira, M.F.R., Orfao, J.J.M., et al., Adsorption of simple aromatic compounds on activated carbons. *Journal of Colloid and Interface Science*, 2005. In Press, Corrected Proof.
86. Warhurst, A.M., McConnachie, G.L., and Pollard, S.J.T., Characterisation and applications of activated carbon produced from *Moringa oleifera* seed husks by single-step steam pyrolysis. *Water Research*, 1997. 31(4): p. 759-766.

87. Wu, F.-C. and Tseng, R.-L., Preparation of highly porous carbon from fir wood by KOH etching and CO₂ gasification for adsorption of dyes and phenols from water. *Journal of Colloid and Interface Science*, 2005. In Press, Corrected Proof.
88. Wu, F.-C., Tseng, R.-L., and Hu, C.-C., Comparisons of pore properties and adsorption performance of KOH-activated and steam-activated carbons. *Microporous and Mesoporous Materials*, 2005. 80(1-3): p. 95-106.
89. Wu, F.-C., Tseng, R.-L., Hu, C.-C., et al., Physical and electrochemical characterization of activated carbons prepared from firwoods for supercapacitors. *Journal of Power Sources*, 2004. 138: p. 351-359.
90. Wu, F.-C., Tseng, R.-L., and Juang, R.-S., Pore structure and adsorption performance of the activated carbons prepared from plum kernels. *Journal of Hazardous Materials*, 1999. 69(3): p. 287-302.
91. Wu, F.-C., Tseng, R.-L., and Juang, R.-S., Preparation of highly microporous carbons from fir wood by KOH activation for adsorption of dyes and phenols from water. *Separation and Purification Technology*, 2005. In Press, Corrected Proof.
92. Wu, F.-C., Tseng, R.-L., and Juang, R.-S., Comparisons of porous and adsorption properties of carbons activated by steam and KOH. *Journal of Colloid and Interface Science*, 2005. 283(1): p. 49-56.
93. Hindarso, H., Ismadji, S., Wicaksana, F., et al., Adsorption of benzene and toluene from aqueous solution onto granular activated carbon. *Journal of Chemical and Engineering Data*, 2001. 46(4): p. 788-791.
94. Toles, C.A., Marshall, W.E., and Johns, M.M., Granular activated carbons from nutshells for the uptake of metals and organic compounds. *Carbon*, 1997. 35(9): p. 1407-1414.

95. Toles, C.A., Marshall, W.E., Johns, M.M., et al., Acid-activated carbons from almond shells: physical, chemical and adsorptive properties and estimated cost of production. *Bioresource Technology*, 2000. 71(1): p. 87-92.
96. Chiou, C.T., Porter, P.E., and Schmedding, D.W., Partition equilibriums of nonionic organic compounds between soil organic matter and water. *Environmental science and technology*, 1983. 17(4): p. 227-231.
97. Chatzopoulos, D. and Varma, A., Aqueous-phase adsorption and desorption of toluene in activated carbon fixed beds: Experiments and model. *Chemical Engineering Science*, 1995. 50(1): p. 127-141.
98. Lillo-Rodenas, M.A., Cazorla-Amorós, D., and Linares-Solano, A., Behaviour of activated carbons with different pore size distributions and surface oxygen groups for benzene and toluene adsorption at low concentrations. *Carbon*, 2005. 43(8): p. 1758-1767.
99. Lillo-Rodenas, M.A., Cazorla-Amorós, D., and Linares-Solano, A., Behaviour of activated carbons with different pore size distributions and surface oxygen groups for benzene and toluene adsorption at low concentrations. *Carbon*, 2005. 43(8): p. 1758-1767.
100. Dimotakis, E.D., Cal, M.P., Economy, J., et al., Chemically Treated Activated Carbon Cloths for Removal of Volatile Organic Carbons from Gas Streams: Evidence for Enhanced Physical Adsorption. *Environmental Science and Technology*, 1995. 29(7): p. 1876-1880.
101. Benkhedda, J., Jaubert, J.-N., Barth, D., et al., Experimental and Modeled Results Describing the Adsorption of Toluene onto Activated Carbon. *J. Chem. Eng. Data*, 2000. 45(4): p. 650-653.
102. Inc., N.A., www.norit-america.com.
103. Rouquerol, F., Rouquerol, J., and Sing, K.S.W., *Adsorption by Powders and Porous Solids. Principles, Methods and Applications*. 1999, San Diego: Academic Press.

104. Setoyama, N., Suzuki, T., and Kaneko, K., Simulation study on the relationship between a high resolution $[\alpha]$ -plot and the pore size distribution for activated carbon. *Carbon*, 1998. 36(10): p. 1459-1467.
105. Kruk, M., Li, Z., Jaroniec, M., et al., Nitrogen Adsorption Study of Surface Properties of Graphitized Carbon Blacks. *Langmuir*, 1999. 15(4): p. 1435-1441.
106. Fogler, H.S., Elements of chemical reaction engineering. 2nd edition ed. 1992, New Jersey: Prentice-Hall, Inc.
107. Lei, S., Miyamoto, J.-I., Kanoh, H., et al., Enhancement of the methylene blue adsorption rate for ultramicroporous carbon fiber by addition of mesopores. *Carbon*, 2006. In Press, Corrected Proof.
108. Sathishkumar, M., Binupriya, A.R., Kavitha, D., et al., Kinetic and isothermal studies on liquid-phase adsorption of 2,4-dichlorophenol by palm pith carbon. *Bioresource Technology*, 2006. In Press, Corrected Proof.
109. Bridelli, M.G., Ciati, A., and Crippa, P.R., Binding of chemicals to melanins re-examined: Adsorption of some drugs to the surface of melanin particles. *Biophysical Chemistry*, 2006. 119(2): p. 137-145.
110. Chen, B., Hui, C.W., and McKay, G., Film-Pore Diffusion Modeling for the Sorption of Metal Ions from Aqueous Effluents onto Peat. *Water Research*, 2001. 35(14): p. 3345-3356.
111. Bartholomew, C.H., Mechanisms of catalyst deactivation. *Applied Catalysis A: General*, 2001. 212(1-2): p. 17-60.

Sorption study of organic compounds on highly microporous carbons prepared from Kraft lignin.

V. Torné-Fernández, V. Fierro.

Table 1. State of the art in the phenol and benzene adsorptions on different materials in liquid systems.

Type of AC	Activating agent	Co (ppm)	m _{AC} (mg)	S _{BET} (m ² /g)	V _{microp} (cm ³ /g)	q _{Ph} q _B		Ref.
						(mg/g)		
AC with microorganism		1000	1000			188.2		[24]
AC		800				75.8		[25]
		100	100	803	-	24.0	39.0	[26]
ACF		100	500			160.0		[27]
Almond shells	H ₃ PO ₄	80	100	1416	-	9.0		[28]
Arundo-donax	H ₃ PO ₄	78	200	1194	0.660	22.7		[23]
Bagasses	Vapour		600			308.0		[29]
Bitumen			100	1114	0.130	218.0		[30]
	CO ₂	500	1200			240.0		[31]
Charsorb CP-1300			200	-	-	156.0		[32]
Coffee grain		20				3.5		[33]
Comercial	-					10.6		[34]
Carbon		>300	50			197.6		[35]
		500	800			221.5		[36]
						451.7		[37]
			100	982	0.304	291.7		[38]
		250		1790	0.773	300.0		[39]
		200				309.0		[40]
		50	300			74.2		[41]
		500	1200			131.8		[42]
		100	50			190.0		[43]
		2000	500			142.9		[44]
		5 · 10 ⁶				301.2		[45]
		998	2500			188.2		[46]
			50			258.8		[47]
		400	50000			220.0		[48]
		235	100			207.4		[49]
			100			80.0		[50]
		250				205.0		[51]
			2000			188.2		[52]
		1505	100	1654	0.651	131.8		[53]

		941	50	-	-	117.6		[54]
		550	800	900	-		221.5	[55]
Coconut shell		498.8	1000			141.2		[56]
		998	1000			178.8		[56]
		47	50			45.7		[57]
	ZnCl ₂	200	50			210.0		[58]
	Vapour	1600	100			571.0		[59]
Corn cobs	KOH		50			153.0		[60]
	Vapour	1000	50			178.2		[61]
Date pits	H ₃ PO ₄	100	200			166.0		[62]
Eucalyptus wood		200	100			148.0		[63]
Filtratorb F400		500				169.1		[65]
Firwood		94110	100			240.6		[66]
	Vapour	94110	100	1131	0.056	831.0		[67]
	KOH	200	600			23.1		[68]
	KOH	94	100			257.9		[69]
	Vapour		100			255.9		[69]
	KOH+CO ₂	200	600			274.8		[70]
Garbage waste	Vapour			700	0.280	300.0		[71]
Grain shells			100			209.2		[72]
Graphite			100	310	0.057	85.6		[38]
		1000				4.0		[73]
Hydro-Anthrasit H		1000		1090	-	112.9	258.0	[74]
Lignin	H ₃ PO ₄		10	1459	0.820	170.0		[75]
Molecular sieves		110	100	-	-	59.4	112.9	[76]
Moringa oleifera seed husks		4706	500			235.3		[77]
Olive mill	Vapour+N ₂	1500	200			91.7		[78]
Pecan shell	H ₃ PO ₄	80	100	1267	-		7.8	[79]
PET	Vapour		100			263.5		[80]
	N ₂	470	50			225.9		[81]
Pistachio	KOH	94	100			285.2		[69]
	Vapour	94	100			242.8		[69]
		94110	100			728.3		[82]
Plum kernels		376				257.0		[83]
			100	1160	-	257.4		[84]
Pneumatics						180.0		[85]
			60			200.0		[86]
Rubber	Vapor/CO ₂ +N ₂	235	600			106.0		[87]
Sludge	H ₂ SO ₄	100	500	3	-	54.0		[88]
	H ₂ SO ₄	100				42.0		[89]
Soil		1600		-	-	0.5		[90]
Straw		100	500			197.6		[91]
Wood		100	30			320.0		[92]

Sorption study of organic compounds on highly microporous carbons prepared from Kraft lignin.

V. Torné-Fernández, V. Fierro.

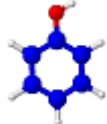
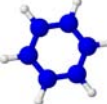
Table 2. Physical properties of the AC used.

	S_{BET}	$V_{0.99}$	$V_{\alpha,\text{micro}}$	$V_{\alpha,\text{super}}$	V_{meso}	Acidic Groups (meq H ⁺ /gAC)	Basic Groups (meq OH ⁻ /gAC)
	(m ² /g)	(cm ³ /g)					
AC-Na	2340	1.338	1.018	0.941	0.428	11.9	16.6
AC-K	2920	1.583	1.332	1.324	0.384	20.4	5.8
AC-P	940	0.442	0.377	0.261	0.118	7.5	0.2
CAC1	1350	0.713	0.458	0.319	0.235	2.6	0.5
CAC2	620	0.637	0.185	0.100	0.407	7.9	1.2
CAC3	1020	0.625	0.334	0.182	0.246	5.0	2.1

Sorption study of organic compounds on highly microporous carbons prepared from Kraft lignin.

V. Torné-Fernández, V. Fierro.

Table 3. Properties of adsorptive molecules.

Molecule	Structure	MW ^a (g/mol)	P _v ^b (mmHg)	T _b ^c (°C)	Solubility (%)	Size ^d (Å)
Ph		94.1	0.4	182	8.3	6
B		78.1	100.8	80.1	0.2	5

MW^a. Molecular weight.

P_v^b. Vapour pressure at 25°C.

T_b^c. Normal boiling point.

Size^a. Size calculated with ACDLABS 8.0.

Sorption study of organic compounds on highly microporous carbons prepared from Kraft lignin.

V. Torné-Fernández, V. Fierro.

Table 4. Kinetic parameters estimated in the adsorption of phenol or benzene on different adsorbates for an initial concentration of 100 ppm.

Adsorbate	General order n (equation 3)				Pseudo-second order (equation 4)
	n	k (g mg ⁻¹ min ⁻¹)	r ²	q _{e,max} (mg g ⁻¹)	k' (g mg ⁻¹ min ⁻¹)
Solute: Phenol					
AC-Na	2.4	7.24	0.98	169.2	5.16
AC-K	2.4	1.30	0.96	165.0	1.54
AC-P	2.1	1.19	0.96	60.6	1.24
CAC1	2.5	2.78	0.97	95.7	3.15
CAC2	2.0	0.11	0.99	74.4	0.46
CAC3	2.2	0.02	0.95	95.3	0.42
Solute: Benzene					
AC-Na	2.1	0.65	0.95	20.1	0.72
AC-K	1.7	0.34	0.98	19.7	0.13
AC-P	2.2	0.40	0.99	7.9	0.56
CAC1	2.3	0.20	0.94	10.6	0.37
CAC2	2.5	0.17	0.96	8.2	0.39
CAC3	2.5	0.07	0.96	9.5	0.49

Sorption study of organic compounds on highly microporous carbons prepared from Kraft lignin.

V. Torné-Fernández, V. Fierro.

Table 5. Isotherms constants for phenol and benzene sorption onto different AC.

	Freundlich			Langmuir				Tempkin		
	k_f	n	r^2	Q_0	b	R_L	r^2	k_1	k_2	r^2
Phenol										
AC-Na	21.20	2.08	0.99	238.10	0.004	0.7	0.97	37.93	0.57	0.97
AC-K	12.96	1.46	0.96	212.77	0.005	0.7	0.97	48.25	0.39	0.98
AC-P	11.73	2.26	0.95	106.38	0.009	0.5	0.97	24.69	0.30	0.96
CAC1	32.48	3.60	0.91	105.26	0.009	0.5	0.98	19.58	2.62	0.89
CAC2	24.58	4.38	0.97	73.53	0.014	0.4	0.98	12.27	2.75	0.98
CAC3	33.84	3.09	0.94	135.14	0.007	0.6	0.98	26.44	1.76	0.97
Benzene										
AC-Na	17.02	1.83	0.99	232.558	0.004	0.7	0.99	48.845	0.37	0.98
AC-K	11.63	1.51	0.99	212.77	0.005	0.7	0.97	45.36	0.33	0.98
AC-P	5.70	1.59	0.97	185.19	0.005	0.7	0.85	39.00	0.12	0.93
CAC1	32.90	2.25	0.93	212.77	0.005	0.7	0.93	39.81	1.45	0.98
CAC2	17.40	2.34	0.99	76.92	0.013	0.4	0.97	22.94	0.78	0.96
CAC3	38.30	2.44	0.93	175.44	0.006	0.6	0.99	36.85	1.82	0.93

Captions of the figures

Figure 1. Experimental data for phenol adsorption kinetic on different AC obtained at 25°C with a initial 100 ppm solution.

Figure 2. Experimental data for benzene adsorption kinetic on different AC obtained at 25°C with a initial 100 ppm solution.

Figure 3. Adsorption capacities for phenol and benzene on different AC related with the supermicropore and mesoporo volume.

Figure 4. Adsorption isotherm for phenol on different ACs at 25°C and its fitted Langmuir isotherm.

Figure 5. Adsorption isotherm for benzene on different ACs at 25°C and its fitted Langmuir isotherm.

Sorption study of organic compounds on highly microporous carbons prepared from Kraft lignin.

V. Torné-Fernández, V. Fierro.

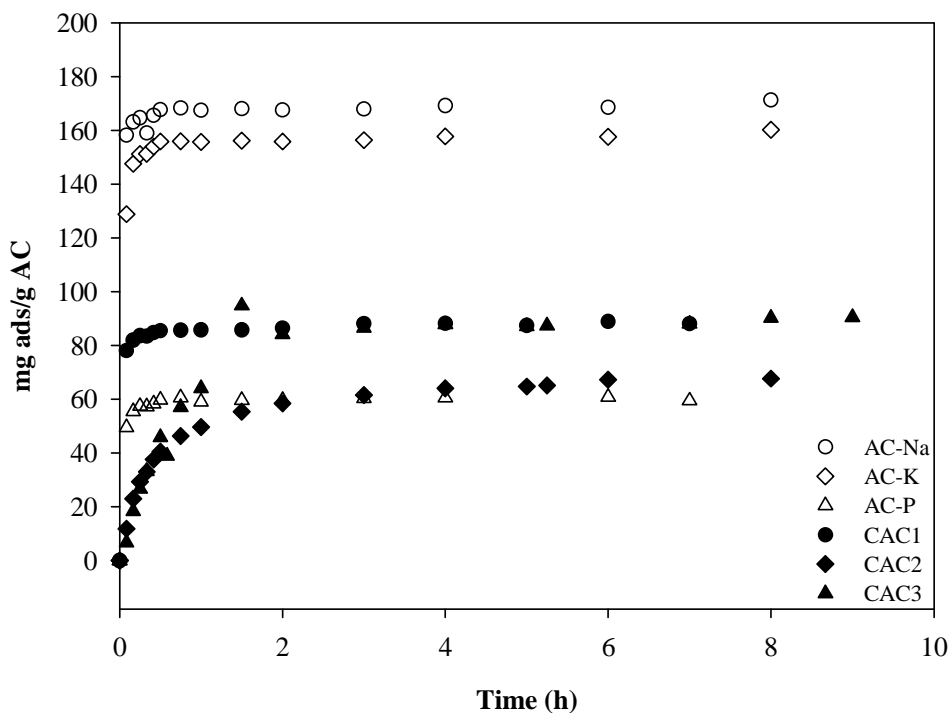


Figure 1
Torné-Fernández, V.; et.al

Sorption study of organic compounds on highly microporous carbons prepared from Kraft lignin.

V. Torné-Fernández, V. Fierro.

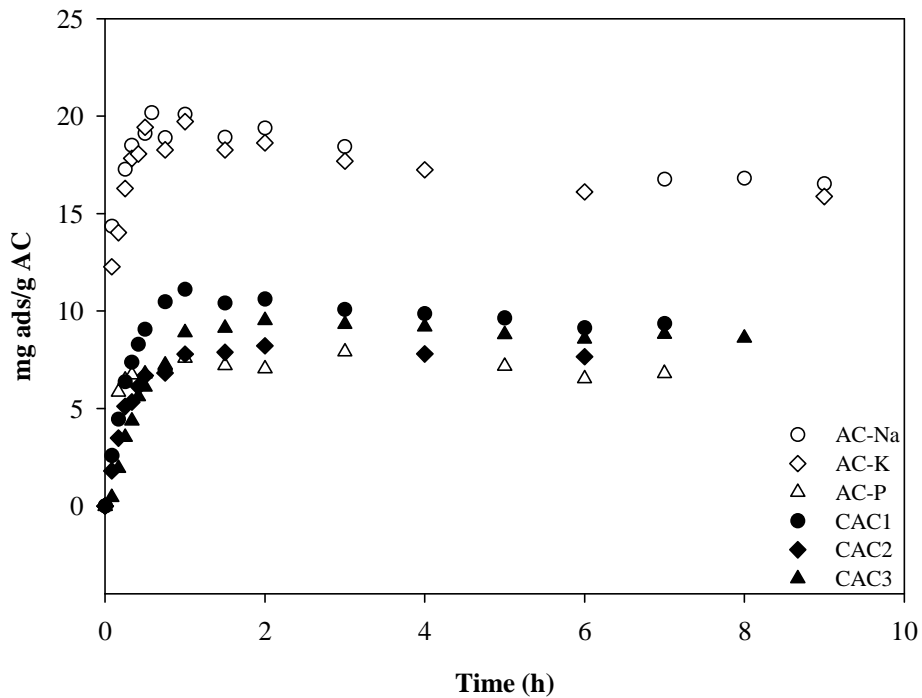


Figure 2
Torné-Fernández, V.; et.al

Sorption study of organic compounds on highly microporous carbons prepared from Kraft lignin.

V. Torné-Fernández, V. Fierro.

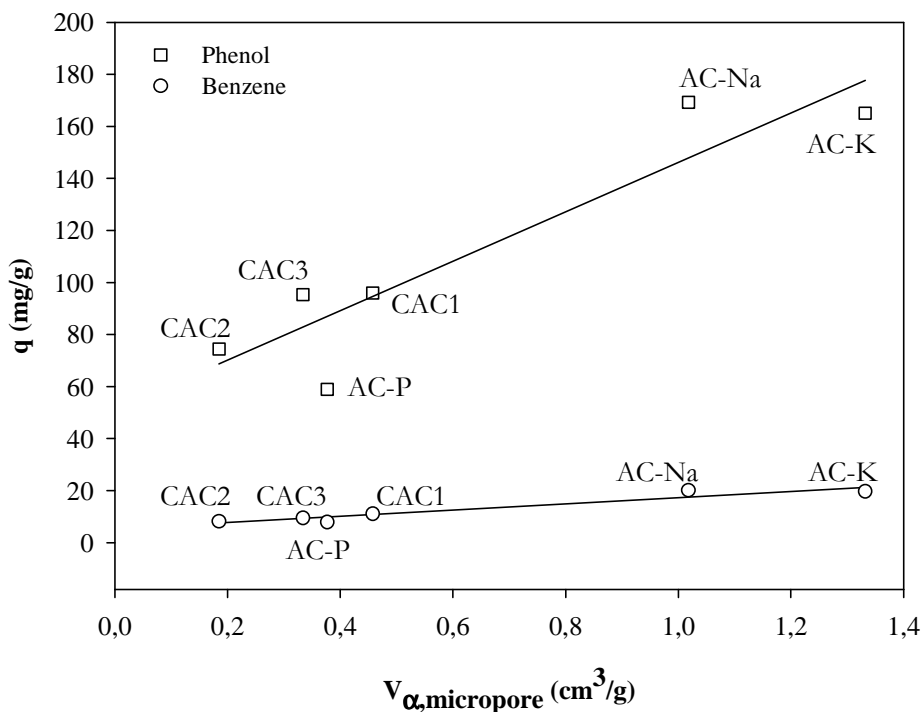


Figure 3
Torné-Fernández, V.; et.al

Sorption study of organic compounds on highly microporous carbons prepared from Kraft lignin.

V. Torné-Fernández, V. Fierro.

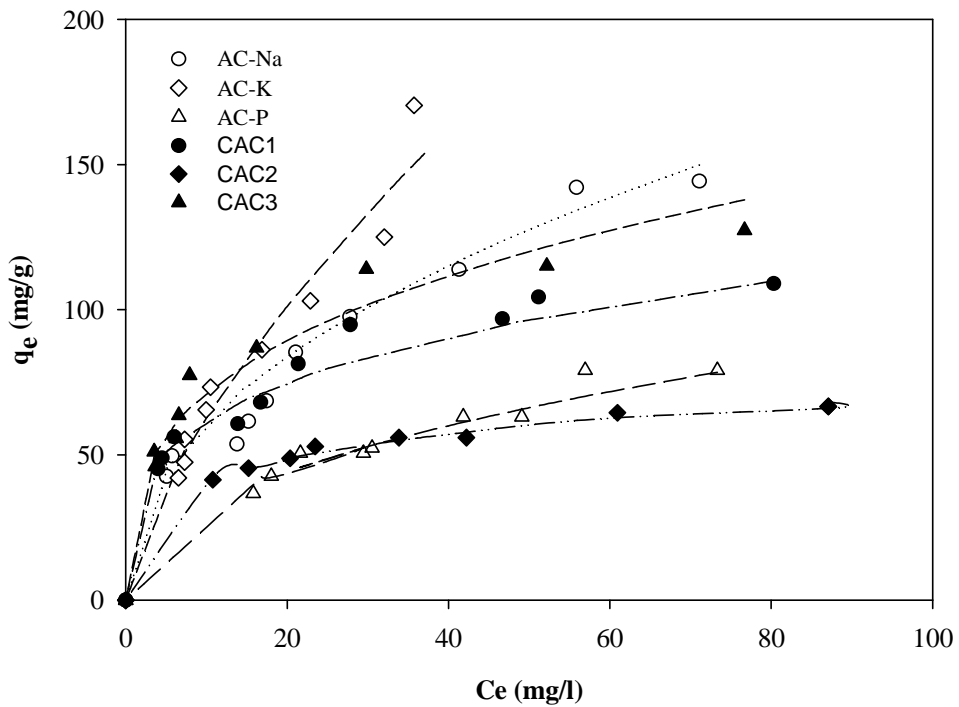


Figure 4
Torné-Fernández, V.; et.al

Sorption study of organic compounds on highly microporous carbons prepared from Kraft lignin.

V. Torné-Fernández, V. Fierro.

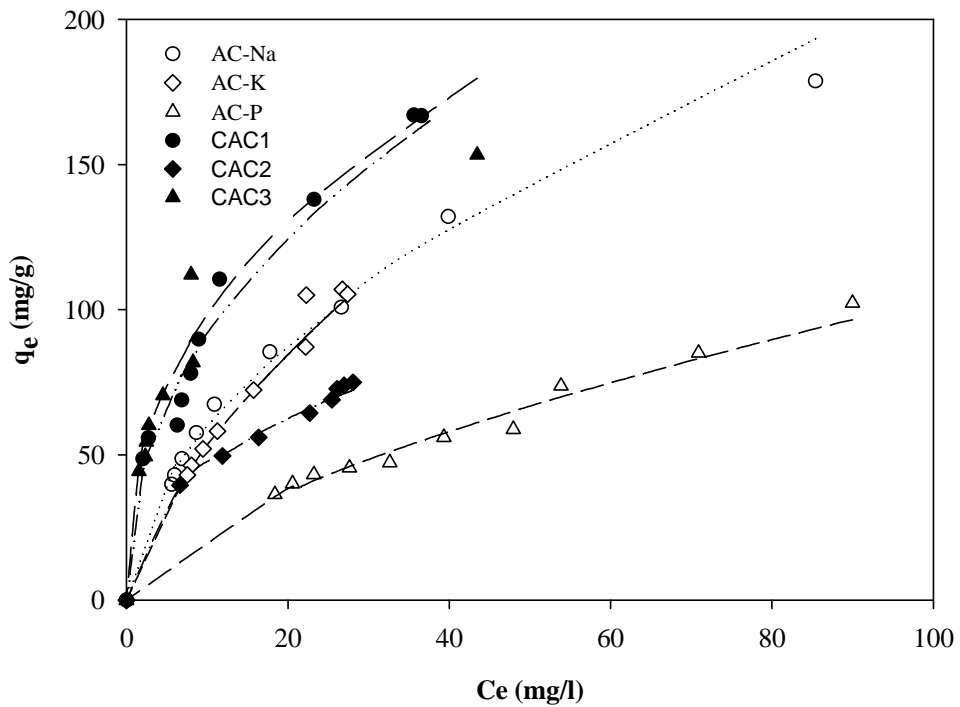


Figure 5
Torné-Fernández, V.; et.al

5.2.4. Polymeric composite membranes based on carbon/PSf

Este artículo se ha publicado en Journal of Membrana Science en 2006 en el volumen 273, páginas 38 a 46.

Otros trabajos relacionados se presentan en el Anexo F donde se presenta el póster “Enzymatic composite membranes based on carbon/polysulfone” publicado en el congreso Engineering with membranes: medical and biological applications.



Available online at www.sciencedirect.com



Journal of Membrane Science 273 (2006) 38–46

Journal of
MEMBRANE
SCIENCE

www.elsevier.com/locate/memsci

Polymeric composite membranes based on carbon/PSf

C. Torras, V. Torné, V. Fierro, D. Montané, R. Garcia-Valls*

*Grup de Biopolímers Vegetals, Departament d'Enginyeria Química, Universitat Rovira i Virgili,
Av. Països Catalans 26, 43007 Tarragona, Catalonia, Spain*

Received 30 June 2005; received in revised form 30 September 2005; accepted 6 October 2005
Available online 29 November 2005

Abstract

Enzymatic membrane reactors were obtained from polymeric membranes and activated carbon, and used for oligosaccharide purification. The activated carbon was used to adsorb the enzyme, directly or via a metal ion as intermediate. We studied the adsorption capacity of two activated carbons (a commercial carbon and a home-made one) and the formation of the complex. In a second step, we studied the activity of the enzymes in batch experiments, and analyzed the synthesis and performance of the membrane reactors. Different kinds of enzymatic membrane reactors were obtained with immobilized solid enzymes. Our results show good agreement between the kinetics of the reactions and the velocity of the flux across the membrane, since both reaction and separation were properly achieved. We also determined optimum amounts of enzyme for obtaining the desired products with a low degree of polymerization and low concentrations of monomer.
© 2005 Elsevier B.V. All rights reserved.

Keywords: Enzymatic membrane reactor; Activated carbon; Oligosaccharides

1. Introduction

Process intensification, in which two unit operations are combined in a single step, is one of the most promising lines of research in chemical engineering. In the area of membrane research, this concept means that the reaction and separation/purification steps are combined in a new single unit. Thanks to their expected selectivity, enzymatic membrane reactors (EMR) offer great potential in this area. In addition to the intrinsic advantages of these systems, the process is continuous, the catalyst component can be re-used and a permeate free of this compound is obtained [1,2].

EMRs include a membrane that holds an active enzyme either by light or by strong bonding. In this project we have used a carbon/PSf composite membrane. The carbon acts as the base surface on which the enzyme bonds [3]. The carbon can hold the enzyme by one of two methods: by holding a metal ion as an intermediate (as IMACS [4]) or by adsorbing the enzyme directly onto the carbon surface. When the metal is used, activated carbons, whose structure is highly microporous, are able

to complexate Cu(II) ions that will act as the intermediate component in an IMAC-like structure.

Several publications related to protein binding due to adsorption processes can be found in the literature. Salins et al. [5] published an interesting application of this technique to a biological process. This technique has also been applied to membranes [6,7].

2. Experimental

Three types of enzyme membrane reactors were obtained. One contained solid enzyme, which was trapped between two membrane layers (without chemical bonds). The other two were prepared with an enzymatic liquid solution, and the enzyme was bound to the activated carbon or to the pair-activated carbon-metal system (to obtain a complex). The difference between these last two reactors was the number of layers of the composite membrane. The monolayer EMR was obtained by adding the complex to the polymeric solution, thus obtaining a homogeneous layer. The two-layer EMR was obtained by adding the complex over the top of the surface of the polymeric film (after casting) before precipitation in the coagulation bath and before the membrane is obtained. Fig. 1 shows schematically these three configurations.

* Corresponding author. Tel.: +34 977 55 96 11.
E-mail address: ricard.garcia@urv.net (R. Garcia-Valls).

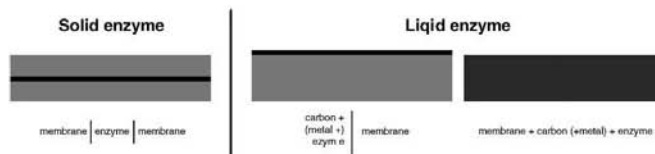


Fig. 1. Scheme of the three types of enzymatic membrane reactor synthesized.

2.1. Membrane synthesis

Membranes were obtained by immersion precipitation (phase inversion) from a polymeric mixture comprising 20% weight of polysulfone (Sigma–Aldrich, Spain) in di-methyl formamide (DMF, Panreac, Spain) as solvent [8]. The polymer was dissolved after 24 h of controlled atmosphere and agitation. The coagulation bath comprised 50% v demineralised water and 50% v DMF. When composite monolayer membranes were obtained, the complex was also added to the polymeric solution with a composition of 0.9%.

The polymeric film was obtained using a casting knife with a thickness of 200 μm applied over a glass support with a controlled and constant velocity using a K-Paint Applicator (R.K. Print Coat Instruments Ltd., United Kingdom).

2.2. Activated carbon

Two kinds of activated carbons were used. One of these was prepared in our laboratories and the other was a Norit Darco 12X40 from Norit Americas Inc. In our laboratories the activated carbon was prepared by phosphoric acid activation (an 85% H_3PO_4 solution from Panreac, Spain) of Kraft lignin (provided by Lignotech Iberica S.A.) by varying the carbonization temperature (400–650 $^\circ\text{C}$) and with a weight ratio of phosphoric acid to lignin of P/L = 0.7–1.75 [9]. Surface area and pore size characterization were performed using a Micromeritics ASAP2020 gas adsorption surface area analyzer. The specific surface area of the samples was determined from the nitrogen isotherms at $-196\text{ }^\circ\text{C}$ and the BET equation. Micropore volume was determined from the t-plot, mesopore volume from the BJH equation and total volume of pores was calculated with a relative pressure (p/p_0) of 0.99.

2.3. Metal

The metal ion used as intermediate in the IMAC-like structures was copper from a solution of $\text{CuCl}_2 \cdot 2\text{H}_2\text{O}$ (Sigma–Aldrich, Spain) with a purity of 99.9% ACS. To study the adsorption capacity of the activated carbon to the metal, an atomic adsorption spectrophotometer (Perkin-Elmer, Spectrometer 3110) was used to determine the copper concentration in solutions. The experiments were carried out by preparing several solutions containing the activated carbon and the metal solution in stirred agitation, and by keeping the temperature and pH constant and controlled. A water bath was used at 25 $^\circ\text{C}$ and the pH

was kept constant at 5 using a basic solution of NaOH 0.5 M (Panreac, Spain).

2.4. Enzymes

We used two kinds of enzymes: a solid enzyme made up of 1,4-beta-xylanase from Sigma–Aldrich (2500 U/g) and a liquid solution made up of a mixture of enzymes (including arabanase, cellulase, β -glucanase, hemi-cellulase and xylanase) from Sigma–Aldrich. To obtain the complex with the liquid enzyme, solutions containing the activated carbon or the activated carbon–metal system, and the enzyme solution were agitated for controlled periods.

2.5. Experimental device

Enzymatic membrane reactors were tested in an experimental system containing a pump piston, a surge suppressor, a back-pressure controller (to keep the pressure constant) and a circular flat membrane module with an effective membrane area of 15 cm^2 . The pressure was fixed at 9 bars. Fig. 2 shows the experimental device (Fig. 2a) and the membrane module (Fig. 2b).

Two different oligosaccharides solutions were tested. A real sample mixture of oligosaccharides obtained in the laboratory by acid hydrolysis from nutshells for the EMR containing the solid enzyme, and a commercial dextrane (Leuconostec, Fluka) of 200 kDa with a concentration of 1 g/L approximate for the EMR containing the liquid enzyme. Oligosaccharides and dextran analysis were performed by gel permeation chromatography (Agilent). A PWXL SS, 12 μm precolumn (Teknokroma, Spain) and a G3000PwXL, SS, 6 μm column (Teknokroma, Spain) were used at 25 $^\circ\text{C}$. A refractive index detector was used at 30 $^\circ\text{C}$ and the mobile phase was a 0.05 M KNO_3 (Panreac, Spain) solution.

In this paper, the results are presented in chromatographic formats related to the logarithm of mass. Table 1 shows the

Table 1
 Relation between the size of several compounds and their logarithm of mass

Compound	Logarithm of mass	Compound (kDa)	Logarithm of mass
Monomer	2.256	Dextrane 12	4.064
Polymer DP=3	2.703	Dextrane 50	4.687
Polymer DP=6	2.996	Dextrane 150	5.169
Dextrane 1 kDa	3.104		

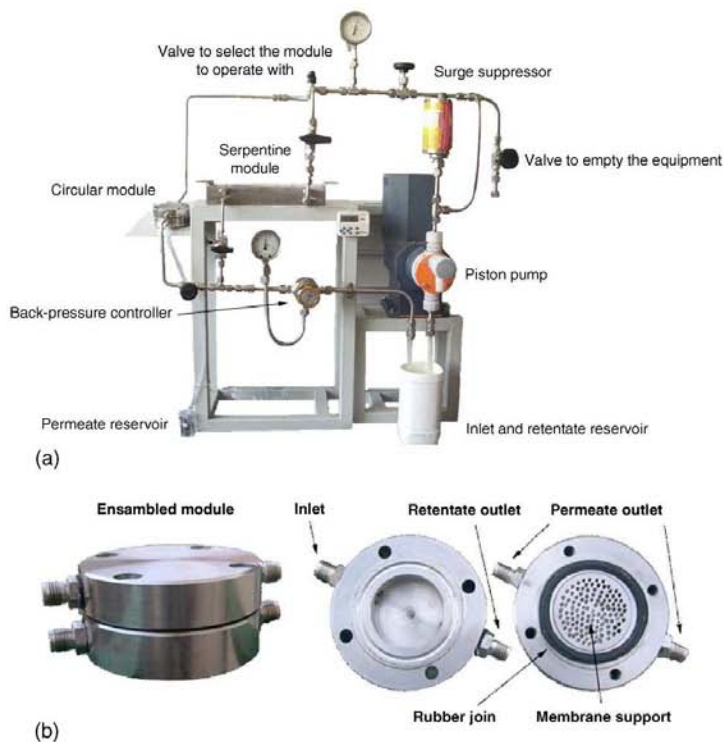


Fig. 2. (a) Experimental device. (b) Membrane module.

equivalence between this number and the size of several compounds.

3. Results and discussion

3.1. Enzymatic activity

3.1.1. Activity of the solid enzyme

The test fluid used to determine the activity of the xylanases (solid enzyme) was a mixture of oligosaccharides obtained by acid hydrolysis from nutshells. Two enzyme concentrations were tested in batch experiments and for each concentration the kinetics were studied. The concentrations considered were 80, 40, 10, 2 and 0.5 g/L. Fig. 3 shows the results for each concentration, as well as the GPC signal of oligosaccharides at several times. We can see that when the enzyme concentration decreases, the activity also decreases. When the activity is high, the main product obtained corresponds to the monomer saccharide. This is the least interesting compound since there are easier ways to obtain it, e.g. hydrolysis at high temperature. The most interesting compounds, which are the most difficult ones to obtain, are those with a low and controlled degree of polymerization, such as the dimmer and trimmer, etc. These compounds are obtained when the enzyme activity is low.

When checking the kinetics of the reaction (Fig. 4), we found that a high percentage of monomer production was carried out in the first few minutes of the reaction. This is interesting because, ideally, the velocity of the reaction should agree with the velocity of the flux across the membrane.

3.1.2. Activity of the liquid enzyme

The test fluid used to evaluate the activity of the liquid enzyme contained a 200 kDa commercial dextrane. As in the previous case, several enzyme concentrations were tested in batch experiments: 100, 10, 2 and 0.44 mL/L. Fig. 5 shows the chromatographic results related to the enzyme and to the dextrans at several times, for the lowest concentrations.

From the reaction we can see that the signals corresponding to the products of the reaction increase with time. This indicates that the reaction occurs, though at a slow rate. Also, our results indicate that the concentration of the enzyme in this case is not a critical factor since the reaction rate is similar in all cases.

3.2. Adsorption capability of the activated carbons

The optimal conditions for the home-made activated carbon were already determined in a previous study [10]. In that study, the adsorption results were best with activated carbon produced

at a carbonization temperature of 450 °C and a phosphoric acid to lignin ratio of P/L = 1.4. We studied how three variables influenced the commercial carbon: the concentration of the metal in solution, the agitation time (24 and 48 h) and the particle size. The particle size of the home-made activated carbon was between 30 and 100 μm. The particles of the commercial carbon were therefore ground and sieved in order to also obtain particles of similar size to those produced in the lab.

Before the activated carbons were tested and their surface characteristics were determined (see Table 2).

These results show that there are small discrepancies between the results provided by the manufacturer and those obtained with the BET. These discrepancies could be due to differences in measurement conditions and type of analyzer, etc. With regard to the differences in particle size, similar results were obtained for all properties, although the smaller particles have a larger surface area. There are clear differences between the commercial and the home-made activated carbon. Our results show that the home-made activated carbon has a larger surface area and a larger micro pore volume, which indicates that the adsorption capability is higher.

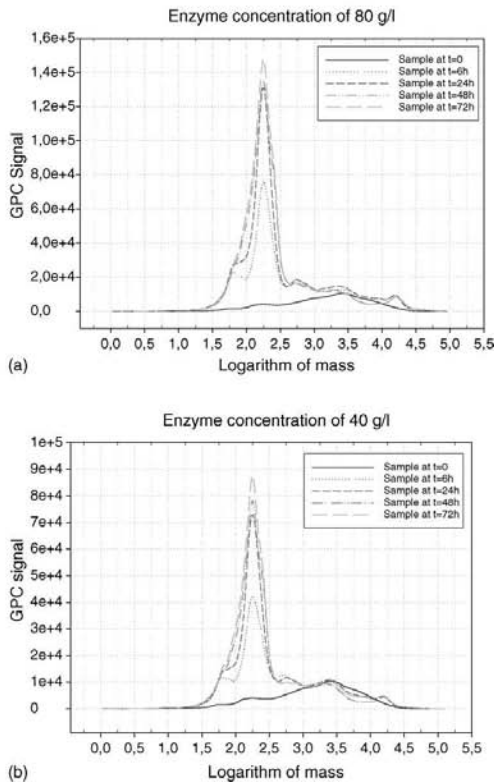


Fig. 3. Chromatographic results of oligosaccharides corresponding to the study of the solid enzyme activity at several concentrations: (a) 80 g/L, (b) 40 g/L, (c) 10 g/L, (d) 2 g/L and (e) 0.5 g/L.

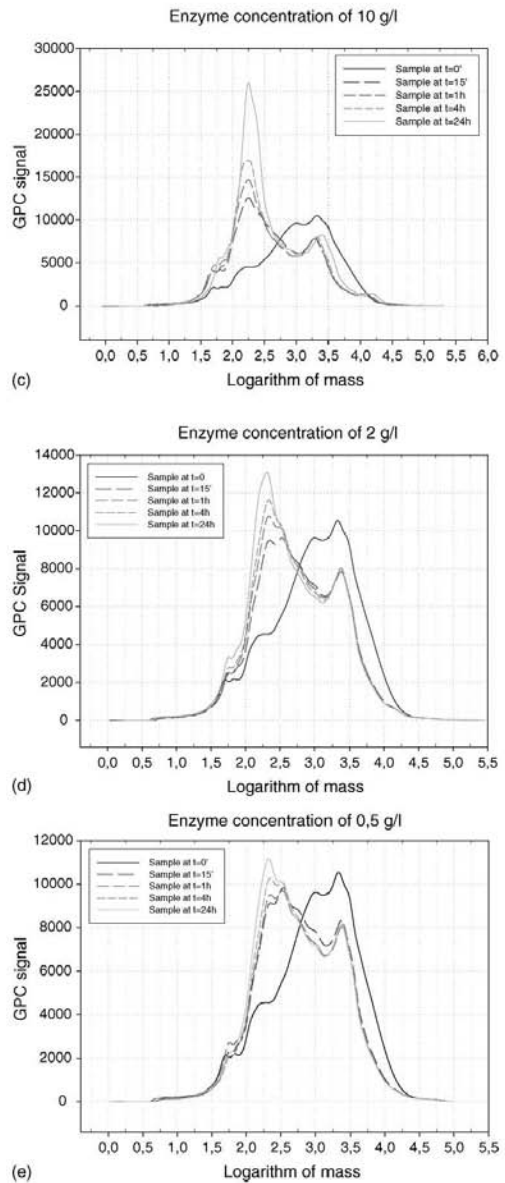


Fig. 3. (Continued).

The results obtained by keeping the metal solution in contact with the activated carbon in batch experiments and using the same variables as before confirmed that there was no variation with time, since the copper adsorbed by the carbon was almost the same for both times. With regard to the concentration of the metal solution, the best results in terms of loading were obtained

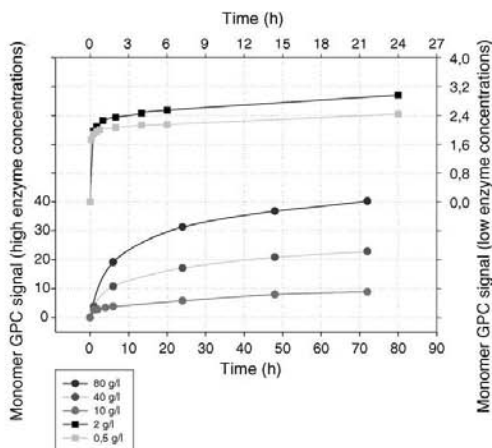


Fig. 4. Kinetics corresponding to the production of the monomer in the reactions carried out with the solid enzyme.

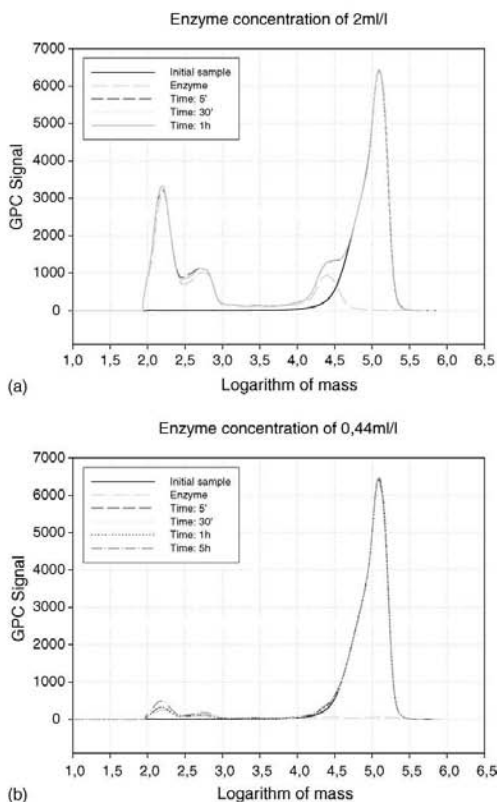


Fig. 5. Chromatographic results of dextrans and enzyme corresponding to the study of the liquid enzyme activity at several enzyme concentrations: (a) 2 mL/L and (b) 0.44 mL/L.

Table 2
 Results of the characterization of the activated carbons with the gas adsorption surface area analyzer

	Surface area	Total pore volume (ml/g)	Micro pore volume (ml/g)
Commercial AC (manufacturer's data)	650	0.93	N/A
Commercial AC (original particle size)	$578 \pm 6 \text{ m}^2/\text{g}$	N/A	0.14
Commercial AC (30–60 μm particle size)	$584 \pm 5 \text{ m}^2/\text{g}$	N/A	0.13
Home-made activated carbon	$1047 \pm 4 \text{ m}^2/\text{g}$	0.51	0.41

at high concentrations, and with regard to particle size, the best results were obtained with small sizes. Variations in these two parameters do not imply significant variations in results. The activated carbon, in agreement with the characterization results, is what really causes different results. The adsorption capability of the home-made activated carbon is about six times higher than that of the commercial membrane (see Fig. 6). Taking into account these results, we performed the following experiments using the home-made activated carbon.

3.3. Batch enzyme loading

As we stated earlier, the enzyme was immobilized with or without a metal ion intermediate but always on the carbon/polysulfone composite. In all cases, two enzyme concentrations were considered with a fixed amount of activated carbon in batch experiments. These concentrations were 100 and 250 mL of enzyme/L of dissolution. The concentrations were high so that the enzyme amount would not be the limiting factor.

All cases showed a reduction in the concentration of the enzyme, because a part of it was bound either to the activated carbon or to the activated carbon–copper system. The concentration decreased the most (about 27% in 48 h) when the initial enzyme concentration was low and with the system containing activated carbon–copper.

Note with regard to the presence of the metal, and despite the previous case, that in the first 24 h, the reduction of enzyme in the solution was greater with the systems that did not contain

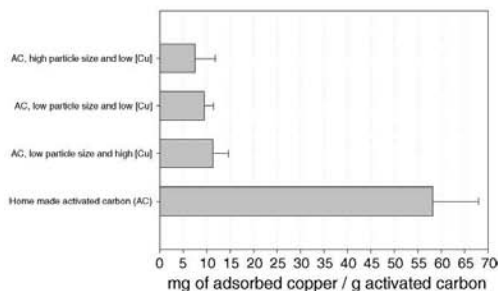


Fig. 6. Results of the metal adsorption capability of the activated carbons.

metal, though the difference in absolute terms was low (9 and 11% versus 4 and 6%). With regard to time, the reduction of enzyme in the solution was always greater at 48 h. It would therefore be suitable to consider longer times to check whether more enzyme can be bound to the precursors. Finally, with regard to concentration, results do not show an optimum configuration.

3.4. Enzymatic membrane reactors

3.4.1. EMR with solid enzyme

To obtain the EMR with the solid enzyme, one polymeric membrane supported the enzyme after dispersing it over the surface of the polymeric film and before immersing it in the coagulation bath to obtain the membrane. Another membrane without the enzyme was then also obtained. The system involved disposing the two membranes in the module, with the layer containing the enzyme located between the two membranes. The enzyme was therefore immobilized in one membrane and encapsulated between the two membranes, and could not escape because the particles were larger than the membrane pores.

The membrane obtained with 20% PSf in DMF and in a coagulation bath containing 50% v DMF and 50% v water has a permeate flux of 0.09 L/m² h bar and a molecular weight cut-off of 28 kDa, measured with the same dextrane samples [11].

Two membrane reactors containing different amounts of solid enzyme were prepared. One of these contained 0.5 g of enzyme and the other contained 3.0 g. Fig. 7 shows the chromatograms corresponding to the initial sample and the permeate of two experiments for each membrane.

These results clearly show that the reaction took place, and that a separation step occurred. In all cases, therefore, some reaction compounds with low molecular weights were produced, and those components with the highest molecular weight were removed from the permeate sample. With the EMR with the largest amount of enzyme, the main component produced in the reaction corresponded to the monomer (in agreement with the results of the batch study of the enzyme activity). With the EMR with the least amount of enzyme, monomer formation was very low and the main component produced was the one corresponding to a molecular weight of about 500 Da.

In the retentate we observed that no reaction products were obtained, which indicates that no reaction occurred, and that the enzyme was properly immobilized in the membranes (which was not in contact with the feed).

Finally, the fluxes measured for the membranes tested were 0.11 and 0.12 L/m² h bar, which is in good agreement to the nominal ones. Note the good agreement between the flux velocity across the membrane and the kinetics of the reaction. This does not occur with the commercial polysulfone membranes, which have larger fluxes (and also larger molecular weight cut-offs). Fig. 8 shows the results obtained using an EMR from a commercial membrane, with a permeability of 10 L/m² h bar and containing 3 g of enzyme, under the same conditions as the previous membrane reactors. Results show that no reaction occurred, though the amount of enzyme was high. This clearly indicates that, in this case, the kinetics of the reaction does not correspond to the membrane flux, which is too high.

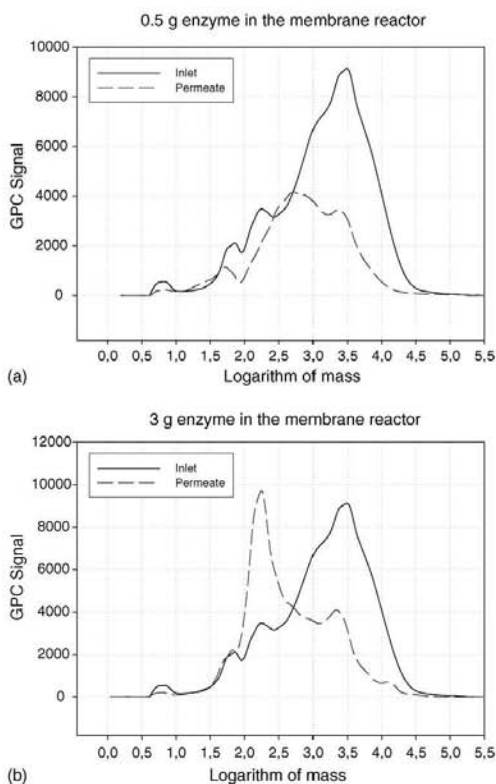


Fig. 7. Chromatographic results of oligosaccharides corresponding to the performance of the EMR containing the solid enzyme in two amounts: (a) 0.5 g and (b) 3 g.

3.4.2. EMR with liquid enzyme

Two types of EMR-containing liquid enzyme were obtained: one monolayer membrane reactor and a two-layer membrane reactor. Fig. 9 shows two photographs of the two type of

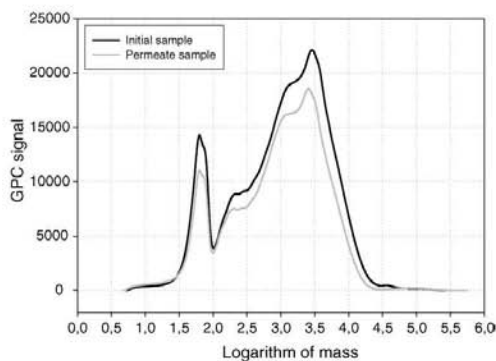


Fig. 8. Chromatographic results of oligosaccharides corresponding to the performance of the EMR containing 3 g of solid enzyme in a commercial membrane.

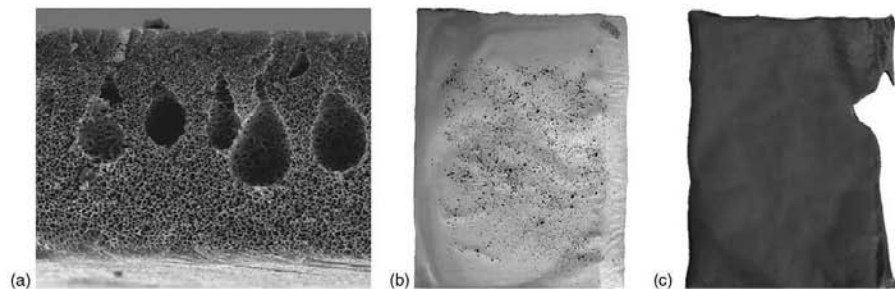


Fig. 9. (a) SEM micrograph of a polymeric membrane obtained with 20% PSF and 50% DMF and 50% H₂O in the coagulation bath. (b) Photograph of a two-layer membrane reactor and (c) one-layer membrane reactor.

membrane reactors, and a cross-section SEM micrograph of the structure of all membranes (which do not change).

For several reasons, the membrane reactors produced with one layer are those with the greatest potential. First, they are the most compact because they comprise a single layer containing the polymeric matrix and the complex-activated carbon–metal–enzyme (or activated carbon–enzyme). Second, the enzyme does not significantly affect the sample feed that does not cross the membrane, so no reaction products are expected to be detected in the retentate stream. Third, the morphological structure of the membrane, determined by the polymeric matrix, does not change when the complex is added (as shown in SEM images and in the conclusions of previous studies [11]). Finally, the presence of the complex throughout the membrane means it can be used in diffusive processes (without pressure and, therefore, without convection) because of the active sites provided by the complex.

On the other hand, this type of membrane reactor presents the most difficulties in its synthesis process because of the greater number of interactions between the components used in the process. Specifically, as is demonstrated in our previous studies [11], the interaction between the solvent (DMF) and the carbon is high. The solvent breaks the carbon particles and may break part of the complex made up of the activated carbon, the metal and the enzyme.

Fig. 10 shows the results from using the monolayer membrane reactor with a test fluid containing a 200 kDa commercial dextrane. These results show that the reaction and the separation were successful. The membrane cut-off is similar to the nominal one, and two basic reaction products were produced—one corresponding to a component of 630 Da and one corresponding to a component of 3200 Da. The signal of the permeate is lower than the one of the initial sample, but if we examine it alone we find that the area occupied by the reaction product is 32% of the total area.

As in the other cases, the retentate stream is free of reaction products. The superficial enzyme of the EMR therefore does not significantly affect the initial sample. The chromatogram shows that, because of the concentration effect of this stream after the most dilute sample crossed the membrane, the height of the signal related to the retentate is slightly higher than that of the initial sample.

Finally, the flux was 0.06 L/m² h bar, which is slightly lower than the nominal flux of the membrane.

The two-layer membrane reactor was obtained with the liquid enzyme. The main advantage of this reactor is the low interaction between the solvent and the enzymatic complex. These reactors can be obtained because the complex particles added on the top

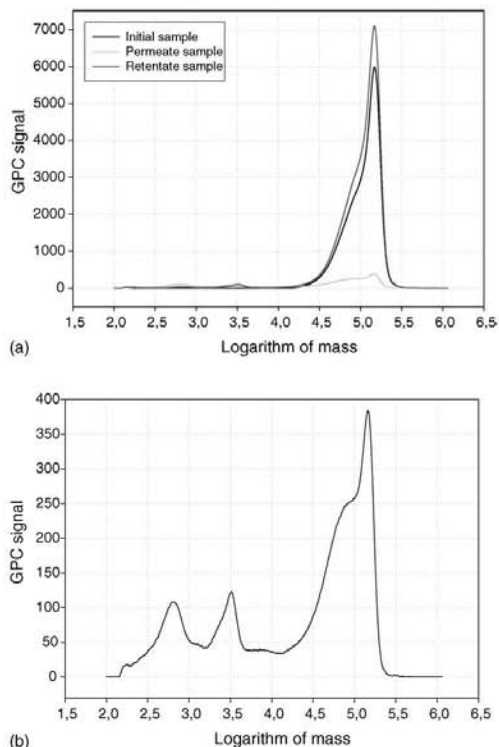


Fig. 10. Chromatographic results of dextrans corresponding to the performance of the monolayer EMR containing the liquid enzyme bound to the activated carbon–metal system: (a) signals corresponding to the initial sample, retentate and permeate, (b) signal corresponding to the permeate.

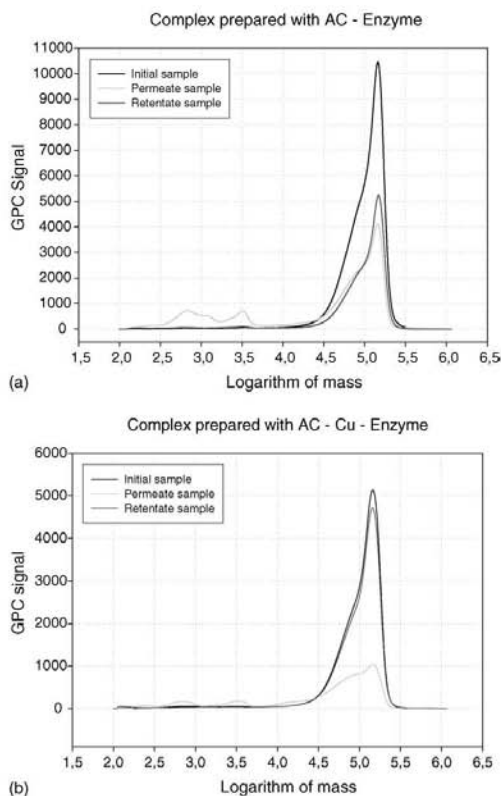


Fig. 11. Chromatographic results of dextrans corresponding to the performance of the two-layers EMR containing the liquid enzyme bound to: (a) activated carbon and (b) activated carbon–metal system.

of the film do not migrate from the membrane after it is immersed into the coagulation bath. In these types of membranes, the entire enzymatic complex is in contact with the initial sample and some reaction products can be formed on the retentate. Finally, this method requires a special technique, both to ensure that the complex deposition over the film is homogeneous and to control the amount of complex added.

Fig. 11 shows the results of the performance with this system. An EMR containing activated carbon–enzyme complex and another containing activated carbon–metal–enzyme were tested. Results are similar to those from the monolayer reactors. In these cases, the signals corresponding to the reaction products in the permeate are higher but they are also part of the feed component, which indicates that the MWCO of the membrane is higher. This always occurs with the two-layer membrane reaction, which suggests that the presence of the complex over the top surface slightly modifies the top nanoporous structure of the membranes. The experiments conducted with these membranes do not show that, overall, results are better with systems that contain metal.

4. Conclusions

In this study, several enzymatic membrane reactors were obtained from polymeric membranes using activated carbon as support to bind the enzyme directly or using a metal ion as precursor. Also, enzymatic membranes reactors were produced without a chemical bond by encapsulating the enzyme between two membrane layers.

Two types of activated carbons were used: a commercial one and a home-made one. Characterization results showed that the surface area was larger for the last one and spectrometer results obtained after the metal was adsorbed by the activated carbon show that adsorption capability was also higher. It is better, therefore, to use the home-made activated carbon.

Using copper to increase the enzyme immobilization with the activated carbon does not provide better overall results, though there is a tendency to increase enzyme adsorption. A more detailed study is needed to obtain more definitive conclusions.

With regard to the membrane reactors, a clear reactivity was demonstrated in all cases and the separation capability of the membrane was maintained, though in some cases this was slightly reduced. The immobilization of the enzymes was also successful in all cases since they were not detected in any stream (permeate and retentate). Also, though optimization was not the aim of this project since it corresponds to future work, there was good agreement in all cases between the kinetics of the reaction and the velocity of the flux across the membrane. The optimal ratio between kinetics and transport did not occur with commercial membranes, in which the velocity of the flux is too high and no reaction occurs.

With regard to the reactors in which the enzyme was encapsulated, although the system corresponds to the less compact EMR produced (two layers are required), it is easy to control the parameters to be considered in the synthesis process (especially the amount of enzyme), the interaction between the compounds that take part in the process is low, and the reactivity levels are satisfactory. In this case, the amount of enzyme should be carefully controlled to avoid the production of monomer.

With regard to the reactors in which the enzyme was adsorbed by the activated carbon or by the pair-activated carbon metal, the one made up of a single layer performs well, since it is compact, it facilitates diffusive transport, the reactivity is satisfactory without the production of monomer, and it maintains the separation capability of the membrane almost intact. The one made up of two layers is easier to produce (because of the fewer interactions between the compounds) and reactivity is higher, but it loses separation capability and is less compact. For these reasons, the reactive membrane with a single layer has the greatest potential.

These results correspond to basic research into this type of enzymatic membrane reactors based on polysulfone and activated carbon. A more detailed study is therefore needed to optimize the various parameters. Promising results are likely, not only in this field of application but also in others.

Acknowledgements

C. Torras acknowledges the Universitat Rovira i Virgili for the doctoral scholarship and Pepa Lázaro for her contribution to the experimental work. This work has been supported by the Spanish Ministry of Science and Technology; project PPQ2002-04201-C02.

Nomenclature

AC	Activated carbon
BET	Gas adsorption surface area analyzer
DMF	Dimethyl formamide
EMR	Enzymatic membrane reactors
GPC	Gel permeation chromatography
MWCO	Molecular weight cut off
PSf	Polysulfone

References

- [1] S. Bouhallab, Les separations par membranes dans les procédés de l'industrie alimentaire, Tech. Doc. Lavoisier, Paris, 1998.
- [2] C.-J. Moon, J.-h. Lee, Use of curdlan and activated carbon composed adsorbents for heavy metal removal, *Process Biochem.* 40 (2005) 1279–1283.
- [3] A. Üçer et al. Immobilisation of tannic acid onto activated carbon to improve Fe(III) adsorption, *Separ. Purif. Technol.*, in press.
- [4] S. Díez, et al., Immobilized soft-metal affinity system for amino acids based on an 8-hydroxyquinoline–Pd(II) complex; characterization using glycine as a model, *Anal. Chim. Acta* 315 (1995) 339–345.
- [5] L.L.E. Salins, S.K. Deo, S. Daunert, Phosphate binding protein as the biorecognition element in a biosensor for phosphate, *Sens. Actuators B* 97 (2004) 81–89.
- [6] M.E. Avramescu, et al., Preparation of mixed matrix adsorber membranes for protein recovery, *J. Membr. Sci.* 218 (2003) 219–233.
- [7] G.L. Lensmeyer, et al., Use of particle-loaded membranes to extract steroids for high-performance liquid chromatographic analyses, improved analyte stability and detection, *J. Chromatogr. A* 691 (1995) 239.
- [8] M. Mulder, *Basic Principles of Membrane Technology*, second ed., Kluwer Academic Publishers, Dordrecht (The Netherlands), 1997, ISBN: 0-7923-4247-8.
- [9] J. Rodríguez-Mirasol, T. Cordero, J.J. Rodríguez, Preparation and characterization of activated carbons from eucalyptus kraft lignin, *Carbon* 31 (1993) 87–95.
- [10] V. Fierro, V. Torné, D. Montané, R. Garcia-Valls, Removal of Cu(II) from aqueous solutions by adsorption on activated carbons prepared from kraft lignin, in: *Conference Proceedings Carbon*, Oviedo, Spain, 2003.
- [11] C. Torras, *Obtenció de Membranes polimèriques selectives*, Ph.D. Thesis, Tarragona (Spain), 2005, pp. 185–203, ISBN: 84-689-3628-6.

5.2.5. Removal of lignin and associated impurities from xylo-oligosaccharides by activated carbon adsorption

Este artículo se ha publicado en el journal Industrial Engineering Chemistry Research en 2006 en el volumen 45, páginas 2294 a 2302.

Removal of Lignin and Associated Impurities from Xylo-oligosaccharides by Activated Carbon Adsorption

Daniel Montané,* Débora Nabarlatz, Anna Martorell, Vanessa Torné-Fernández, and Vanessa Fierro

Departament d'Enginyeria Química, ETSEQ—Rovira i Virgili University, Av. Països Catalans 26, 43007 Tarragona (Catalunya), Spain

This paper studies purification with commercial activated carbons of the xylo-oligosaccharides produced by the autohydrolysis of almond shells. Almond shells are agricultural residues with a high content of xylan that are produced abundantly in some regions with a Mediterranean climate. Adsorption equilibrium was measured in a batch system for three commercial activated carbons using a constant concentration of 20 g/L of crude xylo-oligosaccharides and loads of activated carbon from 1.5 to 50.0 mg/mL. Adsorption for lignin-related products was higher than for xylo-oligosaccharides and the selectivity toward lignin adsorption was better when the carbon was highly microporous and had small mesopore diameters, a low volume of mesopores, a low concentration of basic surface groups to limit xylo-oligosaccharide adsorption, and acidic surface groups to favor the adsorption of the lignin-related products. Column tests were performed at a feed rate of crude xylo-oligosaccharide solution of 6.0 mL/min (35 g/L) in columns packed with 22 g of granular activated carbon and operated in up-flow mode. Average retention was around 64% for lignin products and 21% for carbohydrates for the fraction of treated solution collected during the first 2 h of operation (13.1 bed volumes circulated through the bed). Retention for lignin-derived products was limited because part of them is linked to the xylo-oligosaccharides.

Introduction

Xylose-based oligosaccharides (xylo-oligosaccharides or xylo-oligomers) derived from xylan-rich hemicelluloses are carbohydrates with a high potential for novel applications in food and pharmaceutical products. As they are not metabolized by the human digestive system, xylo-oligosaccharides can be used as low-calorie sweeteners and soluble dietary fiber. They act as prebiotics, providing a source of carbon for the development of intestinal microflora and probiotic microorganisms,^{1–4} and are already used in fortified foods intended for the development of intestinal microflora.^{5,6} In addition, xylo-oligosaccharides have acceptable organoleptic properties and do not exhibit toxicity or negative effects on human health. Ethers and esters prepared from xylan and xylo-oligosaccharides have been synthesized and used as thermoplastic compounds for biodegradable plastics, water soluble films, coatings, capsules, and tablets⁷ and also for the preparation of chitosan–xylan hydrogels.⁸ Xylo-oligosaccharides extracted by autohydrolysis of bamboo have recently been found to possess a cytotoxic effect on human leukemia cells.⁹

The autohydrolysis of xylan-rich biomass is a suitable process for the production of xylo-oligosaccharides. It eliminates the use of important amounts of the chemicals needed in other extraction processes, such as alkali and acid, and since autohydrolysis takes place in slightly acidic media, many of the side chains in the backbone xylose chains, such as acetyl, uronic acids, and phenolic acid substituents, remain in the xylo-oligosaccharides.^{10,11} The differential characteristics of the substituted xylo-oligosaccharides obtained by autohydrolysis have prompted renewed interest in the development of process strategies for achieving a high yield of xylo-oligosaccharides

with consistent reproducibility in purity and composition. Though xylo-oligosaccharides are the main component in the nonvolatile products of biomass autohydrolysis, they are mixed with monosaccharides, ferulic acids, uronic acids, and compounds formed by the partial hydrolysis of lignin, the dehydration and degradation of carbohydrates, and condensation reactions. Lignin-derived products are the largest fraction of the impurities associated with xylo-oligosaccharides. Lignin is a three-dimensional polymer made of phenylpropane units linked randomly through alkyl–aryl ether bonds. It acts as a protecting agent and binder in the cell-wall structure of lignocellulosic materials. During autohydrolysis, lignin is depolymerized partially through cleavage of the ether linkages and yields phenolic monomers and oligomers that are soluble in the aqueous media. Also, some of the xylose units in the xylan backbone are bonded to lignin through ether and ester linkages. Consequently, some of the xylo-oligosaccharides contain lignin oligomers linked to the xylose chain. Various impurities from minor constituents of the lignocellulosic biomass—including inorganic salts, extractives, and, in some cases, proteins—are also present.

Clearly, therefore, the crude xylo-oligosaccharides produced by the autohydrolysis of lignocellulosic biomass will contain large amounts of lignin-derived phenolics, carbohydrate dehydration and condensation products, and ash. For instance, the content of xylo-oligosaccharides in the nonvolatile products has been reported to be 58.3% for almond shells,¹² 54.8% for rice husks,¹³ and only 46.3% for barley residues.¹⁴ Crude xylo-oligosaccharides must be purified in order to obtain a final product that is well characterized chemically and structurally, homogeneous, repetitive, and suitable for food or pharmaceutical applications. Purification sequences based on liquid–liquid and solid–liquid extractions, solvent precipitation, and ion exchange treatments, as well as combinations of these techniques, have been thoroughly studied.^{13,14} Treatment with activated carbon has been shown to be an effective process for removing

* To whom correspondence should be addressed. E-mail: daniel.montane@urv.net. Phone: (+34) 977 559 652. Fax: (+34) 977 558 544.

Table 1. Surface Characteristics of the Commercial Activated Carbons (NORIT) Used in This Study

	Activated Carbons		
	AC-1 (ROX 0.8)	AC-2 (PAC 200)	AC-3 (Darco 12 × 40)
S_{BET} (m ² /g)	1024 (1100*)	1346	616 (650*)
$V_{0.99}$ (mL/g)	0.625	0.713	0.637
$V_{\alpha, \text{mic}}$ (<0.8 nm) (mL/g)	0.152	0.139	0.085
mean pore diam (nm)	2.4	2.1	4.1
iodine number	960 (1000*)	1060 (900*)	635 (600*)
methylene blue (g/(100 g))	22.3 (22*)	47.0	17.4
pHpzc	8.0	8.7	
	Surface Groups (mequiv/g)		
carboxyl	0.2	0.3	0.4
phenolic	4.2	3.0	0.8
lactone	0.1	0.0	0.5
carbonyl	0.5	4.6	0.9
basic groups	2.1	1.2	0.5

* Table data provided by NORIT.

impurities from carbohydrate products, having been tested for the detoxification of xylose solutions from the acid hydrolysis of eucalyptus wood before fermentation to xylitol,¹⁵ for the recovery of xylitol from the fermented hydrolyzates of sugarcane bagasse,¹⁶ for the selective recovery of ferulic acid from hydrolyzates of sugar-beet pulps,^{17,18} for the separation of maltopentaose from other malto-oligosaccharides,¹⁹ and for the decolorization of sugar solutions²⁰ and xylo-oligosaccharides.²¹ However, so far, there has been no detailed study of the performance of activated carbons for the removal of lignin-derived impurities from crude xylo-oligosaccharide solutions or of the characteristics of the carbons that favor the selective adsorption of lignin-related impurities.

In this paper, we study the performance of three commercial activated carbons for the purification of xylo-oligosaccharides by the selective adsorption of lignin-derived compounds and other impurities. Equilibrium experiments were conducted to obtain the adsorption isotherms, and the results were correlated with the physicochemical properties of the carbons. Continuous adsorption experiments were conducted in a packed-bed column to obtain the breakthrough curves for xylo-oligosaccharides and lignin-derived impurities.

Experimental Section

Materials. Samples of three commercial activated carbons supplied by NORIT (NORIT, the Netherlands) were tested for the purification of the xylo-oligosaccharides: ROX 0.8 (AC-1), PAC200 (AC-2), and Darco 12 × 40 (AC-3). ROX 0.8 is an extruded granular activated carbon used for decoloring starch hydrolyzates and sugars. PAC200 is a powdered carbon used for removing taste, odor, and color from water and industrial process applications. The 12 × 40 carbon is a general-purpose granular carbon grade used in a variety of applications including the purification of fine chemicals and food. For the equilibrium experiments, ROX 0.8 and Darco 12 × 40 were ground and sieved to 0.2 mm, while PAC200 was used directly. In the column tests, all the carbons were used as received. The surface characteristics of the carbons were determined in samples of pulverized carbon according to the methods detailed in the analytical methods section (see also Table 1).

Xylo-oligosaccharides were obtained by the autohydrolysis of grounded almond shells at 179 °C for 23 min. Full details of the reactor system and the operational procedure have been provided elsewhere.¹² Xylo-oligosaccharides from two different reaction batches were used in this study. The first batch comprised solid xylo-oligosaccharides recovered from the

autohydrolysis solution by spray drying. This procedure removed water and most of the volatile impurities such as furfural and acetic acid, leaving dry xylo-oligosaccharides (XOs) that still contained all the nonvolatile impurities, such as monosaccharides, organic extractives, lignin-derived phenolics, and inorganic salts. This sample was used for the adsorption equilibrium tests. The second batch comprised an XO solution prepared by autohydrolysis under the same conditions as the first but used directly for the continuous adsorption tests in packed columns. It had a total solids concentration of 35.2 g/L.

Adsorption on Activated Carbon. Adsorption equilibrium was measured in a batch system. A sample of the xylo-oligosaccharides of the first reaction batch recovered by spray drying was dissolved in deionized water at a concentration of 20 g/L. Aliquots of 10 mL of this solution were placed in 20 mL test tubes, and the appropriate amount of activated carbon was added (from 15 to 500 mg). The tubes were capped and placed in a water bath at 30 °C, attached perpendicularly with clamps to a horizontal revolving shaft that had a rotating speed of 2 rpm. After 24 h, the tubes were removed from the bath and the mixture was centrifuged at 4000 rpm for 20 min to precipitate the activated carbon. A sample of the supernatant liquid was filtered through a 0.22 μm nylon syringe filter, placed in an encapsulated HPLC vial, and stored at 5 °C until analysis.

Column tests were performed at room temperature (21 ± 1 °C) using around 22 g of granular activated carbon packed on a 55 mL column, with an inner diameter of 20 mm, made of metacrylate tube and PVC fittings. Activated carbon was submerged in boiling water for 15 min to remove air and fine particles and then extracted and poured immediately into the column, which had previously been filled with water to avoid entrapping air in the carbon bed. The column had wire mesh plates at both ends to prevent the entrainment of carbon particles and was operated in up-flow mode to reduce channeling. The solution of crude xylo-oligosaccharides from the second reaction batch was fed at 6 mL/min with a Watson-Marlow 313F peristaltic pump (Watson-Marlow Bredel, USA), which led to a residence time of 0.15 h. At the end of the experiment, the feed was switched to deionized water for 1 h to clean the column. The product was collected in four fractions—from 0 to 2 h (F1, 13.1 bed volumes circulating through the column), from 2 to 4 h (F2, 26.2 bed volumes), from 4 to 5.5 h (F3, 36 bed volumes), and the washing solution—and the dissolved solids in each fraction were recovered by lyophilization. Also, samples of 2 mL were withdrawn from the outlet stream throughout the experiment, filtered through a 0.22 μm nylon filter, and analyzed by gel permeation chromatography/high-performance liquid chromatography (GPC/HPLC) to determine the instantaneous composition of the product stream, as described below.

Analytical Methods. The surface area and porosity of the activated carbons were determined from their nitrogen adsorption-desorption isotherms obtained at 77 K in an ASAP 2020 surface analyzer (Micromeritics, USA). The samples were previously degassed at 523 K for several hours. N₂ adsorption data for P/P_0 from 10⁻⁵ to 0.99 were analyzed according to (i) the BET method²² for calculating the specific surface area, S_{BET} and (ii) the α_s method²³ using Carboxypack F Graphitized Carbon Black as reference material to calculate the ultramicropore volume²⁴ (pore diameter < 0.8 nm), $V_{\alpha, \text{mic}}$. The total pore volume, $V_{0.99}$, was calculated from nitrogen adsorption at a relative pressure of 0.99. The average pore diameter was calculated from the total pore volume and the surface area with eq 1. The point of zero charge (PZC) was determined by mass titration.²⁵ Various amounts of activated carbon were added to

2296 Ind. Eng. Chem. Res., Vol. 45, No. 7, 2006

a 10 mL solution of 0.1 M NaCl to obtain mixtures with 0.05, 0.1, 0.5, 1.0, and 10% of carbon by weight. The bottles were sealed to eliminate any contact with air and stirred overnight. The equilibrium pHs of the suspensions were measured after 24 h of contact time. The PZC value of the activated carbon was taken as the equilibrium pH of the suspension with the highest concentration of carbon when the change in pH with carbon concentration was low. Methylene blue ($C_{16}H_{18}ClN_3S \cdot 2H_2O$, MB) serves as a model compound for checking the adsorption of medium-size organic molecules from aqueous solutions. A 50 mL portion of a 3.2 mM solution of MB (Scharlau Chemie, Spain) and approximately 50 mg of activated carbon were used in adsorption experiments. The solutions were stirred overnight and filtered to remove the activated carbon in suspension before analysis. The equilibrium concentration of MB in the solution was measured by spectrometry at 664.8 nm in a Dinko Instruments 8500 spectrometer (Dinko Instruments, Spain). The amount adsorbed was calculated from the change in concentration of the solution. The iodine number was provided by NORIT. The oxygenated acid surface groups were determined according to the method of Boehm,²⁶ and the basic groups were determined by titration with hydrochloric acid. A 25 mg portion of carbon was mixed with 25 mL of each of the following solutions: 0.1 N sodium hydroxide, 0.1 N sodium carbonate, 0.1 N sodium bicarbonate, 0.1 N sodium ethoxide, and 0.05 N hydrochloric acid. The vials were sealed and stirred for 48 h, and the solutions were filtered. Samples of 5 mL were taken. These were titrated with 0.05 N HCl or 0.1 N NaOH to determine the excess of base or acid, respectively. The number of acidic sites of each type was calculated under the assumptions that sodium ethoxide neutralizes all the acidic groups (i.e., the carboxylic, phenolic, lactonic, and carbonyl groups), that NaOH neutralizes the carboxylic, phenolic, and lactonic groups, that Na_2CO_3 neutralizes the carboxylic and lactonic groups, and that $NaHCO_3$ neutralizes only the carboxylic groups. The number of surface basic sites was calculated from the amount of HCl consumed by the activated carbon.

$$\bar{d}_p = 4 \frac{V_{0.99}}{S_{BET}} \quad (1)$$

Solid xylo-oligosaccharides were analyzed for their ash content (ASTM D 1102-84 standard method) and for carbohydrates, acetyl groups, and lignin. A sample was dissolved in deionized water and analyzed (i) by HPLC to quantify the free monosaccharides (glucose, xylose, and arabinose), acetic acid, furfural, and hydroxymethyl furfural (HMF) and (ii) by HPLC/GPC to determine the molar mass distribution. Another sample of the XOs was dissolved in 4% sulfuric acid and was quantitatively hydrolyzed at 120 °C for 45 min to convert the oligosaccharides into their constitutive monomers. The hydrolyzate was analyzed by HPLC, and the amount of xylo-oligosaccharides was estimated from the monosaccharides and acetic acid liberated by the quantitative hydrolysis. Lignin was measured as the insoluble residue after the quantitative hydrolysis (Klason-type lignin) by the TAPPI UM 250 method for the acid-soluble lignin. The XO solution from the autohydrolysis reactor (2nd batch of XO) was analyzed with the same procedures. HPLC analyses were performed with a Bio-Rad HPX 87H column at 30 °C (Bio-Rad Laboratories, USA) in an Agilent 1100 series chromatograph (purchased from Agilent, Barcelona, Spain). The solvent was 0.005 M H_2SO_4 at a flow rate of 0.5 mL/min. An Agilent 1100-DAD ultraviolet (UV) diode-array detector and an Agilent 1100-RID refractive index (RI) detector were connected in series. The UV detector was

used to quantify furfural and HMF in the samples that contained low concentrations of these compounds. The RI detector was used for the samples with high concentrations of furfural and HMF and for carbohydrates. The molar mass distribution of the xylo-oligosaccharides was determined by GPC using the same chromatograph and the GPC add-on of the LC Chemstation software (purchased from Agilent, Barcelona, Spain). The analyses were performed with a TSK Gel G3000PWXL column (Toso Haas, purchased from Teknokroma, Barcelona, Spain) at 25 °C using 0.5 mL/min of a 0.05 mol/L solution of KNO_3 with 83 mg of sodium azide as solvent and the refractive index detector. The system was calibrated with xylose, glucose, and low-polydispersity standards of malto-oligosaccharides and dextrans (Fluka). In all cases, the samples were filtered through a 0.22 μm nylon syringe filter prior to HPLC analyses.

Results and Discussion

Adsorption Equilibrium Tests. Adsorption equilibrium tests were developed using a sample of crude xylo-oligosaccharides obtained by spray drying of the hydrolysis liquor (batch 1). This sample comprised 58.3% xylo-oligosaccharide, 5.0% monomer products (2.4% xylose, 1.5% arabinose, 0.78% glucose, 0.27% HMF, and trace amounts of acetic acid and furfural), 4.8% ash, and 16% Klason-type lignin. The remaining 14.9% of the solid was made up of compounds from the almond shells that were solubilized during the autohydrolysis reaction, e.g., extractives, low molar mass phenolics from lignin, and byproducts from the degradation and condensation of monosaccharides and furfural, which were not identified with the analytical procedures we used.

The adsorption of the carbohydrate and lignin-derived fractions of the xylo-oligosaccharides on activated carbons was tested at 30 °C using a constant concentration of crude xylo-oligosaccharides of 20 g/L in deionized water and concentrations of activated carbon of 1.5, 3.3, 10.0, 16.7, 30.0, and 50.0 g_A/L . Figure 1 shows the GPC chromatograms of the feed solution. The UV signal at 254 nm was attributed to the presence of compounds derived from lignin and extractives and from their condensation with furfural, HMF, and other carbohydrate-degradation products, which accounted for around 30% of the mass of the sample. We assumed that the signal of the refractive index detector was caused mainly by carbohydrates and inorganic salts (soluble ashes), since they constituted nearly 70% of the mass in the crude xylo-oligosaccharides, though all the species in the mixture contributed to the signal of this nonselective detector. The retention times for narrow standards of dextran, malto-oligosaccharides, and xylose are included in Figure 1 for comparison. The RI signal shows that the xylo-oligosaccharides had a molar mass below 50 kDa. The most abundant species had a molar mass of between 1 and 5 kDa. There was also a small fraction of the mixture with a molar mass of below 0.15 kDa (xylose). Some of this was inorganic salts (ashes) that eluted after monosaccharides in this chromatographic system. Data from the UV signal revealed two important facts. First, a significant amount of lignin-derived products eluted at the same interval of retention time as did the xylo-oligosaccharides. This was in agreement with the existence of phenolic side groups such as ferulic acids and lignin fragments, which are directly attached to the xylan backbone chains.²⁷ Second, almost half of the lignin-derived products were eluted at a retention time that was well above that of xylose (0.15 kDa). These products were low-molar mass phenolics that eluted from the chromatographic column with a different pattern from that of oligosaccharides, partly because they may have

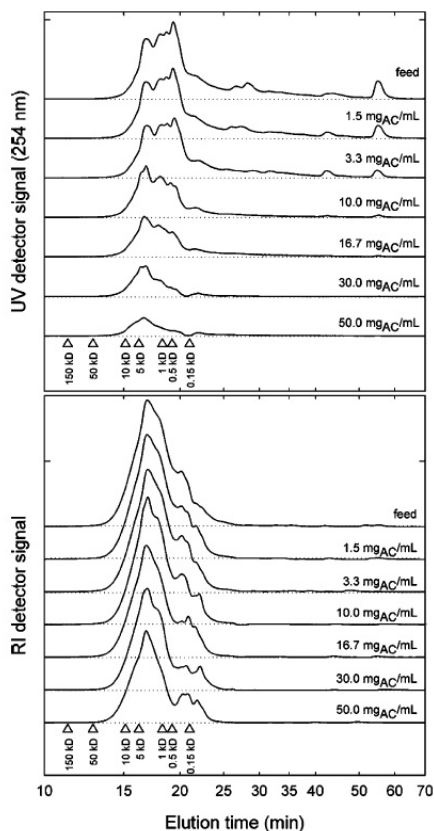


Figure 1. GPC chromatograms (time in log scale) for the xylo-oligosaccharides remaining in solution in the equilibrium adsorption experiments at 30 °C and different loads of the AC-1 activated carbon. The UV signal at 254 nm (top) is caused by lignin-derived phenolics, while the refractive index signal (bottom) is mainly attributed to carbohydrates (oligomers and monomers).

hydrodynamic volumes in 0.05 mol/L KNO_3 that are lower than those of carbohydrates of equivalent molar mass, but mainly because of adsorption on the gel of the GPC column, which increases the elution time. Palm and Zacchi²⁸ observed the adsorption of lignin-derived compounds from wood autohydrolysis on the gel of filtration columns.

Figure 1 also shows the GPC chromatograms for selected samples of the xylo-oligosaccharide solution treated with AC-1. The low molar mass lignin-derived products, which have the longest elution times in the GPC system, are preferentially adsorbed when small amounts of activated carbon are added to the solution. Figure 1 shows that they were completely adsorbed when 16.7 $\text{g}_{\text{AC}}/\text{L}$ was used. The lignin-products in the range of the elution time of oligosaccharides were also adsorbed, but they were still detected even at 50 $\text{g}_{\text{AC}}/\text{L}$ since they are linked to xylose in xylo-oligosaccharides. The adsorption of the carbohydrate fraction was less significant. Below a carbon load of 16.7 $\text{g}_{\text{AC}}/\text{L}$, only species with a molar mass of below 0.5 kDa were adsorbed. At a higher carbon load, there was a reduction in the signal of the sample at all molar masses, but even at 50 $\text{g}_{\text{AC}}/\text{L}$, the total amount of carbohydrates adsorbed was still below 40%. The same qualitative trends were observed for the other activated carbons we tested.

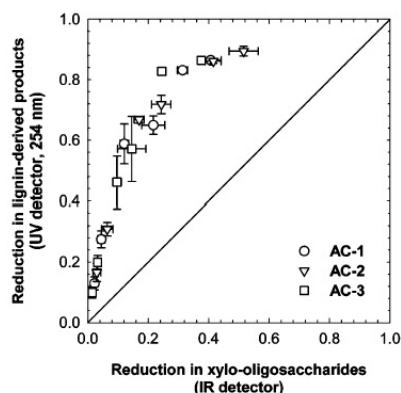


Figure 2. Relation between the reduction in the concentrations of lignin-derived phenolics and carbohydrates at equilibrium for various loads of activated carbon at 30 °C. Error bars are confidence intervals at the 95% probability level.

The reductions in the concentrations of lignin-derived products and carbohydrates ($r_{d,j}$) were calculated from the areas of the GPC chromatograms by assuming constant response factors (eq 2), and the amounts of each solute adsorbed were calculated from a mass balance for the batch system using eq 3, in which j indicates lignin-derived products or carbohydrates, $C_{0,j}$ (g/L) is the concentration of solute in the feed, $C_{e,j}$ (g/L) is the equilibrium concentration of species j in the solution, $C_{\text{Se},j}$ ($\text{g}/\text{g}_{\text{AC}}$) is the concentration of solute j adsorbed on the activated carbon at equilibrium, m is the mass of activated carbon (g_{AC}), and V is the volume of the solution (L). Figure 2 shows the reduction in the concentrations of lignin-derived products and xylo-oligosaccharides in solution for the three activated carbons we tested. Lignin-derived products were preferentially adsorbed over the carbohydrate fraction, especially at low concentrations of AC when the low molar mass aromatics were adsorbed. For instance, when 70% of the lignin-derived compounds were adsorbed, around 80% of the carbohydrates were still in solution. When over 80% of these compounds were adsorbed, the adsorption of carbohydrates dramatically increased.

The adsorption of mixtures of organic solutes onto activated carbons is a complex process that is determined by the chemistry of the carbon surface, the interactions between the solutes and the surface, the interactions of the solutes with the solvent, and those of the solvent with the carbon surface. The molar mass of the solute and the distribution of pore diameters of the carbon also play a significant role in determining the fraction of carbon surface that is actually accessible to a specific solute. The preferential adsorption of lignin-derived species over xylo-oligosaccharides may be attributed to several factors. Lignin-derived species are substituted phenolic monomers and oligomers that are more hydrophobic than carbohydrates. Xylo-oligosaccharides will therefore be more stable in water solution than lignin-derived products especially if, as in activated carbons, the surface of the adsorbent is predominantly hydrophobic.

Average pore diameters were 2.4, 2.1, and 4.1 nm for AC-1, AC-2, and AC-3, respectively. Table 2 shows that the activated carbons had a significant fraction of micropores, while Figure 3 shows that the pore volume distribution, which was calculated with the density functional theory (DFT) model,²⁹ was different for the three carbons. Most of the mesopore volume in the AC-1 carbon corresponded to pores with diameters from 2 to 10 nm, and the rest corresponded to large mesopores (30–50 nm). The

2298 Ind. Eng. Chem. Res., Vol. 45, No. 7, 2006

Table 2. Freundlich Isotherms: Results for the Adsorption of the Carbohydrate Fraction and the Lignin-Derived Products on Commercial Activated Carbons^a

	AC-1 (ROX 0.8)	AC-2 (PAC200)	AC-3 (Darco 12 × 40)
Xylo-oligosaccharides			
n	1.00 ± 0.13	0.81 ± 0.11	0.66 ± 0.09
$K_{XO}[L^{(1/n)} / (g_{ACG}^{(1/n)} - 1)]$	0.0148 ± 0.0046	0.0324 ± 0.0084	0.0249 ± 0.0054
Lignin-Derived Products			
n	0.82 ± 0.06	0.82 ± 0.05	0.62 ± 0.05
$K_{LP}[L^{(1/n)} / (g_{ACG}^{(1/n)} - 1)]$	0.145 ± 0.008	0.184 ± 0.009	0.134 ± 0.007

^a Confidence intervals were calculated at $\alpha = 0.05$.

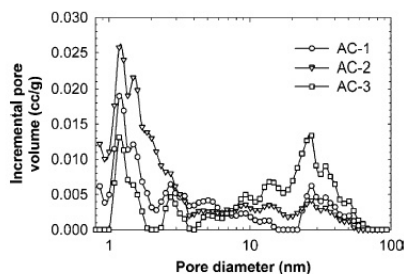


Figure 3. Pore volume distributions for the three activated carbons used in this study.

AC-2 carbon had the largest mesopore pore volume, but it had more pore volume than the AC-1 in the zone of small mesopores and a similar amount of large mesopores. Finally, the AC-3 carbon had very low volume in the small mesopore region, and most of its mesopore volume corresponded to large pores, from 10 to 50 nm. Around half of the lignin-derived compounds and associated impurities that are present in the crude xylo-oligosaccharides had a low molar mass (i.e., around 0.1 kDa) and were easily adsorbed in the three activated carbons, since their entire surface was accessible to these small solute molecules. On the other hand, xylo-oligosaccharides and some of the lignin-derived impurities had molar masses from 1 to 50 kDa, which is roughly equivalent to an interval of molecular diameters from 2 to 10 nm. The area available for the adsorption of the oligomers was therefore dependent on their molar mass: the larger the molar mass, the lower the area they could access. This effect should be more important for carbons AC-1 and AC-2, which have a significant fraction of pores below 10 nm.

However, solute size and the pore diameters are not the only variables governing adsorption. If we compare the GPC chromatograms in Figure 1 for xylo-oligosaccharides and lignin products at a high concentration of carbon AC-1, we can see that the reduction in the concentration of high molar mass solutes was much greater for the lignin products than for xylo-oligosaccharides. The presence of carboxylic and other acidic groups on the surface of the carbon has a definite effect on the adsorption of phenol, since it favors the chemisorption of phenol but hinders physisorption.³¹ We may expect the same to be true for the lignin-derived phenolics present in the crude xylo-oligosaccharides. Finally, electrostatic interactions between charged solutes and the surface of the carbon must also be considered. The pH of the xylo-oligosaccharide solution was 5.7 due to the dissociation of the acetyl groups in the backbone chain of the xylo-oligosaccharides and the carboxyl groups in ferulic acids and in some lignin-derived products. Since this pH is below the pH of zero charge of the activated carbons ($8 < \text{pH}_{\text{PZC}} < 8.7$), we can expect the surface of the carbons to have a positive charge distributed among the basic superficial groups.³¹ This should create favorable electrostatic interactions

between the positive surface and the negatively charged solutes such as the xylo-oligosaccharide chains that contain dissociated acetyl groups.

$$rd_j = 1 - \frac{C_{e,j}}{C_{0,j}} \quad (2)$$

$$C_{Se,j} = \frac{V}{m}(C_{0,j} - C_{e,j}) \quad (3)$$

$$\ln C_{Se,j} = \ln K_j + n_j \ln C_{e,j} \quad (4)$$

Regardless of the complexity of the phenomena involved in the competitive adsorption of mixtures of polydisperse oligomers with dissimilar chemical structures, simple models can provide some insight into the factors that have a determining influence on the selective adsorption of lignin-related species over xylo-oligosaccharides. Adsorption equilibrium was modeled through the Freundlich isotherm, which relates the concentration of a j solute at equilibrium ($C_{e,j}$) to the concentration of j adsorbed on the surface ($C_{Se,j}$). The unit-capacity parameter, K_j , is a measure of the degree of strength of adsorption, and n_j , the site-energy parameter, is an indication of the heterogeneity of the surface adsorption sites. The closer the value of n_j is to unity, the more homogeneous is the energy of the surface sites. The Freundlich isotherm was linearized to calculate the constants n_j and K_j (eq 4). Figure 4 shows the linearized isotherms, and Table 2 shows the best-fit values of n_j and K_j for the three activated carbons and their confidence intervals at 95% probability. Calculations were done using the robust linear regression algorithm implemented in the *robustfit* function of the statistics toolbox of MATLAB (MathWorks Inc., USA). The isotherm provided an acceptable description of the adsorption of both the lignin-derived products and carbohydrates for the three activated carbons, since the model predictions fell within the scattering of the experimental data.

Possible correlations between the main properties of the activated carbons and the parameters of the Freundlich equation for xylo-oligosaccharides and lignin-derived products were analyzed. Figure 5 shows that the unit-capacity parameter for xylo-oligosaccharide adsorption (K_{XO}) increased with the mesopore volume of the activated carbon, while the site-energy parameter increased linearly with the concentration of basic surface groups. The carbons with more developed mesoporous structures had more surface area available for the adsorption of xylo-oligosaccharides with larger molar mass, thus giving higher values for the unit-capacity parameter of the Freundlich isotherm. Also, the higher the number of basic surface groups on the surface, the stronger the electrostatic interactions between the dissociated acetyl groups of the xylo-oligosaccharide chains and the positively charged surface, thus increasing the site-energy parameter n_{XO} for xylo-oligosaccharides adsorption. The K_{LP} parameter for the lignin-derived phenolics grew with the total concentration of acidic superficial groups. In studies on

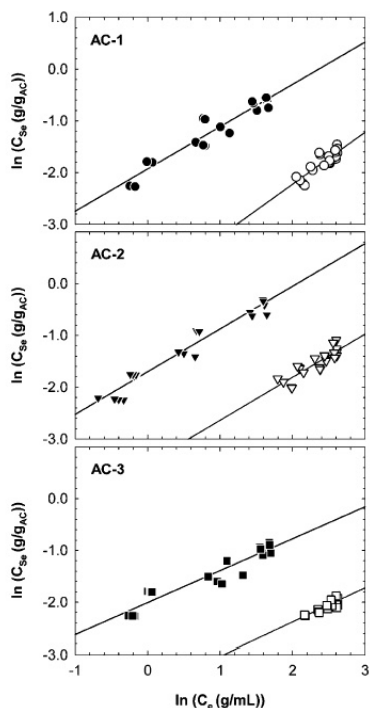


Figure 4. Freundlich isotherms for the adsorption of lignin-derived phenolics (open symbols) and xylo-oligosaccharides (solid symbols) on the three activated carbons at 30 °C.

phenol adsorption from acidic water solutions, the increase in the unit-capacity parameter with the concentration of acidic surface groups has been explained by the existence of two parallel routes: physical adsorption and acid-catalyzed chemisorption.³⁰ We may expect the contribution of chemisorption to the overall adsorption of the low molar mass phenolics present

in the complex mixture of lignin-related products to become more important as the number of acidic surface groups increases, thus increasing K_{LP} . In contrast, the site-energy parameter, n_{LP} , did not have a clear correlation with the concentration of acidic surface groups. Promoting the surface acidic groups by oxidation of an activated carbon reduces the adsorption of phenol from aqueous solution.³¹ More acidic groups should favor chemisorption, but they lower physical adsorption because the acidic groups act as electron acceptors and lower the π -electron density in the carbon planes, thus decreasing the interaction between the aromatic rings and the carbon basal planes. Since physical adsorption is the dominant mechanism, the overall consequence is lower phenol adsorption and a decrease in the site-energy parameter, n , of the Freundlich isotherm.³⁰ In our case, it seems that n_{LP} increased for activated carbons with more acidic surface groups, though the values of n_{LP} for AC-1 (0.82 ± 0.06) and AC-2 (0.82 ± 0.05) were statistically the same even if they had different concentrations of acidic surface groups (6.0 mequiv/g for AC-1 and 7.9 mequiv/g for AC-2). This behavior may be caused by the different nature of the predominant acidic groups in each carbon, which were manufactured from a variety of raw materials using different methods of activation. Phenols are the main acidic group in AC-1 (4.2 mequiv/g), while in AC-2 the main group is carbonyls (4.6 mequiv/g). The relative importance of the chemisorption and physical adsorption paths will therefore be different in each carbon due to the different acidity of these groups. Finally, no direct correlations of the Freundlich parameters with other properties of the activated carbons such as the surface area or the total pore volume were observed.

On the basis of the analysis of the Freundlich isotherms, the purification of xylo-oligosaccharides will require activated carbons with unit-capacity and site-energy parameters that are low for xylo-oligosaccharides and high for lignin-derived products. The AC-1 carbon, with a K_{LP}/K_{XO} of 9.8 ± 3.6 , had a slightly better ratio of unit-capacities than AC-2 (5.7 ± 1.8) and AC-3 (5.4 ± 1.4), while the ratio n_{LP}/n_{XO} did not present significant differences due to the large scattering of the results (0.82 ± 0.17 for AC-1, 1.01 ± 0.20 for AC-2, and 0.94 ± 0.20

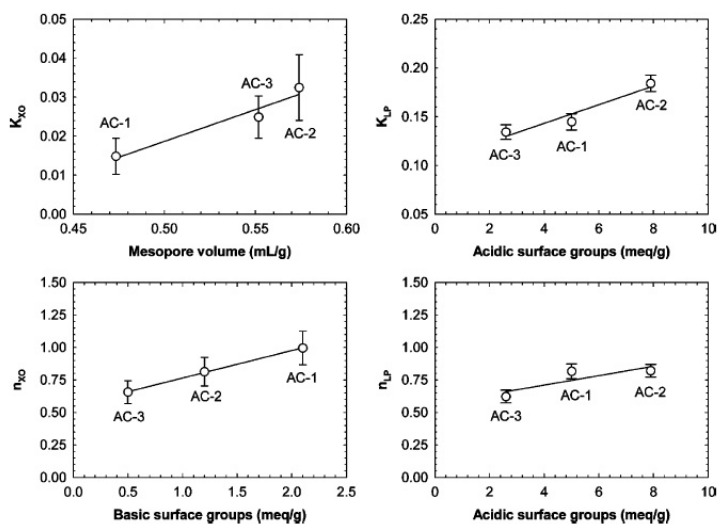


Figure 5. Variation in the constants of the Freundlich isotherms of lignin-derived compounds and xylo-oligosaccharides (K_{LP}) with the surface properties of the activated carbons. The lines only indicate trends.

2300 Ind. Eng. Chem. Res., Vol. 45, No. 7, 2006

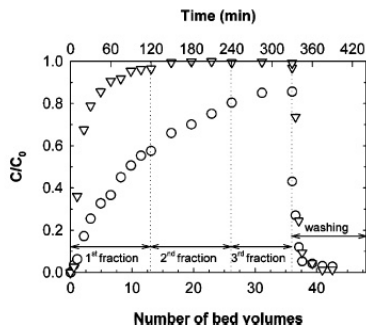


Figure 6. Adsorption of the crude xylo-oligosaccharides from reaction batch 2 on an AC-1 activated carbon column: breakthrough curves for carbohydrates (∇) and lignin-derived products (\circ).

for AC-3). In general, a suitable activated carbon should have small mesopore diameters, a low volume of mesopores, and a low concentration of basic surface groups to limit xylo-oligosaccharide adsorption. It should also be highly microporous and have acidic surface groups to favor the adsorption of the lignin-related products (high K_{LP}).

Column Tests. Column tests were performed with the ROX 0.8 granular activated carbon (AC-1). This carbon was selected because of its slightly better selectivity toward lignin adsorption and because it was readily available in granular form and more suitable for column packing than AC-2 and AC-3. The latter contained fines and caused problems during operation due to the entrainment of carbon particles and because it led to larger pressure drops across the bed. Figure 6 shows the breakthrough curves for an experiment performed using the second batch of xylo-oligosaccharides solution directly. The solution was fed at 6.0 mL/min, and a column loaded with 22.0 g of activated carbon was used. The activated carbon was rapidly saturated with carbohydrates. Retention for carbohydrates was only 10% after 60 min (6.55 bed volumes circulated), while retention for lignin-derived products was over 60%. After 180 min (19.6 bed volumes), the column was completely saturated with carbohydrates and retention was 0.2% but it was still 30% for lignin products. Figure 7 shows the GPC chromatograms for samples of the effluent taken at selected times during the experiment. The lignin-derived products of low molar mass were completely adsorbed on the column during the first 45 min of the experiment, which corresponds to 4.91 bed volumes of feed circulated through the column, but the high molar mass fraction of lignin products associated to carbohydrates was not adsorbed completely even when the volume circulated was small (2.18 bed volumes). The carbohydrate fraction had low adsorption, and there were few differences in the degree of adsorption with molar mass. The fraction collected during the cleaning of the carbon bed with deionized water contained both carbohydrates and lignin-derived species. The latter were detected in the washing stream even after 60 min of cleaning (6.55 bed volumes of water), which suggests that they were strongly adsorbed on the surface of the carbon.

The fractions collected during the experiment were lyophilized to recover the xylo-oligosaccharides (F1, 0–2 h; F2, 2–4 h; F3, 4–5.5 h; F4, washing, 5.5–6.5 h). The dry product was weighed to calculate the yield and analyzed for ash, klason lignin, monomers, xylo-oligosaccharides, and the molar mass distribution. Table 3 shows that the average concentration of nonvolatile soluble products decreased from 35.2 g/L in the feed to 25.2 g/L in the product collected from the column outlet

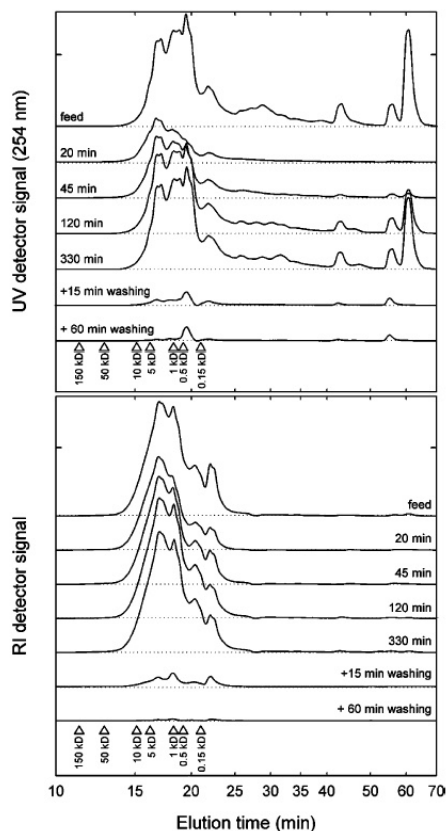


Figure 7. Adsorption of the crude xylo-oligosaccharides from reaction batch 2 on an AC-1 activated carbon column: GPC chromatograms (time in log scale) for the xylo-oligosaccharides remaining in solution. The UV signal at 254 nm (top) is caused by lignin-derived phenolics, while the RI signal (bottom) is mainly attributed to carbohydrates (xylo-oligosaccharides and monomers).

during the first 2 h of the experiment. Analysis of the recovered product shows that monosaccharides and xylo-oligomers were partially adsorbed on the carbon, but the highest adsorption was for lignin-related products and for furfural and HMF, which were almost completely removed from the solution. The product fractions collected afterward (F2 and F3) showed a dramatic decrease in the capacity of adsorption of the column for carbohydrates, although some retention capacity was still observed for furfural, HMF, and lignin-derived species.

The retention for carbohydrates, mainly xylo-oligosaccharides but also monosaccharides, was calculated by integrating the RI signal of the GPC chromatograms of the feed and the samples taken during the experiment, whereas the retention for lignin and carbohydrate-degradation products (furfural and HMF) was calculated from the signal of the UV detector at 254 nm. Retentions for fractions F1–F3 were 20.2, 0.7, and 0.5% for carbohydrates and 64.3, 30.2, and 16.0% for lignin, in accordance with the preferential adsorption of lignin products over carbohydrates we observed earlier. The retentions were also calculated from the mass and composition of the nonvolatile products recovered by lyophilization of the fractions F1, F2, and F3. The results were close to those calculated from the GPC chromatograms, especially for carbohydrates.

Table 3. Adsorption on an AC-1 Activated Carbon Column: Composition of the Lyophilized Samples of the Product Fractions Collected during the Experiment and Retentions Calculated for Xylo-oligosaccharides and Lignin-Related Products (Xylo-oligosaccharide Solution from Reaction Batch 2)

	feed	collected fractions		
		F1 (0–2 h)	F2 (2–4 h)	F3 (4–5.5 h)
avg conc of dissolved products for the fraction (g/L)	35.2	25.2	33.6	33.9
Composition (% of the Dissolved Products in the Feed)				
glucose	1.84	1.28	1.76	1.75
xylose	3.95	2.81	3.96	3.97
arabinose	3.61	2.58	3.58	3.57
acetic acid	3.89	1.74	3.78	3.85
furfural	0.85	0.01	0.40	0.87
hydroxymethyl furfural	0.43	0.03	0.26	0.39
xylo-oligosaccharides	57.8	46.0	59.3	58.6
lignin-related products	6.85	2.90	5.55	5.95
ash	9.02	7.66	7.36	7.60
other (by difference)	11.8	6.78	9.49	9.84
Retention (% of Feed)				
xylo-oligosaccharides (RI signal)	calculated by integration of the GPC chromatograms (data in Figure 7)			
		20.2	0.7	0.5
lignin-related products (UV signal)	calculated from the yield and chemical analysis of lyophilized samples			
		64.3	30.2	16.0
xylo-oligosaccharides ^a		22.5	0.5	0.9
lignin-related products ^b		63.9	23.6	11.4

^a Including monosaccharides, acetic acid, and ash. ^b Including furfural and HMF.

Vegas and co-workers have investigated several sequential treatments for the removal of extractive- and lignin-derived compounds from the aqueous solutions of crude xylo-oligosaccharides of barley residues¹³ and rice husks.¹⁴ After three sequential extraction stages with ethyl acetate, 6.2% of the carbohydrates and 38.2% of non-carbohydrates were removed from the solution in the case of rice husks, while for barley residues removal was 15.9% for carbohydrates and 32.9% for extractives- and lignin-related products. These values are close to those we obtained for fraction F2. Further processing of the ethyl acetate-extracted solutions with a strong anion-exchange resin increased the removal of non-carbohydrates to 78.2 and 54.0% for rice husks and barley residues, respectively, while carbohydrate removal was 22.2 and 20.4%. Our results from the F1 fraction indicate that treatment with activated carbon provides better results than extraction with ethyl acetate and that it may even produce a similar degree of removal of non-carbohydrate compounds to extraction combined with treatment with anion-exchange resins.

Conclusions

The treatment with activated carbon of raw xylo-oligosaccharide solutions obtained by autohydrolysis of lignocellulosics is a feasible option for the removal of extractives- and lignin-derived compounds and carbohydrate-degradation products. The selective adsorption of lignin products over carbohydrates has been observed for three commercial activated carbons at slightly acidic pHs. Selectivity toward lignin adsorption was higher when the carbon was highly microporous and had small mesopore diameters, a low volume of mesopores, a low concentration of basic surface groups to limit xylo-oligosaccharide adsorption, and acidic surface groups to favor the adsorption of the lignin-related products. Further studies into the tailoring of the surface properties of the carbons in order to improve selectivity and adsorption capacity for lignin-products, and into the regeneration of spent carbon beds, are under way.

Acknowledgment

This research was made possible in part by financial support from the Spanish Government (MCYT, project PPQ2002-04201-CO02), the Catalan Regional Government (DURSI,

2001SGR00323 and 2002AIRE), and the ALFA Program of the EU (project ALFA II 0412 FA FI). V.F. acknowledges the MCYT and the Universitat Rovira i Virgili (URV) for the financial support of her "Ramón y Cajal" research contract. D.N. is grateful to the Catalan Regional Government for her Ph.D. scholarship. V.T. is grateful to the URV for her Ph.D. grant, and A.M. is grateful to the Spanish Ministry of Education for economic support. The authors thank the NORIT Company for supplying the samples of their activated carbons.

Literature Cited

- Hudson, M. J.; Marsh, P. D. Carbohydrate metabolism in the colon. In *Human colonic bacteria - role in nutrition, physiology and pathology*; Gibson, G. R., MacFarlane, G. T., Eds.; CRC Press: Boca Raton, FL, 1995; pp 61–73.
- Fooks, L. J.; Gibson, G. R. In vitro investigations of the effect of probiotics and prebiotics on selected human intestinal pathogens. *FEMS Microbiol. Ecol.* **2002**, *39*, 67–75.
- Fooks, L. J.; Gibson, G. R. Mixed culture fermentation studies on the effects of synbiotics on the human intestinal pathogens *Campylobacter jejuni* and *Escherichia coli*. *Anaerobe* **2003**, *9*, 231–242.
- Zampa, A.; Silvi, S.; Fabiani, R.; Morozzi, G.; Orpianesi, C.; Cresci A. Effects of different digestible carbohydrates on bile acid metabolism and SCFA production by human gut micro-flora grown in an in vitro semi-continuous culture. *Anaerobe* **2004**, *10*, 19–26.
- Crittenden, R.; Playne, M. Production, properties and applications of food-grade oligosaccharides. *Trends Food Sci. Technol.* **1996**, *7*, 353–361.
- Kontula, P.; von Wright, A.; Mattila-Sandholm, T. Oat bran β -gluco and xylo-oligosaccharides as fermentative substrates for lactic acid bacteria. *Int. J. Food Microbiol.* **1998**, *45*, 163–169.
- Glasser, W. G.; Jain, R. K.; Sjøstedt, M. A. Thermoplastic pentosan-rich polysaccharides from biomass. U.S. Patent 5,430,142, 1995.
- Gabrieli, I.; Gatenholm, P.; Glasser, W. G.; Jain, R. K.; Kenne, L. Separation, characterization and hydrogel-formation of hemicellulose from aspen wood. *Carbohydr. Polym.* **2000**, *43*, 367–374.
- Ando, H.; Ohba, H.; Sakaki, T.; Takamine, K.; Kamino, Y.; Moriwaki, S.; Bakalova, R.; Uemura, Y.; Hatate, Y. Hot-compressed-water decomposed products from bamboo manifest a selective cytotoxicity against acute lymphoblastic leukemia cells. *Toxicol. in Vitro* **2004**, *18*, 765–771.
- Korte, H. E.; Offermann, W.; Puls, J. Characterization and preparation of substituted xylo-oligosaccharides from steamed birchwood. *Holzforschung* **1991**, *45*, 419–424.
- Puls, J.; Schuseil, J. Chemistry of hemicelluloses: relationship between hemicellulose structure and enzymes required for hydrolysis. In *Hemicellulose and Hemicellulases*; Coughlan, M. P., Hazlewood, G. P., Eds.; Portland Press: London, 1993; pp 1–27.

2302 Ind. Eng. Chem. Res., Vol. 45, No. 7, 2006

- (12) Nabarlaz, D.; Fariol, X.; Montané, D. Autohydrolysis of almond shells for the production of xylo-oligosaccharides: product characteristics and reaction kinetics. *Ind. Eng. Chem. Res.* **2005**, *44*, 7746–7755.
- (13) Vegas, R.; Alonso, J. L.; Domínguez, H.; Parajó, J. C. Manufacture and refining of oligosaccharides from industrial solid wastes. *Ind. Eng. Chem. Res.* **2005**, *44*, 614–620.
- (14) Vegas, R.; Alonso, J. L.; Domínguez, H.; Parajó, J. C. Processing of rice husk autohydrolysis liquors for obtaining food ingredients. *J. Agric. Food Chem.* **2004**, *52*, 7311–7317.
- (15) Parajó, J. C.; Domínguez, H.; Domínguez, J. M. Study of charcoal adsorption for improving the production of xylitol from wood hydrolysates. *Bioprocess Eng.* **1995**, *16*, 39–43.
- (16) Gurgel, P. V.; Mancilla, I. M.; Peçanha, R. P.; Siquiera, J. F. M. Xylitol recovery from fermented sugarcane bagasse hydrolyzate. *Bioresour. Technol.* **1995**, *52*, 219–223.
- (17) Couteau, D.; Mathaly, P. Purification of ferulic acid by adsorption after enzymatic release from sugar-beet pulp extract. *Ind. Crops Prod.* **1997**, *6*, 237–252.
- (18) Couteau, D.; Mathaly, P. Fixed-bed purification of ferulic acid from sugar-beet pulp using activated carbon: optimization studies. *Bioresour. Technol.* **1998**, *60*, 17–25.
- (19) Lee, J. W.; Kwon, T. O.; Moon, I. S. Adsorption of monosaccharides, disaccharides, and maltooligosaccharides on activated carbon for separation of maltopentaose. *Carbon* **2004**, *42*, 371–380.
- (20) Ahmedna, M.; Marshall, W. E.; Rao, R. M. Surface properties of granular activated carbons from agricultural byproducts and their effects on raw sugar decolorization. *Bioresour. Technol.* **2000**, *71*, 103–112.
- (21) Yuan, Q. P.; Zhang, H.; Qian, Z. M.; Yang, X. J. Pilot-plant production of xylo-oligosaccharides from corn cob by steaming, enzymatic hydrolysis and nanofiltration. *J. Chem. Technol. Biotechnol.* **2004**, *79*, 1073–1079.
- (22) Brunauer, S.; Emmett, P. H.; Teller, E. Adsorption of Gases in Multimolecular Layers. *J. Am. Chem. Soc.* **1938**, *60*, 309–319.
- (23) Sing, K. S. W. The use of physisorption for the characterization of microporous carbons. *Carbon* **1989**, *27*, 5–11.
- (24) Kruk, M.; Li, Z. J.; Jaroniec, M.; Betz, W. R. Nitrogen Adsorption Study of Surface Properties of Graphitized Carbon Blacks. *Langmuir* **1999**, *15*, 1435–1441.
- (25) Noh, J. S.; Schwarz, J. A. Effect of HNO₃ treatment on the surface acidity of activated carbons. *Carbon* **1990**, *28*, 675–682.
- (26) Boehm, H. P. Chemical identification of surface groups. *Adv. Catal.* **1966**, *1*, 179–287.
- (27) De Vries, R. P.; Visser, J. *Aspergillus* enzymes involved in degradation of plant cell wall polysaccharides. *Microbiol. Mol. Biol. Rev.* **2001**, *65*, 497–522.
- (28) Palm, M.; Zacchi, G. Separation of hemicellulosic oligomers from steam-treated spruce wood using gel filtration. *Sep. Purif. Technol.* **2004**, *36*, 191–201.
- (29) Olivier, J. P. Improving the models used for calculating the size distribution of micropore volume of activated carbons from adsorption data. *Carbon* **1998**, *36*, 1469–1472.
- (30) Salame, I. I.; Bandosz, T. J. Role of surface chemistry in adsorption of phenol on activated carbons. *J. Colloid Interface Sci.* **2003**, *264*, 307–312.
- (31) Moreno-Castilla, C. Adsorption of organic molecules from aqueous solutions on carbon materials. *Carbon* **2004**, *42*, 83–94.

Received for review September 19, 2005
Revised manuscript received February 1, 2006
Accepted February 6, 2006

IE051051D

6. CONCLUSIONES GENERALES

La preparación de CA a partir de diferentes tipos de agentes activantes ácidos (H_3PO_4) o básicos (NaOH y KOH) a partir de lignina Kraft como material precursor, da como resultado carbones microporosos con altas áreas superficiales, con rendimientos a carbón razonables y con buenas propiedades para ser utilizados en la descontaminación de efluentes líquidos o gaseosos.

Conocer el efecto que la variación de las condiciones de operación produce es muy importante para poder controlar las características finales del producto, que depende de la aplicación que se le quiera dar. Para ello, es importante conocer el mecanismo de activación química que tiene lugar. En el caso de la activación con ácido fosfórico y a partir de datos experimentales, se han explicado los procesos reactivos que tienen lugar durante la pirólisis mediante una serie de reacciones de pseudoprimer orden, como resultado de

la simplificación de los múltiples procesos reactivos involucrados en la descomposición térmica que se ajusta correctamente a los escasos datos bibliográficos obtenidos.

El mecanismo de reacción que se propone se compone de dos etapas. En primer lugar, la mezcla entre la lignina y el ácido fosfórico dan lugar a un complejo generado por la reacción entre el ácido y los sitios reactivos de la lignina que puede durar aproximadamente una hora a temperatura ambiente y que se finaliza antes de comenzar el proceso térmico.

Posteriormente y una vez se comienza con la pirólisis de la muestra, se produce la conversión del exceso de ácido en P_2O_5 después de haberse eliminado por completo el agua presente en la mezcla. La formación de este compuesto está involucrada con el desarrollo de la estructura interna de la muestra ya que actúa como protección de la estructura y cuando seguidamente se evapora y produce la combustión de la muestra. Finalmente, la pirólisis completa del complejo generado en el primer paso, da lugar al CA definitivo y volátiles con lo que se acaba de desarrollar la estructura interna del producto final.

Una vez determinado los fenómenos que se producen en la activación química, es necesario conocer como afectan las condiciones de operación a las propiedades finales del carbón.

En el caso de la activación con H_3PO_4 , los parámetros estudiados son tres: el tiempo de impregnación, la temperatura de activación y la cantidad de ácido empleado.

Por un lado, la reacción de impregnación se completa en una hora y tiempos mayores no tienen ninguna influencia en la producción de carbón, al igual que la realización de isoterma localizadas durante el proceso pirolítico.

Respecto a la relación entre la cantidad de ácido fosfórico añadido y la de lignina Kraft, existe un máximo en el cual se produce la reacción completa de la lignina, situado en valores entre 0.8 y 1.0, y es a partir de este valor, no se producen cambios en el proceso de pirólisis que afecten a sus propiedades más importantes. A relaciones mayores de 1.4 comienza a disminuir el área superficial BET y el volumen total de poros promovido por el agresivo ataque del ácido fosfórico. El uso de ácido fosfórico en exceso produce óxidos de fósforo que protegen la estructura del carbón de la oxidación externa y cuando esta especie se evapora a temperaturas mayores de $580^\circ C$, el carbón se oxida totalmente en aire mientras que en presencia de nitrógeno, la producción de carbón se mantiene constante.

Por último, el aumento de la temperatura de activación de 400°C a 600°C produce un decremento en el volumen de ultramicroporos pero un aumento de la microporosidad total y es a esta temperatura, 600°C, donde se encuentra un óptimo para el desarrollo de la porosidad en este tipo de procesos. A partir de este punto, seguir aumentando la temperatura conlleva la reducción del volumen total de poros y de área superficial BET debido al colapso y al exceso de oxidación del material.

Por tanto, excepto el tiempo de impregnación, el resto de parámetros tienen una importante influencia en las características finales del CA. La disminución de superficie BET viene acompañada de un descenso considerable del rendimiento a carbón y se puede concluir que el valor óptimo respecto al desarrollo de la porosidad a una temperatura de 450°C está entre 1.2 y 1.4. El efecto del tiempo de impregnación es menos importante aunque su aumento provoca una ligera disminución del área superficial y del volumen total de poros. Este efecto tiene más importancia cuando se utilizan también altas temperaturas debido a la descomposición de los enlaces entre el carbón y los fosfatos y polifosfatos.

A parte de las condiciones de operación, otro factor que puede afectar a las condiciones finales del CA es la cantidad de cenizas que contiene la lignina Kraft, tal y como se suministra, en comparación con su uso una vez desmineralizada, es decir, después de proceder a un pretratamiento ácido.

Los análisis realizados por SEM y por espectroscopía de infrarrojo demuestran que el proceso de desmineralización de la materia prima produce un aumento en la polimerización de la lignina y reduce la interacción entre ésta y el ácido fosfórico. De esta manera, se ven afectadas las propiedades finales del AC-P de tal forma que al aumentar la temperatura de pirólisis, aumenta el rendimiento a carbón, la aromaticidad, el área superficial y la cantidad de grupos superficiales en los CA preparados a partir de LK, mientras que la tendencia es opuesta para los CA preparados a partir de LK_d.

En el caso de la activación química con NaOH y KOH, el uso de hidróxidos alcalinos en este tipo de procesos está desarrollando un incremento de interés, por esta razón la posibilidad de preparar CA microporosos a partir de lignina Kraft desmineralizada y KOH o NaOH es parte fundamental de esta memoria.

En este caso, las condiciones de operación estudiadas son cinco: la temperatura de activación, la relación entre agente activante y precursor, el

tiempo de impregnación, el flujo de nitrógeno empleado como atmósfera dinámica en el proceso y por último, la velocidad de calentamiento.

La temperatura de activación es uno de los parámetros que más influencia tiene en este tipo de activaciones. A medida que ésta aumenta y esencialmente a partir de 750°C, los carbones pasan de ser esencialmente microporosos a aumentar la cantidad de mesoporos, ya que a altas temperaturas se produce el colapso de la estructura interna provocando la transformación de los poros más pequeños en poros mayores. A partir de 700°C, se produce un desarrollo pronunciado de la química de superficie. En el caso de la acidez, este aumento viene dado por la presencia de fenoles, alcoholes y carbonilos, aunque depende del tipo de hidróxido empleado como agente activante.

La relación de la cantidad añadida de agente activante y lignina Kraft tiene un efecto muy marcado en la producción de carbón y en el área superficial BET. El aumento de este parámetro, disminuye el rendimiento a carbón obtenido ya que la reacción de activación se ve favorecida y por tanto, se generan más volátiles que a su vez desarrollan la estructura interna. El aumento de hidróxido incrementa el contenido de especies oxigenadas en la superficie del carbón favoreciendo su oxidación y desarrollando tanto la acidez superficial, fundamentalmente mediante fenoles, alcoholes y carbonilos, como la basicidad superficial.

El tiempo de activación no tiene una influencia destacable, ya que principalmente favorece la descomposición de sales superficiales dando lugar a óxidos de carbono que colaboran al desarrollo de la estructura interna de los este tipo de AC. En este caso, no hay un efecto claramente definido sobre el desarrollo de la química superficial ya que si es cierto que se produce un aumento general de la basicidad, el desarrollo de la acidez depende del agente activante utilizado. El uso de hidróxido de potasio favorece el desarrollo de la acidez mediante fenoles y lactonas pero si se utiliza hidróxido de sodio, la acidez disminuye.

El caudal de nitrógeno empleado no es un factor importante en la activación con hidróxidos. Su función principal es la de facilitar la eliminación de los volátiles que se generan durante el proceso térmico aunque si se aumenta de manera pronunciada, y a temperaturas bajas, provoca también la eliminación de agente activante (hidróxido y otras especies como óxidos de carbono y agua) disminuyendo ligeramente la activación. La química de superficie se ve afectada de igual manera, produciendo variaciones poco significativas de la acidez y la basicidad superficial.

Respecto a la velocidad de calentamiento, su aumento produce disminuciones en el área superficial ya que durante el proceso de activación térmica, el hidróxido se funde y la superficie específica aumenta, el tiempo de contacto con el carbón es menor y disminuye la activación producida.

En general, los factores que influyen en mayor manera en los parámetros de estudio son la temperatura de activación y la relación de la cantidad entre agente activante y lignina Kraft que maximizan el área BET hasta $3000\text{m}^2/\text{g}$ aproximadamente, con un volumen de microporos de $1.5\text{ cm}^3/\text{g}$, a 700°C y una R de 3.

Finalmente, una vez se tienen caracterizados los CA preparados por diferentes métodos, estos se pueden aplicar en el campo más adecuado. Una de las principales aplicaciones de estos carbones está en la adsorción de contaminantes, como metales pesados o componentes orgánicos en sistemas líquidos.

En este campo, los carbones preparados a partir de la activación química con ácido fosfórico, también poseen una desarrollada acidez superficial, característica que combinada con su buena PSD, asegura una adsorción favorable de iones metálicos en solución. La temperatura de carbonización es el factor que afecta de manera más significativa ya que, como se ha visto anteriormente, cambia la porosidad del material y degrada la acidez superficial. Las condiciones de preparación del AC-P más adecuadas para maximizar la adsorción de cobre (65 mg Cu/g) son de 500°C de temperatura y una P/L de 1.4.

Optimizar la producción de AC-Na para maximizar su capacidad de adsorción de componentes orgánicos es posible mediante técnicas estadísticas para el diseño de experimentos. La técnica seleccionada fue la Metodología de Respuesta de Superficie debido a que agrupa técnicas tanto matemáticas como estadísticas que resulta de gran ayuda cuando se analizan sistemas donde hay una variable respuesta, la adsorción de azul de metileno, que se ve afectada por varias variables. Como resultado, se obtuvo un carbón activado que adsorbe más azul de metileno que los carbones comerciales utilizados para comparar a unas condiciones de 783°C , un contenido de lignina Kraft desmineralizada en la mezcla inicial del 26.4 %, empleando $200\text{ cm}^3\text{ N}_2/\text{min}$. A estas condiciones, la capacidad de adsorción obtenida fue de 940 mg AM/g CA , la cual se correlaciona con el volumen de microporos de las muestras analizadas y, en menor manera, con la química de superficie, influencia que depende de la naturaleza ácida o básica del compuesto orgánico empleado.

Para el estudio de la eliminación de componentes orgánicos en efluentes líquidos, fenol y benceno, la química de adsorción obedece a una reacción de pseudo segundo orden la cual es más favorable para el fenol que para el benceno. Los CA que se han empleado como adsorbatos en estos análisis son tres carbones derivados de la lignina Kraft y activados con los tres agentes activantes presentados en este estudio, NaOH, KOH y H₃PO₄. No se puede determinar que modelo de adsorción, Freundlich, Langmuir o Tempkin, describe mejor el proceso físico que tiene lugar ya que los tres proporcionan buenos ajustes. Las capacidades de adsorción máximas que se alcanzan han sido de 170 mg fenol/g y 20 mg benceno/g para el carbón activado con NaOH, 165 mg fenol/g y 20 mg benceno/g para el carbón activado con KOH y 60 mg fenol/g y 8 mg benceno/g para el carbón activado con H₃PO₄.

Sin embargo, estos carbones pueden tener otro campo de aplicación como es el de aditivo en membranas o la purificación de oligosacáridos. Así, el AC-P también se ha utilizado para obtener membranas poliméricas compuestas, etapa previa a la obtención de reactores de membranas enzimáticos, utilizando el carbón inmovilizado en la matriz polimérica para adsorber enzimas directamente, o a través de un metal, cobre en este caso, gracias a su buena capacidad de adsorción. A pesar que existen muchos ámbitos de aplicación para este tipo de membranas, en este caso particular, se han utilizado para obtener y separar azúcares de muy bajo peso molecular (cerca del monómero) a partir de azúcares de tamaño superior.

El uso de AC-P en las membranas permite buenas capacidades de separación cumpliendo con el objetivo especificado, y a pesar de que localmente se obtuvo mejor adsorción de enzima con el uso del metal, no se pudo concluir que en general, la utilización de éste implicara mejores resultados. En este sentido, son necesarios más experimentos.

Por último, el uso de carbones comerciales en el tratamiento de xilo-oligosacáridos obtenidos a partir de la autohidrólisis de materiales procedentes de biomasa es factible ya que permite eliminar componentes derivados de la lignina y extractivos. Este proceso debe llevarse a cabo mediante adsorbatos con pH ácido y de gran superficie específica, es decir, muy microporosos y con mesoporosidad poco desarrollada. Las características del carbón necesario para llevar a cabo este tipo de operaciones se adecuan a los carbones obtenidos para la realización de esta tesis. Por tanto, en los siguientes pasos a seguir en este campo de investigación parecen adecuados el uso de AC-P, AC-K y AC-Na.

7. BIBLIOGRAFÍA

1. Hayashi, J., Kazehaya, A., Muroyama, K., et al., *Preparation of activated carbon from lignin by chemical activation*. Carbon, 2000. **38**(13): p. 1873-1878.
2. Khezami, L., Chetouani, A., Taouk, B., et al., *Production and characterisation of activated carbon from wood components in powder: Cellulose, lignin, xylan*. Powder Technology
4th French Meeting on Powder Science and Technology, 2005. **157**(1-3): p. 48-56.
3. Teng, H., Yeh, T.-S., and Hsu, L.-Y., *Preparation of activated carbon from bituminous coal with phosphoric acid activation*. Carbon, 1998. **36**(9): p. 1387-1395.
4. Gonzalez-Serrano, E., Cordero, T., Rodriguez-Mirasol, J., et al., *Removal of water pollutants with activated carbons prepared from H₃PO₄ activation of lignin from kraft black liquors*. Water Research, 2004. **38**(13): p. 3043-3050.

5. Gonzalez-Serrano, E., Cordero, T., Rodríguez-Mirasol, J., et al., *Development of Porosity upon Chemical Activation of Kraft Lignin with ZnCl₂*. Industrial & Engineering Chemical Research, 1997. **36**(11): p. 4832-4838.
6. Rodríguez-Mirasol, J., Cordero, T., and Rodríguez, J.J., *Preparation and characterization of activated carbons from eucalyptus kraft lignin*. Carbon, 1993. **31**(1): p. 87-95.
7. del Bagnò, V.D., Miller, R.L., and Watkins, J.J., *On site production of activated carbon from Kraft Black Liquor*. 1978: U.S.
8. *Activated carbon compendium. A collection of papers from the journal Carbon 1996-2000*. 1^a ed, ed. H. Marsh. 2001, North Shields (UK): Elsevier.
9. Cooney, D.O., *Adsorption design for wastewater treatment*. 1999, Boca Ratón: Lewis Publisher.
10. Lin, S.Y., Jr., S.E.L., and LignoTech USA, I., *Lignin*, in *Kirk-Othmer Encyclopedia of Chemical Technology*. 2000.
11. Lin, S.Y. and Lin, I.S., *Lignin*. Ullmann's Encyclopedia of industrial chemistry, ed. S.H. Barbara Elvers, Gail Schulz. Vol. A15. 1990, New York. 305-315.
12. Hynek, S., Fuller, W., and Bentley, J., *Hydrogen storage by carbon sorption*. International Journal of Hydrogen Energy, 1997. **22**(6): p. 601-610.
13. Das, L.M., *On-board hydrogen storage systems for automotive application*. International Journal of Hydrogen Energy, 1996. **21**(9): p. 789-800.
14. Imamura, H. and Sakasai, N., *Hydriding characteristics of Mg-based composites prepared using a ball mill*. Journal of Alloys and Compounds Proceedings of the International Symposium on Metal-Hydrogen Systems-Fundamentals and Applications, 1995. **231**(1-2): p. 810-814.
15. Imamura, H., Sakasai, N., and Kajii, Y., *Hydrogen absorption of Mg-Based composites prepared by mechanical milling: Factors affecting its characteristics*. Journal of Alloys and Compounds, 1996. **232**(1-2): p. 218-223.
16. Imamura, H., Sakasai, N., and Fujinaga, T., *Characterization and hydriding properties of Mg-graphite composites prepared by mechanical grinding as new hydrogen storage materials*. Journal of Alloys and Compounds, 1997. **253-254**: p. 34-37.
17. Carpetis, C. and Peschka, W., *A study on hydrogen storage by use of cryoadsorbents*. International Journal of Hydrogen Energy, 1980. **5**(5): p. 539-554.
18. Chand Bansal, R., Donnet, J.-B., and Stoeckli, F., *Active Carbon*. 1988, New York and Basel.
19. Chambers, A., Park, C.R., Baker, T.K., et al., *Hydrogen Storage in Graphite Nanofibers*. Journal of Physical Chemistry B, 1998. **102**(22): p. 4253-4256.
20. Dillon, A.C., Jones, K.M., Bekkedahl, T.A., et al., *Storage of hydrogen in single-walled carbon nanotubes*. Nature, 1997. **386**: p. 377-379.

21. *General applications of activated carbon.* in *Ciencia y Tecnología del carbón activo.* 1994. Alicante.
22. Girgis, B.S. and El-Hendawy, A.-N.A., *Porosity development in activated carbons obtained from date pits under chemical activation with phosphoric acid.* *Microporous and Mesoporous Materials*, 2002. **52**(2): p. 105-117.
23. Smisek, M. and Cerny, S., *Active carbon: Manufacture, properties and applications*, ed. Elsevier. 1970, Amsterdam.
24. Rand, B. and Marsh, H., *The process of activation of carbons by gasification with CO₂-III. Uniformity of gasification.* *Carbon*, 1971. **9**(1): p. 79-85.
25. Schafer, H.N.S., *U. S. Patent 4.* 1977. p. 473.
26. Kraehenbuehl, F., Stoeckli, H.F., Addoun, A., et al., *The use of immersion calorimetry in the determination of micropore distribution of carbons in the course of activation.* *Carbon*, 1986. **24**(4): p. 483-488.
27. Suárez-García, F., Martínez-Alonso, A., and Tascón, J.M.D., *Pyrolysis of apple pulp: chemical activation with phosphoric acid.* *J. Annal. Appl. Pyrolysis.*, 2002. **63**(2): p. 283-301.
28. Guo, Y.P., Yang, S.F., Yu, K.F., et al., *The preparation and mechanism studies of rice husk based porous carbon.* *Materials Chemistry and Physics*, 2002. **74**(3): p. 320-323.
29. Qiao, W., Ling, L., Zha, Q., et al., *Preparation of a pitch-based activated carbon with a high specific surface area.* *Journal of Materials Science*, 1997. **32**(16): p. 4447-4453.
30. Sun, J., Rood, M.J., Rostam-Abadi, M., et al., *Natural gas storage with activated carbon from a bituminous coal.* *Gas Separation & Purification Carbon-Based Materials*, 1996. **10**(2): p. 91-96.
31. Hsu, L.-Y. and Teng, H., *Influence of different chemical reagents on the preparation of activated carbons from bituminous coal.* *Fuel Processing Technology*, 2000. **64**(1-3): p. 155-166.
32. Teng, H. and Wang, S.-C., *Preparation of porous carbons from phenol-formaldehyde resins with chemical and physical activation.* *Carbon*, 2000. **38**(6): p. 817-824.
33. Ahmadvour, A. and Do, D.D., *The preparation of activated carbon from macadamia nutshell by chemical activation.* *Carbon*, 1997. **35**(12): p. 1723-1732.
34. Guo, Y.P., Yu, K.F., Wang, Z.C., et al., *Effects of activation conditions on preparation of porous carbon from rice husk.* *Carbon*, 2000. **41**(8): p. 1645-1648.
35. Maciá-Agulló, J.A., Moore, B.C., Cazorla-Amorós, D., et al., *Activation of coal tar pitch carbon fibres: Physical activation vs. chemical activation.* *Carbon*, 2004. **42**(7): p. 1367-1370.
36. Lillo-Rodenas, M.A., Lozano-Castello, D., Cazorla-Amoros, D., et al., *Preparation of activated carbons from Spanish anthracite II. Activation by NaOH.* *Carbon*, 2001. **39**(5): p. 751-759.

37. Lillo-Rodenas, M.A., Cazorla-Amoros, D., and Linares-Solano, A., *Understanding chemical reactions between carbons and NaOH and KOH. An insight into the chemical activation mechanisms*. Carbon, 2003. **41**(2): p. 267-275.
38. Caballero, J.A., Marcilla, A., and Conesa, J.A., *Thermogravimetric analysis of olive stones with sulphuric acid treatment*. Journal of Analytical and Applied Pyrolysis, 1997. **44**(1): p. 75-88.
39. Manya, J.J., Velo, E., and Puigjaner, L., *Kinetics of Biomass Pyrolysis: a Reformulated Three-Parallel-Reactions Model*. Industrial Engineering Chemical Research, 2003. **42**(3): p. 434-441.
40. Orfao, J.J.M., Antunes, F.J.A., and Figueiredo, J.L., *Pyrolysis kinetics of lignocellulosic materials--three independent reactions model*. Fuel, 1999. **78**(3): p. 349-358.
41. Varhegyi, G., Antal, M.J., Szekely, T., et al., *Kinetics of the thermal decomposition of cellulose, hemicellulose, and sugarcane bagasse*. Energy & Fuels, 1987. **3**(3): p. 329-335.
42. Jagtoyen, M. and Derbyshire, F., *Activated carbons from yellow poplar and white oak by H₃PO₄ activation*. Carbon, 1998. **36**(7-8): p. 1085-1097.
43. Montané, D., Torné-Fernández, V., and Fierro, V., *Activated carbons from lignin: kinetic modeling of the pyrolysis of Kraft lignin activated with phosphoric acid*. Chemical Engineering Journal, 2004. **Submitted**.
44. Díaz-Terán, J., Nevskaja, D.M., Fierro, J.L.G., et al., *Study of chemical activation process of a lignocellulosic material with KOH by XPS and XRD*. Microporous and Mesoporous Materials, 2003. **60**(1-3): p. 173-181.
45. Stavropoulos, G.G., *Precursor materials suitability for super activated carbons production*. Fuel Processing Technology, 2005. **86**(11): p. 1165-1173.
46. Park, S.-J. and W.-Y. Jung, *Preparation and structural characterization of activated carbons based on polymeric resin*. Journal of Colloid and Interface Science, 2002. **250**(1): p. 196-200.
47. Guo, Y.P. and Lua, A.C., *Textural and chemical characterization of adsorbent prepared from palm shell by potassium hydroxide impregnation at different stages*. Journal of Colloid and Interface Science, 2002. **254**(2): p. 227-233.
48. Guo, Y.P., Qi, J.R., Yang, S.F., et al., *Adsorption of Cr(VI) on micro- and mesoporous rice husk-based active carbon*. Materials Chemistry and Physics, 2002. **78**(1): p. 132-137.
49. Guo, Y.P., Zhang, H., Tao, N.N., et al., *Adsorption of malachite green and iodine on rice husk-based porous carbon*. Materials Chemistry and Physics, 2003. **82**(1): p. 107-115.
50. Guo, Y.P., Yang, S.F., Fu, W.Y., et al., *Adsorption of malachite green on micro- and mesoporous rice husk-based active carbon*. Dyes and Pigments, 2003. **56**(3): p. 219-229.

51. Lillo-Rodenas, M.A., Juan-Juan, J., Cazorla-Amoros, D., et al., *About reactions occurring during chemical activation with hydroxides*. Carbon, 2004. **Article in press**.
52. www.fao.org/livestock/agap/frg/afris/espanol/document/tfced8/Data/495.HTM, *Madera y subproductos de la madera*.
53. www.fibra-salud.com/.%5CObra%5C9.htm, *Lignina*.
54. Goldstein, I.S., *Productos químicos derivados de la madera*. Unasylva. Chemicals from wood., 1979. **31**(125).
55. www.gtiuruguay.com/lignina.htm, *Lignina*.
56. Northey, R.A. *Low-Cost Uses of Lignin, Emerging Technology of Materials and Chemicals from Biomass*. in *ACS Symposium Series 476*. 1992. Washington D.C.
57. Adler, E., *Lignin chemistry-Past, Present and Future*. Wood Science Technology, 1977. **11**: p. 169-218.
58. Fengel, D. and Wegener, G., eds. *Wood. Chemistry, ultrastructure, reactions*. 1983, Walter de Gruyter: Berlin, New York. 145.
59. Institute, I.L., www.ili-lignin.com/ili_presentation.html. 2005.
60. Goheen, D.W. and Hoyt, C.H., *Lignin*. Third Edition ed. Kirk-Othmer Encyclopedia of Chemical Technology, ed. I. John Wiley & Sons. Vol. 14. 1981, New York: Wiley-Interscience. 294-313.
61. Mansouri, N.-E.E. and Salvado, J., *Structural characterization of technical lignins for the production of adhesives: Application to lignosulfonate, kraft, soda-anthraquinone, organosolv and ethanol process lignins*. Industrial Crops and Products, 2006. **24**(1): p. 8-16.
62. Sarkanen, K.V. and Ludwig, C.H., *Lignins: Occurrence, Formation, Structure and Reactions*. 1971, New York: Wiley-Interscience.
63. Ballerini, A., Ewert, R., and Solís, M., *Utilización de Ligninas en la formulación de adhesivos para tableros contrachapados*. Maderas: Ciencia y Tecnología, 1998. **1**(1).
64. Crawford, D.L., Pometto, A.L., and Crawford, R.L., *Production of useful modified lignin polymers by bioconversion of lignocellulose with Streptomyces*. Biotechnology Advances, 1984. **2**(2): p. 217-232.
65. Mansilla, H., Lizama, C., Gutarra, A., et al., *Tratamiento de residuos líquidos de la industria de celulosa y textil*.
66. Amarasekera, G., Scarlett, M.J., and Mainwaring, D.E., *Development of microporosity in carbons derived from alkali digested coal*. Carbon, 1998. **36**(7-8): p. 1071-1078.
67. Guo, Y. and Rockstraw, D.A., *Physical and chemical properties of carbons synthesized from xylan, cellulose, and Kraft lignin by H₃PO₄ activation*. Carbon, 2006. **44**(8): p. 1464-1475.

68. Fierro, V., Torné-Fernández, V., and Celzard, A., *Highly microporous carbons prepared by activation of Kraft lignin with KOH*. Studies in Surface Science and catalysis, 2005: p. 607-614.
69. *Standard Test Method for methylene blue active substances*, in D3172-89. 2002.
70. Coleman, P.B., *Practical Sampling Techniques for Infrared analysis*. 1993, Boca Raton (EEUU): CRC Press.
71. Muller, M.P. and Griffiths, P.R., *Diffuse reflectance measurements by infrared Fourier transform spectrometry*. Anal. Chem. Vol. 50. 1906-1910.
72. Kendall, D.V., *Applied Infrared Spectroscopy*. 1996: Reinhold Publishing GB.
73. Perkins, W.D., *Fourier Transform- Infrared Spectroscopy*, in *J. Chem. Edu.* 1986. p. A5-A10.
74. Noble, D., *FTIR spectroscopy. It's all done with mirrors*. Anal. Chem. Vol. 6. 1995. 381 A-385 A.
75. Roeges, N.P.G., *Guide to the complete Interpretation of Infrared Spectra of Organic Structures*, ed. C. GB. 1994: John Wiley & Sons.
76. Smith, B., *Infrared Spectral Interpretation. A systematic approach*. 1999, Boca Raton (EEUU): CRC press.
77. Skoog, D.A., Holler, F.J., and Nieman, T.A., *Principios de Análisis Instrumental*. 5ª ed. ed. 2001: McGraw-Hill.
78. Shim, J.-W., Park, S.-J., and Ryu, S.-K., *Effect of modification with HNO₃ and NaOH on metal adsorption by pitch-based carbon fibers*. Carbon, 2001. **39**(11): p. 1635-1642.
79. Oh, G.H. and Park, C.R., *Preparation and characteristics of rice-straw-based porous carbons with high adsorption capacity*. Fuel, 2002. **81**(3): p. 327-336.
80. Moreno-Castilla, C., Carrasco-Marín, F., Maldonado-Hódar, F.J., et al., *Effects of non-oxidant and oxidant acid treatments on the surface properties of an activated carbon with very low ash content*. Carbon, 1998. **36**(1-2): p. 145-151.
81. Chiang, H.-L., Huang, C.P., and Chiang, P.C., *The surface characteristics of activated carbon as affected by ozone and alkaline treatment*. Chemosphere, 2002. **47**(3): p. 257-265.
82. Gregg, S.J., *Adsorption, surface area and porosity*. 1967, London: Academic Press.
83. Lowell, S. and Shield, J.F., *Powder surface area and porosity*, ed. T. Edition. 1979.
84. Rouquerol, F., Rouquerol, J., and Sing, K.S.W., *Adsorption by Powders and Porous Solids. Principles, Methods and Applications*. 1999, San Diego: Academic Press.
85. Kruk, M., Li, Z., Jaroniec, M., et al., *Nitrogen Adsorption Study of Surface Properties of Graphitized Carbon Blacks*. Langmuir, 1999. **15**(4): p. 1435-1441.

86. Tschumper, A. and Prins, R., *Kinetic study of the zeolite catalyzed isomerization of aniline*. Applied Catalysis A: General, 1998. **174**(1-2): p. 129-135.
87. Weeb, P.A., Orr, C., Camp, R.W., et al., *Analytical methods in fine particle technology*. 1997: Micromeritics Instrument Corporation.
88. Setoyama, N., Suzuki, T., and Kaneko, K., *Simulation study on the relationship between a high resolution [alpha]-s-plot and the pore size distribution for activated carbon*. Carbon, 1998. **36**(10): p. 1459-1467.
89. www.vu.union.edu/, *Surface area and pore measurements*.
90. Boehm, H.P., *Some aspects of the surface chemistry of carbon blacks and other carbons*. Carbon, 1994. **32**(5): p. 759-769.
91. Boehm, H.P., *Surface oxides on carbon and their analysis: a critical assessment*. Carbon, 2001. **40**(2): p. 145-149.
92. Contescu, A., Contescu, C., Putyera, K., et al., *Surface acidity of carbons characterized by their continuous pK distribution and Boehm titration*. Carbon, 1997. **35**(1): p. 83-94.
93. Toles, C.A., Marshall, W.E., and Johns, M.M., *Surface functional groups on acid-activated nutshell carbons*. Carbon, 1999. **37**(8): p. 1207-1214.
94. Boehm, H.P., *Chemical Identification of surface groups*. Advances in catalysis, 1966. **16**: p. 179-225.
95. Garten, V.A. and Weiss, D.E., *A new interpretation of the acidic and basic structures in carbons. II. The chromene-carbonium ion couple in carbon*. Australian Journal of Chemistry, 1957. **10**: p. 309.
96. Figueiredo, J.L., Pereira, M.F.R., Freitas, M.M.A., et al., *Modification of the surface chemistry of activated carbons*. Carbon, 1999. **37**(9): p. 1379-1389.
97. Pereira, M.F.R., Soares, S.F., Orfao, J.J.M., et al., *Adsorption of dyes on activated carbons: influence of surface chemical groups*. Carbon, 2003. **41**(4): p. 811-821.
98. *Standard Test Method for methylene blue active substances*, in D 2330 - 02. 2002.
99. Sarmiento, C., Sánchez, J., García, C., et al., *Preparación de carbón activado mediante la activación química de carbón mineral*, in *Ciclo Básico de la Facultad de Ingeniería*: Universidad del Zulia. Maracaibo (Venezuela).
100. Marsh, H., Heintz, E.A., and Rodríguez-Reinoso, F., *Activated carbon: structure, characterization, preparation and applications*, in *Introduction to Carbon Technologies*, S.d.P. Universidad de Alicante, Editor. 1997: Alicante.
101. Rozada, F., Calvo, L.F., Garcia, A.I., et al., *Dye adsorption by sewage sludge-based activated carbons in batch and fixed-bed systems*. Bioresource Technology, 2003. **87**(3): p. 221-230.
102. *Standard Test Method for determination of iodine number of activated carbon*, in D 4607 - 94. 1999.

103. Dabrowski, A., *Adsorption -- from theory to practice*. Advances in Colloid and Interface Science, 2001. **93**(1-3): p. 135-224.
104. El-Hendawy, A.-N.A., *Surface and adsorptive properties of carbons prepared from biomass*. Applied Surface Science, 2005. **252**(2): p. 287-295.
105. Ayranci, E. and Duman, O., *Adsorption behaviors of some phenolic compounds onto high specific area activated carbon cloth*. Journal of Hazardous Materials, 2005. **124**(1-3): p. 125-132.
106. Wu, F.-C. and Tseng, R.-L., *Preparation of highly porous carbon from fir wood by KOH etching and CO₂ gasification for adsorption of dyes and phenols from water*. Journal of Colloid and Interface Science, 2005. **In Press, Corrected Proof**.
107. de Oliveira Pimenta, A.C. and Kilduff, J.E., *Oxidative coupling and the irreversible adsorption of phenol by graphite*. Journal of Colloid and Interface Science, 2005. **In Press, Corrected Proof**.
108. Villacanas, F., Pereira, M.F.R., Orfao, J.J.M., et al., *Adsorption of simple aromatic compounds on activated carbons*. Journal of Colloid and Interface Science, 2005. **In Press, Corrected Proof**.
109. Juang, R.-S., Lin, S.-H., and Cheng, C.-H., *Liquid-phase adsorption and desorption of phenol onto activated carbons with ultrasound*. Ultrasonics Sonochemistry, 2005. **In Press, Corrected Proof**.
110. Khezami, L., Chetouani, A., Taouk, B., et al., *Production and characterisation of activated carbon from wood components in powder: Cellulose, lignin, xylan*. Powder Technology, 2005. **In Press, Corrected Proof**.
111. Otero, M., Zabkova, M., and Rodrigues, A.E., *Adsorptive purification of phenol wastewaters: Experimental basis and operation of a parametric pumping unit*. Chemical Engineering Journal, 2005. **110**(1-3): p. 101-111.
112. Wu, F.-C., Tseng, R.-L., and Hu, C.-C., *Comparisons of pore properties and adsorption performance of KOH-activated and steam-activated carbons*. Microporous and Mesoporous Materials, 2005. **80**(1-3): p. 95-106.
113. Tanthapanichakoon, W., Ariyadejwanich, P., Japthong, P., et al., *Adsorption-desorption characteristics of phenol and reactive dyes from aqueous solution on mesoporous activated carbon prepared from waste tires*. Water Research, 2005. **39**(7): p. 1347-1353.
114. Namane, A., Mekarzia, A., Benrachedi, K., et al., *Determination of the adsorption capacity of activated carbon made from coffee grounds by chemical activation with ZnCl₂ and H₃PO₄*. Journal of Hazardous Materials, 2005. **119**(1-3): p. 189-194.
115. Alvarez, P.M., Garcia-Araya, J.F., Beltran, F.J., et al., *Ozonation of activated carbons: Effect on the adsorption of selected phenolic compounds from aqueous solutions*. Journal of Colloid and Interface Science, 2005. **283**(2): p. 503-512.

116. Wu, F.-C., Tseng, R.-L., and Juang, R.-S., *Comparisons of porous and adsorption properties of carbons activated by steam and KOH*. Journal of Colloid and Interface Science, 2005. **283**(1): p. 49-56.
117. Lee, K.M. and Lim, P.E., *Bioregeneration of powdered activated carbon in the treatment of alkyl-substituted phenolic compounds in simultaneous adsorption and biodegradation processes*. Chemosphere, 2005. **58**(4): p. 407-416.
118. Rio, S., Faur-Brasquet, C., Coq, L.L., et al., *Experimental design methodology for the preparation of carbonaceous sorbents from sewage sludge by chemical activation--application to air and water treatments*. Chemosphere, 2005. **58**(4): p. 423-437.
119. Tancredi, N., Medero, N., Moller, F., et al., *Phenol adsorption onto powdered and granular activated carbon, prepared from Eucalyptus wood*. Journal of Colloid and Interface Science, 2004. **279**(2): p. 357-363.
120. Terzyk, A.P., *Molecular properties and intermolecular forces--factors balancing the effect of carbon surface chemistry in adsorption of organics from dilute aqueous solutions*. Journal of Colloid and Interface Science, 2004. **275**(1): p. 9-29.
121. Nakagawa, K., Namba, A., Mukai, S.R., et al., *Adsorption of phenol and reactive dye from aqueous solution on activated carbons derived from solid wastes*. Water Research, 2004. **38**(7): p. 1791-1798.
122. Roostaei, N. and Tezel, F.H., *Removal of phenol from aqueous solutions by adsorption*. Journal of Environmental Management, 2004. **70**(2): p. 157-164.
123. Nevskaiia, D.M., Castillejos-Lopez, E., Guerrero-Ruiz, A., et al., *Effects of the surface chemistry of carbon materials on the adsorption of phenol-aniline mixtures from water*. Carbon, 2004. **42**(3): p. 653-665.
124. Salame, I.I. and Bandosz, T.J., *Role of surface chemistry in adsorption of phenol on activated carbons*. Journal of Colloid and Interface Science, 2003. **264**(2): p. 307-312.
125. Otero, M., Rozada, F., Calvo, L.F., et al., *Elimination of organic water pollutants using adsorbents obtained from sewage sludge*. Dyes and Pigments, 2003. **57**(1): p. 55-65.
126. Tryba, B., Morawski, A.W., and Inagaki, M., *Application of TiO₂-mounted activated carbon to the removal of phenol from water*. Applied Catalysis B: Environmental, 2003. **41**(4): p. 427-433.
127. Podkoscielny, P., Dabrowski, A., and Marijuk, O.V., *Heterogeneity of active carbons in adsorption of phenol aqueous solutions*. Applied Surface Science, 2003. **205**(1-4): p. 297-303.
128. Ariyadejwanich, P., Tanthapanichakoon, W., Nakagawa, K., et al., *Preparation and characterization of mesoporous activated carbon from waste tires*. Carbon, 2003. **41**(1): p. 157-164.

129. Tseng, R.-L., Wu, F.-C., and Juang, R.-S., *Liquid-phase adsorption of dyes and phenols using pinewood-based activated carbons*. Carbon, 2003. **41**(3): p. 487-495.
130. El-Hendawy, A.-N.A., *Influence of HNO₃ oxidation on the structure and adsorptive properties of corncob-based activated carbon*. Carbon, 2003. **41**(4): p. 713-722.
131. San Miguel, Guillermo, Fowler, G.D., and Sollars, C.J., *A study of the characteristics of activated carbons produced by steam and carbon dioxide activation of waste tyre rubber*. Carbon, 2003. **41**(5): p. 1009-1016.
132. Bae, S.-D., Sagehashi, M., and Sakoda, A., *Activated carbon membrane with filamentous carbon for water treatment*. Carbon, 2003. **41**(15): p. 2973-2979.
133. Klimenko, N., Winther-Nielsen, M., Smolin, S., et al., *Role of the physico-chemical factors in the purification process of water from surface-active matter by biosorption*. Water Research, 2002. **36**(20): p. 5132-5140.
134. Chen, X., Jeyaseelan, S., and Graham, N., *Physical and chemical properties study of the activated carbon made from sewage sludge*. Waste Management, 2002. **22**(7): p. 755-760.
135. Galiatsatou, P., Metaxas, M., Arapoglou, D., et al., *Treatment of olive mill waste water with activated carbons from agricultural by-products*. Waste Management, 2002. **22**(7): p. 803-812.
136. Juang, R.-S., Wu, F.-C., and Tseng, R.-L., *Characterization and use of activated carbons prepared from bagasses for liquid-phase adsorption*. Colloids and Surfaces A: Physicochemical and Engineering Aspects, 2002. **201**(1-3): p. 191-199.
137. Laszlo, K. and Szucs, A., *Surface characterization of polyethyleneterephthalate (PET) based activated carbon and the effect of pH on its adsorption capacity from aqueous phenol and 2,3,4-trichlorophenol solutions*. Carbon, 2001. **39**(13): p. 1945-1953.
138. Hu, Z., Srinivasan, M.P., and Ni, Y., *Novel activation process for preparing highly microporous and mesoporous activated carbons*. Carbon, 2001. **39**(6): p. 877-886.
139. Koh, S.-M. and Dixon, J.B., *Preparation and application of organo-minerals as sorbents of phenol, benzene and toluene*. Applied Clay Science, 2001. **18**(3-4): p. 111-122.
140. Juang, R.-S., Wu, F.-C., and Tseng, R.-L., *Mechanism of Adsorption of Dyes and Phenols from Water Using Activated Carbons Prepared from Plum Kernels*. Journal of Colloid and Interface Science, 2000. **227**(2): p. 437-444.
141. Okolo, B., Park, C., and Keane, M.A., *Interaction of Phenol and Chlorophenols with Activated Carbon and Synthetic Zeolites in Aqueous Media*. Journal of Colloid and Interface Science, 2000. **226**(2): p. 308-317.

142. Brasquet, C., Rousseau, B., Estrade-Szwarczkopf, H., et al., *Observation of activated carbon fibres with SEM and AFM correlation with adsorption data in aqueous solution*. Carbon, 2000. **38**(3): p. 407-422.
143. Hsieh, C.-T. and Teng, H., *Influence of mesopore volume and adsorbate size on adsorption capacities of activated carbons in aqueous solutions*. Carbon, 2000. **38**(6): p. 863-869.
144. Koh, M. and Nakajima, T., *Adsorption of aromatic compounds on C_xN-coated activated carbon*. Carbon, 2000. **38**(14): p. 1947-1954.
145. Wu, F.-C., Tseng, R.-L., and Juang, R.-S., *Pore structure and adsorption performance of the activated carbons prepared from plum kernels*. Journal of Hazardous Materials, 1999. **69**(3): p. 287-302.
146. Laszlo, K., Bota, A., Nagy, L.G., et al., *Porous carbon from polymer waste materials*. Colloids and Surfaces A: Physicochemical and Engineering Aspects, 1999. **151**(1-2): p. 311-320.
147. Tai, H.-S. and Jou, C.-J.G., *Application of granular activated carbon packed-bed reactor in microwave radiation field to treat phenol*. Chemosphere, 1999. **38**(11): p. 2667-2680.
148. Hu, Z. and Srinivasan, M.P., *Preparation of high-surface-area activated carbons from coconut shell*. Microporous and Mesoporous Materials, 1999. **27**(1): p. 11-18.
149. Khan, A.R., Ataullah, R., and Al-Haddad, A., *Equilibrium Adsorption Studies of Some Aromatic Pollutants from Dilute Aqueous Solutions on Activated Carbon at Different Temperatures*. Journal of Colloid and Interface Science, 1997. **194**(1): p. 154-165.
150. Khan, A.R., Al-Bahri, T.A., and Al-Haddad, A., *Adsorption of phenol based organic pollutants on activated carbon from multi-component dilute aqueous solutions*. Water Research, 1997. **31**(8): p. 2102-2112.
151. Shu, H.-T., Li, D., Scala, A.A., et al., *Adsorption of small organic pollutants from aqueous streams by aluminosilicate-based microporous materials*. Separation and Purification Technology, 1997. **11**(1): p. 27-36.
152. Warhurst, A.M., McConnachie, G.L., and Pollard, S.J.T., *Characterisation and applications of activated carbon produced from Moringa oleifera seed husks by single-step steam pyrolysis*. Water Research, 1997. **31**(4): p. 759-766.
153. Laszlo, K., Bota, A., and Nagy, L.G., *Characterization of activated carbons from waste materials by adsorption from aqueous solutions*. Carbon, 1997. **35**(5): p. 593-598.
154. Tamon, H., Atsushi, M., and Okazaki, M., *On Irreversible Adsorption of Electron-Donating Compounds in Aqueous Solution*. Journal of Colloid and Interface Science, 1996. **177**(2): p. 384-390.
155. Leng, C.-C. and Pinto, N.G., *Effects of surface properties of activated carbons on adsorption behavior of selected aromatics*. Carbon, 1997. **35**(9): p. 1375-1385.

156. Singh, B., Madhusudhanan, S., Dubey, V., et al., *Active carbon for removal of toxic chemicals from contaminated water*. Carbon, 1996. **34**(3): p. 327-330.
157. Streat, M., Patrick, J.W., and Perez, M.J.C., *Sorption of phenol and para-chlorophenol from water using conventional and novel activated carbons*. Water Research, 1995. **29**(2): p. 467-472.
158. Moreno-Castilla, C., Rivera-Utrilla, J., López-Ramón, M.V., et al., *Adsorption of some substituted phenols on activated carbons from a bituminous coal*. Carbon, 1995. **33**(6): p. 845-851.
159. Nevskaja, D.M., Santianes, A., Munoz, V., et al., *Interaction of aqueous solutions of phenol with commercial activated carbons: an adsorption and kinetic study*. Carbon, 1999. **37**(7): p. 1065-1074.
160. Sabio, E., González-Martín, M.L., Ramiro, A., et al., *Influence of the regeneration temperature on the phenols adsorption on activated carbon*. Journal of Colloid and Interface Science, 2001. **242**: p. 31-35.
161. Wu, F.-C., Tseng, R.-L., Hu, C.-C., et al., *Physical and electrochemical characterization of activated carbons prepared from firwoods for supercapacitors*. Journal of Power Sources, 2004. **138**: p. 351-359.
162. Ghiaci, M., Abbaspur, A., Kia, R., et al., *Equilibrium isotherm studies for the sorption of benzene, toluene, and phenol onto organo-zeolites and as-synthesized MCM-41*. Separation and Purification Technology, 2004. **40**(3): p. 217-229.
163. Basso, M.C. and Cukierman, A.L., *Arundo donax - Based activated carbons for aqueous-phase adsorption of volatile organic compounds*, Programa de investigación y desarrollo de fuentes alternativas de materias primas y energía (PINMATE): Buenos Aires. p. 42.
164. Hindarso, H., Ismadji, S., Wicaksana, F., et al., *Adsorption of benzene and toluene from aqueous solution onto granular activated carbon*. Journal of Chemical and Engineering Data, 2001. **46**(4): p. 788-791.
165. Torras, C., *Obtenció de membranes polimèriques selectives.*, in *Chemical Engineering*. 2005, Universitat Rovira i Virgili: Tarragona.

8. NOMENCLATURA

$\%ML_{P/L}$	Porcentaje de masa pérdida debido a la reacción entre el ácido fosfórico y la lignina
α	Factor de referencia usado en el método α_s
α'	Coefficiente de reacción
α_{LP}	Orden de reacción para la activación de la lignina
α_w	Orden de reacción para transformación de agua
ΔT	Incremento de temperatura ($^{\circ}C$)
μm	Micrómetros

a

AA, AAS	espectroscopía de absorción atómica
AC, ACs	Carbón Activo
AC-K	Carbón activado químicamente con hidróxido de potasio
AC-Na	Carbón activado químicamente con hidróxido de sodio
AC-P	Carbón activado químicamente con ácido fosfórico
ACF	Fibras de carbón activo
AgA	Agente activante
ATD	Análisis térmico diferencial
Atm	Atmósfera utilizada durante el proceso de pirólisis
ATR	Reflexión total atenuada

b

B	Constante de Langmuir referente a la energía de adsorción (l/mg)
BDDT	Codificación según Bruneaur, Deming, Deming y Teller
BET	Teoría de Brunauer-Emmett-Teller

c

$^{\circ}C$	Grados centígrados
C	Cantidad de carbono (%)
C	Normalidad del filtrado residual
$C_{e,j}$	Concentración de la especie j en el equilibrio
$C_{0,j}$	Concentración de soluto en la alimentación
$C_{Se,j}$	Concentración de la especie j adsorbida en la superficie
C_e	Concentración en el equilibrio (mg/l)
C_{LP}	Concentración del complejo lignina-ácido fosfórico
C_{PA}	Concentración de ácido fosfórico

C_{ws}	Concentración de agua
CA	Carbón Activo
CEC	Capacidad de intercambio de cationes (meq/g)

d

$\overline{d_p}$	Diámetro medio de poro
DAD	Detector de diodo
df/dt	Velocidad de reacción de la disminución de la fracción másica inicial restante en el sólido
DFT	Teoría de la densidad funcional
DMF	dimetilformamida
DR	Ecuación de Dubinin-Radushkevich
DRX	Difracción de rayos X

e

E_j	Energía de activación (kJ/mol)
E_o	Energía característica entre el nitrógeno y el carbón (kJ/mol)
EMR	Reactor enzimático de membrana

f

f	Fracción de masa inicial restante en el sólido
f_∞	Fracción de masa inicial restante en el sólido al final de la termogravimetría
f_{ij}^{cal}	Valor calculado de f en un momento i
f_{ij}^{exp}	Valor experimental de f en un momento i
f_{AC}	Fracción de masa inicial de carbón activo restante en el sólido final
f_j	Fracción de másica de la especie j respecto a la masa inicial de la muestra
f_{LP}	Fracción de masa inicial de lignina restante en el sólido final
f_{LPo}	Fracción de masa inicial de lignina en el sólido inicial
f_{PA}	Fracción de masa inicial de ácido fosfórico restante en el sólido final
f_{PO}	Fracción de masa inicial de óxido de fósforo restante en el sólido final
f_w	Fracción de masa inicial de agua restante en el sólido final
f_{ws}	Fracción de masa inicial de vapor restante en el sólido final
F_{wo}	Fracción de masa inicial de agua en el sólido inicial

g

g	Gramos
g_{AC}	Gramos de carbón activado
GA	Gases ligeros
GPC	Cromatografía de permeación de gel

h

h	Adsorción inicial
h	Constante de Freundlich relacionado con la intensidad de adsorción
h	Horas
H	Cantidad de hidrógeno (%)
H	Tipo de carbón con pH básico
HK	Método de Horwath-Kawazoe
HMF	Hidroximetil furfural
HPLC	Cromatografía líquida de alta precisión

i

IMAC	Técnica de cromatografía de afinidad con ión metálico inmovilizado
IR	Espectroscopía de infrarrojo
ISO	International Organization for Standardization
IUPAC	International Union of Pure and Applied Chemistry

k

k	Constante de reacción
k	Parámetro de Langmuir relacionado con la intensidad de adsorción
K	Grados kelvin
K_{0j}	Factor de frecuencia (1/s)
k_b, K_j	Constante de Freundlich relacionado con la capacidad de adsorción
k_{LP}	Constante de Arrhenius para la volatilización de la lignina activada
k_w	Constante de Arrhenius para la volatilización del agua
kDa	Kilodalton
kg	Kilogramo

l

l	litro
L	Lignina
L	Tipo de carbón con pH ácido
Lo	Amplitud media de los microporos (nm)
LK, KL	Lignina Kraft
LK _d	Lignina Kraft desmineralizada
LP	Complejo lignina-ácido fosfórico
LP	Productos derivados de la lignina

m

m	Masa de carbón activado
M	Molaridad (moles/litro)
m _∞	Masa residual al final de la termogravimetría
M ₀	Masa inicial de la muestra
m _{0LP}	Masa inicial de lignina activada
m _{0w}	Masa inicial de agua
m _{1LP}	Masa de lignina activada
m _w	Masa de agua
MB	Azul de metileno
mequiv	Miliequivalentes
mg	Miligramos
min	Minutos
mM	Milimolar
ml, mL	Mililitro
MW _{AC}	Masa molar de carbón activo
MW _j	Masa molar de la especie j
MW _L	Masa molar aparente de la lignina
MW _{PA}	Masa molar de ácido fosfórico
MW _{PO}	Masa molar de óxido de fósforo
MW _{LP}	Masa molar de complejo lignina-ácido fosfórico
MW _{ws}	Masa molar de vapor
MWCO	Peso molecular del cut-off

n

N	Cantidad de nitrógeno (%)
N	Normalidad (equivalentes/litro)
n(i)	Número de puntos

n_i	Constante de Freundlich
nm	Nanómetros
NOC	Componentes orgánicos no iónicos

O

O	Cantidad de oxígeno (%)
---	-------------------------

P

P	Cantidad de fósforo (%)
P/L	Relación másica entre ácido fosfórico y materia prima
P/P ₀	Presión relativa
PA	Ácido fosfórico
PAS	Detector fotoacústico
pH	Concentración de iones [H ⁺]
pH _{PZC}	Potencial de carga cero
pK	Constante de equilibrio ácido-base
PO	Óxido de fósforo
POS	Evaporación de óxido de fósforo
PSD	Distribución de tamaño de poros
PSf	Polisulfona
PVC	Polivinilo clorado

q

Q ₀	Constante de Langmuir referente a la capacidad de adsorción
q _e	Cantidad adsorbida en el equilibrio (mg/g)
Q _{N₂} , f _{N₂}	Cabal de nitrógeno (cm ³ /min)
q _t	Cantidad adsorbida en un tiempo t (mg/g)

r

R	Relación másica entre agente activante y materia prima
r	Velocidad de calentamiento (°C/min)
R _L	Parámetro de equilibrio de Langmuir
rd _j	Reducción de la especie j
RI	Índice refractivo
RID	Detecto de índice refractivo
RMN	Resonancia magnética nuclear
rpm	Revoluciones por minuto
RRIFT	Reflectancia difusa

S

S	Cantidad de azufre (%)
S_{BET}	Área superficial efectiva (m^2/g)
SEM	Microscopía electrónica de barrido

t

t	Tiempo (h ó min)
T	Temperatura ($^{\circ}\text{C}$)
T_a, T_{carb}	Temperatura de activación ($^{\circ}\text{C}$)
TEM	Microscopía electrónica de transmisión
TG	Termogravimetría
T_p, t_{carb}	Tiempo de activación (h)
TPD, TPDR	Desorción a temperatura controlada

U

UV	Ultravioleta
----	--------------

V

V	Volumen
$V_{\text{DR}}, V_{\mu\text{DR}}$	Volumen de microporos calculado según Duvinin-Radushkevich (cm^3/g)
$V_{\text{macroporo}}$	Volumen de macroporos (cm^3/g)
V_{mesoporo}	Volumen de mesoporos (cm^3/g)
$V_{\text{microporo}}$	Volumen de microporos (cm^3/g)
$V_p, V_{0.99}, V_{\text{total}}$	Volumen total de poro (cm^3/g)
$V_{\alpha_{\text{micro}}}$	Volumen de microporo calculado por el método α_s (cm^3/g)
$V_{\alpha_{\text{super}}}$	Volumen de supermicroporo calculado por el método α_s (cm^3/g)
$V_{\alpha_{\text{ultra}}}$	Volumen de ultramicroporo calculado por el método α_s (cm^3/g)
VO	Volátiles

W

W	Agua
WS	Agua evaporada

Z

$\frac{X}{M}$

Índice de iodo

M

x_m

Parámetro de Langmuir relacionado con la máxima capacidad de adsorción (mg/g AC)

XO(s)

Xylo-oligosacárido(s)

XPS

Espectroscopía fotoelectrónica de Rayos X

XRF

Fluorescencia de rayos X

Compuestos químicos

C	Carbono
$C_{16}H_{18}ClN_3S \cdot 2H_2O$	Azul de metileno (cloruro)
CO	Monóxido de carbono
CO ₂	Dióxido de Carbono
Cu (II)	Cobre (II)
$CuCl_2 \cdot 2H_2O$	Cloruro de cobre dihidratado
H ₂	Hidrógeno
HCl	Ácido clorhídrico
H ₂ O	Agua
HPO ₃	Ácido metafosfórico
H ₃ PO ₄	Ácido fosfórico
H ₄ P ₂ O ₇	Ácido pirofosfórico
H _{n+2} P _n O _{3n+1}	Ácido polifosfórico
H ₂ SO ₄	Ácido sulfúrico
He	Helio
I ₂	Yodo
K	Potasio metálico
K ₂ CO ₃	Carbonato de potasio
KNO ₃	Nitrato de potasio
KOH	Hidróxido de potasio
K ₂ O	Óxido de potasio
N ₂	Nitrógeno
Na	Sodio
NaCl	Cloruro de sodio
Na ₂ CO ₃	Carbonato de sodio
NaHCO ₃	Bicarbonato de sodio
Na ₂ O	Óxido de sodio
NaOC ₂ H ₅	Etóxido de sodio
NaOH	Hidróxido de sodio
Na ₂ S	Sulfuro de sodio
Na ₂ SO ₄	Sulfato de sodio
O ₂	Oxígeno
P ₂ O ₅	Óxido de fósforo
Zn	Zinc
ZnCl ₂	Cloruro de zinc

ANEXOS

Anexo A.

Use of Kraft lignin for Cu(II) removal in industrial water.

Anexo B.

Activated carbons prepared from Kraft lignin by phosphoric acid impregnation.

Anexo C.

Removal of Cu (II) from aqueous solutions by adsorption on activated carbons prepared from Kraft lignin.

Anexo D.

Uptake of Cu(II) and Zn from aqueous solution by Kraft lignin.

Anexo E.

Highly microporous carbons prepared by activation of Kraft lignin with KOH.

Anexo F.

Enzymatic composite membranes based on carbon/polysulfone.

Anexo G.

Influence of the ash content on the microporosity of activated carbons derived from Kraft lignin.

ANEXO A

**USE OF KRAFT LIGNIN FOR CU (II) REMOVAL IN
INDUSTRIAL WATER.**

9TH MEDITERRANEAN CONGRESS (PÓSTER).

BARCELONA - CATALUNYA (2002).



USE OF KRAFT LIGNIN FOR Cu(II) REMOVAL IN INDUSTRIAL WATER

E. Novellon, V. Fierro*, V. Torné, R. García-Valls, D. Montané

Departament d'Enginyeria Química. Grup de Biopolimers Vegetals. Escola Tècnica Superior d'Enginyeria Química. Universitat Rovira i Virgili. Campus Sescelades 43007 Tarragona, España. e-mail: vfierro@etseq.urv.es Tel. 977558546

The presence of heavy metals in industrial wastewater is one of the major sources of aquatic pollution since they are non biodegradable and accumulate in living tissues, thus becoming concentrated throughout the food chain.

The Kraft process produces a residue call as black liquors composed by lignin (30-40%) and other inorganic compounds, after evaporation black liquors are burnt to recover energy and the remaining inorganic reactants. The separation of kraft lignin could be an alternative to incineration since lignin is a bountiful and renewable resource that can be used as feedstock for the fabrication of complexing agents as it can contain active sites (carboxyl, hydroxyl, sulfonate or amine groups) responsible for the complexation of metal ions.

The purpose of this work is to test the ability of a commercial lignin (Kraft lignin - Curan 1052 provided by Lignotech Ibérica S.A.) as a complexing/adsorption agent to remove copper ions.

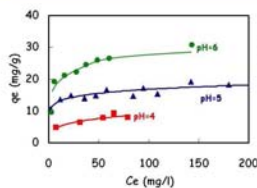
EXPERIMENTAL

150 mg of lignin are added to each 250-ml Erlenmeyer flask containing 150 ml of deionized water. Varying amounts of Cu(II) Chloride (p.a. quality from Aldrich) are added to each flask and maintained under stirring for 24h at 25°C. The resulting Cu(II) concentration is analyzed by atomic absorption (AA). The amount of adsorbed copper is obtained by calculating the difference of each concentration before and after adsorption.



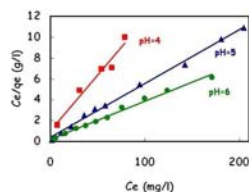
Experimental set up

RESULTS



Maximum Cu(II) removal is obtained at pH=6

q_e (mg/g) equilibrium capacity
 C_e (mg/l) equilibrium concentration
 Q_0 (mg/g) adsorption capacity
 b (l/mg) Langmuir constant
 R_L equilibrium parameter



pH	Q_0 (mg/g)	b (l/mg)	r^2	R_L
4	9.35	0.11	0.96	0.50
5	19.38	0.13	0.99	0.29
6	27.40	0.18	0.99	0.17

Cu(II) removal data fit adequately the Langmuir isotherm

Comparison of adsorption capacity of Cu(II) onto various adsorbents

Adsorbent	Q_0 (mg g ⁻¹)	Reference
Polymerized onion skin	7.55	Kumar et al. 1981
Rice hull	5.58	Suemitsu et al. 1986
Melon seed husk	5.9	Okieman et al. 1989
Red mud	15.0	Zouboulis et al. 1993
Fly ash	0.683	Viswakarma et al. 1989
Ash treated with NaCl	14.54	Hawash et al. 1994
Fe(III)/Cr(III) hydroxide	22.94	Narasivayam et al. 1994
Peanut hull carbon	53.65	Periasamy et al. 1995
Soyabean hull	89.52	Marshall et al. 1995
Bituminous coal	6.47	Singh et al. 1997
<i>Aspergillus niger</i>	1.1	Kapoor et al. 1997
Crab shell	55.88	An et al. 2001
Coirpith carbon	62.5	Kadirvelu et al. 2001
Kraft lignin (pH=6)	27.4	This work

Kraft lignin shows an intermediate capacity for Cu(II) removal

CONCLUSIONS

This study shows that lignin is a good agent for removing Cu(II). As it is used without further modification, its application in the treatment of polluted water could be commercially viable.

ANEXO B

**ACTIVATED CARBONS PREPARED FROM KRAFT
LIGNIN BY PHOSPHORIC ACID IMPREGNATION.**

CARBON (PÓSTER).

OVIEDO – ESPAÑA (2003).



Activated Carbons Prepared from Kraft Lignin by Phosphoric Acid Impregnation

V. Fierro, V. Torne, D. Montané and J. Salvadó

Departament d'Enginyeria Química, ETSEQ, Universitat Rovira i Virgili, Avinguda dels Països Catalans 26, Campus Sescelades, Tarragona 43007, Spain e-mail:vfierro@etseq.urv.es Tel: +34 977 55 85 46 Fax: +34 977 55 85 44

Lignin can be used as precursor for activated carbon as it has been reported on physical activation of eucalyptus Kraft lignin by CO₂ partial gasification¹ and on chemical activation of this precursor by using zinc chloride². However, the use of ZnCl₂ has declined due to the environmental problems³ and phosphoric acid is preferred as activating-dehydrating agent.

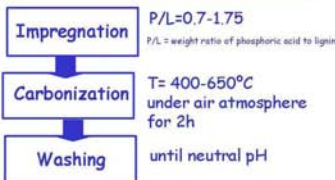
Here we examine the influence of preparation conditions (carbonization temperature, phosphoric-lignin weight ratio and impregnation time) on the carbon yield, surface area and pore size distribution.

EXPERIMENTAL

Lignin Analyses (wt. %)

Proximate (wt. % humid basis)		Elemental (wt. % ash and moisture free)	
Moisture	14.45	Carbon	59.46
Ash	9.50	Hydrogen	5.07
Volatile matter	44.93	Nitrogen	0.05
Fixed carbon*	31.12	Sulfur	2.15
		Oxygen*	33.27

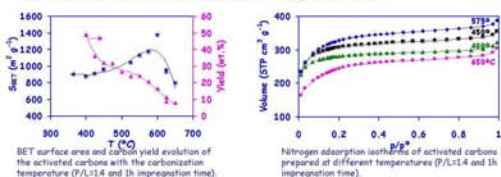
* Estimated by difference



Surface area and pore size characterization were performed using a Micromeritics ASAP2000 gas adsorption surface area analyzer. The specific surface area of the samples was determined from the nitrogen isotherms at -196°C and by using the BET equation. Micropore volume was determined using t-plot, mesopore volume using the BJH equation and total volume of pores was calculated at a relative pressure (p/p⁰) of 0.99.

RESULTS AND DISCUSSION

Effect of the carbonization temperature

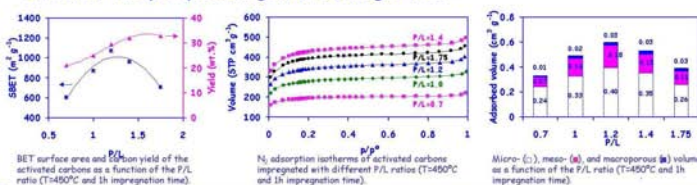


Increasing carbonization temperature carbon yield decreased from 49% at 400°C to 8% at 650°C.

S_{BET} increased between 400 and 600°C, with a maximum of more than 1350m²g⁻¹ at 600°C. At higher temperatures the surfaces areas were considerably reduced.

N₂ isotherms approached type I (Langmuir) with small upward bending at higher pressure, indicating an essentially microporous character with some contribution of wider pores.

Effect of the phosphoric/lignin (P/L) weight ratio

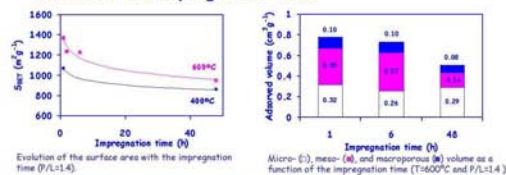


P/L ratio strongly affects the pore structure.

Low P/L ratios promotes the creation of micropores whereas P/L>1.0 slightly affect to the pore size distribution.

P/L ratio has a clear effect on the total volume of pores, there is an optimum for the development of porosity at P/L=1.2.

Effect of the impregnation time



Increasing impregnation times reduces BET surface areas and the total pore volume.

Impregnation time also affects to the pore size distribution of activated carbons.

The effect of impregnation time is more important at high carbonization temperatures due to decomposition of phosphate and polyphosphate bridges crosslinking parts of the carbon structure.

CONCLUSIONS

Pyrolysis of lignin impregnated with phosphoric acid produces essentially microporous activated carbons.

A carbonization temperature of 450°C together with a P/L ratio of 1.2 and low impregnation times produce activated carbons with high specific surfaces areas and reasonable yield.

REFERENCES

- [1] J. Rodríguez-Minasol, T. Cordero, J.J. Rodríguez, Carbon 31 (1993) 87-95.
- [2] E. González Serrano, T. Cordero, J. Rodríguez-Minasol, J.J. Rodríguez Ind. Eng. Chem. Res. 36 (1997) 4832-4838.
- [3] H. Teng, T.S. Yeh, L.Y. Hsu, Carbon 36 (1998) 1387-1395.



ANEXO C

**REMOVAL OF CU (II) FROM AQUEOUS SOLUTIONS BY
ADSORPTION ON ACTIVATED CARBONS PREPARED
FROM KRAFT LIGNIN.**

CARBON (PÓSTER).

OVIEDO - ESPAÑA (2003).



Removal of Cu (II) from Aqueous Solutions by Adsorption on Activated Carbons Prepared from Kraft Lignin

V. Fierro, V. Torne, D. Montané and R. Garcia-Valls

Departament d'Enginyeria Química, ETSEQ, Universitat Rovira i Virgili, Avinguda dels Països Catalans 26, Campus Sescelades, Tarragona 43007, Spain e-mail:vfierro@etseq.urv.es Tel: +34 977 55 85 46 Fax: +34 977 55 85 44

The presence of heavy metals in industrial wastewater is one of the major sources of aquatic pollution since they are non biodegradable and accumulate in living tissues.

This work was undertaken to study the feasibility of the utilization of activated carbon produced from Kraft lignin by chemical activation¹ with phosphoric acid for the removal of heavy metal cations from water solutions. The influence of carbonization temperature and phosphoric acid to lignin weight ratio on Cu adsorption are analyzed.

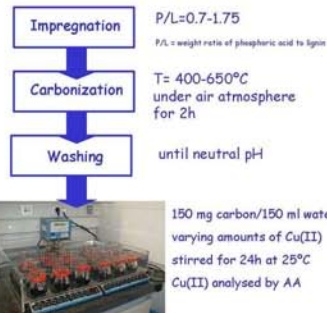
EXPERIMENTAL

Lignin Analyses (wt.%)

Proximate (wt.%, humid basis)		Elemental (wt.%, ash and moisture free)	
Moisture	14.45	Carbon	59.46
Ash	9.50	Hydrogen	5.07
Volatile matter	44.93	Nitrogen	0.05
Fixed carbon*	31.12	Sulfur	2.15
		Oxygen*	33.27

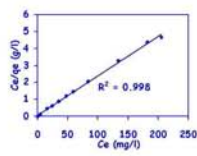
* Estimated by difference

The specific surface area of the carbons was determined from the nitrogen isotherms at 77K and by using the BET equation. Micropore volume was determined using t-plot, mesopore volume using the BJH equation and total volume of pores was calculated at a relative pressure (p/p⁰) of 0.99. Cation exchange capacity (CEC) was measured, after adding NaOH in excess, by titration with HCl and expressed in meq H⁺ g⁻¹.



RESULTS AND DISCUSSION

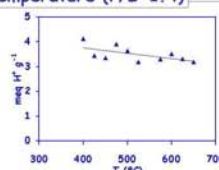
The Langmuir model was applied to the experimental equilibrium data:
 $C_e/q_e = 1/X_m K + C_e/X_m$
 X_m and K are parameters related to the maximum adsorption capacity and intensity of adsorption. X_m was used to study the effect of T and P/L ratio on Cu adsorption. The Langmuir isotherm model describes satisfactorily Cu adsorption on the carbon prepared from Kraft lignin.



Langmuir isotherms for the sorption of Cu on carbon prepared at 450°C and P/L=1.4 (Cu initial concentration: 10-250 ppm)

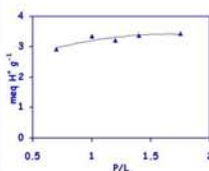
Effect of the carbonization temperature (P/L=1.4)

As temperature increases phosphate and polyphosphate bridges acting as crosslinking parts of the carbon structure decompose and it also could affect to surface phosphorous compounds that are degraded.



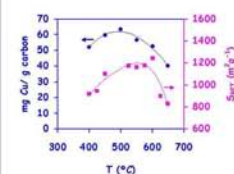
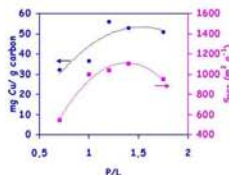
The concomitant effects of T on the CEC and on BET surface explain the existence of a maximum in Cu adsorption for activated carbons prepared at temperatures between 450 and 550°C. At temperatures higher than 600°C, the shrinkage of the structure together with the decreasing tendency of CEC with temperature would explain the Cu adsorption observed.

Effect of the P/L ratio (T = 450°C)



Functional groups increase with P/L ratio but the value remains approximately constant from P/L=1.0. As H₃PO₄ reacts with the hydroxyl groups of lignin it would exist a maximum in the P/L ratio and so a maximum in the phosphorous-containing acids attached to the surface.

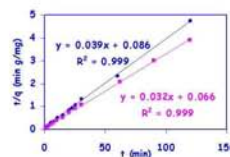
The high CEC together with the no existence of diffusional limitations in carbons at P/L=1.75 explain the slight decrease in copper adsorption even if the surface area decreased greatly from 959 m²g⁻¹ at P/L=1.4 to 704 m²g⁻¹ at P/L=1.75.



Adsorption of Cu on carbon proceeds via a pseudo-second order mechanism

$$t/q_t = 1/h + 1/q_e t$$

where h is the initial sorption, q_e is the equilibrium sorption capacity and the rate constant k can be determined experimentally from the slope and intercept of a plot of t/q_t versus t being $h = k q_e^2$.



Pseudo-second order sorption kinetics for the sorption of Cu²⁺ ions at 300 K and initial concentrations: C₀ = 50ppm; m₀, C₀ = 100ppm

CONCLUSIONS

Activated carbons produced from Kraft lignin can be tailored to have a high surface concentration of acidic groups and a pore size distribution favorable for adsorption of metallic ions from solutions. Carbonization temperature strongly affects to metal adsorption by changing porosity distribution and degrading phosphorous-acidic groups. The P/L ratio does not influence the amount of copper adsorbed if the added phosphoric acid is enough to allow the complete reaction of lignin.

Pyrolysis of lignin with phosphoric acid at temperatures about 500°C and P/L ratio of 1.0 produces activated carbons with a favorable pore size distribution and enough surface acidic groups for removal of copper ions.

REFERENCES

[1] V. Fierro, V. Torné, D. Montané, J. Salvadó also in Carbon'03, Oviedo (Spain) 2003.



ANEXO D

**UPTAKE OF CU(II) AND ZN FROM AQUEOUS
SOLUTION BY KRAFT LIGNIN.**

**4TH EUROPEAN CONGRESS IN CHEMICAL
ENGINEERING (PÓSTER).**

GRANADA - ESPAÑA (2003).



Uptake of Cu(II) and Zn from Aqueous Solution by Kraft Lignin

G. Nastrunisku, V. Fierro*, V. Torné, R. García-Valls, D. Montané

Departament d'Enginyeria Química, ETSEQ, Universitat Rovira i Virgili, Avinguda dels Països Catalans 26, Campus Sescelades, Tarragona 43007, Spain e-mail: vfierro@etseq.urv.es Tel: +34 977 55 85 46 Fax: +34 977 55 85 44

Kraft lignin (KL) is produced upon wood pulping with a NaOH + Na₂S solution. The lignin fraction of wood is solubilized in chemically modified form, representing the main component of the black liquors, which are separated from cellulose. These black liquors bear a very high pollution load and once concentrated by evaporation, they serve primarily as in-house fuel required for the recovery of chemicals. The separation of KL could be an alternative to incineration since lignin is a bountiful and renewable resource and represents an attractive field for future industrial chemistry.

The presence of heavy metals in industrial wastewater is one of the major sources of aquatic pollution since they are non biodegradable and accumulate in living tissues, thus becoming concentrated throughout the food chain. Therefore, their immobilization is a question of primary interest. Lignin contains active sites (carboxyl, hydroxyl, sulfonate or amine groups) responsible for the complexation of metal ions. The advantages of using lignin are its low toxicity and the re-use of a residue in the production chain, which may reduce pollution levels.

EXPERIMENTAL

Kraft lignin (KL) was provided by Lignotech Iberica S.A. Elemental analysis was carried out in an EA1108 Carlo Erba Elemental Analyzer. The proximate analysis was carried out following ISO standards.

Lignin Analyses (wt.%)

Proximate (wt.%, humid basis)	Elemental (wt.%, ash and moisture free)		
Moisture	14.45	Carbon	59.46
Ash	9.50	Hydrogen	5.07
Volatile matter	44.93	Nitrogen	0.05
Fixed carbon ^a	31.12	Sulfur	2.15
		Oxygen ^a	33.27

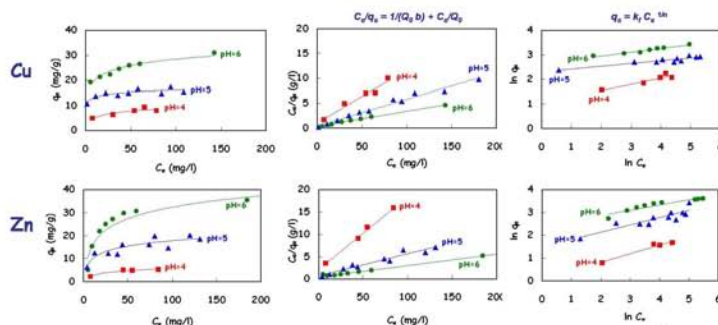
^a Estimated by difference

150 mg of lignin are added to each 250-ml Erlenmeyer flask containing 150 ml of deionized water. Varying amounts of Cu(II) Chloride (p.a. quality from Aldrich) are added to each flask and maintained under stirring for 24h at 25°C. The resulting Cu(II) concentration is analyzed by atomic absorption (AA). The amount of adsorbed copper is obtained by calculating the difference of each concentration before and after adsorption.



Experimental set up

RESULTS AND DISCUSSION



Cu and Zn adsorption onto KL increases with pH from 4 to 6 and the linear plot of q_e/q_m versus C_e showed that both obeys the Langmuir model.

R_L that is defined by

$$R_L = 1 / (1 + b C_0)$$

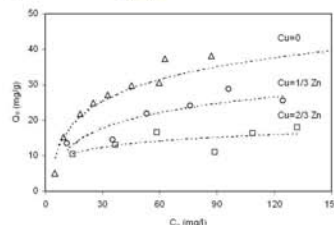
in this study $0 < R_L < 1$ for both metals and at the pH range of this study.

At pH = 6 the maximum Cu(II) removal is of 27.4 mg/g KL whereas reached the maximum Zn removal was 39.22 mg/g lignin. A previous work [1] reported a maximum of Zn²⁺ adsorption of 73.24 mg/g lignin at 30°C but in that case the lignin was intensively purified and washed.

The adsorption did not followed the Freundlich model as well as the Langmuir model. K_f and n were determined. According to Treyball [2], n values between 1 and 10 represents beneficial adsorption. The table shows that n increases with pH and it is always between 1 and 10 for the adsorption of both metals.

pH	Langmuir constants				Freundlich constants		
	Q_0 (mg/g)	b (l/mg)	R_L	R^2	K_f	n	R^2
Cu	4	9.35	0.11	0.086	2.82	3.93	0.90
	5	19.38	0.13	0.073	10.12	4.16	0.89
	6	27.40	0.18	0.053	14.15	6.57	0.96
Zn	4	6.16	0.08	0.117	1.04	2.61	0.96
	5	20.37	0.07	0.126	4.44	3.13	0.80
	6	39.22	0.05	0.155	11.21	4.42	0.89

q_e (mg/g)	equilibrium capacity	K_f	Freundlich constant related to sorption capacity
C_e (mg/l)	equilibrium concentration	n	Freundlich constant related to the sorption intensity
Q_0 (mg/g)	adsorption capacity		
b (l/mg)	Langmuir constant		
R_L	equilibrium parameter		



Zn adsorbed at equilibrium versus the equilibrium concentration at pH=6 for adsorption of Zn and simultaneous adsorption of Cu and Zn at Cu/Zn (w/w) equal to 1/3 and 2/3.

The data fit adequately de Langmuir adsorption model. The maximum Zn removal when Cu is incorporated to the solution decreases from 39.22 to 32.3 and 19.3 for Cu/Zn (w/w) equal to 1/3 and 2/3 respectively.

CONCLUSIONS

This study shows that lignin is a good agent for removing Cu(II) and Zn. The adsorption of metal depends on pH of the solution and maximum metal uptake is obtained at pH=6. Langmuir and Freundlich parameters shows that Cu(II) and Zn adsorption on KL are favorable. As KL is used without further modification, its application in the treatment of polluted water could be commercially viable.

REFERENCES

- [1] S.K. Srinivastava, A.K. Singh, A. Sharma, *Environmental Technology* 1994, 15, 353.
- [2] R.E. Treyball, *Mass Transfers Operations*, 3rd edn, McGraw, New York, 1980.

ANEXO E

**HIGHLY MICROPOROUS CARBONS PREPARED BY
ACTIVATION OF KRAFT LIGNIN WITH KOH.**

**7TH INTERNATIONAL SYMPOSIUM ON THE
CHARACTERIZATION OF POROUS SOLIDS (PÓSTER).**

AIX-EN-PROVENCE - FRANCIA (2005).

Highly microporous carbons prepared by activation of kraft lignin with KOH



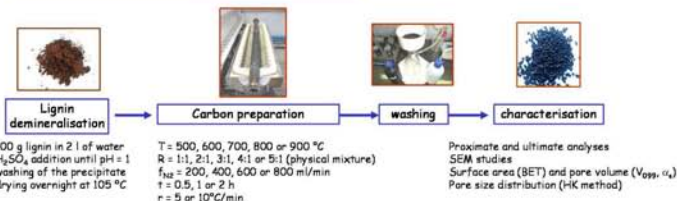
V. Fierro^a, V. Torné-Fernández^a and A. Celzard^b



^a Departament d'Enginyeria Química, Universitat Rovira i Virgili, Campus Sescelades, 43007 Tarragona, Spain
^b Laboratoire de Chimie du Solide Minéral, UMR CNRS 7555, Université Henri Poincaré, 54506 Vandoeuvre-lès-nancy Cédex, France

Highly microporous carbon materials with high apparent BET surface areas (up to ~3000 m² g⁻¹) were obtained by heat treatment of mixtures of demineralised kraft lignin (KL_d) and KOH. The effects of five parameters: temperature of activation (T), KOH/KL_d ratio (R), nitrogen flow rate (f_{N₂}), time of activation (t) and heating rate (r) on carbon yield, surface area, pore volume and pore size distribution were investigated.

EXPERIMENTAL



RESULTS

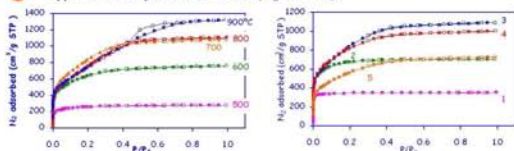
Proximate and ultimate analyses of KL and KL_d (wt. %)

	Proximate Analysis (wt %, dry basis)			Ultimate Analysis (wt %, dry)					
	Fixed Carbon	Volatile matter	ash	C	H	N	S	O*	
KL	36.4	52.5	11.1	59.5	5.1	0.1	2.2	33.3	
KL _d	39.7	60.1	0.2	65.8	5.9	0.0	0.5	27.8	

* Estimated by difference

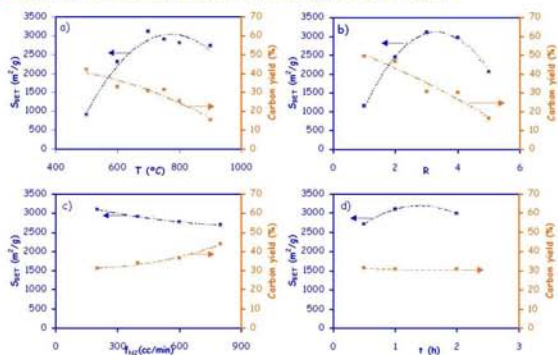
KL has a high ash content, basically Na and Ca combined with S and C inside the phase Na₂CO₃, 2 Na₂SO₄. Lignin demineralisation is very effective: ash content was reduced from 11.1 to 0.2 %.

● Type of adsorption isotherms (N₂ at 77K)



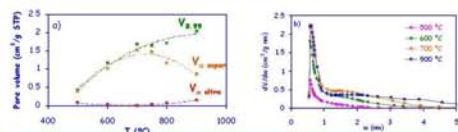
All the isotherms are of type I (Langmuir), characterising microporous solids. Carbons prepared at 500 °C and with R=1 have an essentially microporous character. As T and R increase, the knee of the isotherms widens, indicating a widening of the pores. Carbon prepared at 900 °C shows a hysteresis loop, evidencing a well-developed mesoporosity.

● Effect of activation parameters on both S_{BET} and carbon yield

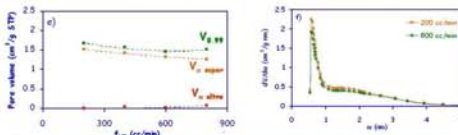


T and R have the most marked effect on both carbon yield and S_{BET}. Increasing the N₂ flow removes part of the activator: carbon yield increases and S_{BET} decreases. The variation of t or r (not shown here) slightly modifies the activated carbon produced.

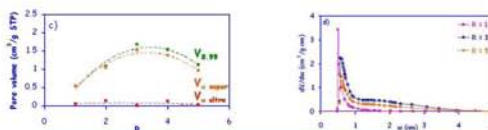
● Effect on both pore volume and pore size distribution



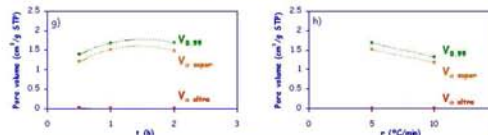
The total pore volume increases with activation temperature but, at temperatures higher than 700 °C, micropores progressively widen to form mesopores.



N₂ flow does not change the PSD but decreases the number of pores.



Pore volumes within the whole pore diameter range are reduced for R > 3; increasing R increases the fraction of wider pores.



1h of activation time is enough to activate the carbon. An increase of the heating rate from 5 to 10 °C/min produces a lowering of the pore volumes.

CONCLUSIONS

- This study evidenced the possibility of preparing highly microporous active carbons from demineralised Kraft lignin, using KOH in suitable experimental conditions.
- The most relevant parameters were found to be activation temperature and mass ratio KOH/lignin. Thus, the best materials (surface area ~3000 m²/g, micropore volumes ~1.5 cm³/g) were obtained at 700 °C and KOH/KL_d = 3.
- Modifying the experimental conditions easily leads to a range of active carbons, from almost purely microporous to mesoporous.

ANEXO F

**ENZYMATIC COMPOSITE MEMBRANES BASED ON
CARBON/POLYSULFONE.**

**ENGINEERING WITH MEMBRANES: MEDICAL AND
BIOLOGICAL APPLICATIONS (PÓSTER).**

CAMOGLI - ITALIA (2005).

Enzymatic composite membranes based on carbon/polysulfone

Carles Torras, Vanessa Torné, Vanessa Fierro, Daniel Montané & Ricard Garcia-Valls

ricard.garcia@urv.net, +34.977.55.96.11



Wood Biopolymers Group
 Department of Chemical Engineering
 Escola Tècnica Superior d'Enginyeria Química
 Universitat Rovira i Virgili
 Av. Països Catalans, 26. 43007 Tarragona (Catalonia - Spain)

Introduction

Versatile materials that have selective properties are of high interest. The objective of these materials is their application in membrane selective reactors. In these reactors, the separation and reaction steps are combined in a single unit. In order to obtain an optimized reactor, the base material (support) is of great importance. In this work, the support is a composite polysulfone membrane that contains activated carbon.

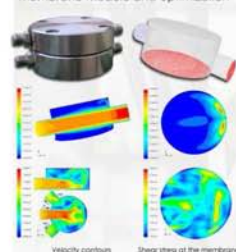
Methods and materials.

- ❖ Membranes. Obtained from Psf (20%w) by immersion precipitation. Solvent: DMF, Non-solvents: IPA & H₂O.
- ❖ Activated carbon. From residual lignin with carbonization at 450°C. Characterized by Micromeritics ASAP 2020. (gas adsorption surface area analyzer).
- ❖ Enzyme. Xylanase (from Sigma-Aldrich), 2.5 u/mg.
- ❖ Fluid: Oligosaccharides from acid hydrolysis of nuts shells up to 40kDa.
- ❖ Experiments carried out in a flat membrane module.

Micromeritics ASAP 2020



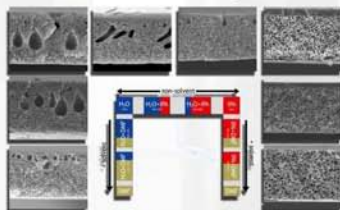
Membrane module and optimization



1. Membranes, activated carbon & composite membranes.

- ❖ Membranes: Cut-off range: 20-600 kDa.
- ❖ Activated carbon. Type I (Langmuir). Microporous character (0.41 cm³/g). BET surface area: 1047 m²/g. Total volume pores: 0.51 cm³/g.
- ❖ Composite membranes. Addition of 0.9% w AC. Membranes morphology & performance do not change.

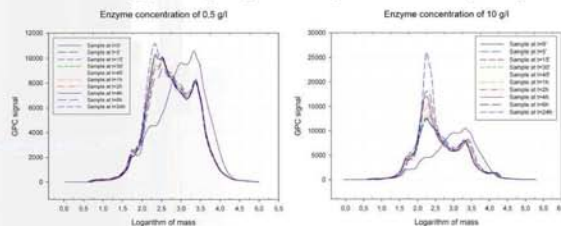
Membrane obtained from several coagulation baths



2. The activity of the enzymes

- ❖ Conditions to obtain chains of 2/3 monomers: Enzyme concentration: low/very low. Reaction time: 0-5'

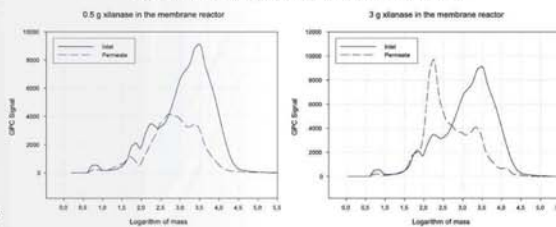
Chromatographs illustrating the degradation of the oligosaccharides due to the enzyme activity



3. The membrane reactor

- ❖ Enzyme was immobilized over the composite membranes.
- ❖ Results show evidence of separation and reaction.
- ❖ With a membrane of 40kDa MWCO and with low amounts of enzyme, a retention of 90% for a sugar size of 17kDa was obtained and also, the permeate contains mainly oligosaccharides of DP=3. This evidences a good equilibrium between the kinetics of the reaction and the separation.
- ❖ With an enzyme concentration too high, the kinetics is not adequate and monomers are mainly obtained.

Chromatographs illustrating the performance of two membrane reactors



Conclusions, references & acknowledgements

- ❖ Activated carbon does not change the morphology and the performance of the membranes.
- ❖ Membranes capable to hold a separation and reaction process have been successfully obtained.
- ❖ Although an optimization should be done, the kinetics of the reactions is consistent with the kinetics of the separation.
- ❖ The immobilization of the enzyme on the carbon-metal complex is in process.
- ❖ C. Torras & R. Garcia-Valls. Quantification of membrane morphology by interpretation of scanning electron microscopy images. *Journal of Membrane Science*, 233 (2004) 119-127.
- ❖ L. Ballinas, C. Torras, V. Fierro & R. Garcia-Valls. Factors influencing activated carbon-polymeric composite membrane structure and performance. *Journal of Physics and Chemistry of Solids*, 65 (2004) 633-637.

C. Torras acknowledges the Rovira i Rovira University for a doctoral scholarship. This work has been supported by the Spanish Ministry of Science and Technology, project PPQ2002-04201-C02.

ANEXO G

**INFLUENCE OF THE ASH CONTENT ON THE
MICROPOROSITY OF ACTIVATED CARBONS DERIVED
FROM KRAFT LIGNIN.**

CARBON (PÓSTER).

COREA (2005).

Influence of the ash content on the microporosity of activated carbons derived from Kraft lignin



Vanessa Fierro^a, Vanessa Torné^a and A. Celzard^b

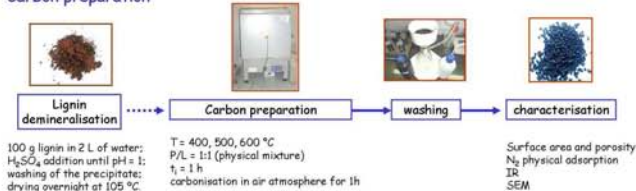


^a Departament d'Enginyeria Química, Universitat Rovira i Virgili, Campus Sescelades, 43007 Tarragona, Spain
^b Laboratoire de Chimie du Solide Minéral, UMR CNRS 7555, Université Henri Poincaré, 54506 Vandoeuvre-lès-nancy, France

This work focuses on ACs produced from the thermal decomposition of mixtures of orthophosphoric acid (PA) and either as-received Kraft lignin, KL, or demineralised one, KL_d. The yield, surface area and porosity were determined, and the effect of the demineralisation process was investigated.

EXPERIMENTAL

Carbon preparation



RESULTS AND DISCUSSION

	Proximate Analysis (wt %, dry basis)			Ultimate Analysis (wt %, daf)					
	Fixed Carbon	Volatile mat.	ash	C	H	N	S	O*	
KL	36.4	52.5	11.1	59.5	5.1	0.1	2.2	33.3	
KL _d	39.7	60.1	0.2	65.8	5.9	0.0	0.5	27.8	

* Estimated by difference

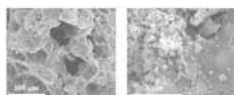
KL has an ash content (11.1% daf basis) that is nearly removed (0.2% daf basis) after the treatment with H₂SO₄.

SEM images of lignins



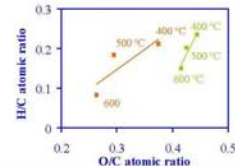
KL particles (left) have a rounded shape with widely open volumes inside. After acid washing, KL_d particles (right) are much bigger and sharp.

SEM images of carbons



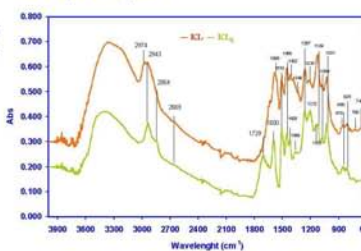
Carbons from KL activated at 400 °C. After carbonisation, the original shape of the particles is lost and a porous structure is revealed.

Van Krevelen diagram



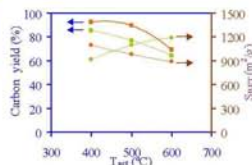
The ACs become more aromatic when T_{act} increases. ACs produced from KL are more aromatic than those from KL_d, and aromaticity increases with T_{act}.

IR analysis of lignins



The most important changes introduced by acid-washing are the reduction of hydroxyl groups and the elimination of carbonates. An intense band in KL_d spectrum centered at 1729 cm⁻¹, which indicates C=O (ketones, aldehydes or carboxyl groups) not associated to aromatic rings, appeared after acid washing.

Carbon yield and S_{BET}

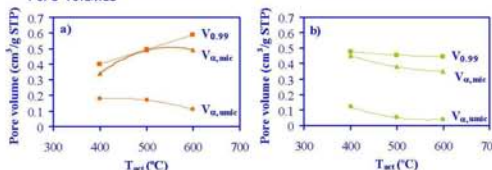


DR model

T (°C)	V _{DR} (cm ³)/(g·mol)	E ₀	L ₀ (nm)
Raw lignin as carbon precursor			
400	0.38	22.2	1.0
500	0.54	19.9	1.3
600	0.51	18.9	1.5
Washed lignin as carbon precursor			
400	0.45	19.1	1.4
500	0.40	17.9	1.7
600	0.37	17.6	1.7

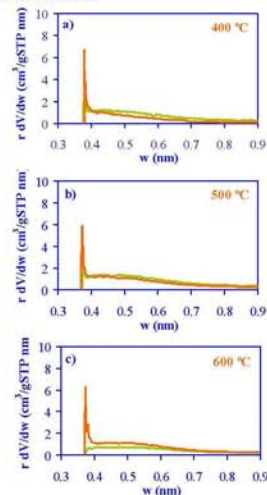
Carbon yield decreases with increasing T_{act} and is always higher for carbons from KL. Opposite evolutions of S_{BET} with T_{act} were found, depending on the precursor. The parameters calculated by applying the DR method are also affected. Carbons from KL_d have a smaller micropore volume, and wider pores.

Pore volumes



ACs from KL_d have higher micropore volumes at 400 °C. However, their pore volumes decrease with increasing T_{act}, contrary to those from KL.

H-K distributions



For ACs from KL, the amount of pores at 0.37 nm is always higher and increases with T_{act}. ACs from KL_d show a wider mean pore size, and a decrease of porosity of width 0.37 nm is observed when ACs were prepared at 600 °C.

CONCLUSIONS

- Carbon yield, surface area, porosity and surface chemistry are affected by the removal of the mineral matter. Carbon yield is higher for activated carbons prepared by activation of the raw Kraft lignin (KL) and such ACs also show a higher aromaticity.
- The activated carbons prepared by activation of KL and demineralised one (KL_d) are essentially microporous with surface areas higher than 800 m²/g. The highest surface area determined in this work, of nearly 1200 m²/g, corresponds to the AC prepared from KL at 600 °C.
- The different characteristics of the ACs are due to the demineralisation process, which produces lignin polymerisation and reduces its ability to react with PA.

NOTAS PARTICULARES

Notas Particulares

Notas Particulares

Notas Particulares

